The Functional Expression of N-Methyl-D-Aspartate Glutamate-Type Receptors by Megakaryocytes and Platelets

Hobbs, Catherine

Award date:
2010

Awarding institution:
University of Bath

THE FUNCTIONAL EXPRESSION OF *N*-METHYL-*D*-ASPARTATE GLUTAMATE-TYPE RECEPTORS BY MEGAKARYOCYTES AND PLATELETS

Catherine Mary Hobbs

A thesis submitted for the degree of Doctor of Philosophy

University of Bath

Department of Pharmacy and Pharmacology

May 2010

TABLE OF CONTENTS

TABLE OF FIGURES

TABLE OF TABLES

ABBREVIATIONS

5,7-DCKA, 5,7-dichlorokynurenic acid; **AA,** arachidonic acid; **ACD**, acid-citrate-dextrose; **ACPD (trans),** (9)-1-aminocyclopentane-trans-1,3-dicarboxylic acid; **AD,** Alzheimer's Disease; **ADP,** adenosine diphosphate; **AM,** acetylmethyl ester; **AMPA**, α-amino-3-hydroxyl-5-methyl-4-isoxazole-propionate; **AMPAR,** AMPA receptor; **ALS,** amyotrophic lateral sclerosis; **ASA,** acetyl salicylic acid; **ATP,** adenosine triphosphate; **ATPA,** 2-amino-3-(5-*tert*-butyl-3-hydroxy-4-isoxazolyl)propionic acid**;** **BFU-MK,** burst forming unit-megakaryocyte; **biotin-HDPD,** *N*-[6-(biotinamido)hexyl]-3'-(2'-pyridyldithio)propionamide; **BSA**; bovine serum albumin; **$CaCl_2$,** calcium chloride; **CBP,** CREB binding protein; **CLP,** common lymphoid progenitor; **CNQX,** 6-cyano-7-nitroquinoxaline-2,3-dione; **CNS,** central nervous system; **COX,** cyclo-oxygenase; **CPP,** 3-(2-Carboxypiperazin-4-yl)propyl-1-phosphonic acid; **CREB,** cAMP response element-binding protein; **D-AP5**, D-2R-Amino-5-phosphonovaleric acid; **DAG,** diacylglycerol; **DMSO,** dimethyl sulfoxide; **dNTP;** deoxyribonucleotide triphosphate; **DTT,** dithiothreitol; **EAAT,** excitatory amino acid transporter; **ECL**, enhanced chemiluminescence detection reagent; **EDTA,** ethylene diaminetetraacetic acid; **EGTA**, ethylene glycol tetraacetic; **eNOS,** endothelial nitric oxide synthase; **ER,** endoplasmic reticulum; **ERK,** extracellular related kinase; **FBS,** foetal bovine serum; **FGF-4;** fibroblast growth factor-4; **FITC,** fluorescein isothiocyanate; **Fli-1,** Friend leukaemia integration 1; **FOG-1,** Friend of GATA-1; **GABA,** γ-butyric acid; **G-CSF,** granulocyte stimulating factor; **GLAST,** glutamate/ aspartate transporter; **GLT-1,** glutamate transporter-1; **GM-CSF,** granulocyte-macrophage stimulating factor; **GP,** glycoprotein; **Grb2,** growth factor-receptor-bound protein-2; **HCl,** hydrochloric acid; **HEPES,** 4-(2-hydroxyethyl)-1-piperazineethanesulfonic acid; **HPP-CFU-MK,** high proliferative potential colony forming unit megakaryocyte; **HSC,** haemopoietic stem cell; **HSP70,** heat-shock protein 70; **Ig,** immunoglobulin; **iGluR,** ionotropic glutamate receptor; **IL,** interleukin; **IP_3,** inositol triphosphate; **JAK2,** Janus kinase 2; **KCl,** potassium chloride; **LAPD,** L-(+)-2-amino-4-phosphonobutyric acid; **LTP,** long-term potentiation; **KAR,** kainate receptor; **MAPK,** mitogen-activated protein kinase; **MEK,** mitogen-activated/ extracellular-regulated kinase; **MEP,** megakaryocyte/ erythrocyte progenitor; **$MgCl_2$,** magnesium chloride; **miRNA,** microRNA; **mGluR,** metabotrophic glutamate receptor; **MK,** megakaryocyte; **MK-801**, dizocilpine hydrogen maleate; **MMTS**, methyl methanethiosulfonate; **MR,** maximum response; **NaCl,** sodium chloride; **NaF,** sodium fluoride; **NaOH,** sodium hydroxide; **$NaNO_2$,** sodium nitrite; **Na_3VO_3,** sodium orthovanadate; **NF-E2,** nuclear factor erythroid-2; **NMDA,** *N*-methyl-*D*-aspartate; **NMDAR,** NMDA receptor; **nNOS,** neuronal nitric oxide synthase; **NO,** nitric oxide; **NOS,** nitric oxide synthase; **PAGE,** polyacrylamide gel electrophoresis; **PAR,** protease activated receptor; **PBS,** phosphate buffered saline; **PCR,** polymerase chain reaction; **PDK-1,** phosphoinositide-dependent kinase-1; **PE,** phycoerythrin; **PF4,** platelet factor 4; **PIP_3,** phosphotidylinositol (3, 4, 5)-triphosphate; **PI,** propidium iodide; **PI3K,** phosphoinositol-3-kinase; **PIC,** protease inhibitor cocktail; **PKB,** protein kinase B (Akt); **PKC,** protein kinase C; **PL,** phospholipid; **PLC,** phospholipase C; **PMA,** phorbol 12-myristate 13-acetate; **PMSF,** phenylmethylsulphonyl fluoride; **PPP,** platelet poor plasma; **PRP,** platelet rich plasma; **PVDF,** polyvinylidene fluoride membrane; **RT,** room temperature; **RT-PCR,** reverse transcription-PCR; **SCF,** stem cell factor; **SDF-1,** stromal-derived factor-1; **SDS,** sodium dodecyl sulphate; **SH2,** Src homology domain 2; **SHIP1,** SH2 containing inositol phosphatase; **SHP2,** SH2-domain containing tyrosine

phosphatase; **SNAP,** synaptosomal associated protein; **SNOB,** *S*-nitrosylation binding agent; **SNOC,** *S*-nitrosocysteine; **SNOSID,** SNO-site identification; **SOCs,** suppressor of cytokine signalling proteins; **SOS,** son-of-sevenless; **STATs,** signal transducers and activators of transcription; **TAE,** tris-acetate-EDTA; **TAR,** trans activating response; **TbA_2,** thromboxane A_2; **TEMED,** tetramethylethylenediamine; **TF,** transcription factor; **TPO,** thrombopoietin; **TRAP,** thrombin receptor-activating peptide; **vWF,** von Willebrand factor; **VGLUT,** vesicular glutamate transporter; **WBC,** white blood cells; **WT,** wild type.

ACKNOWLEDGEMENTS

Firstly, I would like to thank my supervisor Dr Amanda MacKenzie for all of her support and encouragement over the last four years, in particular when things were getting a little 'aggregating'.

Thanks also go to past and present members of 5W2.43 and 5W2.48, in particular Dr James Hewinson for putting up with all of my daft questions and confusion, Dr Vanesa Lopez Valverde for her help in setting up this project, Dr Belinda Thompson for assistance with Western blotting and gin, and Dr Samantha Moore for her help with calculations, listening to my ranting and general merriment. My thanks also go to Dr Mike Storm, Dr Heather Bone and all the members of 7W3.11 for their assistance and guidance with the RT-PCR.

I would like to thank all of my donors, without whose blood this project would not have been possible, and Jo Carter, without whom the blood could not have been extracted.

Many thanks to my friends for everything over the course of this thesis, and in particular to Lisa and Annah for all the coffee, cake and crazy chats, as well as to the CS theory group at Bristol for letting me camp in their office. Thanks also go to my family for all of their love and encouragement, especially when I decide to do a crazy thing like a PhD.

Thanks go to Cadburys, Tetleys and Gordons for their assistance in the writing of this thesis.

And, last but definitely not least, all my love and thanks to Ashley, without whose support and expert tea making skills this thesis would not have been written.

ABSTRACT

This study investigated the role of NMDARs in the differentiation of MEG-01 cells and in the activation of human platelets. This investigation demonstrated that the NR1, NR2D and NR3 subunit proteins are expressed in human platelets, with the NR1 subunit also expressed in MEG-01 cells. The NR2A subunit protein was not detectable in either MEG-01 cells or human platelets. PMA-induced differentiation of MEG-01 cells did not appear to stimulate changes in expression of any of the subunit proteins tested. Using assays to measure the changes in $[Ca^{2+}]_i$ and ATP secretion, it was determined that donors could be separated into those who responded to the agonists applied and those who did not; responses also decreased over time in both assays. Human platelets from responding donors demonstrate an increase in $[Ca^{2+}]_i$ in response to extracellular glutamate, and that increases in ATP secretion are detected at a 10-fold lower concentration. The same is also true with extracellular glycine. Increases in $[Ca^{2+}]_i$ were elicited on the addition of extracellular NMDA; extracellular D-serine had no effect. NMDAR inhibitors, MK-801 and D-AP5, inhibited ATP secretion evoked by either glutamate alone or in combination with glycine. D-serine inhibited responses elicited by extracellular glycine. NMDARs play a role in MK differentiation, with the adhesion of MEG-01 cells cultured on a fibrinogen-surface and differentiated with PMA reduced by both inhibitors. PMA-treated MEG-01 cells increased both in size and irregularity, with the addition of NMDAR-specific inhibitors having no effect. *S*-nitrosylation also inhibits activation of NMDAR, and a new molecule has been developed which can detect *S*-nitrosylated proteins through a single step process in live cells. Overall, this study has shown that both human platelets and MEG-01 cells express NMDAR subunits, which have been demonstrated to form functional receptors in human platelets.

CHAPTER 1
INTRODUCTION

Studies from two separate groups have highlighted an important role for glutamate and glutamate binding receptors in the function of both megakaryocytes (MKs) and circulating blood platelets (Genever *et al*, 1999; Hitchcock *et al*, 2003; Franconi *et al*, 1996 and 1998). Extracellular glutamate has been implicated in the differentiation of bone marrow derived MKs through to the production of platelets and platelet function in the blood. In this study, I have investigated the expression of a specific subtype of glutamate receptor, the *N*-methyl-*D*-aspartate (aspartate analogue; NMDA) activated receptor (NMDAR), in both human platelets and MKs.

1.1. Megakaryocytes

MKs are highly specialized precursor cells that differentiate to generate blood borne platelets. Platelets were first identified as "extremely minute…granules" in 1841 by Addison, and were subsequently termed platelets in 1882 (Bizzozero). Bone marrow derived MKs were identified as the source of platelets in 1906 (Wright). MKs are produced via megakaryopoiesis from pluripotent haematopoietic stem cells (HSCs), and are found primarily in the bone marrow, where they constitute less than 1 % of myeloid cells, as well as in the lungs and peripheral blood (Patel et al, 2005). Thrombopoietin (TPO) has been identified as the primary cytokine required for HSC differentiation and the eventual production of platelets (Bartley *et al*, de Sauvage *et al*, Lok *et al*, and Kaushansky *et al*; 1994). HSCs are maintained in the G_0 phase of the cell cycle in the bone marrow, re-entering the cell cycle upon stimulation with TPO alone or in combination with interleukin-3 (IL-3), IL-6, stem cell factor (SCF) or granulocyte colony-stimulating factor (G-CSF) (Ku *et al*, 1996; Sitnicka *et al*, 1996). Various combinations of factors are required at each stage of megakaryopoiesis, however TPO alone has been found to be sufficient to stimulate the entire process from HSCs to platelets (table 1) (Kaushansky *et al*, 1995).

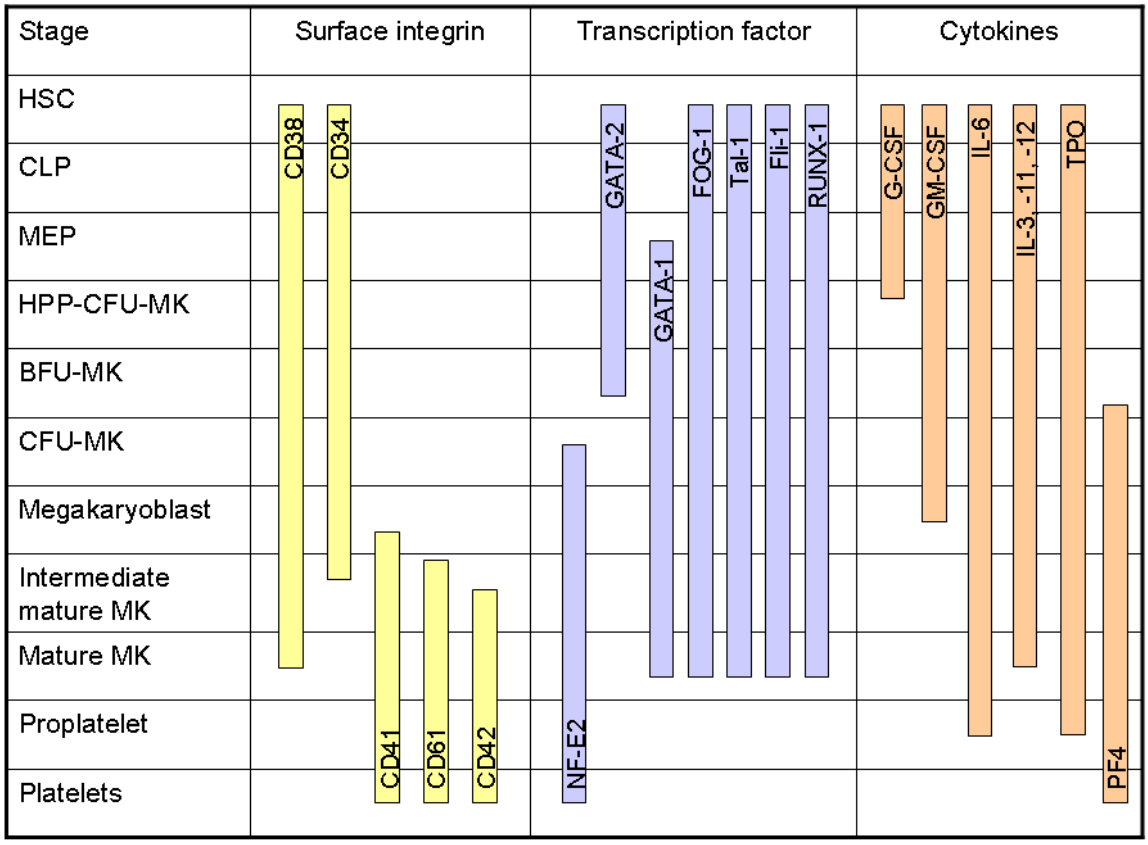

Table 1. **Table illustrating the stages of haematopoiesis when surface integrins, transcription factors and cytokines are expressed** (Szalai *et al*, 2006; Pang *et al*, 1995; Kaushansky *et al,* 1995; Lambert *et al*, 2007). CLP, common lymphoid progenitor; MEP, MK/ erythrocyte progenitor; HPP-CFU-MK, high proliferative potential colony forming unit megakaryocyte; BFU-MK, burst forming unit- megakaryocyte; CFU-MK, colony forming unit-megakaryocyte; IL, interleukin; G-CSF, granulocyte colony stimulating factor; GM-CSF, granulocyte-macrophage colony stimulating factor; PF4, platelet factor 4.

1.1.1. Cytokines and chemokines

TPO is a cytokine constitutively expressed by the liver and has been demonstrated to be the main regulator of megakaryopoiesis (Szalai *et al*, 2006). It was identified in 1994 by 4 different groups, Bartley *et al*, de Sauvage *et al*, Lok *et al*, and Kaushansky *et al*, and consists of 332 amino acids with a molecular mass of approximately 70 kDa (Muto *et al*, 2000). The TPO receptor was originally identified from the oncogene *v-mpl* of the mutant murine myeloproliferative leukaemia virus, which is capable of transforming haematopoietic progenitor cells, and by its homology to other members of the cytokine receptor superfamily (Vigon *et al*, 1992). The proto-oncogene, c-mpl, was identified as the cellular counterpart of *v-mpl* with the genes encoding human and mouse c-mpl isolated in

1992-3, and identified as the TPO receptor (Vigon *et al*, 1992; Vigon *et al*, 1993). The N-terminal domain of TPO binds to the high affinity c-mpl receptor expressed on the surface of haematopoietic cells leading to receptor activation (Linden *et al*, 2000; Muto *et al*, 2000).

The c-mpl protein is constitutively expressed and contains both extracellular and intracellular domains, with TPO binding to the extracellular domain and the intracellular containing 2 conserved membrane-proximal boxes (box 1 and 2) constitutively bound to Janus kinase 2 (JAK2). Binding of TPO to c-mpl induces the formation of c-mpl dimers, which moves the 2 JAK2 kinases closer together, leading to their mutual activation which stimulates phosphorylation of c-mpl tyrosine residues (amino acids 112 and 117) (Gedis *et al*, 2002; Drachman and Kaushansky, 1997). Phosphorylation of other proteins is then triggered through activation of Src homology 2 (SH2) domain-containing tyrosine phosphatase (SHP2), which binds the complex formed of growth factor-receptor-bound protein-2 (Grb2) and Son of Sevenless (SOS). This activates Ras, a GTPase, which then activates the mitogen activated protein kinase (MAPK) pathway. Phosphorylated extracellular related kinase (ERK) translocates to the nucleus where it has been shown to phosphorylate GATA-1 and Friend leukaemia integration-1 (Fli-1) stimulating megakaryopoiesis. ERK is also hypothesised to regulate Bad, a proapoptotic factor (Scheid *et al*, 1999). Phosphoinositol-3-kinase (PI3K) is activated by TPO binding, stimulating protein kinase B (PKB/ Akt) (Pasquet *et al*, 2000). STATs (signal transducers and activators of transcription) 3 and 5 are phosphorylated, then translocate to the nucleus and stimulate transcription of genes including cyclin D and Bcl-x_L (Miyakawa *et al*, 1996; de Groot, 2000). Other factors activated by TPO binding are known to have an inhibitory role, such as SHIP1 (SH2 containing inositol phosphatase), a negative regulator of the PI3K pathway, and SOCs (suppressor of cytokine signalling proteins) (Drachman and Kaushansky, 1997). SOCs also act as a negative regulator, inhibiting further activation of GP130 through IL-6 mediation by binding to the phosphorylated activation loop of the JAK kinase domain via its SH2 domain (Schmitz *et al*, 2000). Activation of these pathways regulates the transcription of genes (e.g. SOCS and c-fos) determining the fate of the cells (figure 1).

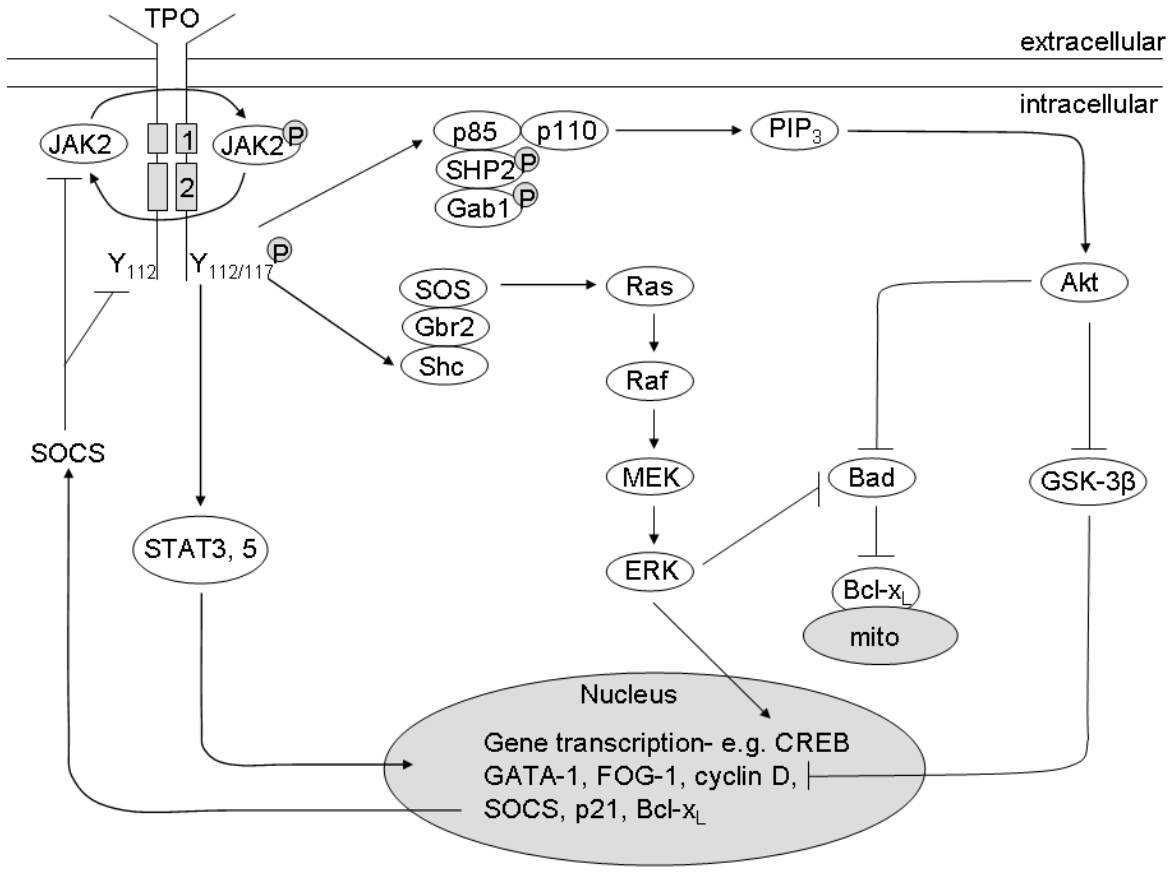

Figure 1. JAK/ STAT pathway. Illustrating some of the intracellular pathways triggered by binding of thrombopoietin (TPO) to its receptor, c-mpl. JAK, Janus kinase; 1/ 2, box 1/ 2; STAT, signal transducers and activators of transcription; SOCS, suppressor of cytokine signalling proteins; SHP2, Src homology 2 domain-containing tyrosine phosphatase; SOS, son-of-sevenless; Grb2, growth factor-receptor-bound protein-2; MEK, mitogen-activated/ extracellular-regulated kinase; ERK, extracellular-regulated kinase; CREB, cAMP response element-binding protein; FOG, friend of GATA; PIP_3, phosphotidylinositol (3, 4, 5)-triphosphate; GSK-3β, glycogen synthase kinase-3β; mito, mitochondria; P, phosphorylation.

Levels of free circulating TPO within the bloodstream are regulated by platelets, which have been found to express 25-100 copies of the c-mpl receptor per platelet (Broudy *et al*, 1997; Li *et al*, 1999). TPO binds to the c-mpl receptor forming a complex, which is then internalised and degraded, reducing the amount of free TPO (Li *et al*, 1999). If platelet numbers in the blood become too high, levels of unbound TPO decrease, leading to a reduction in the number of maturing MKs and therefore a decrease in platelet production. Equally, when the platelet number decreases, the level of free TPO is higher, stimulating a higher level of platelet production to return platelet levels to normal.

While TPO is able to direct megakaryopoiesis alone, under normal physiological conditions other factors are also involved at specific stages of differentiation. For example, IL-3 is involved during the early stages of differentiation around the colony forming unit MK (CFU MK) stage (table 1) (Quesenbury *et al*, 1985; Robinson *et al*, 1987). G-CSF is implicated in stimulating HSCs back into the cell cycle; however it is postulated to have another, inhibitory role in the latter stages of differentiation, controlling the levels of platelet release (Ku *et al*, 1996; Saito *et al*, 1996). Granulocyte-macrophage colony stimulating factor (GM-CSF) has also been implicated in the early stages of megakaryopoiesis, with IL-11 shown to be required during the intermediate stages (Robinson *et al,* 1987; Neben *et al*, 1993).

Platelet factor 4 (PF4 or CXCL4) has been shown to have 2 different roles, assisting in stimulation of megakaryopoiesis from approximately the BFU-MK until the mature MK stage, then switching to an inhibitory role negatively regulating platelet production. PF4 is produced by MKs and is present in α-granules (Briquet-Laugier *et al*, 2004). The PF4 content of platelets has been shown to be inversely proportional to platelet number and knocking down PF4 in mice has been demonstrated to increase the number of mature MKs in comparison to the wild-type (WT) (Lambert *et al*, 2007). It is hypothesised that PF4 is released from mature MKs and platelets inhibiting further differentiation of immature MKs.

1.1.2. TPO-independent differentiation

Both $TPO^{-/-}$ and $c\text{-}mpl^{-/-}$ mice are viable with normal clotting behaviour, but have only 10 % of the normal level of platelets present in WT mice (Bunting *et al*, 1997). This indicates that other pathways and regulators are present which are able to maintain a level of haematopoiesis in the absence of TPO or TPO binding, for example IL-6/ GP130.

1.1.2.1. IL-6/ GP130

IL-6 acts via the membrane-bound glycoprotein GP130, stimulating the JAK/ STAT and the Ras/ Raf/ MAPK pathways, and has been shown to stimulate MK differentiation and platelet production in the presence and absence of TPO. GP130 conditional knockout mice have shown that when IL-6 is unable to bind the glycoprotein, the number of immature MKs and white blood cells (WBCs) increases as the cells are unable to differentiate to form more mature MKs (Jenkins *et al*, 2002). GP130, like TPO, has been shown to be

constitutively bound to JAK2, as well as to JAK1, which are able to phosphorylate SHP2 and STAT 1 and 3 (Stahl *et al*, 1994). As with TPO, a range of pathways are stimulated, leading to activation of CREB binding protein (CBP) and the MAPK pathway for example (figure 1), and eventually to regulation of gene transcription (Schmitz *et al*, 2000; Scheid *et al*, 1999).

The loss of GP130 causes embryonic lethality due to severe thrombocytopenia. A postnatal conditional knockout however leads to only a mild decrease in platelet numbers (Yoshida *et al*, 1996; Betz *et al*, 1998). The number of MKs in the bone marrow is not affected by the loss of GP130, suggesting that its role is in maintaining platelet production rather than in the early stages of differentiation (Jenkins *et al*, 2002).

1.1.3. HSC differentiation

The differentiation of HSCs to platelets can be tracked by following the changes in expression of transcription factors (TFs) and surface integrins together with changes in morphology (table 1).

1.1.3.1. Transcription factors

Several different TFs have been demonstrated to be involved with megakaryopoiesis, including RUNX1, GATA-1 and -2 and Friend-of-GATA-1 (FOG-1), and are detailed in table 2.

1.1.3.2. Surface integrins

Differentiation of bone marrow stem cells can be tracked through the expression of the CD integrins on the surface of the cells. Different combinations of CD integrins are expressed at each stage of megakaryopoiesis, for example HSCs in humans are $CD34^+$ $CD38^{-/lo}$ while human platelets are $CD41^+$ $CD42^+$ $CD61^+$ (Chang *et al*, 2007) (table 1). CD integrin expression can be used to determine the maturity of MKs with methods such as flow cytometry. These markers also combine to form receptor complexes such as the GPIIb/IIIa (CD41/CD61; $\alpha_{IIb}\beta_3$) that binds von Willebrand factor (vWF), vitronectin, fibronectin and fibrinogen (Szalai *et al*, 2007). CD42 (GPIb) has also been shown to bind vWF and has been linked to increasing expression of c-mpl, and two collagen receptors, GPVI and the $\alpha_2\beta_1$ integrin (Chang *et al*, 2007; Atkinson *et al*, 2003). A collagen binding complex formed of the glycoproteins GPIb, GPIX and GPV is expressed on the surface of platelets.

TRANSCRIPTION FACTOR	DESCRIPTION	EXPRESSION	INTERACTIONS
GATA-1 and GATA-2	DNA-binding proteins expressed in cis-regulatory sequences N-terminus binds FOG-1, C-terminus binds DNA directly at (A/T)GATA(A/G)	From MEP to mature MK (GATA-1) and from HSC to CFU-MK (GATA-2)	FOG-1
FOG-1	9-fingered haematopoietic-specific TF	HSC to mature MK	4 of the zinc-fingers interact with either GATA-1 or GATA-2
Fli-1	Contains winged helix-loop-helix DNA binding (Ets) domain, binds GGA(A/T) (Ets binding sequence)	HSC to mature MK	Transcriptionally activates genes with Ets binding sequence in promoter region GATA-1, PF4, c-mpl
NF-E2 (nuclear factor erythroid-2)	Basic leucine zipper protein p45 subunit with either MafK or MafG	CFU-MK to platelet	Regulates β-tubulin expression
Tal-1	Basic helix-loop-helix	HSC to mature MK	Required for commitment to initiate haematopoiesis Implicated in NF-E2 regulation

Table 2. Main transcription factors involved in haematopoiesis. Szalai *et al*, 2006; Chang *et al*, 2007; Elagib *et al*, 2003.

1.1.3.3. Morphology and cell structure

Once MKs are fully mature, they cease to proliferate and instead increase in size to approximately 50 to 100 μm in diameter (Italiano *et al*, 2005). They undergo mitosis, but do not pass through anaphase B or cytokinesis in a process called endomitosis. This results in the nucleus increasing in size and becoming multi-lobed, with the number of single sets of chromosomes (ploidy) increasing from 2N up to 128N (Italiano *et al*, 1999) (figure 2). Demarcation membranes form and increase within the MK together with the number of organelles present in the cells and the synthesis of proteins such as vWF. There is an increase in the number of mitochondria and electron dense granules that contain serotonin, adenosine nucleotides and calcium (Ca^{2+}) (Italiano Jr *et al*, 2003). These changes form the preparatory step prior to the production of proplatelets.

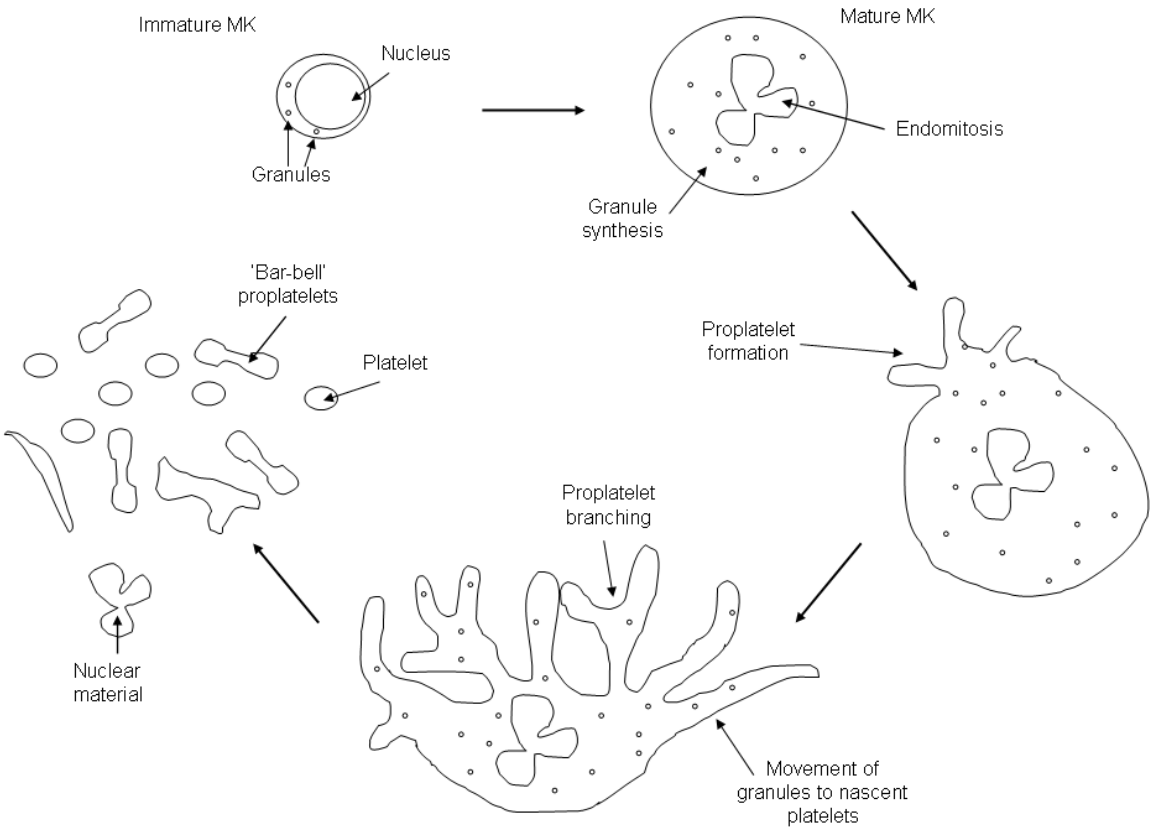

Figure 2. Changes in MK morphology during proplatelet production. The MK enlarges as it matures, increasing the number of granules and developing a multilobed nucleus. Proplatelets then start to form once the cell has stopped increasing in size. They branch and granules move along microtubules, becoming trapped in the developing platelets. The platelets eventually separate from the parent cell to enter the bloodstream either singularly or in a 'bar-bell' where 2 platelets are joined by a fragment of proplatelet, eventually separating.

1.1.3.3.1. Proplatelet formation

It has been demonstrated that proplatelet formation starts from one point on the MK surface, with 5-10 proplatelets forming per cell each of which can reach 50-100 μm in length (Italiano Jr *et al*, 2003). Proplatelets have been shown to form at a rate of 0.85 μm min^{-1}, taking between 4 and 10 h for the whole MK to be formed into platelets (Patel *et al*, 2005). The remaining nucleus, membrane and cytoplasmic material are then degraded by apoptosis.

The main driving force for proplatelet formation is the reorganisation of microtubules within the MK. These are formed of αβ-tubulin dimers, and have been shown to form in immature MKs coupled to the centrosome, growing towards, then parallel to the cell cortex (Patel *et al*, 2005). Microtubule production at the centrosome halts immediately prior to proplatelet formation, and the microtubules converge at the cell cortex. As the proplatelets form, microtubules extend in both directions, aided by the presence of the minus-end microtubule motor protein, dyenin (Patel *et al*, 2005). Platelets are formed at the end of each proplatelet by microtubules looping around themselves 8-12 times before re-entering the proplatelet shaft (Freson *et al*, 2005). Actin is also present throughout proplatelets and is implicated in the branching process, which is thought to be driven by the actin-based molecular motor, myosin; higher concentrations of actin are found at these points (Italiano *et al*, 1999; Italiano and Shivdasani, 2003). Organelles and granules are trafficked from the parent MK bidirectionally along the microtubules contained within the proplatelet eventually becoming trapped within developing platelets. This transport occurs through a combination of microtubule sliding and movement of the positive-end microtubule motor protein, kinesin (Richardson *et al*, 2005)

1.1.3.3.2. Platelet release

The mechanism of platelet release from proplatelets is not yet fully understood. Platelets are released into the blood stream through the blood sinusoids that link the bone marrow to the blood stream. Immature MKs have been shown to express CXCR4, the receptor for stromal-derived factor-1 (SDF-1) which has been demonstrated to form a gradient guiding the cells along the sinusoids from the osteoblastic niche to the vascular niche as they differentiate (Avecilla *et al*, 2004). The adhesion of the cells to the bone marrow endothelium is enhanced by fibroblast growth factor-4 (FGF-4), with SDF-1 assisting MK migration between the cells forming the endothelium barrier (Avecilla *et al*, 2004). The

junctions are too small for whole MKs to move into the sinusoids; however proplatelets are able to pass through. They separate from the remnants of the parent MK through retraction of the membranes such that platelets are released individually or more commonly as a 'bar-bell' where 2 platelets are joined by a proplatelet branch and then finally separate in the bloodstream (Italiano *et al*, 1999). MK fragments are able to pass into the sinusoids, and have been found in the bloodstream following platelet release (Junt *et al*, 2007).

The remnants of the parent cell are then degraded by apoptosis (Radley and Haller, 1983), and it has been demonstrated that pro-apoptotic factors are expressed during later stages of megakaryopoiesis, with anti-apoptotic factors expressed earlier during the process. Pro-apoptotic factors located within MKs include caspases-3 and -9 and nitric oxide (NO). Both procaspase-3 and procaspase-9 are compartmentalised in the cytoplasm of MKs, and have been shown to be present in mature platelets (de Botton *et al*, 2002). Both are activated prior to proplatelet production, with caspase-3 playing the major role. Previous work has shown that the inhibition of caspases induces thrombocytopenia (low platelet number, $< 1 \times 10^8$ platelets ml^{-1}), and it has been hypothesised that caspases-3 and -9 are implicated in the formation of proplatelets (de Botton *et al*, 2002). Caspase-12 is also present in mature MKs and has been demonstrated to link G-protein coupled receptors to $\alpha_{IIb}\beta_3$ activation. While it has been hypothesised to play a role in platelet aggregation, the mechanism by which this occurs has not been determined (Kerrigan *et al* 2004). NO has also been implicated in MK apoptosis using 2 cell lines, MEG-01 and HEL (Battinelli and Loscalzo, 2000), and there is also evidence to suggest its involvement in platelet production, where treatment of MEG-01 cells with NO assisted in the induction of platelet-like particle production (Battinelli *et al*, 2001). Several anti-apoptotic factors have been identified, including Bcl-2, whose overexpression leads to reduced platelet counts (Ogilvy *et al*, 1999). The expression of Bcl-2 has been shown to be regulated by a proapoptotic factor Bim, the loss of which has been shown to approximately halve the number of platelets produced (Bouillet *et al*, 1999). Another factor is Bcl-x_L, overexpression of which has also been shown to inhibit proplatelet formation (Kaluzhny *et al*, 2002). Both Bcl-2 and Bcl-x_L have been potentially implicated in platelet survival (Zhang *et al*, 2007).

1.2. Platelets

Platelets are small, anucleate cell fragments which circulate freely in the bloodstream, until they become activated and form a platelet aggregate. The average platelet count in an adult human is between 1.5 and 4.0 x 10^8 platelets ml^{-1} with approximately 1 x 10^{11} platelets produced each day; this can increase by more than 10 fold when required (Kaushansky, 2005). Platelets have been shown to contain 3 different types of granules each with specific contents- α, dense and lysosomal granules, which are released upon activation for example in thrombus formation (table 3).

α-GRANULES	DENSE GRANULES	LYSOSOMES
P-selectin	ATP	Acid phosphatase
vWF	ADP	Arylsuphatase
von Willebrand antigen II	Calcium	Carboxypeptidase A
Fibrinogen	Serotonin	Carboxypeptidase B
Fibronectin	Pyrophosphate	Proline carboxypeptidase
PF4	Glutamate	Cathepsin D
Protein S		Cathepsin E
Factor V		
Factor VIII		
Albumin		
Platelet-derived collagenase inhibitor		
Vitronectin		
Osteonectin		
IgG, IgA, IgM		
Plasminogen		
Neutrophil-activating protein II		

Table 3. The contents of platelet secretary granules. PF4, platelet factor 4; vWF, von Willebrand factor; IgG, immunoglobulin G; IgA, immunoglobulin A; IgM, immunoglobulin M; ATP, adenosine triphosphate; ADP, adenosine diphosphate (Nicol *et al*, 1999).

1.2.1. Coagulation cascade

The coagulation cascade contains two pathways through which platelets can be activated, the extrinsic which is triggered by vascular injury and subsequent exposure of tissue factor, and the intrinsic, which is triggered by the activation of factor XII, in turn stimulating the activation of factor XI (Davie *et al*, 1991) (figure 3). The pathways lead to activation of factors X and V, which combine to form the prothombinase complex that cleaves prothrombin, leading to the release of thrombin, a serine protease (Orkutt and Krishnaswamy, 2004; Tracey and Mann, 1983). Thrombin then stimulates the conversion of fibrin from fibrinogen in addition to activating factor XIII, which triggers the formation of crosslinks between the fibrin monomers, strengthening the clot (Davies *et al*, 1991). The site of clot formation is regulated by the location of the exposed tissue factor, an integral membrane glycoprotein, preventing formation where it is not required. Clot formation is limited by the activity of thrombomodulin located on the viable endothelial membranes. Thrombomodulin binds active thrombin removing it from the blood stream and leading to the activation of Protein C. Active Protein C subsequently inhibits FVa and FVIIIa resulting in attenuation of the clotting cascade (Esmon and Owen, 1981; Fulcher *et al*, 1984).

1.2.2. Thrombin

In addition to a role in the coagulation cascade thrombin has been demonstrated to activate the 7-transmembrane G-protein coupled protease activated receptors (PAR) 1 and 4 expressed on the surface of human platelets, by cleaving the extracellular N-terminus between residues Arg-42 and Ser-43 (Vu *et al*, 1991). The new N-terminus acts as a tethered ligand, binding to the body of the receptor and activating intracellular signalling (Vu *et al*, 1991). Each PAR can only be activated once before desensitising and uncoupling from the induced signalling pathway. The receptor is internalised by endosomes within the first 60 s of activation (Hoxie *et al*, 1993). The internalised receptors are then targeted to the lysosomes for degradation (Trijo *et al*, 1998). PAR-1 has been localised to both the cell surface and the demarcation membrane of platelets (Molino *et al*, 1997), and in megakaryocytic cells, it has been demonstrated that new receptors can be synthesised and transported to the cell surface. However, due to an apparent lack of machinery to synthesise new proteins this is not possible within platelets, and no further reserve of receptors other than those at the demarcation membrane has been determined (Molino *et al*, 1997).

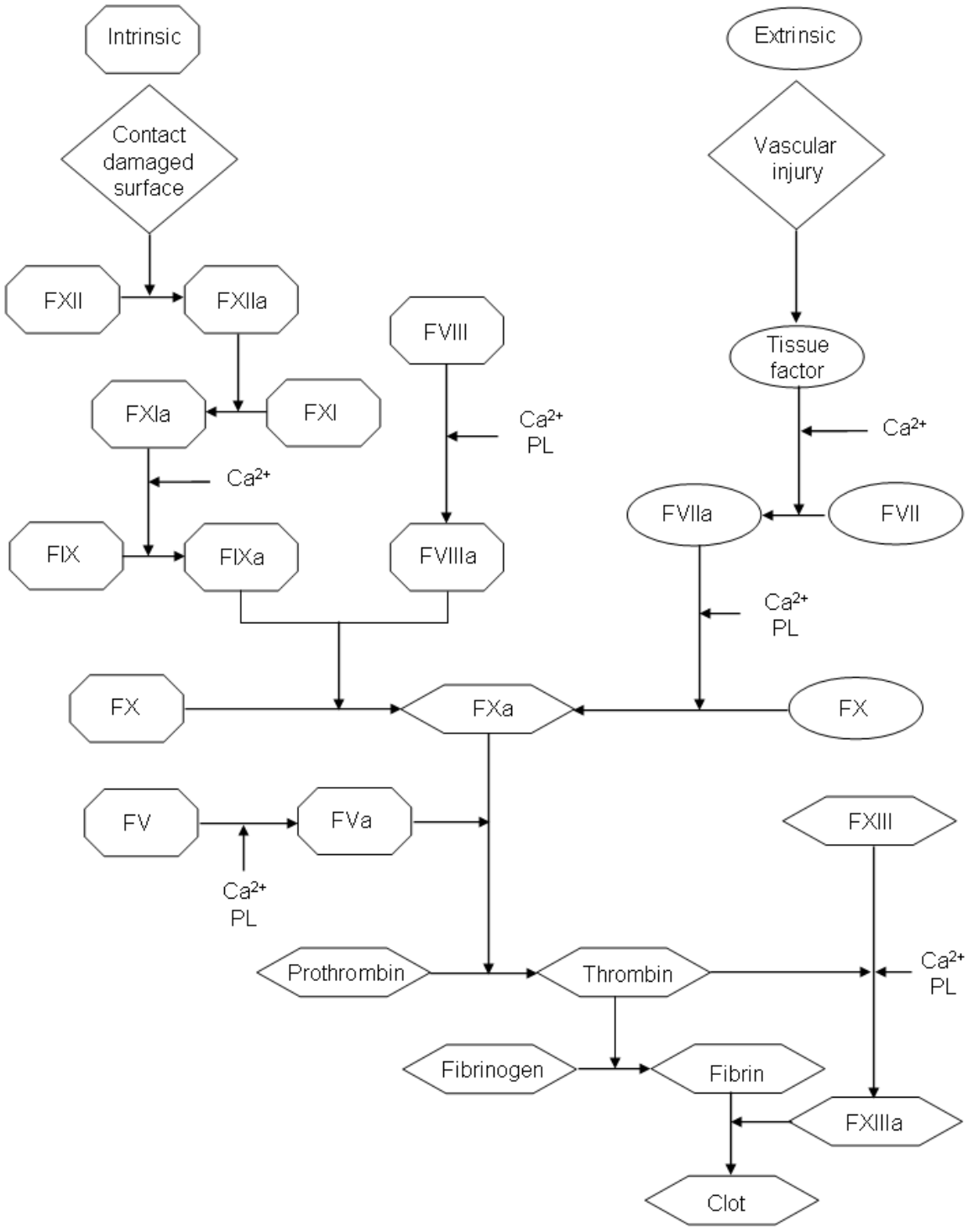

Figure 3. Intrinsic and extrinsic pathways of the coagulation cascade which end in the formation of a cross-linked fibrin clot. Initiation of the coagulation cascade occurs following vascular injury, triggering the extrinsic pathway (right hand side; ⬭). The intrinsic pathway is triggered by FXII binding to exposed collagen (left hand side; ⬭) The pathways converge (⬭) to trigger activation of FX which leads to the generation of thrombin from prothrombin and the conversion of fibrin from fibrinogen, from which an insoluble clot forms. PL, phospholipid; F, factor; a, activated; numbers are in Roman numerals where I= 1, V= 5, X= 10.

The sensitivity of the receptors to thrombin has been shown to vary, with the EC_{50} for PAR-4 shifting from 20 (platelets- endogenous receptors) to 100 fold (oocytes- transfected receptors) greater than for PAR-1 (Kahn *et al*, 1998; Xu *et al* 1998; Covic *et al*, 2000), indicating that while PAR-1 is the main mediator of platelet stimulation, PAR-4 is able to participate in platelet activation at high concentrations. There is evidence that the response to thrombin is biphasic with the more rapid initial phase due to PAR-1 activation, and the second, slower, sustained response mediated by PAR-4 (Kahn *et al*, 1999). Also in comparison to the rapid desensitisation of PAR-1, the desensitisation of PAR-4 is slower, indicating a role in sustaining a response to thrombin (Shapiro *et al*, 2000).

PAR-1 and -4 have also been demonstrated to stimulate different intracellular pathways. PAR-1 has been shown to trigger $G_{\alpha i}$ which inhibits the production of adenylyl cyclase, and thus the production of cAMP, $G_{q/\ 11}$ which activates phospholipase C (PLC), and $G_{12/\ 13}$ which have both been shown to stimulate RhoA kinase. In comparison, PAR-4 has been shown to activate only the $G_{\alpha q}$ pathway, but potentially also the G_{12} pathway (Farugi *et al*, 2000) (figure 4).

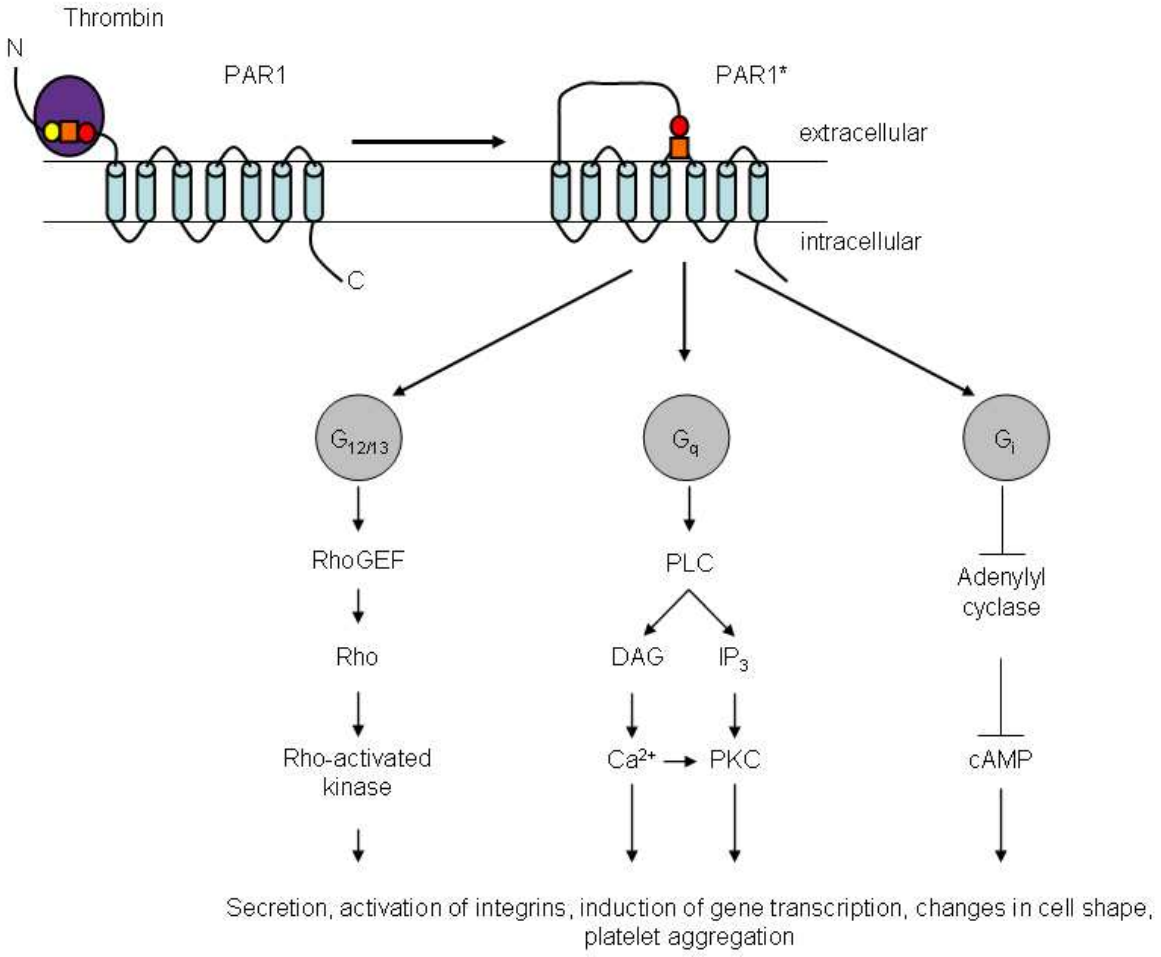

Figure 4. Pathways linked to activation of protease activated receptor 1 (PAR1) by thrombin. The N-terminus is cleaved by thrombin exposing a new N-terminus, which binds to the receptor leading to activation. PLC, phospholipase C; DAG, diacylglycerol; IP_3, inositol triphosphate; PKC, protein kinase C; *, activated receptor.

1.2.3 Platelet activation

Inactive platelets are discoid in shape, but upon activation they swell, becoming spherical and extend pseudopods (figure 5). The peripheral microtubule rings contract and break down, and the granules become centralised (Klages *et al*, 1999). The granules then fuse with the membrane invaginations of the open canalicular system, and release their contents into the surrounding environment (Lemons *et al*, 1997).

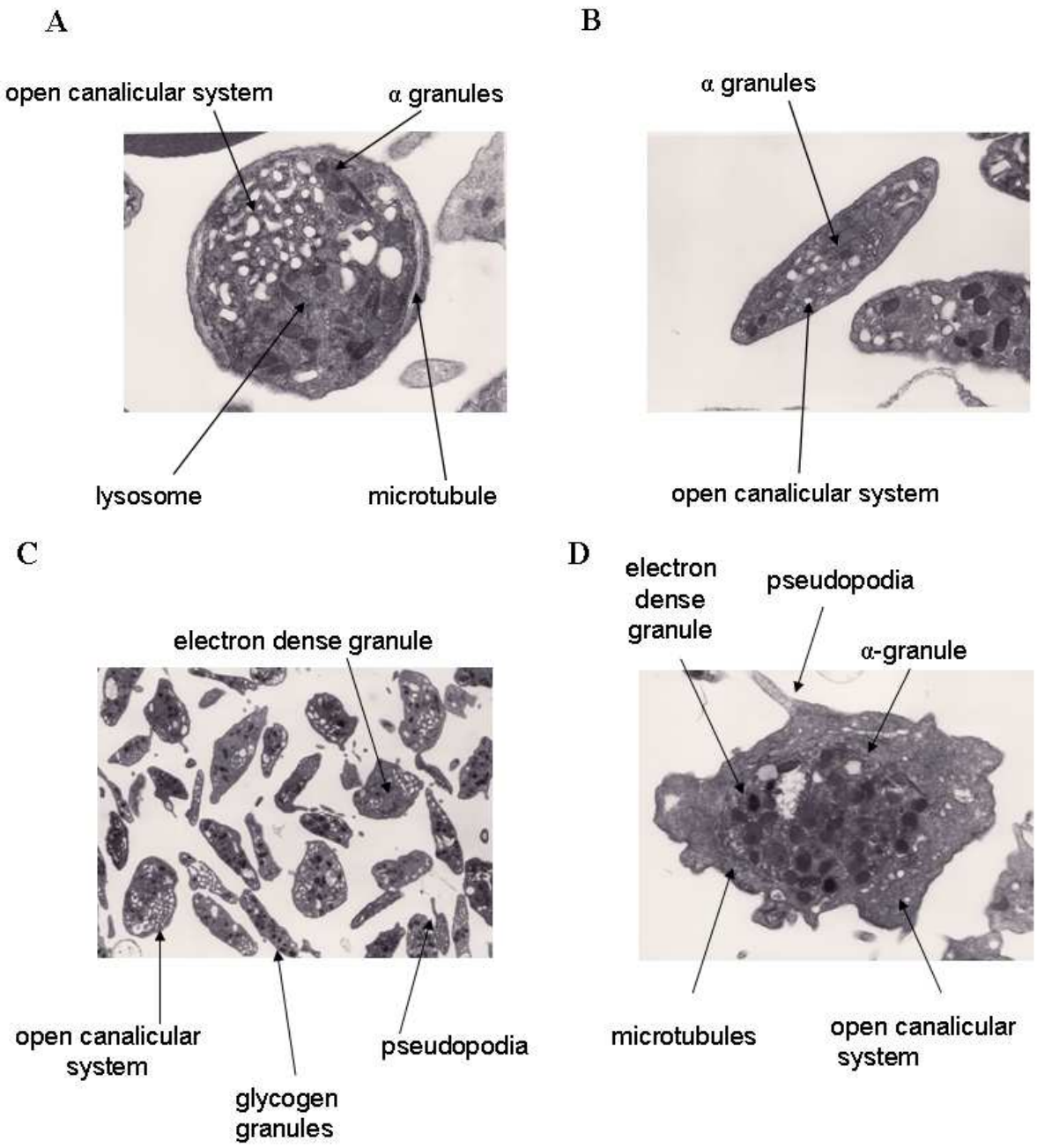

Figure 5. Changes in platelet structure upon activation. A, B, Transmission electron micrograph of platelets following 5 min incubation at 37 ^{o}C in nominally Ca^{2+}-free saline, prior to fixation. **C, D,** The effects of stimulation in the presence of 1mM extracellular calcium, followed by immediate fixation (MacKenzie, 1996).

Platelets become activated upon exposure to collagen, P-selectin or tissue factor revealed by injury to the vascular wall, production of thrombin or factors released from previously activated cells. Initial binding, or tethering, of platelets is rapidly reversible, for example when platelet GPIbα binds to endothelial P-selectin, the platelet then rolls and binds more securely to exposed collagen via GPVI (Frennete *et al*, 1995). This process activates the

platelet causing the granules to migrate to the open canalicular system to release their contents into the surrounding environment, and adhesion proteins are exposed. This stimulates the activation of other platelets in the immediate environment, that bind to the platelets already present through surface $\alpha_{IIb}\beta_3$, using fibrinogen as a bridge, and through expressed vWF which binds GPIb/IX/V (Szalai *et al*, 2006). The formation of fibrin through the extrinsic coagulation cascade (figure 3) occurs alongside platelet activation, which acts to strengthen and stabilise the forming thrombus (Furie and Furie, 2005). This process continues in an autocrine and paracrine manner, as contents released from activated platelets further stimulates the original platelets together with those around them. It has been determined that the gap between platelets ranges between 0-50 nm (Skaer *et al*, 1979), enabling the connection of platelets for example by $\alpha_{IIb}\beta_3$ receptors linked by fibrinogen. It also limits the distances factors released from activated platelets have to diffuse, for example ATP which is rapidly broken down to ADP and AMP by ecto-ATPases following release, and is able to activate the ionotropic $P2X_1$ receptor which is involved in the initiation of platelet aggregation (Toth-Zsamboki *et al*, 2003). The integrin $\alpha_{IIb}\beta_3$ is present in an inactive state on the surface of resting platelets. Upon platelet stimulation, more integrins translocate to the cell membrane, enabling the platelet to bind to both stimulated and unstimulated platelets through binding to vWF or fibrinogen (Niiya *et al*, 1987). vWF is a multimeric protein synthesised in both endothelial cells and MKs, which binds GPIbα and collagen as well as the β_3 integrin, giving it a multifaceted role in platelet activation and aggregation (Muira *et al*, 2000; Romikjn *et al*, 2001; Ruggeri, 2007). Talin, a cytoskeletal protein has also been shown to bind to the β_3 cytoplasmic domain, leading to activation of the integrin through inside-out signalling (Calderwood *et al*, 1999).

1.2.4. Storage and secretion of glutamate

1.2.4.1. Bone marrow

The MEG-01 cell line has been demonstrated to express the glutamate/ aspartate transporter, GLAST (also called excitatory amino acid transporter 1 (EAAT1)) together with the vesicular glutamate transporter, VGLUT1, suggesting that glutamate is taken up by MKs and stored (Genever *et al*, 1999; Thompson *et al*, 2010). MKs are located within the bone marrow in close proximity to osteoblasts and osteoclasts, which are responsible for maintaining the bone marrow matrix. Both osteoclasts and osteoblasts have been shown to express EAAT1 (Mason *et al*, 1997), with osteoclasts found to take up glutamate into the vesicles through the VGLUT1 transporter (Morimoto *et al*, 2006). The cells have been demonstrated to secrete the contents of these vesicles through transcytosis (Morimoto *et al*, 2006). This process is stimulated by depolarisation of the cells causing the vesicles to move across the cell and release their contents (glutamate and other bone degradation products) into the extracellular surroundings (Morimoto *et al*, 2006). Osteoblasts are also thought to express a vesicular glutamate transporter (Hinoi *et al*, 2002), and have been shown to release glutamate through a vesicular pathway, which mimics release from presynaptic glutamatergic neurones involving Rab, synaptosomal-associated protein-25 (SNAP-25) and syntaxin (Bhangu *et al*, 2001). The glutamate transporter GLT-1 (EAAT2) usually expressed on glia cells is also expressed on marrow cells, indicating that levels of glutamate in the bone marrow are tightly regulated (Mason *et al*, 1997).

1.2.4.2. Platelets

Glutamate is stored within the dense granules of platelets, which express EAAT1, 2 and 3 at both protein and mRNA levels (Zoia *et al*, 2004). EAATs are sodium-dependent transporters, and it has been suggested that activation of platelets by thrombin stimulates the translocation of EAAT2 from α-granules to the dense granules and the cell surface, enabling the influx of glutamate into the cells (Hoogland *et al*, 2005). EAAT1 is found in platelet membranes, with EAAT3 also located at the membranes as well as within the cytoplasm, suggesting that it is also able to translocate to the membranes when required (Zoia *et al*, 2004). Uptake can be affected detrimentally by changes in EAAT expression, for example in amyotrophic lateral sclerosis (ALS) where a decrease in expression of EAAT2 occurs in the brain, spinal cord and in platelets (Ferrarese *et al*, 2001). EAAT1 has been shown to decrease in expression with age, but has been demonstrated to decrease further in patients with Alzheimer's disease (AD) (Zoia *et al*, 2004). Platelets have also

been found to express the transporters, VGLUT1 and 2, with the latter only found previously on glutamatergic axon terminals (Tremolizzo *et al*, 2006). VGLUTs transport glutamate from the cytoplasm of cells into vesicles, using an H^+-ATPase-driven H^+ electrochemical gradient to drive the process (Ikemoto *et al*, 2003).

1.2.4.2.1. Role of glutamate in platelet function

Glutamate is released by platelets upon activation for example by collagen, with the vesicles and dense granules fusing with the open canalicular system and plasma membrane (Tremolizzo *et al*, 2006). This increases the level of extracellular glutamate which can be taken up by neighbouring platelets. Glutamate levels in the blood can increase rapidly, for example during an ischemic event, and removal of glutamate from the area is important as part of limiting the damage caused, for example by platelets as well as neurones and glia (Káradóttir *et al*, 2005). Moreover, the increased circulating glutamate associated with ischemic events such as stroke may be associated with the increased pro-thrombotic state.

There is conflicting evidence in the literature for the role of glutamate in platelet activation. Earlier studies report an anti-aggregatory action of the NMDA-activated glutamate receptor leading to an inhibition of thromboxane A_2 (TbA_2) synthesis from exogenous arachidonic acid (AA), but did not alter TbA_2-mediated platelet aggregation (Franconi *et al*, 1996). However, despite the reported anti-aggregatory action, extracellular NMDA was demonstrated to elicit an increase in intracellular Ca^{2+} (Franconi et al, 1998). Platelet sensitivity to glutamate has been demonstrated to increase in both schizophrenia and depression, with increases in intracellular calcium higher in platelets from patients with these disorders than in control patients (Berk *et al*, 2000). Overall this demonstrates that the role of glutamate in platelet activation has only started to be understood and requires further investigation.

1.3. Glutamate receptors

Glutamate is a non-essential amino acid which was originally known for its role in the Krebs and urea cycles in addition to the production of γ-butyric acid (GABA) (Watkins and Jane, 2006). It has more recently been demonstrated to play a major signalling role in both the central nervous system (CNS) and in non-excitable cells (table 6).

Glutamate was identified as having an excitatory role in 1954 by Hayashi, where L-glutamate triggered convulsions following injection into the brain, leading to its proposal as a central synaptic transmitter. Further studies by Curtis *et al* (1960 and 1961) demonstrated that the application of glutamate to neurones elicited a rapid response that quickly returned to baseline. In addition, aspartate had been demonstrated to elicit responses from cells which also responded to glutamate, and subsequent work determined that glutamate receptors could be divided into those receptors that responded to NMDA, an aspartate analogue, and those which did not (Watkins and Evans, 1981). The latter group responded to both quisqualate and kainate; however they could be divided into those which were activated preferentially by quisqualate (later refined as those which responded to the more specific agonist (S)-α-amino-3-hydroxy-5-methylisoxazole-4-propionic acid (AMPA)) and those preferentially activated by kainate. The discovery of the glutamate-like compounds L-(+)-2-amino-4-phosphonobutyric acid (L-AP4) and (9)-1-aminocyclopentane-trans-1,3-dicarboxylic acid (trans-ACPD) that induced excitatory responses which were not inhibited by known glutamate antagonists led to the cloning of the first metabotropic receptor (mGluR) subunit, mGluR1 (Masu *et al*, 1991; Houamed *et al*, 1991). This in turn led to the discovery of other members of the mGluR family, found to be G-protein coupled receptors, demonstrating that glutamate signalling is not limited to only ionotropic receptors (Tanabe *et al*, 1992). The mGluR family has been divided into 2 based on their coupled G-protein, either $G_{\alpha i}$ (group I) or $G_{\alpha q}$. Those acting via $G_{\alpha q}$ are further subdivided into groups II and III, depending on the effects of L-AP4 (group III) or trans-ACPD (group II) (Hollman and Heinemann, 1994; Hall *et al*, 1979; Nicoletti *et al*, 1986) (figure 6). At the time of commencing my studies, there was no evidence in the literature indicating the presence of functional AMPA or kainate receptors (AMPARs or KARs) in human MKs or platelets. My thesis therefore investigates the expression of the NMDA-activated glutamate receptor in human MKs and platelets.

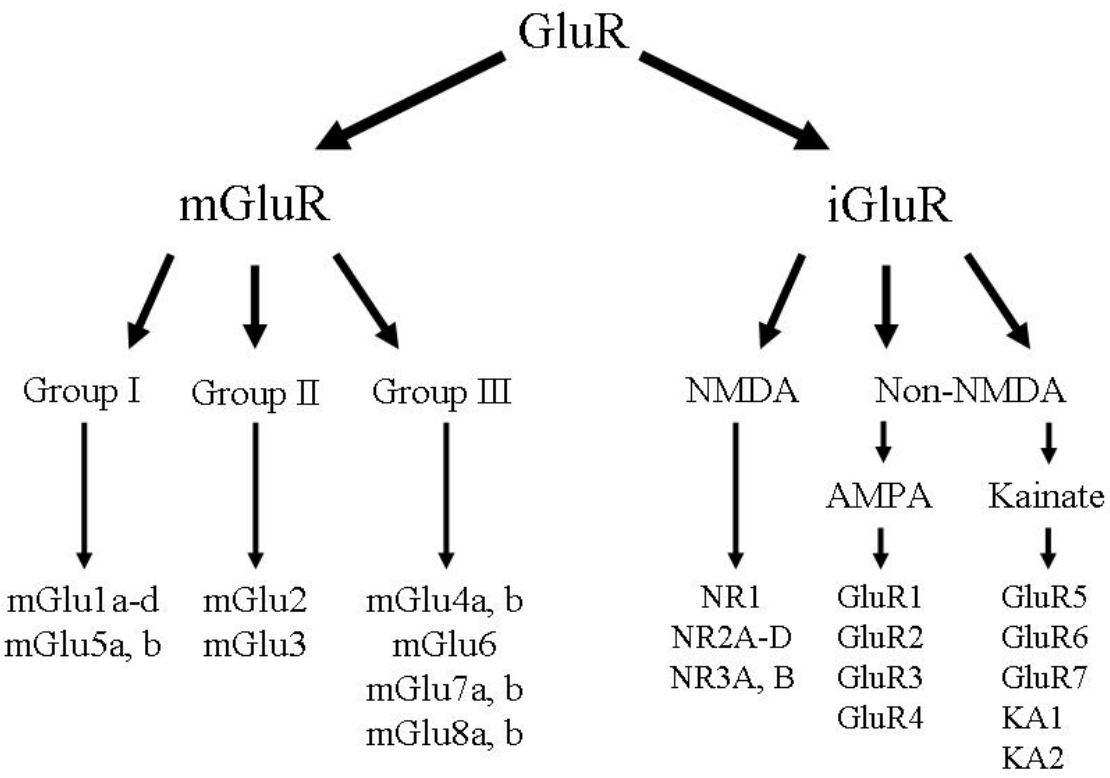

Figure 6. Classification of glutamate receptors. GluR, glutamate receptors; mGluR, metabotrophic glutamate receptors; iGluR, ionotropic glutamate receptors

1.3.1. NMDA receptor, an ionotropic glutamate receptor

The first NMDAR subunit was identified in 1991 by Moryoshi *et al*, and denoted NR1. The NR2 subunit was identified by several groups in the early 1990s, with 4 different subtypes cloned, NR2A-D (Meguro *et al*, 1992; Monyer *et al*, 1992; Kutsuwark *et al*, 1992; Ishii *et al*, 1993). A third subunit, NR3A was discovered in 1995 (Ciabarra *et al*; Sucher *et al*), with a second subtype, NR3B identified a few years later (Chatterton *et al*, 2002). No subtypes of NR1 have been determined; however 8 splice variants are known (McBain and Mayer, 1994). Each subunit varies in amino acid number and molecular mass, detailed in table 4. Sequence homology varies between NR1 and the 4 NR2 subtypes from 19-22 %, with 36-53 % homology between the NR2 subtypes. The sequence homology between the 2 NR3 subtypes is 47 % and they have 17-21 % homology with the NR1 and NR2 subunits (Chatterton *et al*, 2002). The main differences in sequences have been found in the M2 re-entrant loop and the C-terminus, particularly between the NR1 and NR2 subunits (figure 7).

SUBUNIT	MOLECULAR MASS (kDa)	AMINO ACID NUMBER
NR1	105.5	938
NR2A	178.0	1464
NR2B	165.9	1482
NR2C	136.5	1250
NR2D	147.5	1340
NR3A	124.5	1115
NR3B	109.0	1002

Table 4. Comparing the molecular mass and amino acid numbers of the NMDAR subunits (Moriyoshi *et al*, 1991; Ishii *et* al, 1993; Sucher *et al*, 1995; Ciabarra *et al*, 1995; Chatterton *et al*, 2002).

The NMDAR is tetrameric in composition, containing 2 NR1 subunits together in combination with NR2 and NR3 subunits (Schüler *et al*, 2008). It has been shown that NR1 subunits are required for the formation of stable, functioning receptors and that translocation from the endoplasmic reticulum (ER) to the cell membrane requires the formation of dimers of subunits consisting of 1 NR1 subunit and 1 other, either an NR2 or NR3 subunit (Pérez-Otano *et al*, 2001). While it is possible for 2 NR1 subunits to form a dimer and translocate to the cell membrane, they are unable to form functional receptors (Schüler *et al*, 2008). Dimers of 2NR2, NR2/NR3 or 2NR3 subunits are retained within the ER and are not released to the cell membrane (Pérez-Otano *et al* 2001). Upon reaching the cell membrane, dimers converge forming functional tetrameric receptors from dimers of dimers (Schüler *et al*, 2008; Schorge and Colquhoun, 2003). It is therefore possible for NMDARs to contain 2 different NR2 subunits e.g. NR1/ NR2A/ NR2D, 2 different NR3 subunits e.g. NR1/ NR3A/ NR3B, or even a mix of 3 different subunits (tri-heteromeric), for example NR1/ NR2D/ NR3B (Pérez-Otano *et al* 2001).

The structure of the NMDAR subunits has been determined through comparisons with potassium channels using a range of techniques including hydrophobicity plots and crystallisation studies, demonstrating that they consist of 3 transmembrane domains (M1, M3 and M4) with a re-entrant loop (M2), which forms the pore of the receptor (figure 7) (Wood *et al*, 1995). In the open state, the pore of the receptor is blocked by a magnesium ion (Mg^{2+}), which is released upon depolarisation of the membrane, allowing the

movement of Ca^{2+} and sodium (Na^{+}) ions into, and potassium (K^{+}) ions out of, the cell. The strength of the bonds retaining the Mg^{2+} within the pore is dependent on the subunits present in the receptor, for example if NR2A is present, a greater stimulus is required to remove the magnesium block than if NR2D is present (table 5) (Qian and Johnson, 2006; Clarke and Johnson, 2006). NR1/NR3 receptors have been shown to be less sensitive to block by magnesium ions than NR1/NR2 receptors (Chatterton *et al*, 2002).

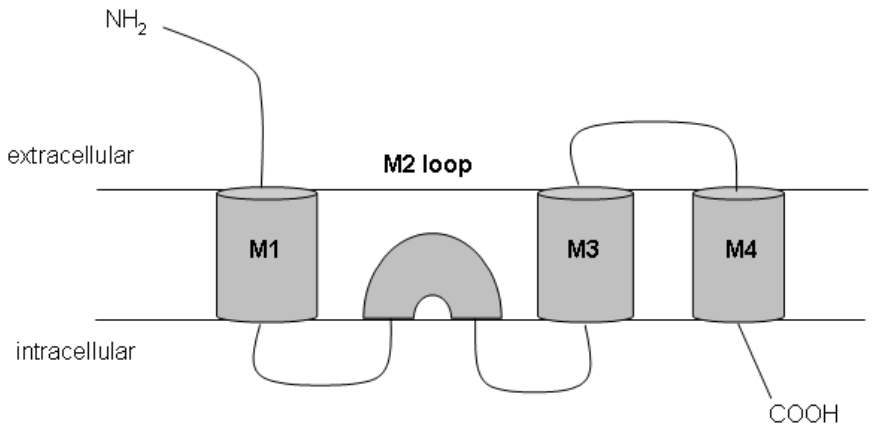

Figure 7. Structure of an NMDA receptor subunit. Illustrating the 3 transmembrane regions (M1, M3 and M4), and the re-entrant loop (M2). The intracellular N- (NH_2) and extracellular C- (COOH) termini are also shown.

Extracellular glutamate and NMDA are the main agonists of classical NR1/ NR2 NMDARs and bind to the NR2 subunit. Full activation requires the binding of a co-agonist to the NR1 subunit, either glycine or D-serine (Matsui *et al*, 1995) (figure 8). In comparison, the NR1/ NR3 combination requires only the binding of glycine to both subunits for activation, forming an excitatory glycine receptor (Chatterton *et al*, 2002). A further difference between the combinations is that D-serine acts as an inhibitor rather than a co-agonist for NR1/ NR3 receptors (Chatterton *et al*, 2002) (figure 8).

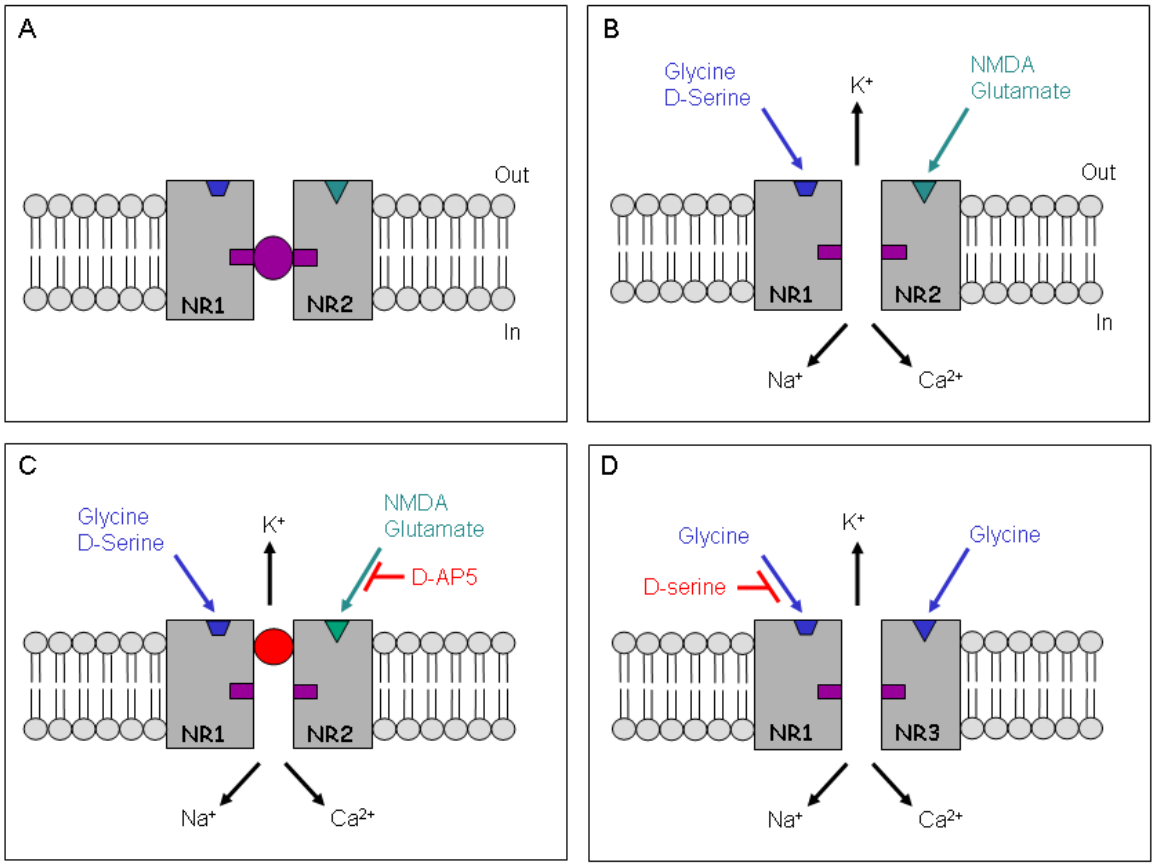

Figure 8. Pharmacology of the NMDA receptor. A, the classic NMDAR subunit conformation, NR1/NR2, the pore of which is blocked by a magnesium ion (purple circle). The receptor is activated by binding of either NMDA or glutamate together with either of the co-agonists, glycine or D-serine (**B**), following removal of the magnesium (Mg^{2+}) block through desensitisation of the membrane. This allows movement of the Ca^{2+} and Na^{+} into, and K^{+} out of, the cell. **C**, activation can be inhibited through the application of either MK-801, an open channel blocker (red circle), or D-AP5, a competitive inhibitor which binds to the glutamate/ NMDA binding site. **D**, a third NMDA receptor subunit is known, NR3. In combination with NR1 an excitatory glycine receptor is formed, which does not require glutamate for activation. Here, D-serine acts as an inhibitor, and the pore is not blocked by Mg^{2+}.

NMDAR SUBUNIT	AGONIST	ANTAGONIST	ION PERMEABILITY	Mg^{2+} BLOCK
NR1/NR2	Glutamate with glycine or D-serine	D-AP5 MK-801	Higher permeability to Ca^{2+} than Na^{+} in K^{+} out	Block varies with NR2 subunit: EC_{50}- NR1/NR2A or NR2B 1-10 μM - NR1/NR2C or NR2D ~130μM
NR1/ NR3	Glycine	D-serine MK-801 5,7- (DCKA)	Higher permeability to Na^{+} than Ca^{2+} K^{+} out	Low sensitivity to magnesium block

Table 5. Comparing agonists and antagonists for different NMDA receptor subunit combinations. 5,7-dichlorokynurenic acid (5,7-DCKA)- glycine receptor antagonist; D-AP5 (McBain and Mayer, 1994; Dingledine *et al*, 1999; Chatterton *et al*, 2002)

NMDARs form complexes with other proteins located at the plasma membrane of cells, and activation of the NMDAR leads to the stimulation of the complexed proteins as well as an influx of Ca^{2+} causing the formation of a localised region of high Ca^{2+} (Ca^{2+} microdomain) close to the intracellular face of the receptor (Hardingham *et al*, 2001). One such protein is RasGRF1, which is stimulated by the increase in $[Ca^{2+}]_i$ and activates Ras, leading to phosphorylation and activation of ERK, part of the the MAPK pathway (Bading and Greenberg, 1991). This has in turn been demonstrated to play a role in signalling to downstream transcription factors leading to modulation of gene transcription and activation e.g. CREB (Hardingham *et al*, 2001; Klages *et al*, 1999).

NMDAR activity can be modulated through post-translational modifications such as the *S*-nitrosylation of cysteine (cys) residues within the extracellular regions of the NR1 and NR2A subunit proteins by nitric oxide (NO). This inhibits NMDARs and desensitises those already active (Choi *et al*, 2000). *S*-nitrosylation of NMDARs has been demonstrated to occur within the brain and is hypothesised to limit their activation during excitotoxic events such as an ischemic attack where localised concentrations of glutamate are greatly

raised, leading to increased receptor activity (Choi *et al*, 2002, Jaffrey *et al*, 2001). This suggests a potential regulatory role in platelet NMDAR activation for NO which is constitutively released by endothelial NO synthase (eNOS) into the blood stream (Dimmler *et al*, 1999; Fulton *et al*, 1999).

1.3.2. Receptor localisation

NMDARs have been well characterised in the CNS where they have been localised both pre- and postsynaptically in neurones, glia and astrocytes. Several studies have demonstrated that NMDARs are implicated in the generation of long-term potential (LTP), an important facet of the learning and memory processes (Do *et al*, 2002), and NMDARs have also been shown to be expressed in peripheral, non-neuronal locations (table 6). NMDARs are widely expressed in bone cells particularly in osteoclasts and osteoblasts (Patton *et al*, 1998). These are known to release glutamate (section 1.2.4.1.) and this release has been demonstrated to activate NMDAR in the neighbouring cells. However, the function of NMDARs in these cells appears to be limited and is not well understood (Gu and Publicover, 2000). Other locations include skin, heart, lung, pancreas and the urogenital tract (table 6). My thesis focuses on the expression of NMDARs in human platelets and MKs.

	CELL TYPE	FUNCTION
CNS	Neurones Glia Astrocytes	Synaptic signalling, mediate ischemic injury (Dingledine *et al*, 1999) Synaptic signalling, mediate ischemic injury (Vekhratsky and Kirchhoff, 2007) Synaptic signalling, mediate ischemic injury (Schipke *et al*, 2001)
Bone	Osteoblasts Osteoclasts Megakaryocytes	Bone resorption (Patton *et al*, 1998*) Bone formation (Patton *et al*, 1998*) Platelet formation (Genever *et al*, 1999a)
Blood	Platelets	Anti-platelet aggregation (Franconi *et al*, 1996*, 1998*)
Skin	Keratinocytes	Production of keratin, skin development (Genever e*t al*, 1999b*)
Pancreas	B-cells and islets of Langerhans	Regulate secretion of insulin (Molńar *et al*, 1995)
Heart	Atrial and ventricular cells	Modulate cardiac function (Leung *et al*, 2002; Skerry and Genever, 2001)
Lung	Lung	Induce excitotoxicity (Dickman *et al*, 2004)
Urogenital tract	Renal medulla and cortex Bladder and prostate	Cytoprotective (Skerry and Genever, 2001; Leung *et al*, 2001) Reproduction (in males) (Gonazlez-Cadavid *et al*, 2000*)

Table 6. Location of NMDA receptors in different tissues and cell types with their function.

*= studies in which endogenous receptors were studied rather than recombinant receptors.

1.3.2.1. Ionotropic glutamate receptor expression in megakaryocytes and platelets

1.3.2.1.1. NMDA receptor expression in megakaryocytes

NMDARs have previously been identified in $CD34^+$-derived MKs from umbilical cord blood and MEG-01 cells (Genever *et al,* 1999; Hitchcock *et al*, 2003). In the initial study by Genever *et al* (1999), it was demonstrated that mRNA for the NR1 and NR2D subunits are expressed in human MEG-01 cells and rat bone marrow derived MKs. The NR1 protein was expressed in both untreated MEG-01 cells and those treated with phorbol 12-myristate 13-acetate (PMA) for 3 d. In comparison, mRNA was detected for NR1 and all NR2 subtypes in rat brain samples. Immunolocalisation studies detected the NR1 subunit protein in human MKs and MEG-01 cells as well as in human platelets. NMDARs were involved in PMA-mediated MEG-01 differentiation, where treatment with PMA increased the expression of CD41 attenuated by treatment with an NMDAR antagonist MK-801. This effect was also observed with the expression of CD61. The corresponding increase in MEG-01 cell size with PMA was also inhibited by the presence of MK-801. In addition, the adhesion of MEG-01 cells was investigated as another marker of differentiation. Adhesion was shown to increase with the presence of PMA, and then decrease with increasing concentrations of either MK-801 or D-AP5, another NMDA receptor specific inhibitor. The addition of NMDAR-specific inhibitors was demonstrated not to affect either the cell number or viability over the experiment. The adhesion experiments were repeated using the CMK cell line to confirm that the adhesion is not just specific to the MEG-01 cell line. The CMK cell line was derived from a Down's syndrome patient suffering from acute megakaryoblastic leukaemia, and demonstrated to be an accurate megakaryocytic model (Sato *et al*, 1989). Therefore the effects of the inhibitors are indicative that NMDA receptors are expressed by MEG-01 cells and that they have a functional role.

A second study extended this work using MKs derived from umbilical cord blood $CD34^+$ cells (Hitchcock *et al*, 2003). Here expression of NR2A and NR2D mRNA was shown. Proplatelet formation and cell size was investigated, and both shown to be reduced by the presence of MK-801; the MK-801 treated cells were found to be approximately half the size of the untreated cells. No difference was determined in the number or viability of the cells between treated and untreated cells. TPO-mediated increases in CD41a, CD42a and CD61 expression were reduced upon addition of MK-801. The ultrastructure of native MKs was also investigated following culture with TPO present, and either with and

without MK-801. This revealed that changes indicative of differentiation such as increasing cell size, formation of a multilobed nucleus and dilated demarcation membrane were lacking in MK-801 treated cells. This study indicates that NMDARs are implicated in differentiation of MKs derived from umbilical cord blood. My thesis will extend these studies to investigate the protein expression of the NR2 subunits and the contribution of NMDAR to the adhesion of MEG-01 cells to different substrates.

1.3.2.1.2. NMDAR expression in platelets

The first evidence to suggest the expression of NMDARs in platelets came from studies demonstrating binding of phencyclidine to platelet membranes (Jamieson *et al*, 1992). Phencyclidine (an NMDAR antagonist) is reported to bind with high affinity to NMDARs, thus suggesting the expression of this receptor in platelets; it has subsequently been demonstrated to also bind dopamine D_2 receptors and serotonin $5HT_{2A}$ receptors, both of which are known to be expressed at the platelet surface membranes (Dean and Copolov, 1989; Kapur and Seeman, 2002). Further binding studies demonstrated that [^{3}H]glutamate and [^{3}H]MK801 bound to platelet membranes with affinities comparable to neuronal membranes (Franconi *et al*, 1996). Addition of NMDA only partially displaced [^{3}H]glutamate binding. However [^{3}H]glutamate binding was not increased by MK801 as would be predicted from studies in neurones. The expression of the NMDAR NR1 subunit has been demonstrated in human platelets by immunohistochemistry (Genever et al, 1999). As previously mentioned in section 1.2.4.2.1, NMDAR functional expression has been demonstrated in assays of intracellular calcium and implicated in anti-aggregatory responses (Franconi *et al*, 1996 and 1998). To date the functional expression of NMDARs in human platelets is poorly understood. My thesis therefore investigates the expression of NMDAR subunits, pharmacological properties and their role in ATP secretion.

1.4. Current model of glutamate signalling in megakaryocyte and platelet function

Glutamate has been shown to play a range of roles in MK and platelet function, through glutamate uptake via EAAT1-3 or through the binding of glutamate to NMDARs. The figure below illustrates the different roles of glutamate receptors in both MKs and platelets using the evidence gained from previous studies.

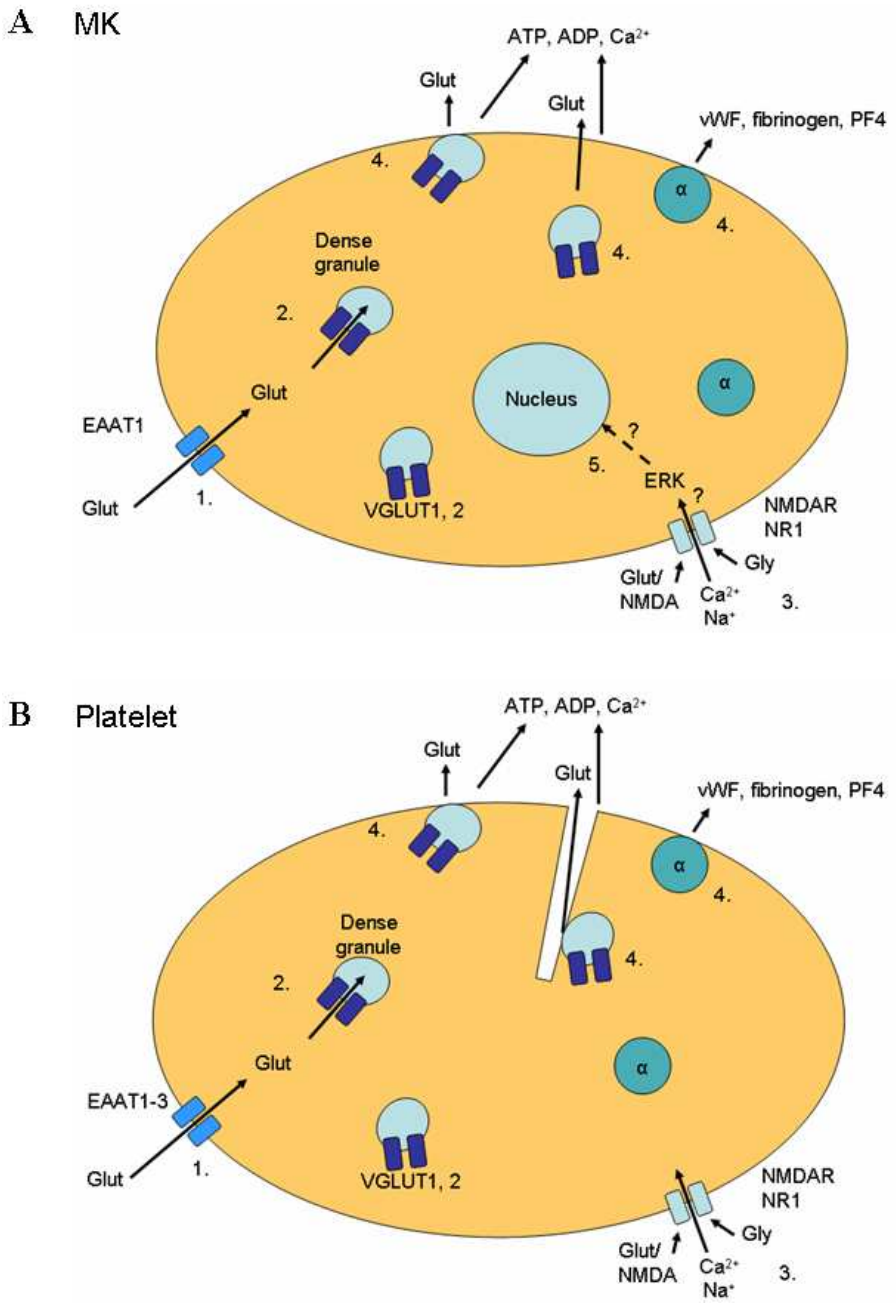

Figure 9. Demonstrating the different glutamate signalling pathways in MKs and platelets. **1.** Glutamate is taken up by both platelets (**B)** and MKs (**A**) through EAATs (excitatory amino acid transporters) and stored in dense granules via vesicular glutamate transporters (VGLUT) (**2.**). Activation of the cells, potentially by NMDARs (**3.**) triggers the release of the granule contents (**4.**) including glutamate into the extracellular space, which is able to further activate the NMDARs. This leads to increases in $[Na^+]_i$ and particularly $[Ca^{2+}]_i$ leading to the formation of Ca^{2+} microdomains close to the intracellular face of the NMDAR which have been demonstrated to stimulate ERK activation via activation of RasGRF1 in MKs (**5.**), and potentially leading to modulation of gene transcription in the nucleus e.g. CREB phosphorylation (Hardingham *et al*, 2001; Bading and Greenberg, 1991).

1.5. Aims of this study

The hypothesis of this study is that functional NMDARs are expressed in the human megakaryocytic cell line, MEG-01, and primary human platelets, based on previous evidence in the literature which has reported the expression of the NMDA NR1 subunit protein and suggested a role for NMDARs in both MK and platelet function (Franconi *et al*, 1996 and 1998; Genever *et al*, 1999; Hitchcock *et al*, 2003). There was no evidence at the start of my study that functional AMPAR and KARs were expressed in either human MKs (neither native nor cell line) or human platelets, therefore the role of these in MK differentiation and platelet were not investigated.

The overall aim of this study is therefore to determine the expression and role of NMDARs in the human megakaryocytic cell line, MEG-01, and primary human platelets.

The individual aims are to:

- determine which NMDAR subunits are expressed by MEG-01 cells and platelets. Evidence in the literature has demonstrated the expression of the NR1 subunit protein and treatment of native MKs with MK-801 inhibited MK differentiation. NR1 subunits are unable to form functional receptors alone, therefore other NMDAR subunits are required to form a functional receptor (NR2A-D, NR3A, B), which have yet to be identified.
- evaluate the functional expression of NMDARs in human platelets and MKs. The expression of NMDR subunits does not necessarily determine that functional receptors are formed, therefore the responses induced by classic agonists can determine whether the receptors present are comparable to the properties of the same receptors described in the literature.
- assess the pharmacological properties of platelet NMDARs. The sensitivity of NMDARs expressed in human platelets requires further determination from that ascertained in the published literature, such as dose responses to glutamate or NMDA and the role of inhibitors such as MK-801 and D-AP5
- establish the functional role of platelet and MK NMDARs. Determining the expression and pharmacology of the receptors can help in ascertaining their role in both MK differentiation and platelet production, as well as in platelet activation and aggregation.

CHAPTER 2

METHODS

2.1. Materials

Table 7. General Reagents

REAGENT	SUPPLIER
Acetic acid (glacial)	Fisher Scientific (Loughborough, UK)
Acetone	Sigma Aldrich (Dorset, UK)
Acetyl salicylic acid (ASA; aspirin)	Sigma Aldrich (Dorset UK)
Acrylamide mix (30 % protogel)	Fisher Scientific (Loughborough, UK)
Ammonium persulphate	Fisher Scientific (Loughborough, UK)
Apyrase VII	Sigma Aldrich (Dorset, UK)
Bradford proteins assay concentrate	Bio-Rad (Hemel Hemstead, UK)
Broad range biotinylated standards	Bio-Rad (Hemel Hemstead, UK)
Calcium chloride ($CaCl_2$)	Sigma Aldrich (Dorset, UK)
Chloroform	Fisher Scientific (Loughborough, UK)
Coomassie brilliant blue R-250	Bio-Rad (Hemel Hemstead, UK)
Crystal violet	Sigma Aldrich (Dorset, UK)
L-cysteine	Sigma Aldrich (Dorset, UK)
D-(+)-Glucose	Sigma Aldrich (Dorset, UK)
D-(2*R*)-amino-5-phosphonovaleric acid (D-AP5)	Sigma Aldrich (Dorset, UK)
Dimethyl sulfoxide	Sigma Aldrich (Dorset, UK)
Dithiothreitol (DTT)	Sigma Aldrich (Dorset, UK)
Disodium ethylenediamine tetraacetate (Na_2EDTA)	Sigma Aldrich (Dorset, UK)
D-serine	Sigma Aldrich (Dorset, UK)
Ethidium bromide	Sigma Aldrich (Dorset, UK)
Ethylene diaminetetraacetic acid (EDTA)	Sigma Aldrich (Dorset, UK)
Ethylene glycol tetraacetic acid (EGTA)	Sigma Aldrich (Dorset, UK)
Enhanced chemiluminescent (ELC™) Western Blotting detection reagents	GE Healthcare (Amersham, UK)
Ethanol	Fisher Scientific (Loughborough, UK)

Fibrinogen	Sigma Aldrich (Dorset, UK)
L-glutamate	Sigma Aldrich (Dorset, UK)
Glycine (Western blotting buffers)	Fisher Scientific (Loughborough, UK)
Glycine (≥ 99 %; agonist)	Sigma Aldrich (Dorset, UK)
4-(2-hydroxyethyl)-1-piperazineethanesulfonic acid *(*HEPES)	Sigma Aldrich (Dorset, UK)
Hydrochloric acid (HCl)	Fisher Scientific (Loughborough, UK)
Ionomycin	Sigma Aldrich (Dorset, UK)
Isopropanol	Fisher Scientific (Loughborough, UK)
Magnesium chloride ($MgCl_2$)	Sigma Aldrich (Dorset, UK)
Methanol	Fisher Scientific (Loughborough, UK)
(+)-Dizocilpine hydrogen maleate (MK-801)	Sigma Aldrich (Dorset, UK)
Nitrocellulose membrane (0.2 μm)	Bio-Rad (Hemel Hemstead, UK)
N-methyl-D-aspartate (NMDA)	Sigma Aldrich (Dorset, UK)
Nonidet P-40 (NP-40)	Pierce (Cramlington, UK)
DEA NONOate	Sigma Aldrich (Dorset, UK)
Phosphate buffered saline (PBS)	Sigma Aldrich (Dorset, UK)
Pluronic acid F-127	Sigma Aldrich (Dorset, UK)
Polyvinylidene fluoride membrane (PVDF) (Hybond; 0.2 μm)	GE Healthcare (Amersham, UK)
Potassium chloride (KCl)	Sigma Aldrich (Dorset, UK)
Precision plus protein standards (kaleidoscope)	Bio-Rad (Hemel Hemstead, UK)
Protease inhibitor cocktail (General use)	Sigma Aldrich (Dorset, UK)
Protein inhibitor cocktail (cell and tissue extract; PIC)	Sigma Aldrich (Dorset, UK)
RNaseA	Invitrogen (Paisley, UK)
Sample buffer 2x	Sigma Aldrich (Dorset, UK)
Skimmed milk powder	Sigma Aldrich (Dorset, UK)
Sodium chloride (NaCl)	Sigma Aldrich (Dorset, UK)
Sodium dodecyl sulphate (SDS)	Fisher Scientific (Loughborough, UK)

Sodium fluoride (NaF)	Sigma Aldrich (Dorset, UK)
Sodium hydroxide (NaOH)	Sigma Aldrich (Dorset, UK)
Sodium nitrite ($NaNO_2$)	Sigma Aldrich (Dorset , UK)
Tetramethylethylenediamine (TEMED)	Sigma Aldrich (Dorset, UK)
Thrombin (bovine)	Sigma Aldrich (Dorset, UK)
Tris (hydroxymethyl)-methylamine	Fisher Scientific (Loughborough, UK)
Tris base (Trizma)	Sigma Aldrich (Dorset, UK)
Trisodium citrate	Fisher Scientific (Loughborough, UK)
Triton X-100	Sigma Aldrich (Dorset, UK)
Trizol Reagent	Invitrogen (Paisley, UK)
Tween-20	Sigma Aldrich (Dorset, UK)

Table 8. Cell culture

REAGENT	**SUPPLIER**
Inactivated foetal bovine serum (FBS)	Invitrogen (Paisley, UK)
L-glutamine	Invitrogen (Paisley, UK)
Penicillin/ streptomycin	Invitrogen (Paisley, UK)
Phorbol 12-myristate 13-acetate (PMA)	Sigma Aldrich (Dorset, UK)
RPMI-1640	Sigma Aldrich (Dorset, UK)
Thrombopoietin (recombinant human; TPO)	Peprotech (London, UK)
Trypsin/ EDTA	Invitrogen (Paisley, UK)

Table 9. Polymerase chain reaction reagents

REAGENT	SUPPLIER
Total RNA, human cerebellum	Stratagene (Stockport, UK)
DNase	Ambion (Warrington, UK)
10 x DNase buffer	Ambion (Warrington, UK)
DNase stop solution	Qiagen (Crawley, UK)
RNAsin PLUS	Promega UK (Southampton, UK)
Oligo dT	Qiagen (Crawley, UK)
5 x RT buffer	Invitrogen (Paisley, UK)
Superscript II	Invitrogen (Paisley, UK)
dATP	Qiagen (Crawley, UK)
dCTP	Qiagen (Crawley, UK)
dGTP	Qiagen (Crawley, UK)
dTTP	Qiagen (Crawley, UK)
5 x Green Flexi buffer	Promega UK (Southampton, UK)
Dithiothreitol (DTT)	Promega UK (Southampton, UK)
Magnesium chloride ($MgCl_2$)	Promega UK (Southampton, UK)
Go-Taq	Promega UK (Southampton, UK)

Table 10. Antibodies

ANTIBODY	SUPPLIER
Polyclonal rabbit anti-β-actin	Sigma Aldrich (Dorset, UK)
Monoclonal mouse anti-NMDA NR1	BD Bioscience (Oxford, UK)
Polyclonal rabbit anti-NR2A	R&D Systems (Oxford, UK)
Polyclonal goat anti-NR2D	Santa Cruz Biotechnology (Wembley, UK)
Monoclonal mouse anti-glutamate NMDA receptor NR3A/B	Cambridge Bioscience (Cambridge, UK)
Neutravidin-HRP	Pierce (Cramlington, UK)
Polyclonal Rabbit Anti-Mouse IgG/HRP	DakoCytomation (Ely, UK)
Polyclonal Swine Anti-Rabbit IgG/HRP	DakoCytomation (Ely, UK)
Polyclonal Rabbit Anti-Goat IgG/HRP	DakoCytomation (Ely, UK)

Table 11. Fluorescent indicators

REAGENT	SUPPLIER
Adenosine 5′-triphosphate (ATP) assay mix	Sigma Aldrich (Dorset, UK)
Fluo-4 AM	Invitrogen (Paisley, UK)

2.2. Solutions

Table 12. Nominally (Ca^{2+})-free salt solution (saline)

REAGENT	CONCENTRATION (mM)
NaCl	145
HEPES	10
Glucose	10
KCl	5
$MgCl_2$	1

Adjust final solution to pH 7.3 with 0.1 M NaOH.

Table 13. Tris-acetate-EDTA (TAE) buffer

REAGENT	CONCENTRATION (mM)
Tris base (Trizma)	40
Na_2EDTA	1

Adjust pH to 7.6 with glacial acetic acid

2.3. Cell isolation and cell culture

2.3.1. Platelet preparation

Table 14. Acid-citrate-dextrose (ACD)

REAGENT	CONCENTRATION (mM)
Glucose	111
Trisodium citrate	85
Citric acid	78

Human platelets were isolated as previously described by MacKenzie *et al*, 1996. Venous blood was taken with informed consent from healthy volunteers who had not taken any medicine, particularly aspirin, its derivatives or other anti-clotting agents, for 2 weeks prior to donation. The pool of donors used consisted of 46 people, of whom 31 were male (24 aged between 18 and 40 years, and 7, 40 years and over), and 15 female (10 aged between 18 and 40 years, and 5 aged 40 and over) with 42 white European and the remaining 4 of other extraction. The blood was taken by the department phlebotomist, Mrs Jo Carter, in the departmental phlebotomy room. The isolated blood was immediately mixed with an anticoagulant (acid-citrate-dextrose; ACD; table 14) in the ratio 8.5 ml blood to 1.5 ml ACD. Platelet rich plasma (PRP) was obtained by centrifugation of whole blood for 5 min at 750 *x*g in a Beckman CS-15R centrifuge with S4180 rotor, and removing the upper (PRP) layer. PRP was maintained at 37 ^{o}C, and used within 6 h following isolation from whole blood and within 2 h of removal from plasma. Aspirin (100 μM) and 0.32 U ml^{-1} apyrase VII were added to the PRP immediately after isolation to minimise platelet activation by spontaneously released thromboxane or adenosine nucleotides respectively. Apyrase and aspirin were not added when platelets were required for Western blotting samples as they were lysed immediately after isolation from PRP (see section 2.4.2).

2.3.2. Culture of MEG-01 cells

Table 15. Complete culture medium

REAGENT	CONCENTRATION
RPMI-1640	
Inactivated FBS	10 %
L-glutamine	2 mM
Penicillin	100 U ml^{-1}
Streptomycin	100 μg ml^{-1}

The human megakaryoblastic cell line MEG-01 (American Type Culture Collection (ATCC), Middlesex, UK) was maintained in complete culture media (table 15) at 37 ^{o}C in a humidified atmosphere of 5 % CO_2 and 95 % air. Undifferentiated cells were both loosely adherent and in suspension (Ogura, M. *et al,* 1985). Both cell populations were collected by pipetting without trypsin/ EDTA. The cells were centrifuged at 240 *x*g for 4 min in a Beckman CS-15R centrifuge with S4180 rotor with the resulting suspension of cells resuspended and maintained in fresh complete culture medium at a cell density of 1 x 10^5 cells ml^{-1} twice a week. Cells were maintained in culture for 5 weeks, after which fresh cells were thawed.

2.3.2.1. MEG-01 differentiation

Two different methods were used to differentiate MEG-01 cells. In the first (method 1), MEG-01 cells were counted and resuspended in complete culture media at 1 x 10^5 cells ml^{-1}, then treated acutely (2 h) with 10 nM PMA. Cells were centrifuged at 240 *x*g for 4 min, resuspended at the same density in complete culture medium, and cultured for 3 d as described in section 2.3.2. Alternatively, method 2, cells were resuspended at 2.4 x 10^5 cells ml^{-1} and treated chronically in complete medium with 10 nM PMA for 3 d. The cells were maintained at 37 ^{o}C as described in section 2.3.2.

2.3.2.1.1. Cell morphology studies

For analysis of cell morphology studies, bright field images were taken of the cells after 3 d in culture using an Olympus Camedia digital camera (C-4040ZOOM) connected to an Olympus IX51 microscope. The area of the cells was measured using ImageJ software 1.41o (NIH, USA), and the data analysed using GraphPad Prism version 4 (section 2.10).

2.3.2.1.2. Cell number studies

MEG-01 cells were transferred from their culture flasks/ dishes into fresh tubes either by pipetting, or, when culturing on fibrinogen, adding enough 0.5 % trypsin/ EDTA to cover the cells and warming at 37 ^{o}C for 2-3 min before pipetting to ensure that all the cells were removed from the base of the container. A sample was then taken from each tube, counted 5 times to give an average number of cells and the total number determined in each tube of cells. The results were collated and analysed using GraphPad Prism version (section 2.10).

2.3.3. Freezing cells for storage

Table 16. Freezing medium

REAGENT	VOLUME (%)
RPMI complete media	80
FBS	10
DMSO	10

Cells were counted and resuspended in freezing medium at 1 x 10^6 cells ml^{-1}. 1 ml volumes of resuspended cells were aliquoted into cryotubes, and placed into a Cryo-freezing container (named commercially as 'Mr Frosty' (containing ispropan-2-ol; Nalgene Labware) overnight at -80 ^{o}C. This slows the cooling of the cells to 1 ^{o}C min^{-1}, reducing the risk of dehydration or ice crystals forming within the cells, maintaining their viability until required. The cells are then transferred to long-term storage in liquid nitrogen.

2.3.4. Thawing cells

Cells were removed from liquid nitrogen storage and thawed gently at 37 ^{o}C. They were removed from the cryotube and 4 ml complete medium added slowly drop-wise. The cells were then centrifuged at 240 *x*g for 4 min to remove the freezing medium, resuspended gently into 5 ml fresh complete medium, transferred into a T25 and placed at 37 ^{o}C as described in section 2.3.2.

2.3.5. Fibrinogen-coating

Fibrinogen is a soluble glycoprotein produced in the liver by hepatocytes, and MKs (Haidaris *et al*, 1989). It is involved in platelet adhesion and clot formation, forming a link between platelets by binding to the integrin $\alpha_{IIb}\beta_3$, which is expressed on their surfaces and

helping to strengthen the forming thrombus (Ni *et al*, 2000). Fibrinogen has been located in the blood marrow sinusoids, towards which MKs migrate as they start to differentiate, following a concentration gradient of stromal-derived factor-1 (SDF-1) (Wang *et al*, 1998). MKs bind to the fibrinogen via the $\alpha_{IIb}\beta_3$ integrin in the sinusoids, and reach terminal differentiation producing proplatelets. These extend into the bloodstream, eventually releasing individual platelets (Larson and Watson, 2006). Where indicated, fibrinogen-coated surfaces were used to differentiate MEG-01 cells.

Fibrinogen was solubilised by layering on top of warmed PBS and mixed gently on a warming magnetic stirrer (Stuart Scientific SB302, Lutterworth, UK) to give a 100 µg ml^{-1} solution, which was filtered using a 0.22 µm filter. Clear 96-well plates were coated with 30 µl in each well, and 5 cm dishes (Nunc, Loughborough, UK) were coated with 1 ml. These were incubated at 37 ^{o}C for either 2 h or overnight, and any remaining solution removed (Larson and Watson, 2006; van Os *et al*, 2003). They were then used for either crystal violet experiments (clear 96-well plates; section 2.6) or MEG-01 differentiation (5 cm dishes; section 2.3.2.1).

2.4. Polymerase chain reaction

All stages of the polymerase chain reaction (PCR) must be carried out using sterile tips and tubes to prevent contamination or degradation of the RNA isolated or the products produced by PCR.

2.4.1. Isolation of total RNA

MEG-01 cells were cultured as described in section 2.3.2. Samples of 1.5 x 10^6 cells were taken and the cells washed in sterile PBS. The PBS was removed, each sample of cells resuspended in 500 µl of Trizol in the fume hood due to the phenol content of Trizol, then stored at -80 ^{o}C until required. The samples were defrosted at RT for approximately 5 min. All of the following steps were carried out in a fume hood due to the toxic nature of the phenol in Trizol. 0.1 ml of chloroform was added to each sample which was then shaken vigorously for 15 s to ensure that the 2 solvents were completely mixed, incubated at RT for 2- 3 min, then centrifuged at 18000 *x*g at 4 ^{o}C for 15 min in an Eppendorf Centrifuge 5417R centrifuge with an FA45-24-11 rotor. The clear, colourless upper layer containing the RNA was carefully removed to a fresh eppendorf tube, then mixed gently with 250 µl isopropanol and incubated at RT for 10 min. These were then centrifuged at 18000 *x*g at

4 ^{o}C for 10 min, and the supernatant discarded. The gelatinous pellet was washed by the gentle addition of 1 ml 75 % cold ethanol, without resuspending the pellet, then centrifuged again at 18000 *x*g for 10 min at 4 ^{o}C. The supernatant was discarded, removing as much as possible before leaving the pellets in air dry in the fume hood. Once dry, the pellets were resuspended in 10 µl RNase-free water, and can be stored at -80 ^{o}C until required or used immediately.

2.4.2. Quantification of RNA

Before the RNA can be reversed transcribed to cDNA, the concentration of RNA within each sample must be determined. A sample of the RNA obtained in section 2.3.2 was diluted 100 x in RNase-free water to give a final volume of 100 µl, with the remaining sample left on ice. The RNA quantification was carried out using a Pharmacia Biotech Gene Quant II, with a path length of 10 and dilution factor of 100. Milli Q water was used as a reference sample to give an absorbance setting of 0. The diluted RNA samples were then read and the concentration of RNA determined. The rest of the original RNA samples were stored at -80 ^{o}C until required.

2.4.3. Reverse transcription

In this step the RNA is reverse transcribed using PCR (RT-PCR) to generate single strands of cDNA. The samples were treated with DNase to remove any DNA present in the samples and RNasin PLUS to prevent degradation of the RNA present (table 17) and heated at 37 ^{o}C for 30 min in PCR tubes.

Table 17. Reaction mix for DNAse treatment of RNA

REAGENT	**VOLUME (µl)**
2 µg RNA	x
DNase (2000 U ml^{-1})	1.0
10 x DNase buffer	0.5
RNA-free water	x
RNAsin PLUS (40 U ml^{-1})	0.5
Total volume	5.5 µl

Where the volume of RNA from each sample prepared in section 2.4.1 and quantified in 2.4.2 together with the water, total 3.5 µl.

1 µl DNase stop solution was then added to each sample and heated at 65 ^{o}C for 10 min to inactivate the DNase, as the following step reverse transcribes the isolated RNA to cDNA and any active DNase would degrade this. Olio dT was then added to each sample, providing an anchor at poly-A tails of mRNA aiding the start of reverse transcription (Krug and Berger, 1987), and incubated for another 5 min at 65 ^{o}C. The samples were then briefly centrifuged to ensure that all of the liquid was at the bottom of the tubes, then incubated on ice for at least 1 min. 13 µl of RT-PCR stock solution (table 18) was subsequently added to each sample and mixed gently before being incubated at 42 ^{o}C for 50 min, follow by 15 min at 72 ^{o}C to inactivate the reverse transcriptase (Superscript II) in a Techne TC-512 Thermal Cycler.

Table 18. RT-PCR stock solution

REAGENT	**VOLUME (µl)**
PCR water	6
5 x RT buffer	4
DTT (100 mM)	1
dNTPs (10 mM)	1
Superscript II (200 U μl^{-1})	1
Total	13 µl

dNTPs- deoxyribonucleotide triphosphates; Superscript II, reverse transcriptase.

2.4.4. PCR- β-actin and NMDAR subunits

The reverse transcribed samples were then set up for PCR in PCR tubes containing, using primers detailed in tables 20 or 21:

Table 19. PCR stock solution

REAGENT	VOLUME (µl)
Water	15.6
5 x Flexi buffer	5.0
dNTPs (10 mM)	0.5
$MgCl_2$ (25 mM)	2.0
Forward primer (25 pM)	0.4
Reverse primer (25 pM)	0.4
Go-Taq	0.1
Total	24.0 µl

Table 20. Primer sequences- β-actin

		PRIMER SEQUENCE	EXPECTED SIZE (BP)
B-actin	Forward	5’ – TAGGCACCAGGGTGTGATGG	
	Reverse	5’ - CATGGCTGGGGTGTTGAAGG	282

Obtained with kind permission from Dr Heather Bone

Table 21. Primer sequences- NMDAR subunits

SUBUNIT		PRIMER SEQUENCE	EXPECTED SIZE (BP)
NR1	Forward	5’-CTTTCTGCCAGCGAGGACG	
	Reverse	5’- CATACTTGGAAGACATCAGC	336
NR2A	Forward	5’- ATGTGGTGAGATGGAGGAGC	
	Reverse	5’- TCTTGAGGAGTTCATGTTGG	391
NR2B	Forward	5’- TGGTATGATTGGAGAGGTGG	
	Reverse	5’- TTTGCCGATGGTGAAAGAGG	338
NR2C	Forward	5’- CAGTGACAAGAAGTTTCAGC	
	Reverse	5’- ATGCCGTAGCCAGTGGTAGC	304
NR2D	Forward	5’-GCTCACGCCCAAGGAGAAGG	
	Reverse	5’-AACCAGACGTAGCCAGATCC	366
NR3A	Forward	5'- TCCAACCAGAACTTGCTCTC	
	Reverse	5'- GGATGCTCAATCAGGGTAA	352
NR3B	Forward	5'- CATGGTCGGGGACAAGAC	
	Reverse	5'- GGACAGGTTGGAGGTGAGC	385

1 µl of cDNA was added to each tube and mixed gently. The tubes were then placed in a Techne TC-512 Thermal Cycler and run on the programme required (table 22). Optimisation was required for the annealing step for the NMDAR subunit primers, which used a temperature gradient across the Thermal Cycler from 53- 63 ^{o}C, in place of 62 ^{o}C used for the β-actin primers (table 22). The other steps of the programme remained the same.

Table 22. PCR programme for β-actin

	TEMPERATURE (^{o}C)	**TIME (s)**
Heated lid	105	-
Initial denaturation	94	300
25 cycles- denaturation	94	30
- annealing *	62	30
- extension	72	45
Final extension	72	5
Hold	4	-

* the annealing temperature was varied as required the NMDAR primer sets. For optimisation, a temperature gradient was used from 53- 63 ^{o}C.

Once the PCR programme was completed, the samples were run on a 2 % agarose-TAE gel bathed in TAE buffer for 1 h at 80 V. The gel was then soaked in 0.5 µg ml^{-1} ethidium bromide-TAE solution for 30 min, before visualisation using a Syngene UV transluminator using GeneSNAP software version 7.07.

2.5. Western blotting

2.5.1. Determination of protein concentration

The protein concentration for all samples run on Western blots was determined using the Bradford assay (Bradford, 1976). Bradford assay concentrate was diluted 10 fold, and split into 1 ml volumes for each sample. To these, 2 µl of the relevant sample was added and mixed well. 200 µl of each diluted sample was added to a 96 well clear plate in triplicate together with triplicate bovine serum albumin (BSA) standards ranging from 1 to 32 µg ml^{-1}, and the absorbance read at 595 nm. Protein samples were subsequently prepared with a final concentration of 1 µg µl^{-1} with double deionised water, and 5 x sample buffer.

2.5.2. Preparation of MEG-01 cells and platelets

Table 23. Lysis buffer A

REAGENT	CONCENTRATION (%)
Protease inhibitor cocktail (General use)	
Triton X-100	1

Table 24. Lysis buffer B

REAGENT	CONCENTRATION
NaCl	150 mM
Tris (pH to 7.4)	20 mM
$MgCl_2$	1 mM
$CaCl_2$	1 mM
Protease inhibitor cocktail (cell and tissue extract)	2 %
Triton X-100	1 %

Table 25. Laemmli sample buffer (5x)

REAGENT	CONCENTRATION
Tris-HCl (pH 6.8)	200 mM
Glycerol	50 %
2-mercaptoethanol	20 %
SDS	10 %
Bromophenol blue	0.01 %

Protein samples were prepared using either 2 x 10^6 MEG-01 cells or 3 ml PRP, centrifuged at 240 *x*g for 4 min or 350 *x*g for 20 min respectively, and washed once in PBS. The cells were then resuspended in 100 µl lysis buffer A (table 23) containing 1 % Triton X-100 and protease inhibitors, incubated for 10 min on ice, and centrifuged at 19000 *x*g for 15 min at 4 ^oC to pellet cell debris. The supernatant was retained and either used immediately or stored at -80 ^oC. Samples were assayed for protein content using the Bradford assay (section 2.5.1) and diluted as required to a final concentration of 1 µg $µl^{-1}$ with double distilled water and 5x sample buffer, such that approximately 15 µg of protein was loaded per lane. Samples were boiled at 100 ^oC for 10 min prior to loading onto the gel. This step

in combination with sodium dodecyl sulphate (SDS), which confers a negative charge over the whole protein, and 2-mercaptoethanol, which reduces disulphide bonds, in the sample buffer ensures that the protein runs through the gel matrix in a purely size-dependent manner.

A second method with a longer lysis period was also used to solubilise membrane proteins for analysis by Western blot. This method is modified from Young *et al*, 2007, using a tris-based buffer in place of a phosphate-based lysis buffer. The extended lysis period is hypothesised to improve the solubilisation of membrane proteins, for example ion channel subunits. Triton X-100 is a non-ionic detergent which has previously been used for the recovery of membrane proteins for analysis by Western blot, for example by Sheu *et al*, (2004) in the localisation of matrix metalloproteinase-9, Merezhinskaya *et al*, (2006) investigating the expression of monocarboxylate transporter 4 and Jung *et al*, (2008), investigating the membrane localisation of phosphoinositol 4-kinase IIβ.

MEG-01 cells (2×10^6) were washed in ice cold PBS to remove any remaining media, with centrifugation steps of 240 x*g* for 4 min. 3 ml PRP was centrifuged at 350 x*g* for 20 min to pellet the platelets. The platelet poor plasma (PPP) was discarded and the cells washed in warmed PBS. Both cell pellets were resuspended in 50 µl lysis buffer B (table 24) and rocked gently (Stuart Scientific, rocking platform STR9, Lutterworth, UK) at 4 ^{o}C for 60 min. The cells were then centrifuged at 19000 *x*g for 10 min (Beckman CS-15R centrifuge, F3602 rotor). The supernatant containing solubilised membrane proteins was collected and either used immediately or stored at -80 ^{o}C. Samples were assayed for protein content using the Bradford assay (section 2.4.1) and diluted as required to a final concentration of 1 µg μl^{-1} with double distilled water and 5x sample buffer. Samples were boiled at 100 ^{o}C for 10 min prior to loading onto the gel.

2.5.3. SDS-polyacrylamide gel electrophoresis (SDS-PAGE)

Table 26. 8 % resolving gel (5 ml = 1 gel)

REAGENT	VOLUME (ml)
Distilled water	2.3
30 % Acrylamide	1.3
1.5 M Tris (pH 8.8)	1.3
10 % SDS	0.05
10 % Ammonium persulphate	0.05
TEMED	0.003

Table 27. 5 % stacking gel (2ml = 1 gel)

REAGENT	VOLUME (ml)
Distilled water	1.36
30 % Acrylamide	0.34
1 M Tris (pH 6.8)	0.26
10 % SDS	0.02
10 % Ammonium persulphate	0.02
TEMED	0.002

Table 28. Running buffer

REAGENT	CONCENTRATION
Glycine	192 mM
Tris	25 mM
SDS	0.1 %

Table 29. TGS running buffer

REAGENT	CONCENTRATION
Glycine	192 mM
Tris	25 mM
SDS	0.1 %

8 % SDS-polyacrylamide gels were cast in a Bio-Rad gel system (BioRad, UK), and run in a Bio-Rad Mini Protean II system containing running buffer (table 28) at constant 200 V for approximately 30 min. Alternatively, samples lysed in lysis buffer B were run at a constant 150 V for approximately 1 h with the system filled with TGS running buffer. A protein standard was run alongside the samples in both cases to estimate the size of proteins detected.

2.5.4. Immunoblotting

Table 30. Transfer buffer

REAGENT	CONCENTRATION
Glycine	192 mM
Tris	25 mM
SDS	0.1 %
Methanol	20 %

Table 31. Wash buffer

REAGENT	CONCENTRATION
PBS tablets	1 per 200 ml double deionised water
Tween-20	0.5 %

Table 32. TG transfer buffer

REAGENT	CONCENTRATION
Glycine	192 mM
Tris	25 mM
Methanol	20 %

Table 33. TTBS wash buffer

REAGENT	CONCENTRATION
Sodium chloride	500 mM
Tris	20 mM
pH	7.5
Tween-20	0.2 %

Polyvinylidene difluoride (PVDF) membrane is inherently hydrophobic, and requires wetting before use as proteins will not bind to the dry membrane. Soaking the membrane in methanol reduces the hydrophobicity through the formation of hydrogen bonds between the methanol hydroxide groups and the fluoride groups of the PVDF. The membrane is then equilibrated in TG transfer buffer before immunoblotting. PVDF has a greater protein binding capacity than nitrocellulose, 140- 150 μg cm^2 compared to 80- 100 μg cm^2 respectively (Bio-Rad), which enables increased binding of protein to small areas of the membrane giving a higher signal-to-noise ratio, and therefore a clearer final image.

The gels were removed from the glass plates, and transferred into a 'sandwich' containing (in order) sponge, filter paper, gel, nitrocellulose membrane (0.2 μm), filter paper and sponge, where both sponge and filter paper were pre-soaked in transfer buffer[1] (table 30). This was placed into a cassette, and into the Bio-Rad transferring system with transfer buffer, then run at a constant 150 mA for approximately 2 h. Alternatively[2], PVDF membrane (0.2 μm) was used in place of nitrocellulose membrane. PVDF membrane was soaked in methanol for 2 min, followed by 2 min washing in cold TG transfer buffer (table) before placing in the sandwich. In this case transfer was carried out at a constant 350 mA for approximately 40 min, and the tank filled with cold TG buffer[2].

Membranes were incubated overnight in either 5 % skimmed milk-PBS[1] (-TTBS[2] (table 33)) at 4 ^{o}C with constant, gentle rocking. The membrane was then incubated with the required antibody (see table 34) for 90 min at RT with constant rocking. The membrane was washed for 3 x 5 min in either PBS or TTBS, then incubated in secondary antibody diluted in 5 % skimmed milk- PBS (-TTBS) for 60 min at RT with constant rocking. The membrane was washed for 6 x 5 min in either PBS or TTBS and the protein visualised on X-ray film using ECL chemiluminescent detection agent.

[1] Running buffer, transfer buffer and PBS were used when samples were lysed with lysis buffer A
[2] TGS running buffer, TG transfer buffer and TTBS were used when samples were lysed with lysis buffer B

Table 34. Antibody concentrations

ANTIBODY	CONCENTRATION USED
Anti-β-actin	0.8 ng ml^{-1}
Anti-NR1	0.5 µg ml^{-1}
Anti-NR2A	0.2 µg ml^{-1}
Anti-NR2D	0.2 µg ml^{-1}
Anti-NR3A/B	0.32 µg ml^{-1}
Polyclonal Rabbit Anti-Mouse IgG/HRP	0.26 mg ml^{-1}
Polyclonal Rabbit Anti-Goat IgG/ HRP	0.13 mg ml^{-1}
Polyclonal Swine Anti-Rabbit IgG/HRP	0.26 mg ml^{-1}

NB All antibodies were diluted in 5 % skimmed milk-PBS (-TTBS)

2.5.5. Membrane stripping

Table 35. Membrane stripping buffer (5x)

REAGENT	AMOUNT
SDS	10 g
1M Tris-HCl pH 7.4	31.25 ml
Double distilled H_2O	Make up to 100 ml

Table 36. Membrane stripping buffer (1x)

REAGENT	AMOUNT
5x membrane stripping buffer	20 ml
Double distilled H_2O	80 ml
2-mercaptoethanol	770 µl

Membranes were stripped so that they could be re-probed with different antibodies, for example β-actin to validate whether loading of the samples was equal.

The membrane was immersed in 1x stripping buffer such that its upper surface was just covered, and warmed at 60 ^{o}C for 20 min in a water bath. The membrane was then washed at least 3x for 20 min in wash buffer (PBS-tween or TTBS) and blocked in either 5 % BSA or milk as required overnight before probing with a different antibody (section 2.5.4).

2.5.6. Densitometry analysis

The X-ray film onto which the proteins were visualised following immunoblotting (section 2.5.4), was scanned using a Cannon Lide 70 and the image captured using Adobe Photoshop version 7.0. The pictures were then analysed using ImageJ software 1.41o (NIH, USA), where the area of the gel for each sample at the expected size for each subunit protein was identified and framed using a box of the same size for each band, then the arbitrary densitometry value taken. The values were normalised using the arbitrary densitometry value for the matched β-actin bands for each sample; each membrane from SDS-PAGE was split prior to immunoblotting at approximately 70 kDa such that the expression of the subunit proteins (100-180 kDa) could be determined on the top half and that of β-actin (44 kDa) on the lower half. The data was analysed using GraphPad Prism version 4 (section 2.10).

2.6. Coomassie blue staining

Coomassie brilliant blue R-250 binds non-specifically to virtually all proteins enabling visualisation of proteins on an SDS-polyacrylamide gel, and therefore assisting the comparison of the amount and size of proteins within samples.

Table 37. Coomassie blue staining solution

REAGENTS	CONCENTRATION (%)
Methanol	50
Double deionised water	40
Glacial acetic acid	10
Coomassie brilliant blue R-250	0.05 (w/v)

Table 38. Coomassie destaining solution

REAGENTS	CONCENTRATION (%)
Methanol	50
Double deionised water	40
Glacial acetic acid	10

Samples were prepared using the membrane lysis protocol (section 2.5.2) and separated using SDS-polyacrylamide gel electrophoresis (as described in section 2.5.3). The gel was

then immersed in Coomassie blue staining solution (table 39) for approximately 30 min at RT with gentle rocking after which the staining solution (table 40) was replaced with destaining solution. This was in turn replaced approximately every hour with fresh destaining solution, and rocked gently at RT until the gel background was clear and blue bands clearly visible.

2.7. Crystal violet staining

Crystal violet or methyl violet 10B is a cell impermeable dye which is able to bind DNA following fixation of the cells. It is used in the determination of cell viability and adhesion assays (Genever *et al*, 1999)

MEG-01 cells were cultured at 2 x 10^{-5} ml^{-1} in the presence or absence of 10 nM PMA for 3 d in combination with varying concentrations (0-100 μM) of either MK-801 or D-AP5. The cells were washed 3 times with PBS to remove non-adherent cells, then fixed with 70 % ethanol in double deionised water for 15 min at RT. The cells were washed with PBS and stained with 0.5 % crystal violet in double deionised water for 25 min. Excess dye was removed by washing several times with double deionised water. The dye was then eluted by adding a 50 % ethanol/ 0.1 M sodium citrate solution (pH 4.2) to the cells. Absorbance was read on a BMG multi-detection microplate reader (FLUOstar OPTIMA, BMG Labtech, Aylesbury, UK) at 570 nm and the data analysed using Prism Version 4 (GraphPad Software, San Diego, CA, USA).

2.8. Measuring intracellular Ca^{2+} in human platelets

Ca^{2+} responses were detected in acutely isolated human platelets using the fluorescent indicator fluo-4, where an increase in fluorescence is indicative of an increase in intracellular Ca^{2+} (Baier *et al*, 2009; Grynkiewicz *et al*, 1985), and the dye exhibits a K_d (Ca^{2+}) of 345 nm (Gee *et al*, 2000). Human platelets were loaded with fluo-4 using a membrane-permeant analogue, fluo-4AM. The addition of the acetylmethyl (AM) ester converts the charged fluo-4 molecule into an uncharged molecule which becomes membrane permeable. Non-specific esterases cleave the ester group once inside the cell, returning the fluo-4 to its original, charged state, which leaks out of the cells far more slowly than when bound to the AM group (Simpson, 2005).

PRP was prepared as previously described (section 2.3.1) and incubated with 5 μM fluo-4AM and 0.02 % pluronic acid-F127 in the dark. Pluronic acid-F127 is a non-ionic detergent which facilitates solubilisation of water insoluble dyes, such as fluo-4AM, ensuring equal dispersal of the dye throughout the solution during cell dye loading. The PRP was centrifuged for 20 min at 350 *x*g and the PPP discarded. The platelet pellet was resuspended in an equal volume of saline containing 0.32 U ml^{-1} apyrase grade VII. The fluo-4AM loaded suspension was added to a black-walled 96 well plate (Greiner Bio-One, Stonehouse, UK), and the recording started while the cells equilibrated to 37 ^{o}C for 60 s (figure 10). $CaCl_2$ (1 mM) was then manually added to the cells, which were allowed to equilibrate for another 120 s, while still recording the fluorescence produced, after which the agonist or saline were applied using the inbuilt injectors in the microplate reader.

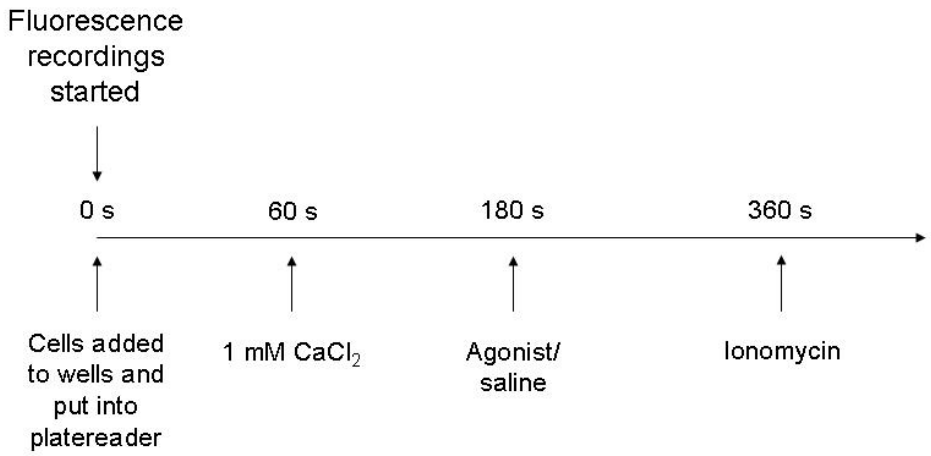

Figure 10. Timeline for the fluo-4 assay. The platelets were maintained at 37 ^{o}C from time= 0 s, and were kept in the dark from loading with fluo-4AM. The first 60 s equilibrated the platelets to 37 ^{o}C, with the following 120 s equilibrating the platelets to the increase in $[Ca^{2+}]$. The addition of ionomycin, an ionophore, leads to the maximal increase in $[Ca^{2+}]_i$.

Ionomycin (1 μg ml^{-1}) was added 180 s after the agonist to obtain maximal fluorescence. Antagonists were added at the start of the experiment (t=0). All measurements were performed at 37 ^{o}C with a BMG multi-detection microplate reader (FLUOstar OPTIMA, BMG Labtech, Aylesbury, UK). Fluo-4 was excited at 488 nm and fluorescence collected at 520 nm every 0.24- 8 s. Each condition was repeated in triplicate for each experiment and values normalised to the baseline and maximal fluorescence readings (equation 1). The increase in fluorescence due to the addition of calcium was subtracted from peak values to give responses solely due to the addition of the agonist. Curve fitting was

performed using Prism Version 4 (GraphPad Software) using a four parameter logistic equation (equation 2).

Equation 1

$$y = \left(\frac{F - F_0}{F_{max}} \right) \text{x } 100$$

Where F is fluorescence, F_0 is fluorescence at time = 0 s, and F_{max} is maximum fluorescence.

Equation 2

$$y = baseline + \frac{\alpha}{1 + 10^{(LogA_{50} - x)n_H}}$$

Where x is the logarithm of the molar concentration of the drug, α is the maxima (max-baseline), $logA_{50}$ is the half maximal response and n_H is the Hill slope.

2.9. Measurement of ATP release from human platelets

Luminescent firefly luciferase was used to detect the secretion of ATP from platelet electron dense granules into the external environment (McNicol and Israels, 1999). Firefly luciferase binds ATP in the presence of luciferin, the substrate for luciferase, leading indirectly to the production of light (figure 11).

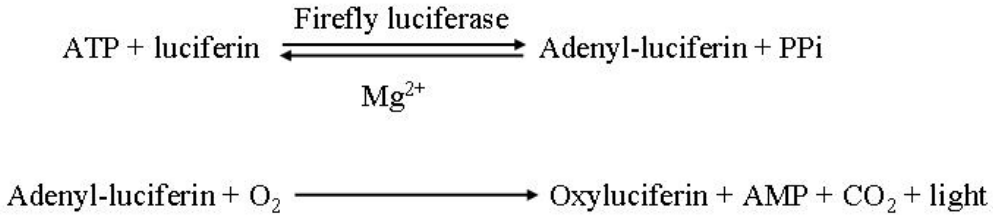

Figure 11. Mechanism of ATP detection by luciferase. Equation showing the process through which ATP is detected by luciferase, leading to the release of light which is detected by the photomultiplier tube in the luminometer (Sigma, www.sigma.co.uk).

A lyophilised powder luciferin-luciferase mix was used containing the firefly enzyme luciferase, luciferin, $MgSO_4$, DTT, EDTA, BSA and tricine buffer salts. This was reconstituted in 5 ml double deionised water to give the stock solution (Sigma).

In all experiments, PRP was centrifuged for 2 min at 140 xg in a Hermle Z160M centrifuge and the platelet pellet resuspended in nominally Ca^{2+}-free salt solution. The platelet suspension (25 µl per well) was placed in a white 96 well plate (Greiner Bio-One, Stonehouse, UK) with 15 µl platelet saline and 40 µl of 10 x diluted luciferin-luciferase mix per well. Antagonists and $CaCl_2$ (1 mM final concentration) were added prior to the start of the assay. Agonists (10 µl) were injected using a computer controlled injector as indicated in figures 24 and 42. All measurements of luminescence were performed with a BMG multi-detection microplate reader (FLUOstar OPTIMA, BGM Labtech, Aylesbury, UK), and, where emitted, light was detected using photomultiplier tube. Luminescence was measured every 21 s.

ATP standards (1 nM- 10 µM) were run alongside each experiment using half log serial dilutions, which were plotted against luminescence detected to produce a standard curve (figure 12). The increase in luminescence from baseline was measured and used to calculate the ATP concentration released using the standard curve determined for each experiment. Analysis was performed using Prism Version 4 (GraphPad Software).

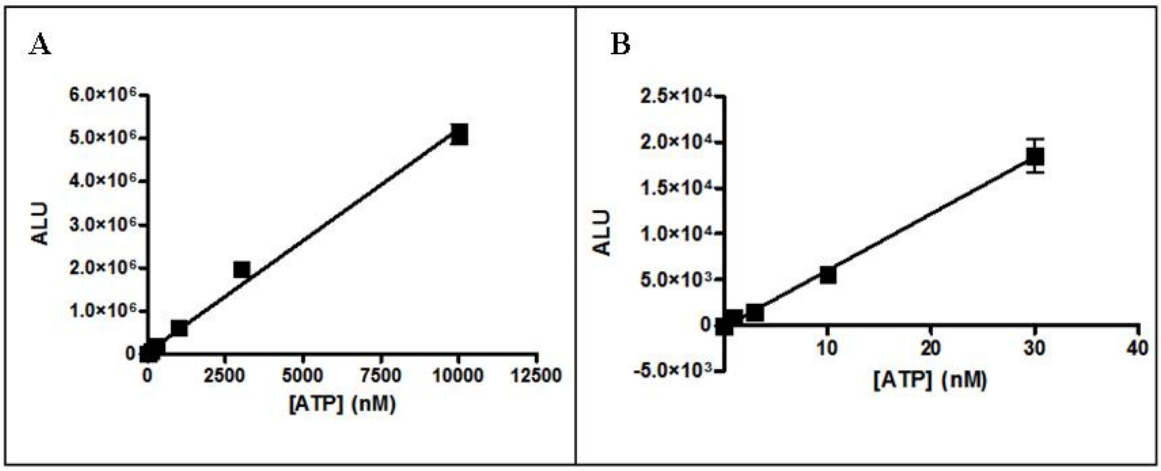

Figure 12. ATP calibration curve. A, to determine the sensitivity of the luciferase assay using known ATP concentrations from 1 nM to 10 µM ATP. B, showing the limit of detection is from 10 nM ATP. Values represent mean ± s.e.m from 4 experiments.

2.10. Analysis

Data analysis and graphical diagrams were produced using Prism Version 4 (Graphpad Software, San Diego CA, USA). Luminescence readings were converted to ATP concentrations using ATP-luminescence calibration curves (section 2.9; figure 12). Statistical significance of differences were analysed either by a one-way ANOVA with a Dunnetts posthoc test, a two-way ANOVA with Bonferroni post-hoc test, or alternatively a 2-tailed, unpaired student's *t* test, as appropriate. Significance was reached when $P < 0.05$ (GraphPad Prism). Data is expressed as mean ± standard error of the mean (± s.e.m), with *n* denoting the number of donors.

CHAPTER 3
GLUTAMATE-GATED ION CHANNELS

3.1. Summary

In this chapter, it has been determined that:

- the NMDA receptor subunit proteins NR1 and NR2D are expressed in human platelets, but not the NR2A subunit protein
- increases in $[Ca^{2+}]_i$ are observed upon external application of either glutamate or NMDA
- ATP release can be elicited from human platelets upon external application of glutamate alone, and in combination with glycine, which can be inhibited by the additional presence of either MK-801 or D-AP5

3.2. Introduction

Previous studies have demonstrated that the NMDA NR1 subunit protein is expressed in human platelets (Genever *et al*, 1999) and have also shown that NMDARs are implicated in platelet activation (Franconi *et al*, 1996 and 1998). These studies have been extended to examine the expression of different NMDA subunit proteins in freshly isolated human platelets; NMDA NR1 subunits that contain the glycine binding site and whose presence is required for the formation of functioning NMDA receptors, together with NR2 subunits which bind glutamate and are inhibited by the binding of the antagonist D-AP5 (Matsui *et al*, 1995).

3.3. Results

3.3.1 Detection of NMDA receptor subunits by Western blot

Figure 13 demonstrates that 4 different human platelet donors express the NMDA NR1 subunit protein at approximately 120 kDa (donors 1, 3-5; with equal loading determined by the expression of β-actin). Donor 3 appears to demonstrate a lower level of expression of the NR1 subunit, however the density of the β-actin band is less than in the other 3 expressing donors (n=6). Secondary bands were detected between 150 and 250 kDa in all donors. These were reduced in intensity by increasing the boiling step prior to loading from 5 to 10 min.

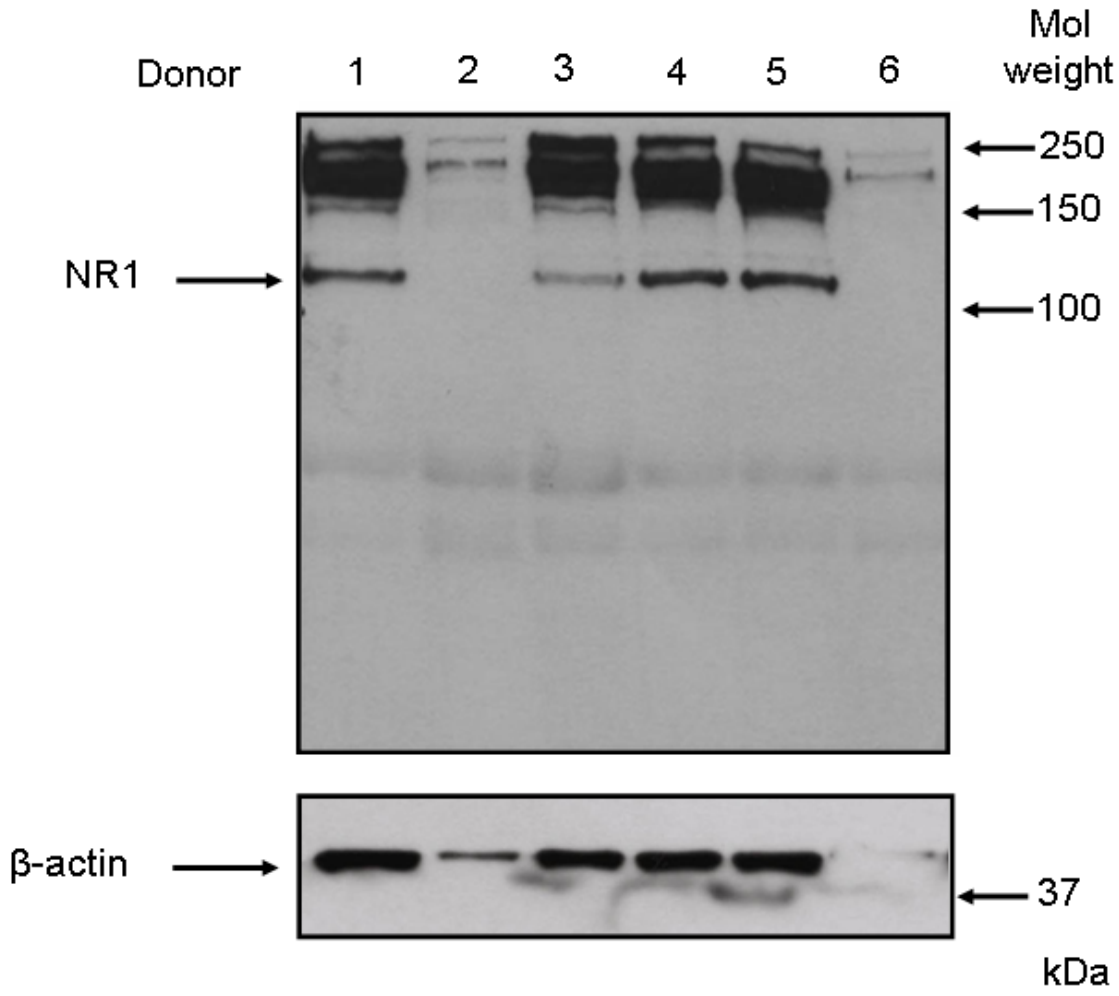

Figure 13. Human platelets express NMDA receptor subunit NR1. Western blot demonstrating variation in expression of the NMDA NR1 subunit between different human donors (1-6), with loading was assessed by blotting for β-actin (expected size 42 kDa), from the same, subsequently stripped membrane. The arrows on the right side indicate sizes predicted by the protein standards (mol weight, molecular weight marker; kDa). Arrow on the left indicates the expected size of the NR1 subunit, 120 kDa. Number above the lanes indicates the donor from which sample was obtained; approximately 15 μg protein loaded of each sample determined by Bradford assay. Representative blot from 15 separate experiments.

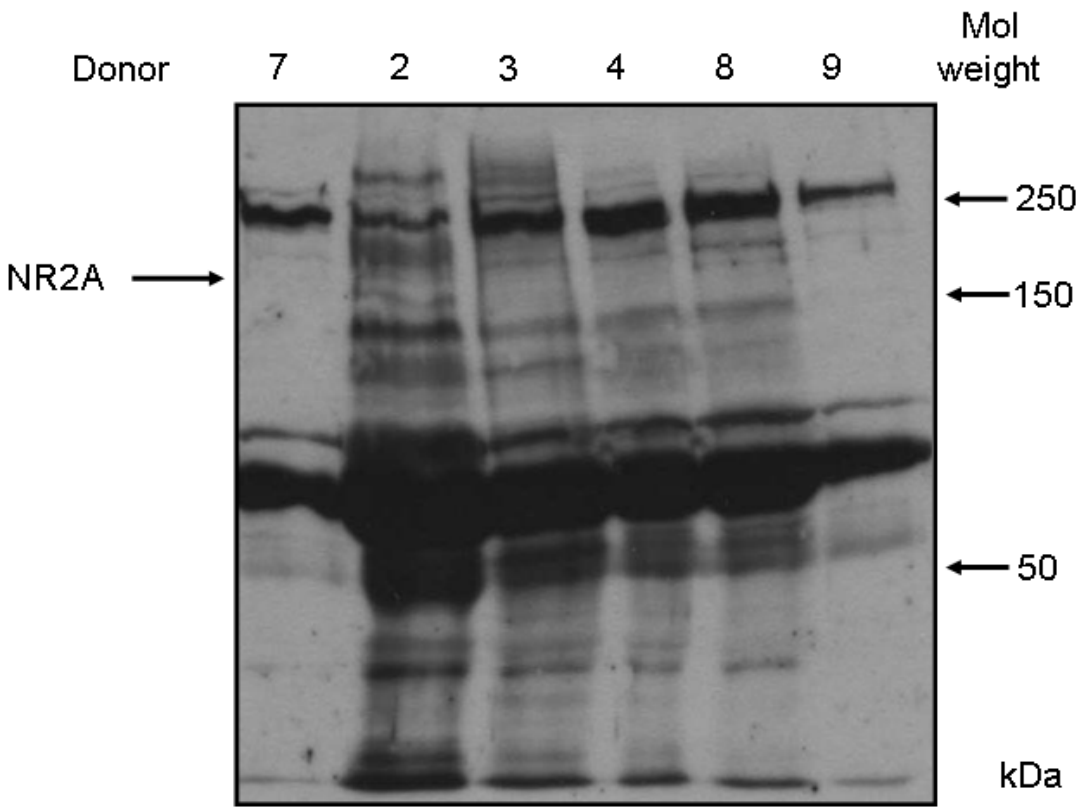

Figure 14. Human platelets do not express detectable NMDA receptor subunit NR2A. Western blot demonstrating that the NMDA NR2A subunit is not detectable in 6 different human donors. The arrows on the right side indicate sizes predicted by the protein standards (mol weight, molecular weight marker; kDa). Arrow on the left indicates the expected size of the protein, 180 kDa. Number above the lanes indicates the donor from which sample was obtained; approximately 15 μg protein loaded of each sample determined by Bradford assay. Representative blot from 4 separate experiments.

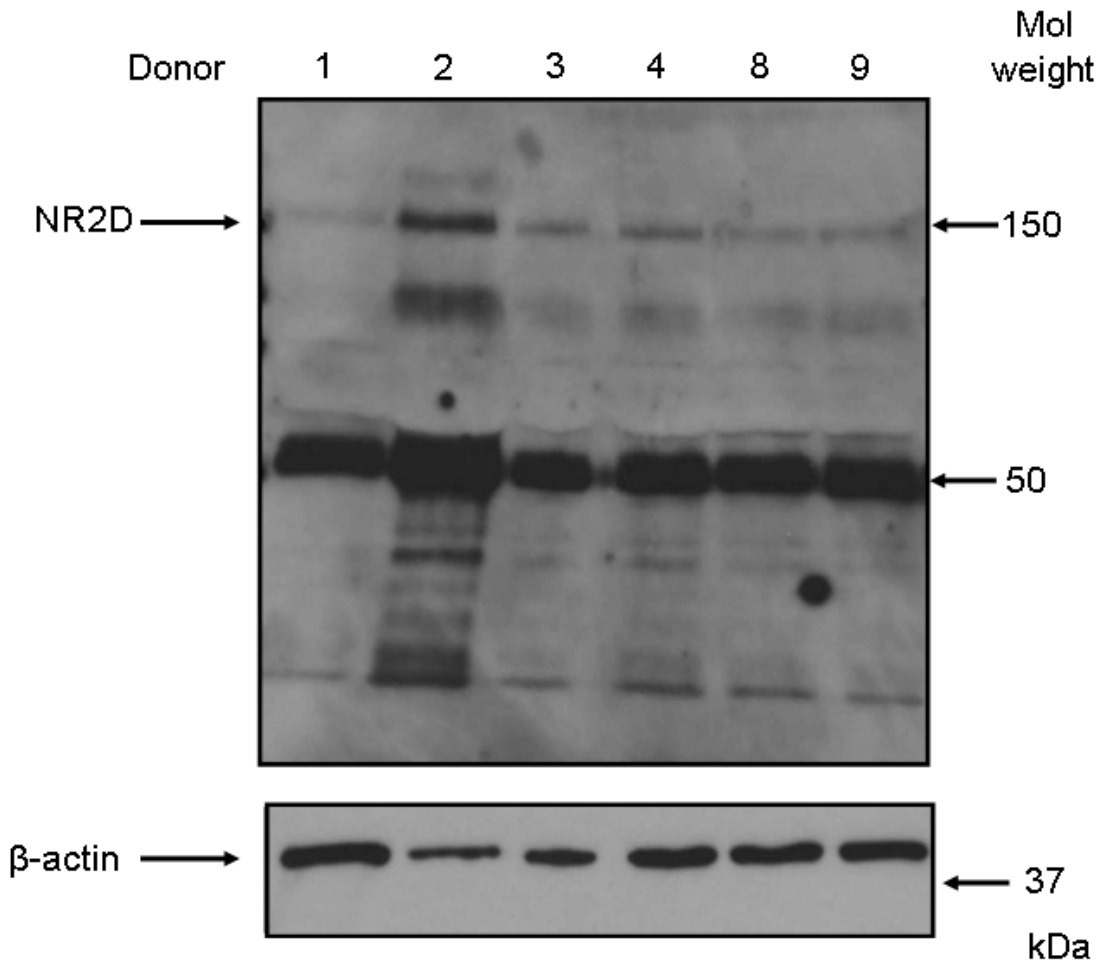

Figure 15. Human platelets express NMDA receptor subunit NR2D. Western blot demonstrating variation in expression of the NMDA NR2D subunit between different human donors with loading was assessed by blotting for β-actin (expected size 42 kDa), from the same stripped membrane. The arrows on the right side indicate sizes predicted by the protein standards (mol weight, molecular weight marker; kDa). Arrow on the left indicates the expected size of the protein, 150 kDa. Number above the lanes indicates the donor from which sample was obtained; approximately 15 μg protein loaded of each sample determined by Bradford assay. Representative blot from 5 separate experiments.

The NR2D subunit protein (estimated molecular weight 150 kDa) is expressed by all 6 donors in figure 15 (*n*= 6) at different levels, with donor 2 clearly expressing the protein in larger amounts than others, while the β-actin blot below indicates that the loading of this sample is less than that for the other 5 donors suggesting that the level of expression is greater in this particular donor. In comparison there is no detectable evidence of NR2A protein expression in human platelets (figure 14), with no bands discernable in the Western blot at the expected size of 180 kDa with the antibody used (*n*= 6).

3.3.2. Intracellular calcium responses to glutamate, NMDA and thrombin

Activation of NMDARs leads to an influx of Ca^{2+} into cells increasing levels of intracellular Ca^{2+}. This can be measured by loading cells with a fluorescent dye, such as fluo-4AM which is used in these experiments (section 2.8). The data obtained is normalised against differences in cell numbers and variation in dye loading by the addition of 1 μg ml^{-1} ionomycin, a Ca^{2+} ionophore, to obtain the maximum fluorescence (100 % response; maximum response; MR) at the end of each experiment, thus giving each experiment an internal control. Each response is then calculated as a percentage of this value. A saline control was added to evaluate background changes in fluo-4 fluorescence, and was shown to evoke a small sustained increase of 10-20 % MR above baseline fluorescence in experiments to evaluate responses to glutamate and NMDA.

3.3.2.1. Glutamate and thrombin responses

The glutamate family of receptors were originally defined by their response to glutamate (Dingledene *et al*, 1999), so initial work investigated the effect of extracellular glutamate on intracellular Ca^{2+} in human platelets. Over the duration of each experiment measurements of changes in fluorescence indicative of changes in $[Ca^{2+}]_i$ were taken between 1.5 and 5 h post isolation of platelets from whole blood. In initial experiments, a glutamate concentration response curve was performed in triplicate using platelets from different donors, with triplicate repeats of thrombin (3 U ml^{-1}) and saline, as positive and negative controls respectively, also measured.

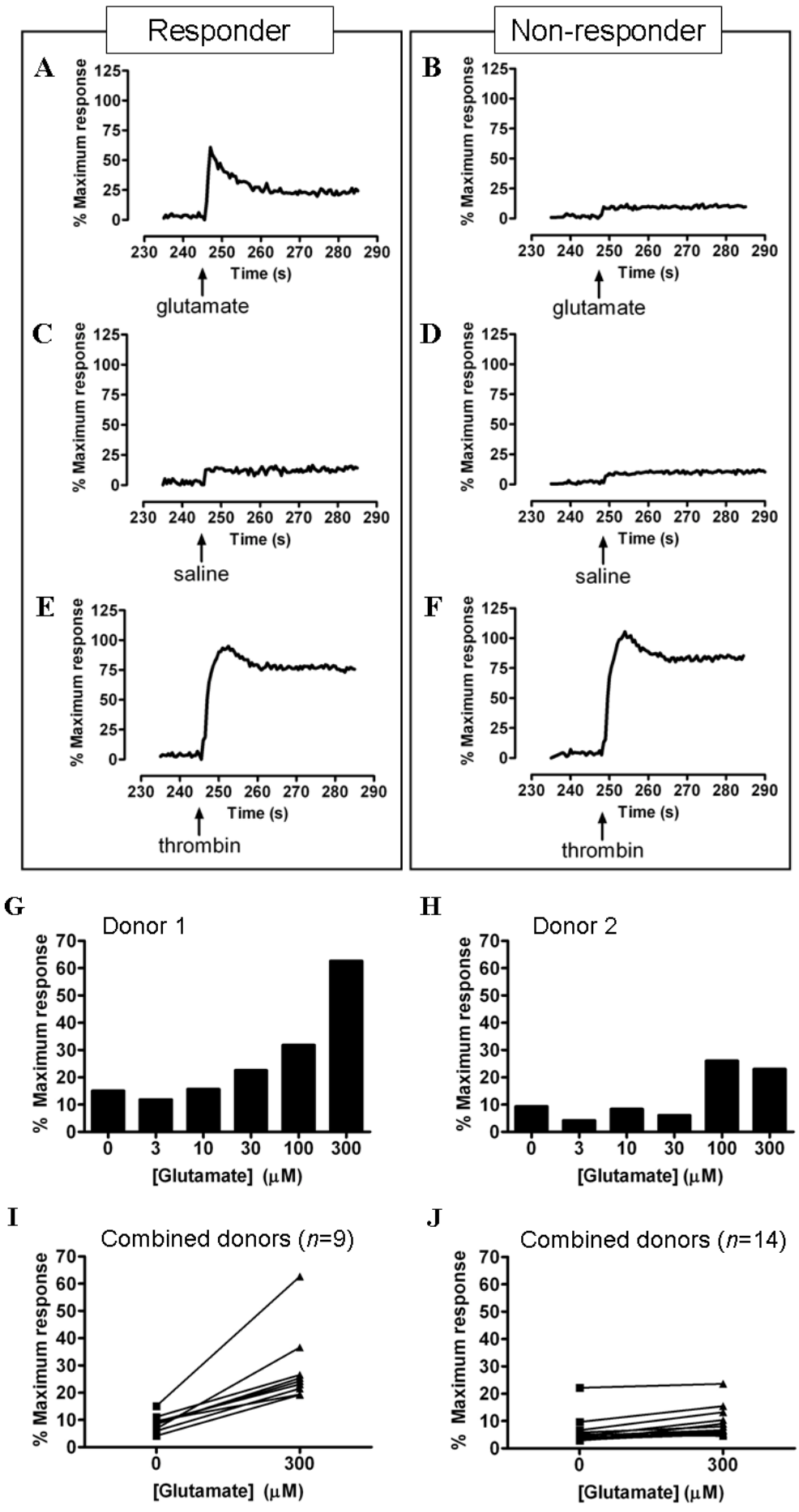
Responder
Non-responder
A
B
C
D
E
F
% Maximum response
Time (s)
glutamate
saline
thrombin
G
H
Donor 1
Donor 2
[Glutamate] (μM)
I
J
Combined donors (n=9)
Combined donors (n=14)

Figure 16. Glutamate evokes an intracellular calcium response in human platelets. Representative traces from 2 different donors exemplifying single kinetic responses to 300 μM glutamate, saline (nominally Ca^{2+}-free salt solution) and 3 U ml^{-1} thrombin. **A, B,** kinetic traces demonstrating that 300 μM glutamate triggers an increase in fluo-4 fluorescence in human platelets. **C, D,** Control responses to the addition of saline alone (nominally Ca^{2+}-free salt solution). **E, F,** Representative traces illustrating the response to the addition of 3 U ml^{-1} thrombin (positive control) from the same donor. The addition of agonists is indicated by an arrow. The % maximum response (% MR; 100 % response) is determined by the addition of 1 μg ml^{-1} ionomycin at the end of each experiment. **G, H,** Each histogram illustrates the peak responses from a single donor obtained within the first 2 h of each experiment (n=1). **I,** Demonstrates the variation in mean responses between responding donors to 0 and 300 μM glutamate (n=9). **J,** Demonstrates the variation in mean response between non-responding donors to 0 and 300 μM glutamate (n=14). Each point represents the mean value from a single experiment for each donor, with the points joined such that the data for each donor at 0 and 300 μM glutamate is linked. All data was obtained within the first 2 h of each experiment.

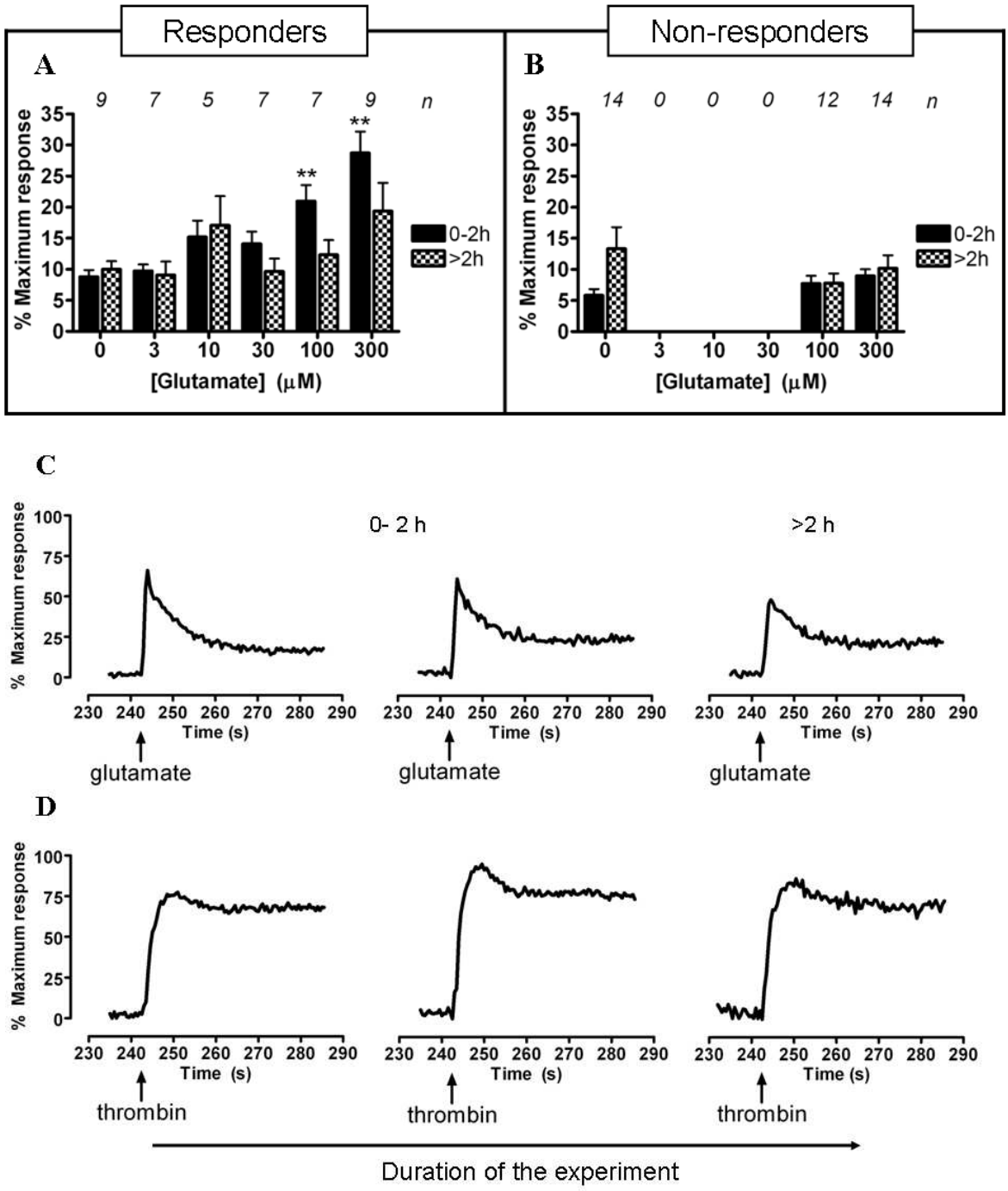

Figure 17. Glutamate evokes an intracellular calcium response in human platelets which varies between donors and decreases over the duration of each experiment. A, B, the data is split into donors which respond to glutamate (A) and those in which a response above control was not observed (B). The solid black bars represent the responses to glutamate in the first 2 h of the experiments with the black checked bars illustrating the responses after 2 h from the start of the experiments. The figures demonstrate that responses to glutamate decrease slightly over time at 30, 100 and 300 μM glutamate with responses to saline remaining static in responding donors. In non-responding donors, all responses to NMDA decrease over time, while responses to saline increase.

The numbers above the columns indicate the number of donors whose data is included (*n*=5-14). **C,** Kinetic traces from 1 experiment using platelets from 1 donor illustrating the decrease in response to 300 μM glutamate over the course of an experiment. **D,** Illustrates the responses to 3 U ml^{-1} thrombin (positive control) in the same experiment demonstrating that while responses to thrombin vary over the course of the experiment, they do not decrease overall. The first 2 responses for both glutamate and thrombin were obtained within the first 2 h of the experiment, with the final response obtained over 2 h from the start of the experiment. Addition of the agonists is indicated by an arrow. The % maximum response (% MR; 100 % response) is determined by the addition of 1 μg ml^{-1} ionomycin at the end of each experiment. The data indicates that there is a dose-dependent effect within the first 2 h of the experiment with responses peaking at 300 μM glutamate. ** $P< 0.01$ compared to 0 μM glutamate using a one-way ANOVA with Dunnetts post-hoc test.

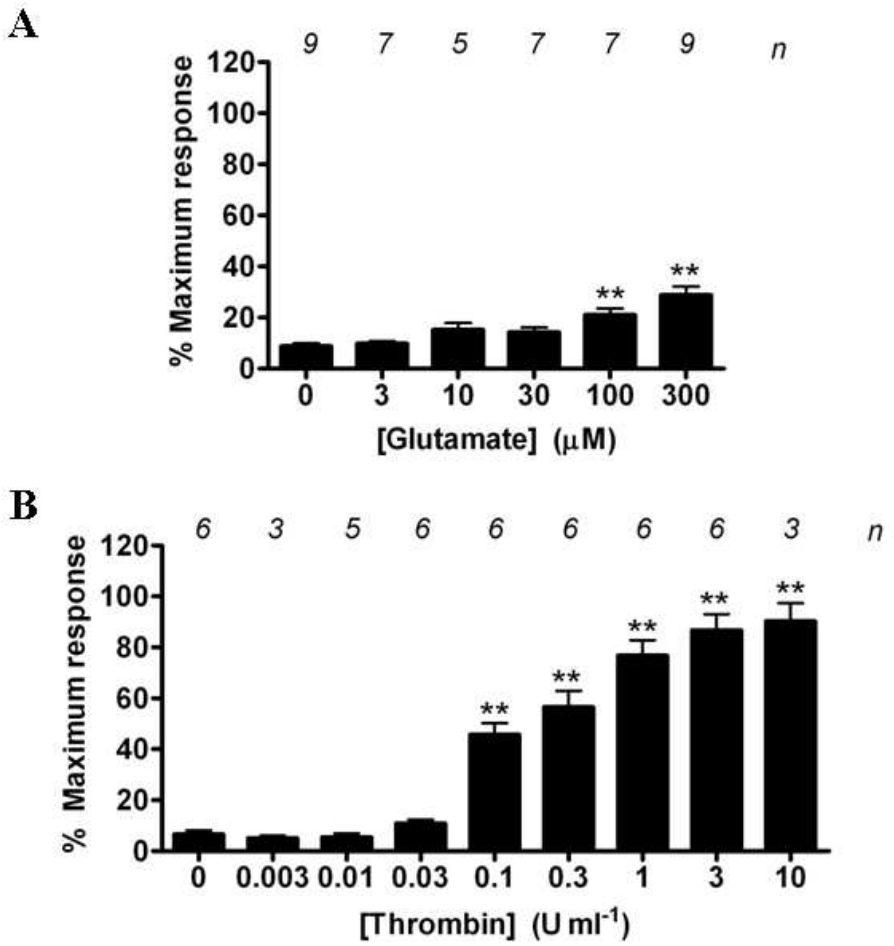

Figure 18. Comparison of the intracellular calcium responses evoked by glutamate and thrombin in human platelets. **A**, Histogram illustrates the peak responses of glutamate-evoked increases in fluo-4 fluorescence in human platelets (*n*=5-9 ± S.E.M), in comparison to those elicited in response to thrombin (**B**) in separate experiments (*n*=3-6 ± S.E.M.). All data was obtained within the first 2 h of each experiment. For the 2 agonists, the fluo-4 fluorescence increases with increasing agonist concentration, where the peak concentration response for glutamate (300 μM) is 58.02 ± 7.17 % MR smaller than that for thrombin (3 U ml^{-1}). The maximum response is determined for each agonist by the addition of 1 μg ml^{-1} ionomycin at the end of each experiment. Numbers above the columns indicates the number of donors from which data has been obtained for each concentration. * P< 0.05; ** P< 0.01 compared to 0 μM glutamate or 0 Uml^{-1} thrombin using a one-way ANOVA with Dunnetts post-hoc test.

It was observed that responses to the extracellular application of glutamate varied between donors (figures 16A and B, G and H), where figure 16A demonstrates a rapid transient increase in response to glutamate in comparison to figure 16B which illustrates a response similar to that elicited by the addition of saline (figures 16C and D). As such I defined parameters to identify a clear 'responder' platelet sample from a 'non-responder' to the addition of extracellular glutamate. For the purpose of this study, a response to glutamate ws defined as an increase of at least 10 % MR above that evoked by the application of saline alone. This figure was used as the majority of responses to saline were between 10- 20 % MR (10 % range) above baseline, therefore to determine whether the agonist had an effect above that of saline the fluorescence response needed to be greater than 10 % MR. Samples which did not elicit an increase 10 % MR or greater than that obtained with saline were designated non-responders (figure 16A and B). However, apparent non-responders were not excluded from the study and all data is summarised as mean responses as well as the individual response for each experiment (figures 16 and 17)

The data was also separated into responses obtained within the first 2 h from the start of an experiment and that obtained after 2 h to determine whether the response desensitised over the duration of the experiment (figure 17). The responses elicited following the application of extracellular glutamate were determined to decrease slightly over time, while maintaining the rapid, transient kinetic shape (figure 17E). The largest response in responding donors throughout the whole duration of the experiments is shown to be evoked with 300 μM glutamate in the first 2 h of the experiments (28.72 ± 3.44 % MR), decreasing after 2 h to 19.34 ± 4.55 % MR (n=9). The mean background response to saline varied slightly over time from 8.79 ± 1.07 to 9.98 ± 1.33 % MR and maintained a small sustained kinetic response throughout (figure 16C). In non-responding donors, saline responses were observed to increase from 5.81 ±1.02 to 13.31 ± 3.48 % MR (n=14) over the duration of the experiments. A small increase occurred in the first 2 h on the addition of 30 μM glutamate in non-responders (11.33 ± 0.71 % MR), which did not reach the 10 % MR increase above saline to reach a response.

In comparison, thrombin was shown to stimulate a rapid sustained response to thrombin at 3 U ml^{-1} both in responding and non-responding donors, which varied slightly over time (figure 16F). The peak thrombin response shifts from 10 to 3 U ml^{-1} during the experiments with mean responses of 90.29 ± 7.09 (0-2 h) and 92.21 ± 14.49 (>2 h) % MR

respectively (*n*=3 and 6) (Appendix I). It was decided to use 3 Uml^{-1} thrombin as a positive control in the rest of the study. The response elicited with 3 Uml^{-1} thrombin was shown to be 61.57 ± 7.86 % MR larger than the peak response in responding donors to glutamate (300 μM) (figure 18). From these data it was determined that the responses to glutamate become slightly desensitised over the course of the experiments and only data from the first 2 h of any experiment will be used for analysis.

The data for all responding donors from the first 2 h of each experiment was pooled to demonstrate the variation in responses to 300 μM glutamate (figure 16I), where the data from non-responders was combined in figure 16J. These illustrate that fluorescence increases in 9 different donors with a mean increase of 19.93 ± 3.60 % MR above saline (responders), while the mean increase in non-responders is 3.14 ± 1.96 % MR above control. This illustrates the variation in responses observed upon the addition of glutamate to isolated human platelets.

3.3.2.2. NMDA and thrombin responses

The ionotropic glutamate receptor family is subdivided by reactivity to NMDA (Dingledene *et al*, 1999), and the expression of the NR1 and NR2D subunit proteins together with responses elicited to extracellular glutamate suggested the presence of NMDARs on human platelets,. The study was therefore extended to investigate the effect of NMDA on platelet functionality.

As described in section 3.3.2.1, triplicate NMDA concentration response curves were performed together, with triplicate repeats of thrombin (3 U ml^{-1}) and saline (positive and negative controls respectively) also assessed. Variation between donors was observed as illustrated in figure 19, with figure 19A illustrating a rapid, transient increase in response to extracellular NMDA in contrast to a small sustained response, comparable to that stimulated with saline (figure 19D). Therefore the data was again separated into that from responders and non-responders as previously (section 3.3.2.1).

The responses were also observed to decrease over the course of the experiments, and data was again separated into that obtained within the first 2 h and that obtained afterward (figure 19). Increases in fluorescence at least 10 % MR above that induced by saline were shown to occur between 3 and 100 μM NMDA in responding donors (figure 20A), with

the peak responses elicited at 3 and 100 μM (30.08 ± 3.75 % MR (*n*=9) and 29.52 ± 6.41 % MR (*n*=4) respectively). All responses to NMDA decrease after 2 h, where the peak response of 22.45 ± 5.55 % MR is obtained with 3 μM NMDA (*n*=9). Saline is the exception to this, with the responses increasing slightly from 7.30 ± 1.32 to 10.14 ± 2.31 % MR (*n*=9) over the duration of the experiments. In non-responding donors, responses to saline increase over the duration of the experiments from 7.63 ± 1.30 to 13.29 ± 3.12 % MR (*n*=6), above which no concentration of NMDA elicits a response. The kinetic responses remain rapid and transient throughout the experiments in responding donors (figure 20E). Thrombin stimulates a rapid sustained response throughout the experiments (figure 20F), with the addition of extracellular thrombin (3 U ml^{-1}) stimulating a response 70.09 ± 8.019 % MR larger than the peak NMDA response (3 μM) (figure 21).

From these data, it was determined that the responses to NMDA desensitise during the course of the experiments, and only data from the first 2 h of any experiment will be used for analysis.

The data for all donors was separated into that from responders and non-responders and plotted to illustrate the variation in responses to 3 μM NMDA (figures 19I and J). It demonstrates that responses to 3 μM NMDA are highly varied between responding donors with a mean increase of 22.79 ± 4.95 % MR above that of saline, in comparison to the mean increase of 3.42 ± 1.49 % above control in non-responding donors. Overall, these data demonstrate that human platelets respond to both glutamate and NMDA leading to an increase in $[Ca^{2+}]_i$. For both agonists, the responses are variable between donors and desensitise following platelet isolation.

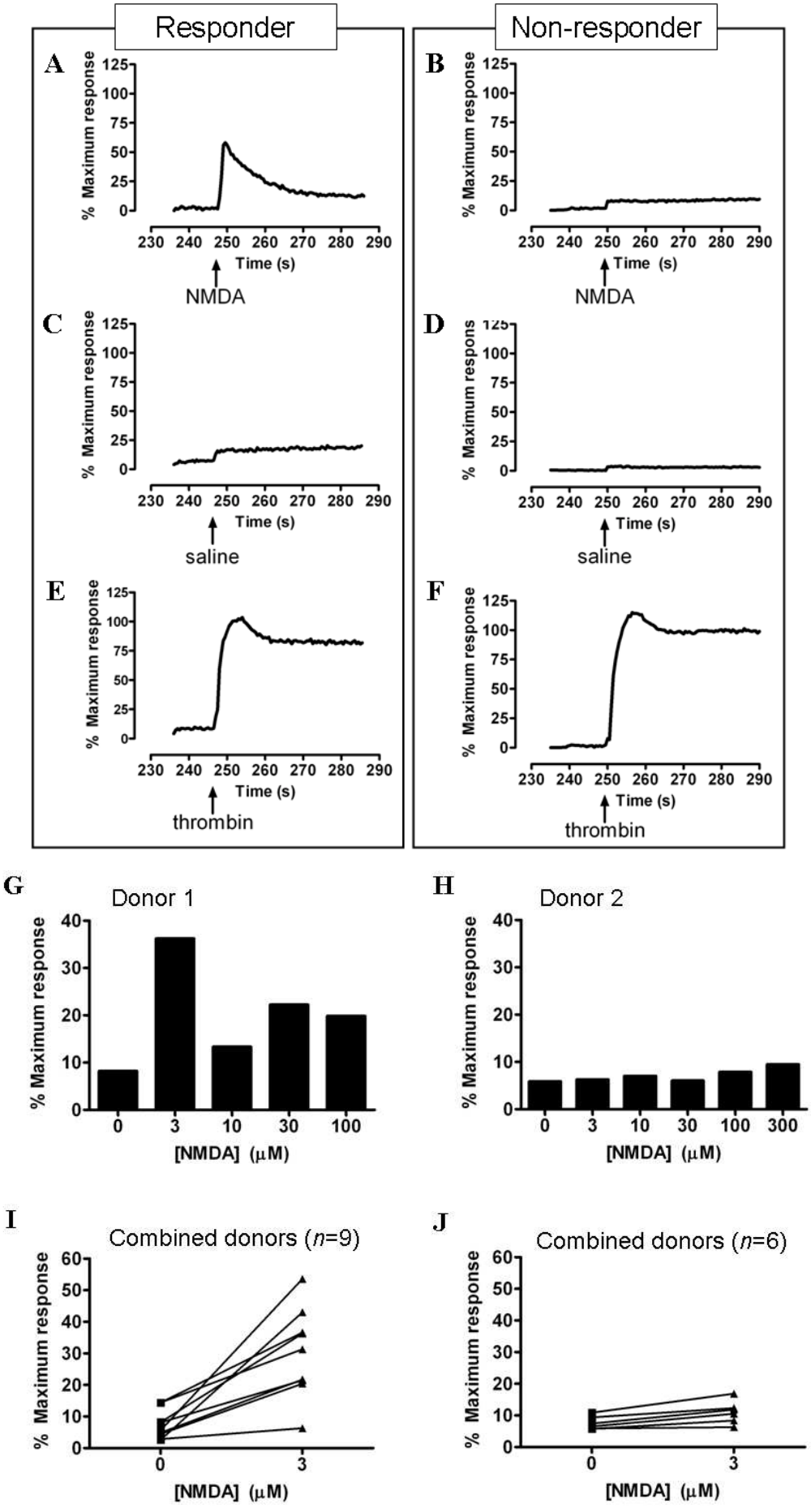
Responder
Non-responder
A
B
C
D
E
F
% Maximum response
Time (s)
NMDA
saline
thrombin
G
Donor 1
H
Donor 2
[NMDA] (μM)
I
Combined donors (n=9)
J
Combined donors (n=6)

Figure 19. NMDA evokes an intracellular calcium response in human platelets. Representative traces from 2 different donors demonstrating single kinetic races in response to 3 μM NMDA, saline (nominally Ca^{2+}-free salt solution) and 3 U ml^{-1} thrombin. **A, B,** Kinetic traces illustrating that 3 μM NMDA elicits an increase in fluo-4 fluorescence in human platelets. **C, D,** Control responses to the addition of saline alone (nominally Ca^{2+}-free salt solution). **E, F,** Representative traces illustrating the response to the addition of 3 U ml^{-1} thrombin (positive control) from the same donor. The addition of agonists is indicated by an arrow. The % maximum response (% MR; 100 % response) is determined by the addition of 1 μg ml^{-1} ionomycin at the end of each experiment. **G, H,** Each histogram illustrates the peak responses from a single donor obtained within the first 2 h of each experiment (*n*=1). **I,** Demonstrates the variation in mean responses between responding donors to 0 and 3 μM NMDA (*n*=9). **J,** Demonstrates the variation in mean responses between non-responding donors to 0 and 3 μM NMDA (*n*=6). Each point represents the mean value from a single experiment for each donor, with the points joined such that the data for each donor at 0 and 3 μM NMDA is linked. All data was obtained within the first 2 h of each experiment.

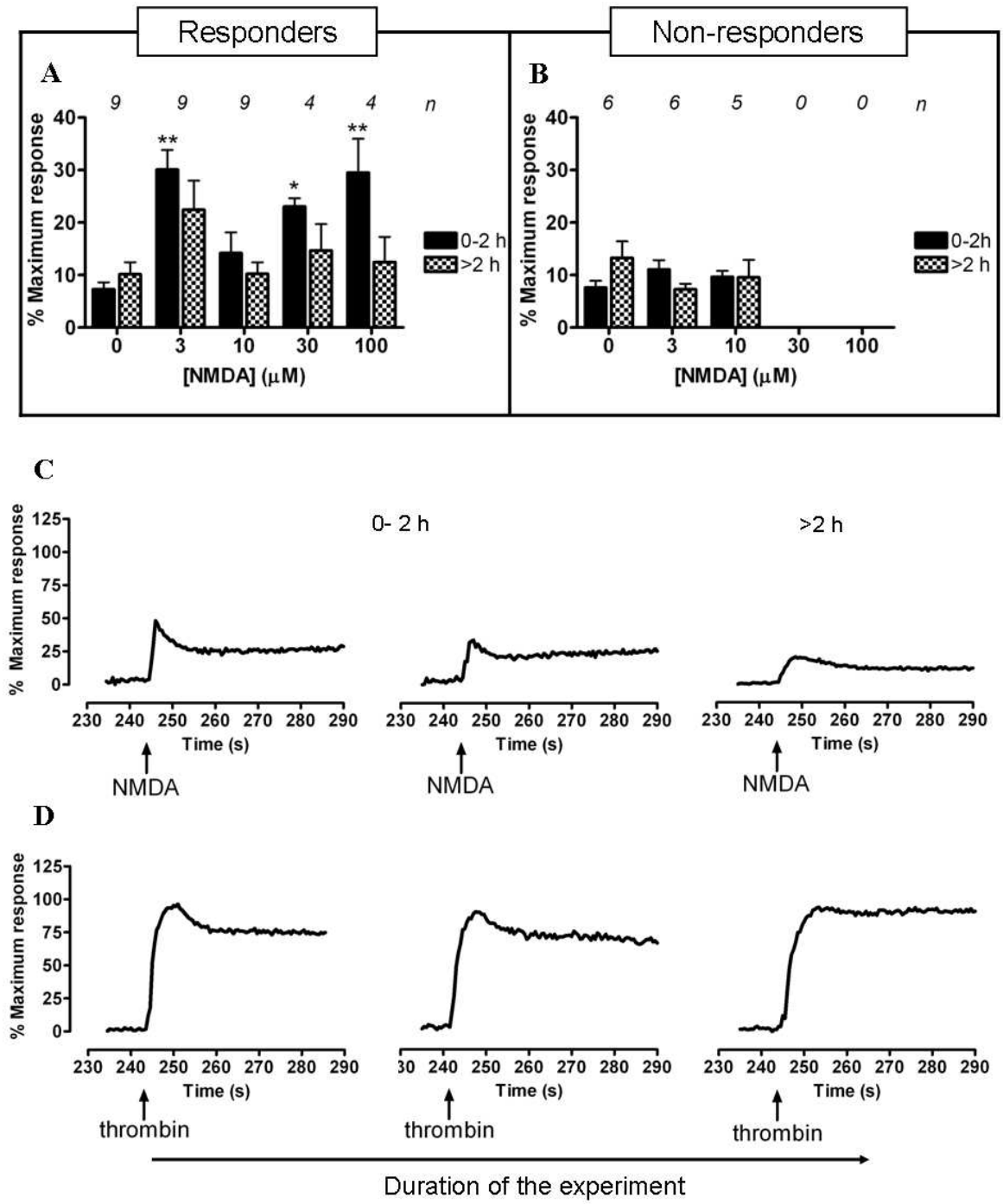

Figure 20. NMDA evokes an intracellular calcium response in human platelets which varies between donors and decreases over the duration of each experiment. A, B, the data is split into donors who respond to NMDA (A) and those in which a response above control was not observed (B). Solid black bars illustrate the responses to glutamate in the first 2 h of the experiments with black checked bars representing the responses after 2 h from the start of the experiments. The figures demonstrate that responses to all concentrations of NMDA decrease over time with responses to saline increasing slightly in both responders and non-responders. The numbers above the columns indicate the number of donors whose data is included (*n*=4-9). **C,** Kinetic traces from

1 experiment using platelets from 1 donor illustrating the decrease in response to 3 μM NMDA over the course of an experiment. **D,** Illustrates the responses to 3 U ml^{-1} thrombin (positive control) in the same experiment demonstrating that while responses to thrombin vary over the course of the experiment, they do not decrease overall. The first 2 responses for both NMDA and thrombin were obtained within the first 2 h of the experiment, with the final response obtained over 2 h from the start of the experiment. Addition of the agonists is indicated by an arrow. The % maximum response (% MR; 100 % response) is determined by the addition of 1 μg ml^{-1} ionomycin at the end of each experiment. The data indicates that there is a dose-dependent effect within the first 2 h of the experiment with increases in response between 3 and 100 μM NMDA, with peaks at 3 and 100 μM NMDA. The smallest decrease over time is observed with 3 μM NMDA. * $P< 0.05$; ** $P< 0.01$ compared to 0 μM glutamate using a one-way ANOVA with Dunnetts post-hoc test.

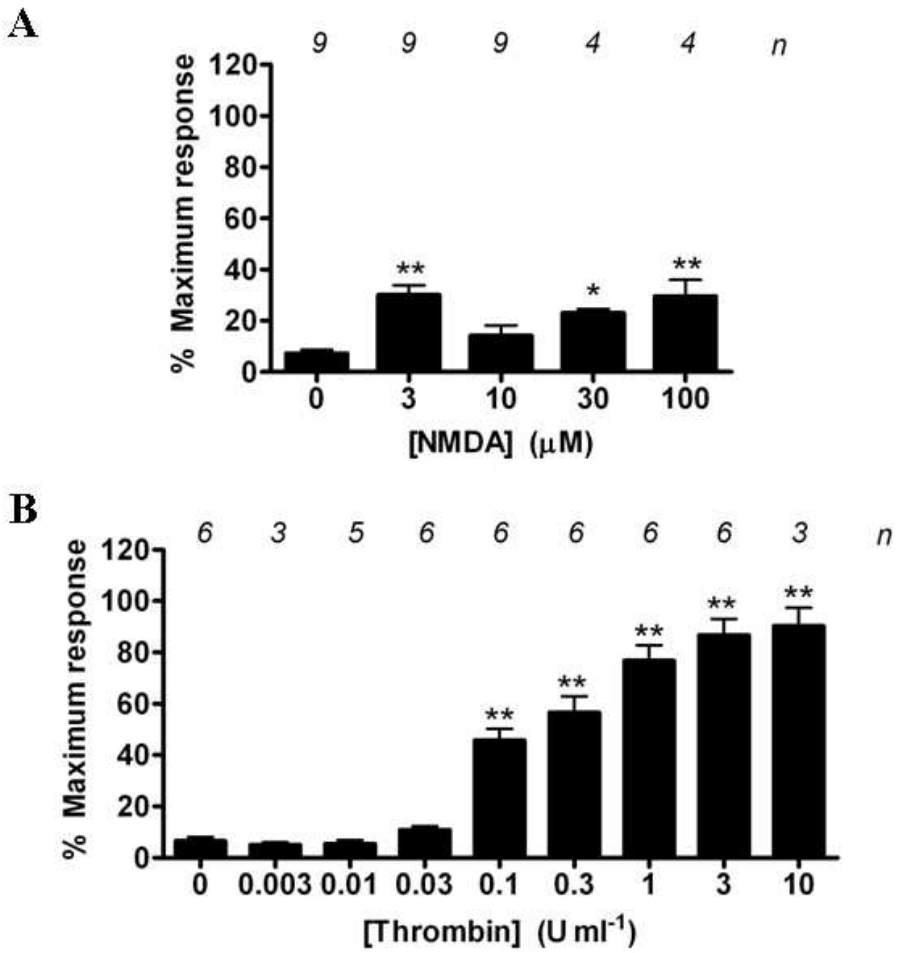

Figure 21. Comparison of intracellular calcium responses evoked by NMDA and thrombin in human platelets. **A**, Histogram illustrates the peak responses of NMDA-evoked increases in fluo-4 fluorescence in human platelets (*n*=8-22 ± S.E.M.), in comparison to those elicited by the addition of thrombin (**B**) in separate experiments (*n*=3-6 ± S.E.M.). All data was obtained within the first 2 h of each experiment. In comparison to thrombin, NMDA-evoked fluo-4 fluorescence is not dose dependent. The maximum response is determined for each agonist by the addition of 1 μg ml^{-1} ionomycin at the end of each experiment. * P<0.05; ** P< 0.01 in comparison to 0 μM NMDA or 0 U ml^{-1} thrombin using a one-way ANOVA with a Dunnetts post-hoc test.

3.3.3. Measurement of extracellular ATP secretion from human platelets

ATP is secreted from activated platelets and can be detected using the firefly enzyme luciferase (Beigi *et al*, 1999). Light is produced in a manner directly proportional to ATP concentration, therefore by running known ATP concentrations for each experiment, the light recorded can be converted into ATP concentrations (figure 12). The sensitivity of the assay to ATP concentration was determined using a range of serial dilutions, and the resulting peak responses used to produce a standard curve. From this, the sensitivity of the method was shown to be > 10 nM ATP (figure 12B).

Previous studies have shown that some chemicals have non-specific effects on the luciferin-luciferase assay (Reigada *et al*, 2006). Therefore, each chemical was tested prior to use in both the presence and absence of 100 nM ATP and compared to their equivalent controls to ensure that this was not the case (figure 22).

3.3.3.1 Glutamate and thrombin responses

Initial work investigated the ATP release from human platelets, where a glutamate concentration response was performed in triplicate, with triplicate repeats of thrombin (3 U ml^{-1}) and paired saline responses (positive and negative controls) also assessed. The responses to extracellular glutamate varied in size between donors with platelets, with responders defined as those who produced an increase in ATP secretion of at least 40 nM ATP above that obtained from the same donor with saline to at least 1 concentration of glutamate. No donors were found who did not give this response to at least 1 glutamate concentration (figure 23). The variation in responses to glutamate is also demonstrated in figures 24A, B, E and F.

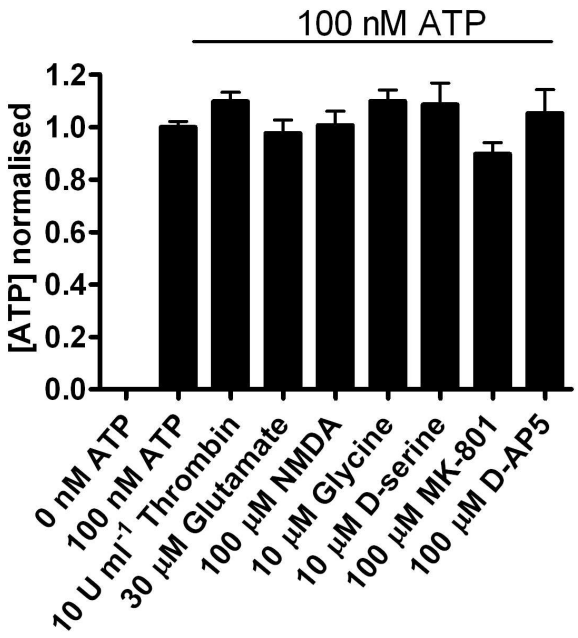

Figure 22. Determining the effects of different chemicals used in this study on the ATP luciferin-luciferase assay under cell-free conditions. None of the agonists or antagonists tested quenched the luminescence produced by the binding of ATP to the luciferase enzyme. This indicates that changes in luminescence observed in the presence of platelets are due to that stimulated by the effect of the chemical on the cells as opposed to the luciferase enzyme. Values represent mean ± s.e.m.; *n*=3. Luminescence was converted to ATP concentrations using calibration curves, and normalised against that obtained when 100 nM ATP was added in absence of NMDAR agonists/ antagonists in cell-free conditions.

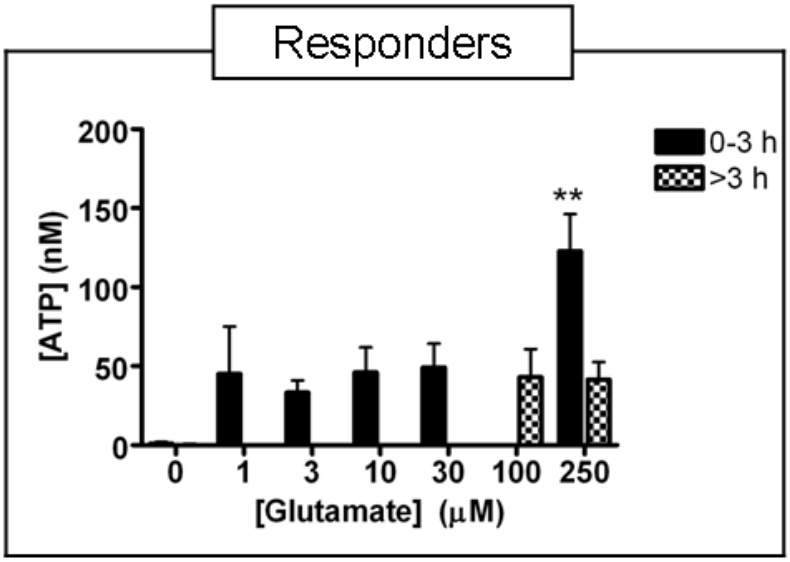

Figure 23. Glutamate-evoked ATP release changes over time. The data shows donors who responded to glutamate. No non-responders were found in the donors tested with extracellular glutamate. Solid black bars represent the responses to glutamate over the first 3 h of the experiments with black checked bars illustrating the responses 3 h from the start of the experiment. They demonstrate that largest responses are obtained with 250 μM glutamate in the first 3 h of the experiments. This effect is lost after 3 h, and the responses become more variable. The responses to saline remain static. The number of donors varies for each concentration of glutamate, with 15 donors for 0 μM (saline); 3 for 0-3 h 1-30 μM; 3 at >3 h, 100 μM; and 13 donors for both bars at 250 μM glutamate. **P< 0.01 in comparison to 0 μM glutamate using a one-way ANOVA with a Dunnetts post-hoc test.

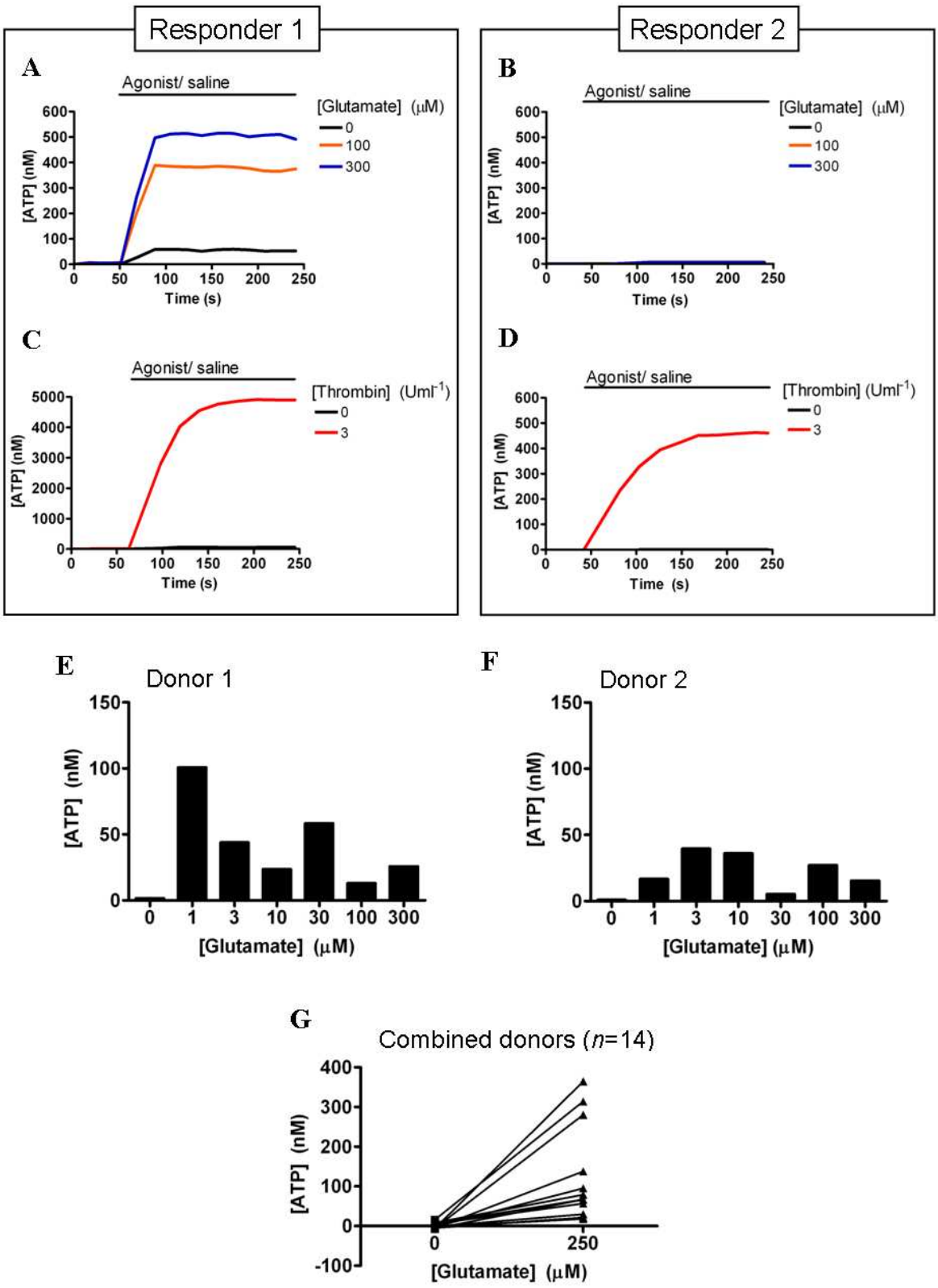
Responder 1
Responder 2
A
Agonist/ saline
[Glutamate] (μM)
0
100
300
[ATP] (nM)
Time (s)
B
C
[Thrombin] (Uml-1)
3
D
E
Donor 1
[Glutamate] (μM)
F
Donor 2
G
Combined donors (n=14)

Figure 24. Glutamate triggers ATP secretion from human platelets. **A, B,** Representative traces from 2 different donors illustrating single kinetic traces in response to 0, 100 and 300 μM glutamate. **C, D,** Representative responses to the addition of thrombin (3 U ml^{-1}; positive control) for the same donors. The duration of agonist application is indicated by the line above each graph. Note the difference in scale for the thrombin response for the responding donor. **E, F,** Each histogram represents the responses from a single donor (*n*=1). **G,** Demonstrates the variation in mean responses between responding donors to 0 and 250 μM glutamate (where the response may not have been obtained on the addition of 250 μM glutamate) (*n*=12). Each point represents the mean value from a single experiment for each donor, with the points joined such that the data for each donor at 0 and 250 μM glutamate is linked. All data was obtained within the first 3 h of each experiment.

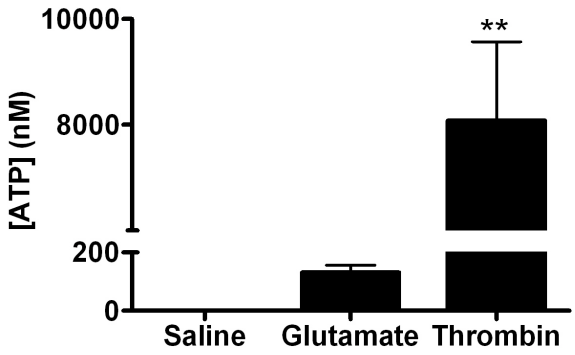

Figure 25. Comparison of peak ATP release elicited by glutamate and thrombin. Histogram comparing the peak responses of glutamate (250 μM) and 3 U ml^{-1} thrombin –evoked ATP release from human platelets; *n*=13 ± S.E.M. for glutamate and control (nominally Ca^{2+}-free salt solution) and *n*=6 ± S.E.M. for thrombin. This illustrates that glutamate-evoked ATP release is 93.31 ± 5.90 % less than that stimulated by thrombin. ** P< 0.01 compared to control using a one-way ANOVA and Dunnetts post-hoc. Data was obtained in the first 3 h of each experiment.

Separating the data into that obtained within the first 3 h of the experiment and that obtained afterwards, demonstrates a dose-dependent trend in the data from responding donors which increases at 250 μM glutamate (122.78 ± 23.49 nM ATP, *n*=13; figure 22A). After 3 h, the response to 250 μM glutamate drops to 41.53 ± 11.09 nM ATP (*n*= 13). The background ATP release in response to saline decreases over time from 1.06 ± 1.02 to -0.46 ± 1.10 nM ATP. In comparison to thrombin responses, peak glutamate responses elicited with 250 μM glutamate are 93.31 ± 5.90 % smaller than that elicited with 3 U ml^{-1} thrombin (figure 25). From these data, it was determined that the ATP release stimulated by extracellular glutamate becomes more variable after 3 h of each experiment, therefore only data from this period of the experiments will be used for analysis.

The data for 13 donors obtained within the first 3 h of their respective experiments was pooled to demonstrate that variation between donors in response to both saline and 250 μM glutamate (*n*=13; figure 24G). It illustrates that the increase in ATP release is highly varied with 3 donors showing a larger mean increase than the other 10 donors (mean ATP release of 319.44 ± 25.62 nM ATP), with another 3 demonstrating either a very small or no ATP release upon the addition of extracellular glutamate (23.10 ± 2.76 nM ATP). The remaining 7 donors demonstrate an average increase of 81.21 ± 11.23 nM ATP. Overall, these data demonstrate that extracellular glutamate triggers ATP secretion in human platelets that varies over time.

3.3.3.2 Glutamate, glycine and inhibitors

Full activation of NMDARs is achieved with the addition of a co-agonist, for example glycine, and the study was extended to investigate the effects of adding 2 different concentrations of glycine, 0.3 and 10 μM, in combination with glutamate. The study was taken further by testing the effect of the NMDAR specific inhibitors MK-801 and D-AP5 on responses elicited by glutamate and glycine to further test the functionality of the hypothesised NMDA receptors. A high concentration of each of the inhibitors (100 μM) was used to ensure that the maximal effect of the inhibitors was obtained. IC_{50} values have been defined as 0.6 μM for MK-801 and 0.9 μM D-AP5 (Lombardi *et al*, 2001).

The addition of 0.3 μM glycine with 250 μM glutamate was found to have no discernable effect on the overall ATP release (*n*=12 and 5 respectively; figure 26). This release is inhibited by the addition of either inhibitor (*n*=5). The data for the 5 donors on which

0.3 μM glycine was used is shown more clearly in figure 26D. It demonstrates that the addition of glutamate stimulates increases in 4 out of 5 donors above saline only, 1 of which shows a further increase with the addition of glycine, 2 demonstrating a decrease in ATP release, with the final 2 showing no observable change in ATP release. The addition of 100 μM MK-801 stimulated a large decrease in 1 donor, with little or no decrease in the other 4. In comparison, the addition of 100 μM D-AP5 caused a decrease in ATP release in 3 donors, and little of no effect in the remaining 5.

Increasing the glycine concentration to 10 μM led to an inhibition of ATP release in comparison to that evoked with 250 μM glutamate alone (50.64 ± 9.25 nM ATP (*n*=8) compared to 131.51 ± 24.63 nM ATP (*n*=12)) (figure 28C). The addition of the inhibitors had no effect on ATP release above that induced with the addition of 10 μM glycine to glutamate (54.54 ± 21.49 nM ATP (*n*=7) with 100 μM MK-801 and 51.53 ± 13.96 nM ATP (*n*=7) with 100 μM D-AP5). Displaying the data differently, figure 28D illustrates the differences in responses between donors. Of the donors tested with glutamate, 5 demonstrate an increase in ATP release in, with little or no increase in the remaining 2 donors. The application of 10 μM glycine together with glutamate causes an increase in response in 1 donor, decrease in 3 donors, and little or no change in the remaining 3 donors. The presence of MK-801 increases ATP release in 2 donor and decreases in another 2. D-AP5 stimulates an increase in 2 donors, decreases in 2 and has no effect in the remaining 3. Overall, overall these data demonstrate that the concentration of glycine used in combination with glutamate affects the ability of the induced ATP secretion from human platelets to be inhibited by MK-801 or D-AP5. This is a small sample of donors with variable responses and further studies are required to fully characterise the action of MK-801 and D-AP5 on responses induced by glutamate alone, and further evaluate the additional action of glycine.

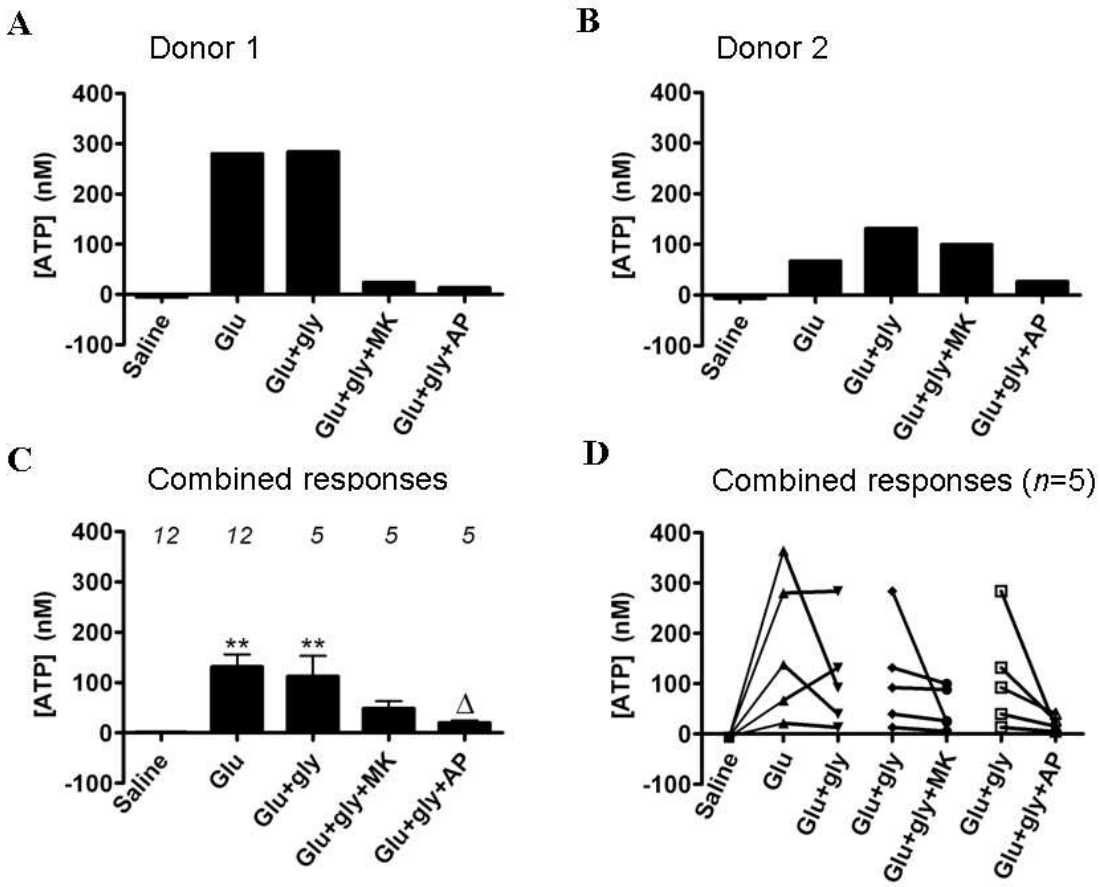

Figure 26. Glutamate and glycine (0.3 μM) trigger ATP release from human platelets which is inhibited by MK-801 and D-AP5. **A, B,** Histograms illustrate the variation in ATP release between 2 different donors in response to 250 μM glutamate alone or in combination with 0.3 μM glycine and the effects of the inhibitors MK-801 or D-AP5 (each 100 μM) (*n*=1). **C**, Histogram illustrates the combined peak data from 5-12 different donors (numbers above the columns indicate the number of donors data is included (*n*=5-12 ± S.E.M.). **D,** Plot illustrates the variation between donors with glutamate increasing the ATP released in 4 donors, with the response further increased by the addition of glycine in 2 of the donors. The responses were inhibited in 3 out of 5 donors by MK-801 and in 4 out of 5 donors by D-AP5. This figure demonstrates that glutamate alone or in combination with glycine stimulates ATP release from human platelets which can be inhibited by either MK-801 or D-AP5 (*n*=5). Saline, nominally Ca^{2+}-free salt solution; glu, glutamate; gly, glycine, MK, MK-801; AP, D-AP5. ** P< 0.01 compared to control using a one-way ANOVA with Dunnetts post-hoc test; Δ P< 0.05 compared to glu + gly using an unpaired, 2-tailed Students *t*-test. All data was obtained within the first 3 h of each experiment.

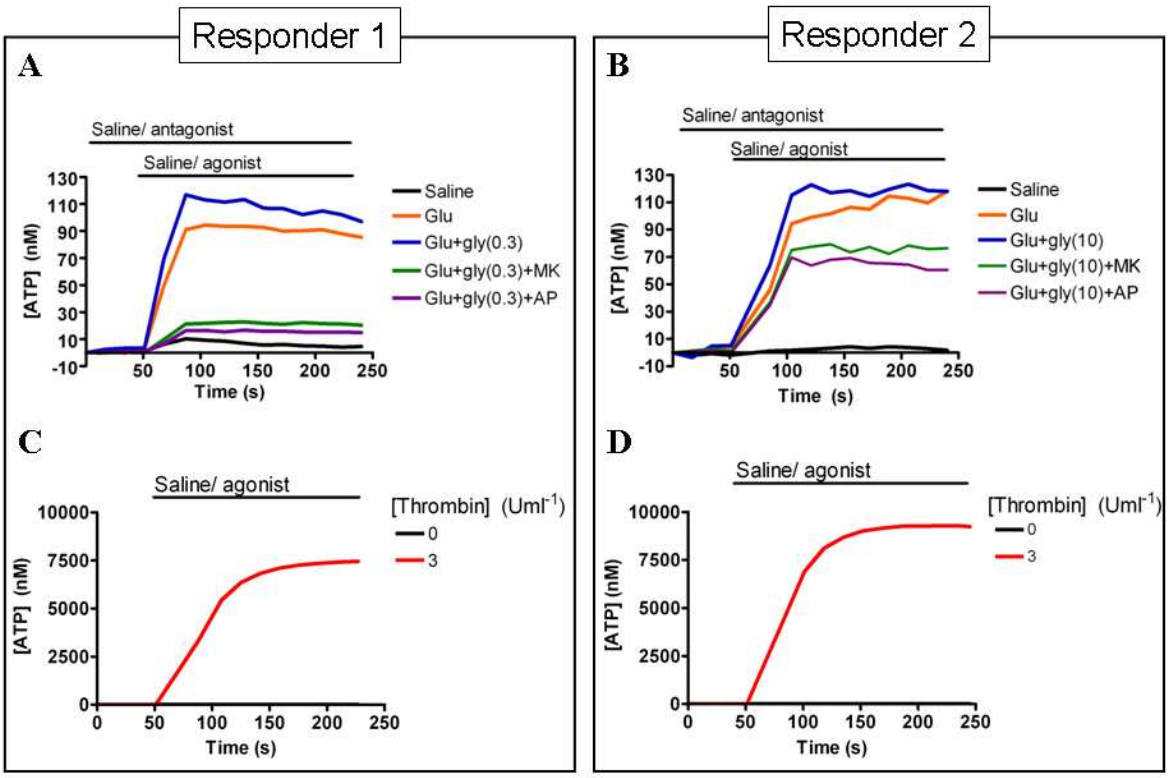

Figure 27. Glutamate and glycine evoke ATP release from human platelets which is inhibited by MK-801 and D-AP5. **A,** Representative single kinetic responses elicited by the addition of 250 μM glutamate in the presence and absence of 0.3 μM glycine, and the effect of the inhibitors, MK-801 and D-AP5 (both 100 μM); **B.** Representative single kinetic responses elicited by the addition of 250 μM glutamate in the presence and absence of 10 μM glycine, and the effect of the inhibitors, MK-801 and D-AP5 (both 100 μM) (Genever *et al*, 1999; Hitchcock *et al*, 2003). Samples were taken from 2 different donors, with one represented in either A or B. Glu- glutamate; gly- glycine; MK- MK-801; AP- D-AP5. **C, D,** Representative traces from the same donors showing responses to 3 U ml^{-1} thrombin (positive control). The lines indicate the duration of application of the agonists, inhibitors and saline (nominally Ca^{2+}-free salt solution). Data was obtained within the first 3 h of each experiment.

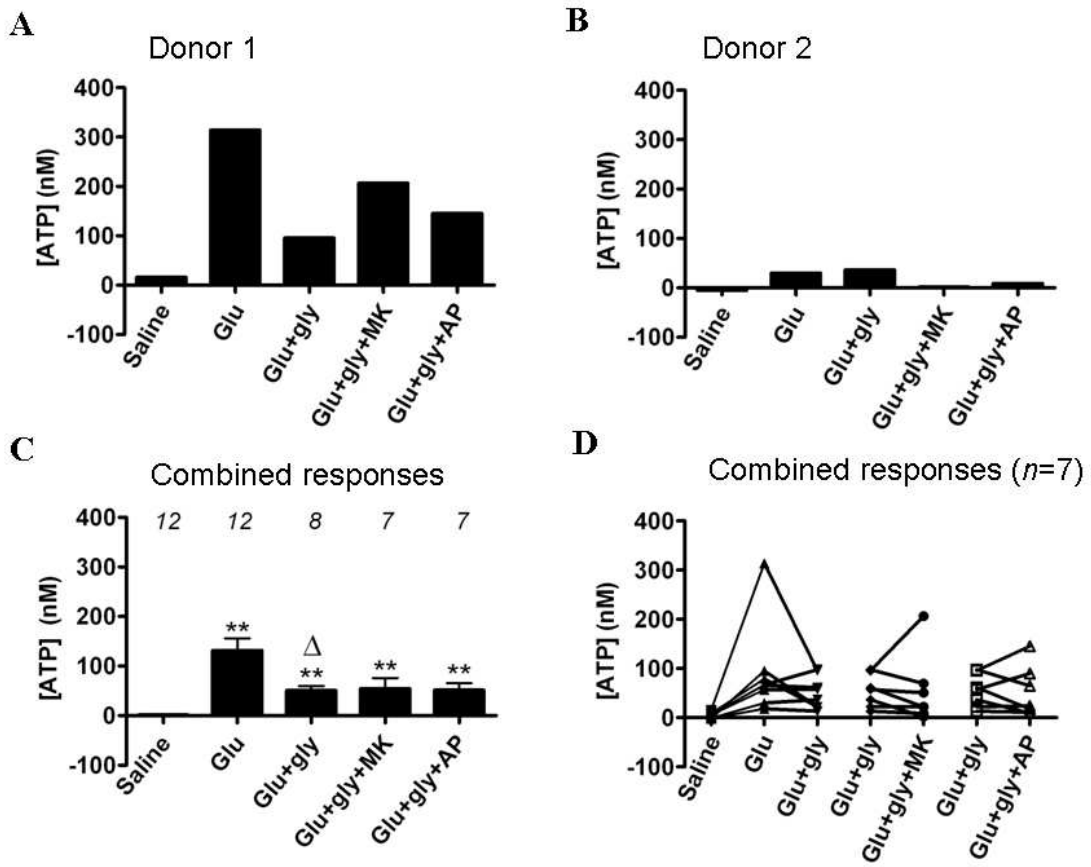

Figure 28. Glutamate and glycine (10 μM) trigger ATP release from human platelets which is not inhibited by MK-801 and D-AP5. A, B, Histograms illustrate the variation in ATP release between 2 different donors in response to 250 μM glutamate alone or in combination with 10 μM glycine and the effects of the inhibitors MK-801 or D-AP5 (each 100 μM) (*n*=1). **C**, Histogram illustrates the combined peak data from 7-12 different donors (numbers above the columns indicate the number of donors' data included (*n*=7-12 ± S.E.M.). **D,** Plot illustrates the variation between donors, with glutamate increasing the ATP released in 5 donors, with the response further increased by the addition of glycine in 1 of the donors, with the response decreasing in another 4 donors. The responses were inhibited in 3 out of 6 donors by MK-801 and in 3 out of 6 donors by D-AP5. In 1 donor the addition of MK-801 caused an increase in ATP release, as with 2 donors with D-AP5. This figure demonstrates that glutamate alone stimulates ATP release, however the addition of 10 μM glycine has an inhibitory affect such that the further addition of inhibitors has no effect on response (*n*=7-8). Saline, nominally Ca^{2+}-free salt solution; glu, glutamate; gly, glycine, MK, MK-801; AP, D-AP5. ** P< 0.01 compared to control using a one-way ANOVA with Dunnetts post-hoc test; Δ P< 0.05 compared to glu + gly using an unpaired, 2-tailed Students *t*-test. All data was obtained within the first 3 h of each experiment.

3.4. Discussion

In this study I have demonstrated that human platelets (i) express NMDAR NR1 and NR2D subunits, (ii) glutamate and NMDA elicit an increase in cytosolic $[Ca^{2+}]_i$ in a percentage of donors and (iii) glutamate evokes ATP secretion sensitive to inhibition by NMDAR antagonists.

3.4.1. NMDA receptor subunit expression

Previous studies have demonstrated the expression of NMDAR NR1, NR2C and NR2D subunit mRNA in the MEG-01 cell line and NR2A and NR2D in native MKs, with the NR1 subunit protein also found to be expressed in human platelets (Genever *et al*, 1999; Hitchcock *et al*, 2003; Hitchcock, 2003). In this study, the expression of both NR1 and NR2D subunit proteins in human platelets has been determined (figures 13 and 15). The mRNA expression of another NR2 subunit, NR2A, has also been determined in primary MKs (Hitchcock *et al*, 2003). However, in this study, expression of the NR2A subunit protein in human platelets has not been detected (figure 14). Expression of the NR1 and NR2D subunit proteins suggests the presence of the classic NMDAR conformation, NR1/NR2 in human platelets, which requires either extracellular glutamate or NMDA for activation (Matsui *et al*, 1995). While the subunit proteins are present, it does not automatically follow that any receptors formed are functional; this therefore requires further investigation into known aspects of platelet activation.

3.4.2. Donor variation

Variation was detected in expression of the NR1 and NR2 subunit proteins between donors (figures 13 and 15), which was also observed during measurements of Ca^{2+} responses, where a Ca^{2+} response to glutamate or NMDA was not detected in 8 out of 24 donors tested. The variations in Ca^{2+} responses may be due to (i) the differences in protein expression or (ii) differences in the number of functional receptors formed. It is possible that the donors which express higher levels of the subunit proteins are more susceptible to glutamate and NMDA, and evoke larger responses. This is however dependent on the subunit proteins expressed forming functional receptors, the number of which may be low even with high levels of expression.

3.4.3. NMDA receptor-evoked calcium responses

NMDAR activation leads to the opening of the receptor's pore, through which cations including Ca^{2+} and Na^{+} pass and are predicted to regulate platelet activation. It can therefore be assumed that if functional NMDARs are expressed on human platelets, stimulation by extracellular glutamate will induce an increase in $[Ca^{2+}]_i$ which can be detected, for example as in this study using the fluo-4 assay (section 3.3.2.).

3.4.3.1. NMDAR desensitisation

In assays investigating changes in $[Ca^{2+}]_i$, it was found that donors could be split into 2 distinct groups; those which respond to extracellular glutamate, and those which do not (figure 16). It was also noted that responses to extracellular glutamate decrease over time, with the greatest decreases observed over 2 h from the start of the experiment, which was in total 3 to 3.5 h from the whole blood being taken from the donor (figure 17). In comparison, the responses to thrombin are only slightly affected by time (figure 17F). Desensitisation of platelet ionotropic receptors is not unknown, with the $P2X_1$ receptor requiring the presence of apyrase (an ADP/ATPase) in the PRP following isolation, to maintain receptor activity (MacKenzie *et al*, 1996). It is predicted that endogenous ATP released from dense granules results in the desensitization of platelet $P2X_1$ receptors (Mackenzie *et al*, 1996). I hypothesise that NMDARs may also undergo desensitisation as glutamate is known to be stored in dense granules and is therefore co-released with ATP (Zoia *et al*, 2004). Release of dense granule contents is important for signalling as it maintains activation of the original platelet and triggers activation of neighbouring cells, finally leading to thrombus formation.

3.4.3.1.1. Calcium

Ca^{2+} has been found to play a role in NMDAR desensitisation, with activation of NMDARs leading to increases in $[Ca^{2+}]_i$ and the formation of Ca^{2+} micro-domains close to the intracellular face of the receptors, reducing the open probability of the NMDARs, leading to desensitisation (Hardingham *et al*, 2001; Rosenmund and Westbrook, 1993). This effect increases with rising extracellular $[Ca^{2+}]$, where maximal desensitisation reached at approximately 1 mM Ca^{2+} (Legrendre *et al*, 1993). This effect is fully reversible, with the rate of clearance from the cytoplasm limited by the movement of Ca^{2+} out of the cells through a combination of Na^{+}/Ca^{2+} exchangers and Ca^{2+} ATPase-pumps located in the plasma membrane, both of which play a functional role in platelets (Harper

and Sage, 2007; Brown and Dean, 2007). In neurones, voltage-gated Ca^{2+} channels have also been implicated in the Ca^{2+} micro-domain formation, and hence NMDAR desensitisation. To date, these channels have not been found to be expressed in platelets (Mahaut-Smith *et al*, 1999), and are not expressed in MKs, with the sole exception of guinea pig MKs (Kawa *et al*, 1990). This suggests that the movement of ions through ion channels plays a more important regulatory role in platelets than in neurones.

3.4.3.1.2. Fibrillar actin

Fibrillar actin (F-actin) has been shown to play a role postsynaptically in NMDAR desensitisation in combination with Ca^{2+} (Rosenmund and Westbrook, 1993b). Ca^{2+} is required for actin depolymerisation and a previous study has shown that treating cells with phalloidin, which inhibits the movement of actin filaments, maintaining them in the polymerised state, prevents Ca^{2+}-induced rundown of NMDARs (Rosenmund and Westbrook, 1993b). This suggests that actin depolymerisation, triggered by the influx of Ca^{2+} into the cell through the NMDAR leads to rundown of the receptor and could potentially be implicated in platelet activation, during which reorganisation of the platelet cytoskeleton is known to occur (Italiano *et al*, 1999; Italiano and Shivdasani, 2003).

NMDAR desensitisation has also been investigated in other expression systems, for example HEK293 cells. Each study has shown variation in their results, demonstrating that responses in transfected cells can be just as varied as in native cells (Krupp *et al*, 1996; Medina *et al*, 1995; Kendrick *et al*, 1998). Therefore data obtained from transfected cells requires comparison with that from native cells to determine whether they represent an accurate model.

3.4.3.2. Glutamate/ NMDA versus thrombin-mediated calcium responses

In comparison to the responses elicited with thrombin, the maximal response obtained on the addition of extracellular glutamate was smaller by 58.02 ± 7.17 % MR (figure 18). Thrombin activates platelets through cleavage of the PAR1 and 4 receptors, which are known to induce platelet activation leading to full aggregation (Gambaryan *et al*, 2010). In contrast, glutamate induces a small, rapid, transient influx of Ca^{2+} into the platelet (figure 16A). It is possible that this small response plays a vital role in platelet activation, such as has already been determined for the extensively studied $P2X_1$ receptor (Toth-Zsamboki *et al*, 2003). Activation of $P2X_1$ elicits a small, very rapid and transient

response to extracellular ATP, which is also smaller than that elicited by activation of GPCRs (MacKenzie *et al*, 1996). This stimulation primes platelets to other activating factors, for example low concentrations of collagen (Toth-Zsamboki *et al*, 2003). This small response has been demonstrated to play an important role in the initiation of thrombus formation using a $P2X_1$ knockout model, and particularly at the high shear rates which occur in the microvascular (Hechler *et al*, 2003). However, $P2X_1$ knockout mice displayed no spontaneous bleeding phenotype and the tail bleeding time was normal in the majority of the $P2X_1$ knockout mice. This normal bleeding time observed in the $P2X_1$ knockout suggests that the absence of P2X1 only has a minor impact on primary haemostasis. Comparable results were observed with the $P2Y_1$ knockout with no spontaneous bleeding phenotype, or GPVI knockout mice which demonstrated a normal tail bleeding time (Léon *et al,* 1999, Kato *et al,* 2003). This data might suggest that these receptors are more relevant to the pathophysiological conditions associated with increased thrombosis (Kato *et al*, 2003). The generation of a knockout model for the NMDAR NR1 subunit protein has been shown to be neonatally lethal (Li *et al*, 1994; Forrest *et al*, 1994), however establishing a conditional knockdown has been previously demonstrated where the mice show a normal phenotype, and only exhibit effects of the loss of NR1 subunit function when required (Cui *et al* 2004). NR2D knockout mice have been shown to demonstrate a normal phenotype, with no detrimental effect on viability. The only change determined was a reduction in spontaneous exploratory behaviour (Ikeda *et al*, 1995). To date, no knockdown studies have been carried out to investigate the role of NMDARs in platelet function. It would therefore be interesting to determine whether, like the $P2X_1$ receptor, it has a role in the initiation of thrombus formation under conditions of elevated shear rate, or in another facet of platelet activation (MacKenzie *et al*, 1996).

A range of concentrations of NMDA, glutamate and glycine are used in the literature, ranging from 1μM to 1mM NMDA, 100 μM to 1mM glutamate with between 10 and 100 μM glycine (Krupp *et al*, 1996; Legrende *et al*, 1993; Choi and Lipton, 2000; Clarke and Johnson, 2006). In this study, two different concentrations of glycine are used, 0.3 and 10 μM, in combination with 250 μM glutamate (figures 26 and 27), demonstrating a decrease in response in combination with 10 μm glycine in comparison to 0.3 μM. Further experiments could investigate whether this effect is specific to ATP secretion from human platelets as these previous studies primarily use electrophysiology to investigate the effects in neurones or transfected cells, or whether it extends to other assays for example

Ca^{2+} influx. Different combinations of NMDA or glutamate with glycine could determine the optimal combination for platelet activation, which could be compared to those determined for neuronal NMDARs to ascertain any differences in concentrations required for activation, and also any differences in the effects of inhibitors.

3.4.3.3. Glutamate-mediated calcium responses versus ATP secretion

In this study, it has been demonstrated that extracellular glutamate triggers the secretion of ATP, which is sensitive to partial inhibition by the NMDAR-specific antagonists MK-801 and D-AP5 (figures 26 and 27). In contrast to the Ca^{2+} response assays, ATP secretion is detected at a ten-fold lower concentration of glutamate (figures 17 and 23). The increased sensitivity to glutamate in ATP assays may result from (i) differences in sensitivity between the measurements of intracellular Ca^{2+} versus ATP or (ii) activation of non-NMDA glutamate receptors with increased glutamate sensitivity, but low Ca^{2+} permeability.

Firstly, the apparent increase in glutamate sensitivity observed in assays of ATP secretion could be due to the formation of Ca^{2+} micro-domains close to the intracellular face of the NMDAR of Ca^{2+} that has entered upon activation of the receptors, and has been demonstrated in hippocampal neurones (Hardingham *et al*, 2001). The rapid increase in $[Ca^{2+}]_i$ may be sufficient to trigger movement of dense granules to the plasma membrane or the open canalicular system of the platelet, leading to the release of ATP, and could disperse too quickly for the increase to be detected by the fluo-4.

Alternatively, as only partial inhibition of ATP secretion with MK-801 or D-AP5 was detected, this indicates that other glutamate-sensitive receptors which couple to ATP secretion are expressed. Two recent studies report the expression of AMPAR and KARs on human platelets, which elicit the influx of Na^+ and have low permeability to Ca^{2+} (Morrell *et al*, 2008; Sun *et al*, 2009). Other studies have also demonstrated Na^+ influx into human platelets via transient receptor potential vanilloid 1 (TRPV1) channels which are activated by AA derivatives, for example leukotrienes, that have been shown to play a role in atherosclerosis (Harper *et al*, 2009). The influx of Na^+ has been shown to stimulate a secretion of serotonin from the dense granules which can then act on $5HT_{2A}$ receptors on the surface of platelets inducing increases in $[Ca^{2+}]_i$ (Harper *et al*, 2009). Release of serotonin from the dense granules suggests that the other contents are also released,

including ATP, ADP and glutamate, suggesting that other receptors are also activated potentiating the increase in Ca^{2+} influx. This work could be extended by loading cells with Ca^{2+}-sensitive dye and measuring the fluorescent peaks stimulated by the entry of Ca^{2+} into the cells (Sigimori *et al*, 1990). This can be calibrated using known concentrations of Ca^{2+} such that the changes in concentration of intracellular calcium can be determined.

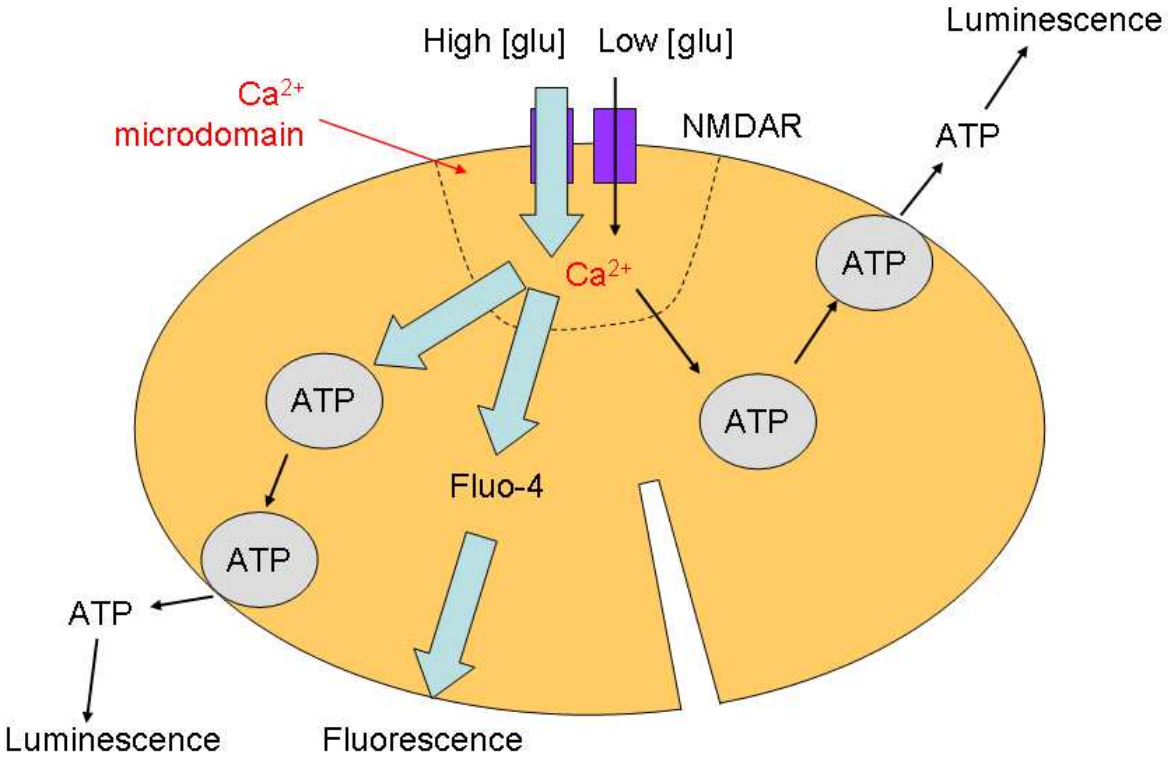

Figure 29. Illustrating the differences in sensitivity between the Ca^{2+} influx and the ATP secretion assays. This demonstrates that while the influx of Ca^{2+} from the activation of the NMDAR with a low concentration of glutamate (glu) might be sufficient to stimulate release of ATP from dense granules, a higher concentration is required for cytoplasmic [Ca^{2+}] to trigger detectable fluorescence through binding to fluo-4.

3.4.4. Previous studies

3.4.4.1. NMDAR function in platelets

Franconi *et al* (1996), have previously demonstrated that NMDARs play an anti-aggregatory role in platelets. Treatment of human platelets with either glutamate or NMDA alone was shown not to induce aggregation, however when the platelets were incubated with NMDA prior to the addition of AA, the aggregation induced by the AA was inhibited. This effect could be inhibited by pre-treatment with MK-801 prior to the addition of NMDA, however it was not observed with D-AP5. NMDA was also found to

inhibit the aggregating effect of ADP in a dose-dependent manner. The generation of cAMP was also investigated, and treatment with increasing concentrations of NMDA shown to increase cAMP production in the presence of extracellular Ca^{2+}.

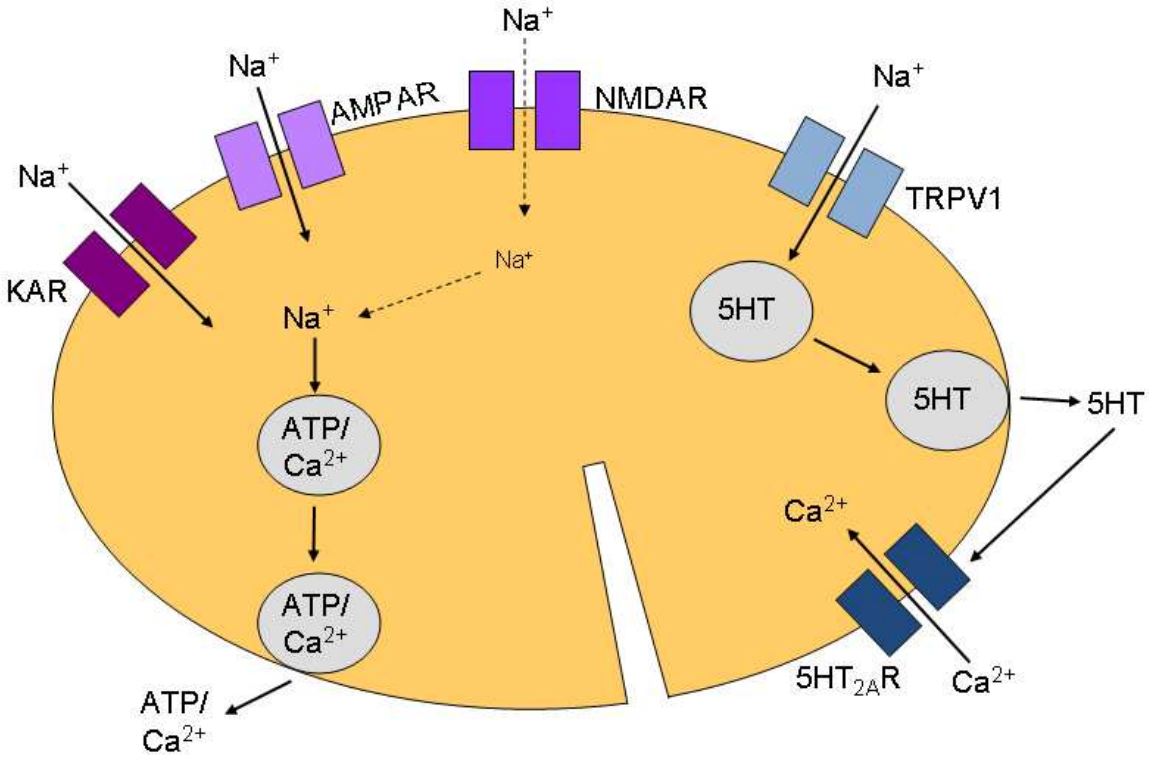

Figure 30. Effect of Na^+ influx into platelets. Na^+ occurs through the AMPA receptors (AMPAR) and kainate receptors (KAR), and to a lesser extent NMDARs (thin arrows). It has been demonstrated that AMPA and kainate alone can not aggregate platelets, but it is suggested that they prime platelets for activation, potentially releasing Ca^{2+} and ATP from the dense granules (grey) to assist in further platelet activation. TRPV1 receptors are also Na^+ permeable which has been shown to stimulate serotonin (5HT) release from dense granules, which in turn activates $5HT_{2A}$ receptors, increasing $[Ca^{2+}]_i$.

In a second paper, this work was extended to determine the effects of NMDA on $[Ca^{2+}]_i$ levels (Franconi *et al*, 1998). Treating human platelets with NMDA alone, demonstrated a dose-dependent increase in $[Ca^{2+}]_i$ with increasing NMDA concentration; this pattern was also shown with AA. Pre-treating the platelets with NMDA had no effect on changes in $[Ca^{2+}]_i$ induced by the addition of AA. However increasing concentrations of NMDA inhibited platelet aggregation at lower concentrations of AA. The addition of NMDA had no effect on thromboxane-stimulated aggregation, but was found to inhibit thromboxane synthesis. Two different anti-aggregating agents were used, indomethacin and ASA to

determine whether inhibition of the cyclo-oxygenase (COX) cascade was implicated. It was found that each of the inhibitors separately reduced the maximum aggregation, the extra addition of increasing concentrations of NMDA caused an almost complete inhibition of aggregation.

Comparing these investigations with this study demonstrates that they all observe increases in $[Ca^{2+}]_i$ stimulated by increasing concentrations of NMDA (figures 19 and 20; Franconi *et al*, 1998). In my study, changes in $[Ca^{2+}]_i$ are detected within seconds of the addition of NMDA or glutamate (figures 19 and 16), however in experiments investigating $[Ca^{2+}]_i$ detailed in Franconi (1998), platelets were pre-incubated with NMDA for 100s before taking readings. Franconi had previously stated that neither glutamate nor NMDA added alone modified platelet functionality (1996), and in 1998 also notes that the anti-aggregatory effect of NMDA does not vary within a 5-40 min interval. This suggests that the role of NMDAR in platelet activation is not sufficient alone to affect aggregation, but potentially plays a role in the initiation of the activation process, and further work is required to fully understand this role.

3.4.4.2. Non-NMDAR expression and function in platelets

It has previously been demonstrated that platelets release glutamate (D'Andrea *et al*, 1991), however the role of glutamate has until recently not been investigated in platelet activation and thrombus formation. In 2008, Morrell *et al*, used an enzymatic probe to show that glutamate is released during thrombus formation. The levels of glutamate in control donors has been shown in previous studies to be approximately 120 μM (Castillo *et al*, 1996), and found to increase to over 200 μM in patients during from a stroke (Castillio *et al*, 1997). In comparison, Morrell *et al* (2008) demonstrated that while baseline levels of glutamate were found to be at approximately 100 μM, levels measured during platelet aggregation were found to reach 400 μM.

The study by Morrell *et al* (2008) then demonstrated that the AMPAR subunit proteins, GluR1-4 are expressed on human platelets. AMPAR are also members of the glutamate ionotropic receptor family (figure 6), and are mainly permeable to Na^+; however when the receptors include GluR2 subunits they are also permeable to Ca^{2+} (Morrell *et al*, 2008). This study demonstrates that glutamate alone is unable to activate human platelets, using changes in the binding of the PAC-1 antibody, which binds to the $\alpha_{IIb}\beta_3$ integrin, the

expression of which increases with platelet activation. Treatment of human platelets with glutamate prior to the addition of thrombin receptor-acting peptide (TRAP) however, increased platelet activation above that induced with TRAP alone. AMPA was found to have a similar pattern of activation as glutamate, which was shown to be inhibited by CNQX, an AMPAR inhibitor. Platelets were then isolated from GluR1 knockout mice and found to express the same baseline level of P-selectin as WT littermates. While an increase was then observed on stimulation with TRAP, when the cells were pre-stimulated with AMPA no further increase was observed in the GluR1$^{-/-}$ platelets. AMPA was then demonstrated to increase $[Na^+]_i$ in platelets, which could be inhibited by CNQX. Electrophysiological data demonstrated the presence of functional AMPARs in bone marrow-derived MKs, the responses of which could be blocked by the addition of CNQX. While expression of the GluR2 subunit was demonstrated in human platelets, treating platelets with the GluR2-specific inhibitor Joro spider toxin had no effect in the Na^+ influx assay, suggesting that while the subunit is expressed, it does not form part of the functional receptors; these are therefore Ca^{2+}-impermeable. The role of AMPA in platelet aggregation was also investigated, and increasing concentrations of CNQX found to inhibit TRAP-induced aggregation. Pre-treatment with AMPA was found to enhance the initial stages of TRAP-induced aggregation, which was not as discernable towards the latter stages. The effects on tail-bleeding were also investigated, with GluR1 knockout and WT mice that were treated with CNQX exhibiting prolonged bleeding times in comparison to untreated WT mouse platelets. This also suggests that AMPARs are implicated in thrombus formation.

This study was extended in 2009 to investigate the role of the KAR, another glutamatergic ionotropic receptor, by Sun *et al*. The KAR subunit proteins, GluR5 and 6 were shown to be expressed in human platelets, with the mRNA for both subunits demonstrated to be expressed in the megakaryoblastic, MEG-01 cell line. The addition of kainate alone to platelets was found to have no effect on platelet activation, however pre-treatment with kainate increased the level of activation in response to TRAP or thrombin. This was also shown using the GluR5 subunit-specific agonist 2-amino-3-(5-*tert*-butyl-3-hydroxy-4-isoxazolyl)propionic acid (ATPA). GluR6 knockout mice were generated, and the activity of their platelets compared to their WT littermates. Thrombin was found to induce an increase in platelet activation which was potentiated by pre-treatment with kainate in WT mice. In GluR6 knockout platelets however, thrombin had no effect at all either with or

without kainate pre-treatment. Human platelets were used to determine whether the application of a specific kainate receptor antagonist, UBP302 (a GluR5-specific antagonist), had an effect on platelet aggregation, and was shown to have an inhibitory effect on platelets pre-treated with kainate then thrombin. Thromboxane production and release was also investigated, with both glutamate and kainate shown to cause increases in levels which could be inhibited by pre-treatment with either UBP301 (KAR antagonist) or indomethacin, a COX inhibitor. The duration of kainate pre-treatment was found to have an effect on platelet activation, which increased up until the final time point of 30 min. Differences in thromboxane production were also investigated between WT and GluR6 knockout mice and found that while treatment with kainate increased thromboxane release slightly above control, in GluR6 knockout littermates, there was a decrease below control. Phosphorylation of MAPK p38 was also investigated, and it was found that treatment with kainate led to an increase in p38 phosphorylation, which was inhibited by UBP301. The phosphorylation of p38 was compared between WT and GluR6 knockout mice and found to be comparable. Treatment with kainate elicited further phosphorylation of p38 in WT platelets, however no further increase was stimulated in GluR6 knockout platelets. Again duration of kainate pre-treatment was investigated, and phosphorylation of p38 was shown to peak at 10 min of pre-treatment. An inhibitor of p38 was shown to prevent release of thromboxane in human platelets treated with kainate. Finally, ferric chloride injury in WT and GluR6 knockout mice demonstrated that vessel occlusion time increased in the absence of GluR6, as did the cessation of bleeding in the tail bleeding test. Vessel occlusion time was also investigated by treating WT mice with UBP302, showing that inhibition of the subunit also increased the time for vessel occlusion.

Both papers suggest that if NMDARs are expressed in human platelets, they are not functional. Morrell *et al* (2008), used pre-treatment with 3-(2-Carboxypiperazin-4-yl)propyl-1-phosphonic acid (CPP), a competitive NMDAR antagonist structurally similar to D-AP5 (Lehmann *et al*, 1987), which had no effect on TRAP-induced P-selectin expression. Sun *et al* (2009), treated human platelets with NMDA then stimulated them with TRAP. The addition of NMDA did not increase platelet activation above that induced by TRAP alone. Overall these two papers determine that the non-NMDARs, AMPA and kainate, play a role in platelet activation as well as in the initiation and continuation of thrombus formation, and suggest that NMDARs are not involved, even though they may be expressed in platelets. In contrast, this study demonstrates that NMDARs are implicated in

platelet activation through increases in $[Ca^{2+}]_i$ and ATP secretion, which can be inhibited by MK-801 or D-AP5. The assays used to determine platelet activation in this study however are not the same as those used by Morrell and Sun, therefore further experimentation is required to determine the effects of NMDARs on TRAP or thrombin-stimulated platelet activation and aggregation. The use of platelets from knockdown mice in combination with *in vivo* studies would also enable further comparison, to determine whether NMDARs are involved in the initiation and continuation of thrombus formation or whether they have a different role in platelet activation. This chapter also suggests that platelets could be used as model cells for these disorders as they express functional NMDARs together with serotonin and dopamine receptors as well as AMPAR and KARs, and are more easily obtainable than human neuronal tissue (Morrell *et al*, 2008; Sun *et al*, 2009; Harper *et al*, 2009; Ricci *et al*, 2001).

3.4.5. Clinical relevance and concluding remarks

Overall, these data demonstrate that human platelets express functional NMDARs, which can be stimulated by glutamate and NMDA to elicit increases in both $[Ca^{2+}]_i$ and ATP secretion. The addition of glycine together with glutamate has been demonstrated to have mixed effects, suggesting that differential expression of receptor subunits plays a role in the outcome of receptor activation. The NMDAR-specific antagonists, MK-801 and D-AP5 have both been found to inhibit responses elicited with glutamate, adding further weight to the functional role of the receptors. While the effect of NMDAR activation appears small in relation to that of thrombin, it is possible that the role of NMDARs is comparable to that of $P2X_1$ receptors, which elicit small Ca^{2+} responses, but play an important role in both the initiation and the development of thrombus formation (Hechler *et al*, 2003).

Glutamate receptors are highly expressed in the CNS and glutamate has been shown to play a major role in neuronal signalling (Vekhratsky and Kirchhoff, 2007; Dingledene *et al*, 1999). Therefore given that platelets can be used as neuronal models, they can be used to investigate the effects of neurodegenerative diseases such as Parkinson's disease (PD) and AD together with schizophrenia, migraine and stroke, all of which have been demonstrated to have a glutamatergic facet, involving NMDARs. Further investigations into their inhibition or regulation could therefore lead to potential new drugs to control their activity, even though the effects induced are highly varied. During a stroke, the

localised level of glutamate increases massively, leading to excitotoxicity and cell death, not only of the cells immediately surrounding the insult, but also those which adjoin this region called the penumbra (Olney and Sharpe, 1969; Olney *et al*, 1971). In PD, glutamatergic signalling has been demonstrated to compensate for damaged dopaminergic signalling particularly in the striatum where the concentration of NMDARs is especially high and it has been demonstrated that treatment with NMDAR antagonists e.g. MK-801, have anti-parkinsonian effects (Porter *et al*, 1994). In AD, over-stimulation of NMDARs has been linked to the formation of neurofibrillary tangles within neurones which are believed to have a toxic effect on cells and detrimentally affect scores in behavioural studies (Couratier *et al*, 1996; Minkeviciene *et al*, 2004). NMDARs have also been implicated in schizophrenia following studies showing that phencyclidine, which blocks NMDARs, induced symptoms similar to schizophrenia in normal humans and enhanced symptoms in schizophrenics (Luby *et al*, 1959). Studies have shown that expression of NMDAR subunits is impaired or reduced and that sensitivity to glutamate is increased (Mohn *et al*, 1999; Berk *et al*, 2000), and it has been suggested that targeting regulation of glycine and D-serine levels in the brain could reduce the symptoms of schizophrenia (Kantrowitz and Javitt, 2010). Glutamate has been shown to play a role in migraine, with release demonstrated from platelets during attacks (D'Andrea *et al*, 1991), and NMDARs implicated in both pain pathways and in the generation of aura (Bereiter *et al*, 1996; Peeters *et al*, 2007). NMDAR antagonists have been demonstrated to reduce both these effects, suggesting that they could potentially be used to treat migraines (Bereiter *et al*, 1996; Peeters *et al*, 2007).

A study in 1984 demonstrated that excessive NMDAR activity underlies the damage caused during an ischemic insult, and suggested that blocking their activity may protect the brain against ischemic-induced damage (Simon *et al*, 1984). Following this discovery, many laboratories investigated the possibility of formulating NMDAR antagonists for medicinal use in humans. Several studies were carried out which reached stage III of clinical trials, but were halted due to concerns over the potential increased death risk and adverse neurological effects including hallucinations, drowsiness, confusion and agitation together with increased cardiovascular instability (Morris *et al*, 1999; Albers *et al*, 1999). One drug, memantine, however has gone through clinical trials and is currently used to treat moderate-severe AD in the US. Memantine is a low affinity, uncompetitive, open channel blocker with a rapid on/off rate, which enables it to prevent excessive NMDR

stimulation while having little to no effect on subsequent normal, physiological signalling, which was a major problem with other drugs trialled (Chen *et al*, 1992). It has been demonstrated to reduce the size of ischemic infarcts up to 2 h after the start of the event (Chen *et al*, 1998) to inhibit migraine-associated aura (Peeters *et al*, 2007), and to reduce neurofibrillary tangles in culture together with improving behavioural scores in AD mouse models (Minkeviciene *et al*, 2004; Li *et al*, 2004). Memantine has also been shown to have no effect on learning or LTP in rats, which has been demonstrated to be due to the drug blocking only extrasynaptic NMDARs, and not those in the synapse, in comparison to other drugs trialled which blocked both (Chen *et al*, 1998). Blocking extrasynaptic NMDARs prevents suppression of CREB activation, which leads to eventual cell death by necrosis. Activation of synaptic NMDARs enables the retention of normal receptor signalling which in turn promotes the continuation of CREB activation promoting the transcription of anti-apoptotic factors such as Bcl-2 (Hardingham *et al*, 2002). This demonstrates that while further investigation is required to fully understand the function of NMDARs in neurological disorders, some progress is being made with the development of memantine suggesting that NMDAR antagonists can play a role, and that platelets can be used as neuronal models in which to test them.

CHAPTER 4
GLYCINE-GATED ION CHANNELS

4.1. Summary

In this chapter, it has been demonstrated that:

- the NMDA NR3 subunit protein is expressed in human platelets
- extracellular application of glycine is shown to induce increases in intracellular calcium, with the additional presence of D-serine having varied effects
- ATP release is stimulated by the addition of extracellular glycine, and inhibited by D-serine

4.2. Introduction

This thesis investigates the role of NMDARs in platelet and MK function. In addition to the classical NMDAR conformation consisting of NR1/ NR2 subunit proteins, the existence of the glycine-binding NR3 subunits has also been determined (Ciabarra *et al*, 1995; Sucher *et al*, 1995; Chatterton *et al*, 2002). To date, the expression of NR3 subunits has been demonstrated in motor neurones (Nishi *et al*, 2001), glia and oligodendrocytes (Verkhratsky and Kirchoff, 2007), and myelinating cells (Káradóttir *et al*, 20005) together with mature myelin (Micu *et al*, 2006). The NR1/NR3 conformation is activated by glycine alone, due to the absence of glutamate-binding NR2 subunits. This activation has been shown to be inhibited by the presence of D-serine (Chatterton *et al*, 2002). In this chapter, the potential functional expression of NR3 subunit containing NMDA receptors in human platelets has been investigated.

4.3. Results

4.3.1. Detection of NMDA proteins by Western blot

The expression of NMDA NR1 subunit proteins by human platelets has been demonstrated in Chapter 3 (figure 13). The expression of NMDA NR3 subunit proteins was investigated by performing Western blots using platelet samples from different human donors. A band running between 100 and 120 kDa was detected with an anti-NR3 antibody in 3 different platelet samples (figure 31), which corresponds to the predicted molecular weight for NR3 of 116 kDa (Ciabarra *et al*, 1995; Sucher *et al*, 1995; Chatterton *et al*, 2002). This suggests the potential for the formation of NMDARs containing both NR1 and NR3 subunit proteins.

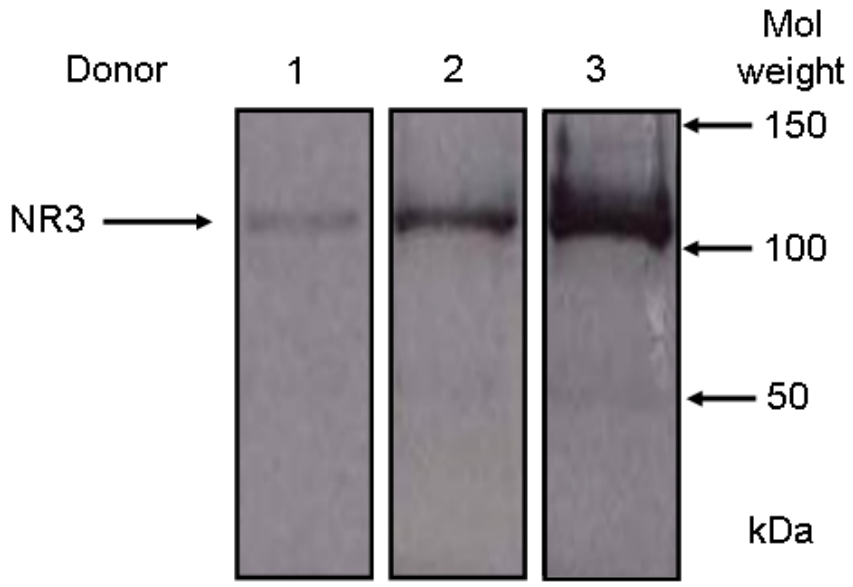

Figure 31. Human platelets express NMDA receptor subunit NR3. Western blots demonstrating expression of the NMDA NR3 subunit in 3 different human donors (1-3). The bands are from 3 different gels indicated by the surrounding boxes. Number above the lanes indicates the donor from which sample was obtained; approximately 15 μg protein loaded of each sample determined by Bradford assay. The arrows on the right side indicate sizes predicted by the protein standards (mol marker, molecular weight marker; kDa) with the arrow on the left side indicating the expected size of the NR3 subunit, 116 kDa.

4.3.2. Intracellular calcium responses to glycine, D-serine and thrombin

4.3.2.1. Glycine and thrombin responses

To determine whether the potential NR1/NR3 combination of subunits is functional, the effect of extracellular glycine on $[Ca^{2+}]_i$ in fluo-4 loaded human platelets was investigated. In these experiments, all responses are normalised to the fluorescence response evoked by the addition of ionomycin, a calcium ionophore, described as the maximal response where responses are expressed as a percentage of the maximal responses (Lui and Hermann, 1978). Moreover, a saline control was added to evaluate background changes in fluo-4 fluorescence. The saline control evoked a small sustained increase, 10-20 % MR above baseline fluorescence in experiments to evaluate the responses to glycine and D-serine (figure 32C and D). This background response was comparable to that detected in Chapter 3 when glutamate responses were evaluated.

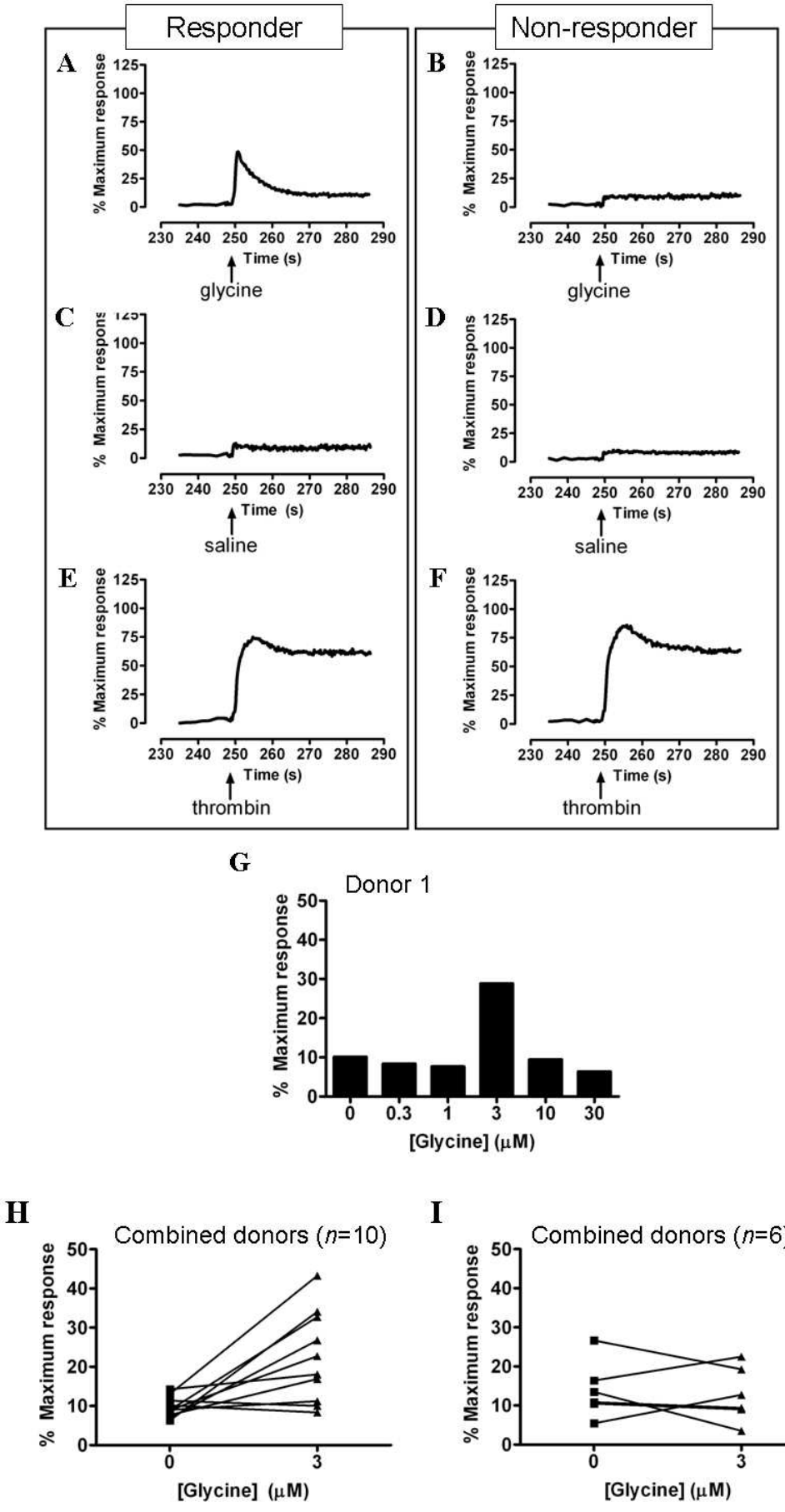
Responder
Non-responder
A
B
C
D
E
F
% Maximum response
Time (s)
glycine
saline
thrombin
G
Donor 1
[Glycine] (μM)
H
Combined donors (n=10)
I
Combined donors (n=6)

Figure 32. Glycine evokes an intracellular calcium response in human platelets. Representative traces from 2 different donors illustrating single kinetic responses to 3 μM glycine, saline (nominally Ca^{2+}-free salt solution) and 3 U ml^{-1} thrombin recorded within the first 2 h of each separate experiment. **A, B,** Kinetic traces comparing the responses to 0.3 μM between the 2 donors, illustrating an increase in fluorescence in 1 donor (responder) but not in the other (non-responder). **C, D,** Representative responses to the addition of saline from the 2 donors. **E, F,** Representative traces illustrating the response to the application of 3 U ml^{-1} thrombin (positive control). The addition of agonists and saline are indicated by an arrow. The % maximum response (% MR; 100 % response) is determined by the addition of 1 μg ml^{-1} ionomycin at the end of each experiment. **G,** Histogram illustrates the peak responses from a single donor obtained within the first 2 h of each experiment (n=1). **H,** Demonstrates the variation in mean responses between donors to 0 and 3 μM glycine (n=10). **I,** Demonstrates the variation in mean response between non-responding donors to 0 and 3 μM glycine (n=6). Each point represents the mean value from a single experiment for each donor, with the points joined such that the data for each donor at 0 and 0.3 μM glycine is linked. All data was obtained within the first 2 h of each experiment.

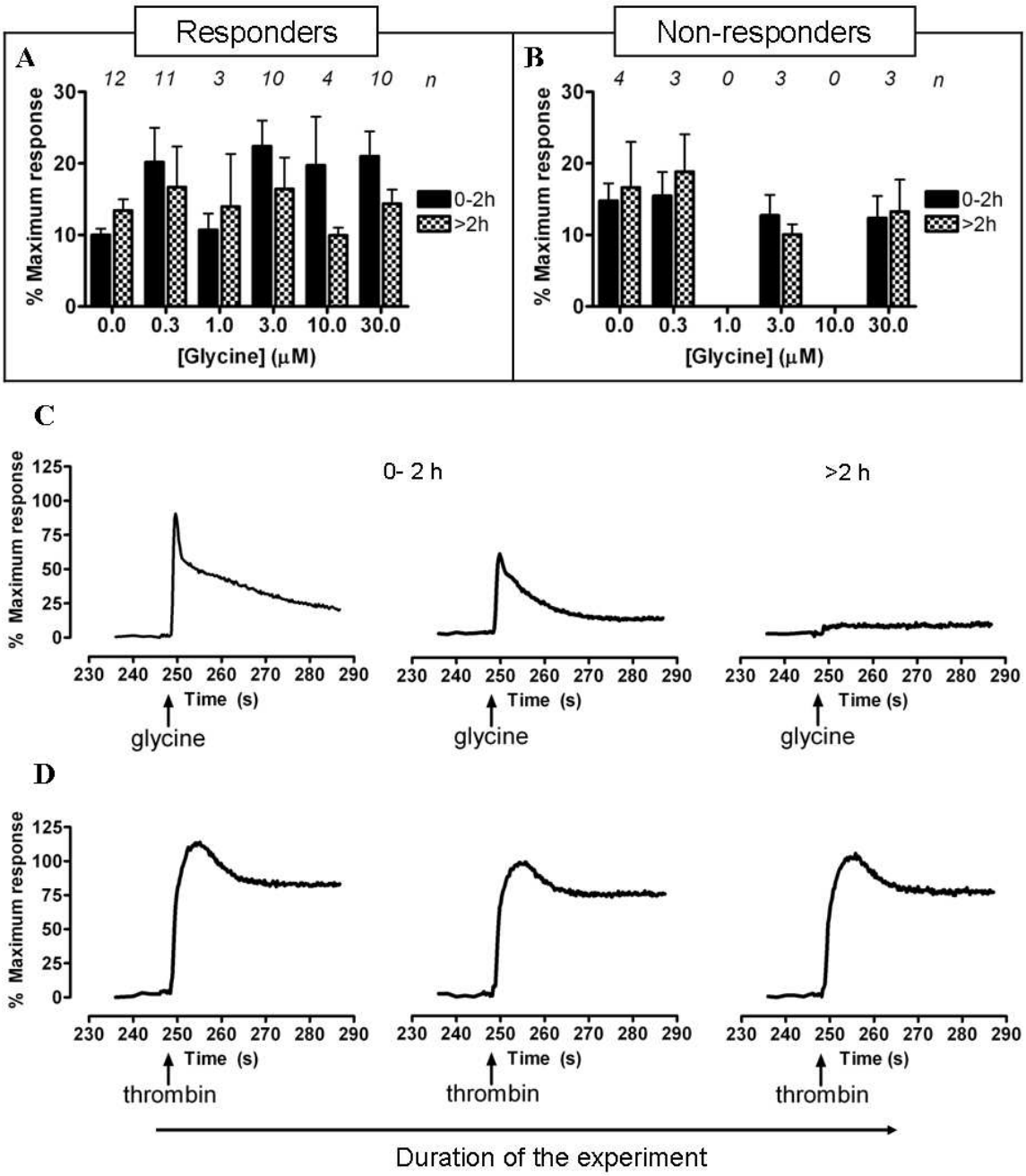

Figure 33. Glycine-evoked intracellular calcium responses vary between donors and decrease over time. A, B, The data is split into donors whose platelets responded to glycine (A) and those in which a response above control was not observed (B). Solid black bars represent the responses to glycine over the first 2 h of the experiments with black checked bars illustrating the responses after 2 h. They demonstrate that the responses to glycine decrease after the first 2 h after the beginning of the experiment, with the responses elicited by saline increasing after this time. The numbers above the columns indicate the number of donors' data included (*n*= 1- 12). **C,** Kinetic traces from 1 experiment using platelets from 1 donor illustrating the decrease in response to 0.3 μM glycine over the course of the experiment. **D,** Illustrates the responses to 3 U ml^{-1} thrombin (positive

control) in the same experiment demonstrating that while the responses to thrombin vary over the course of an experiment, they do not decrease overall. The first 2 responses for both glycine and thrombin were obtained within the first 2 h of the experiment, with the final response obtained over 2 h from the start of the experiment. Addition of the agonists is indicated by an arrow. The % maximum response (% MR; 100 % response) is determined by the addition of 1 μg ml^{-1} ionomycin at the end of each experiment. The data indicates that there is no overall dose-dependent effect of the addition of glycine to human platelets.

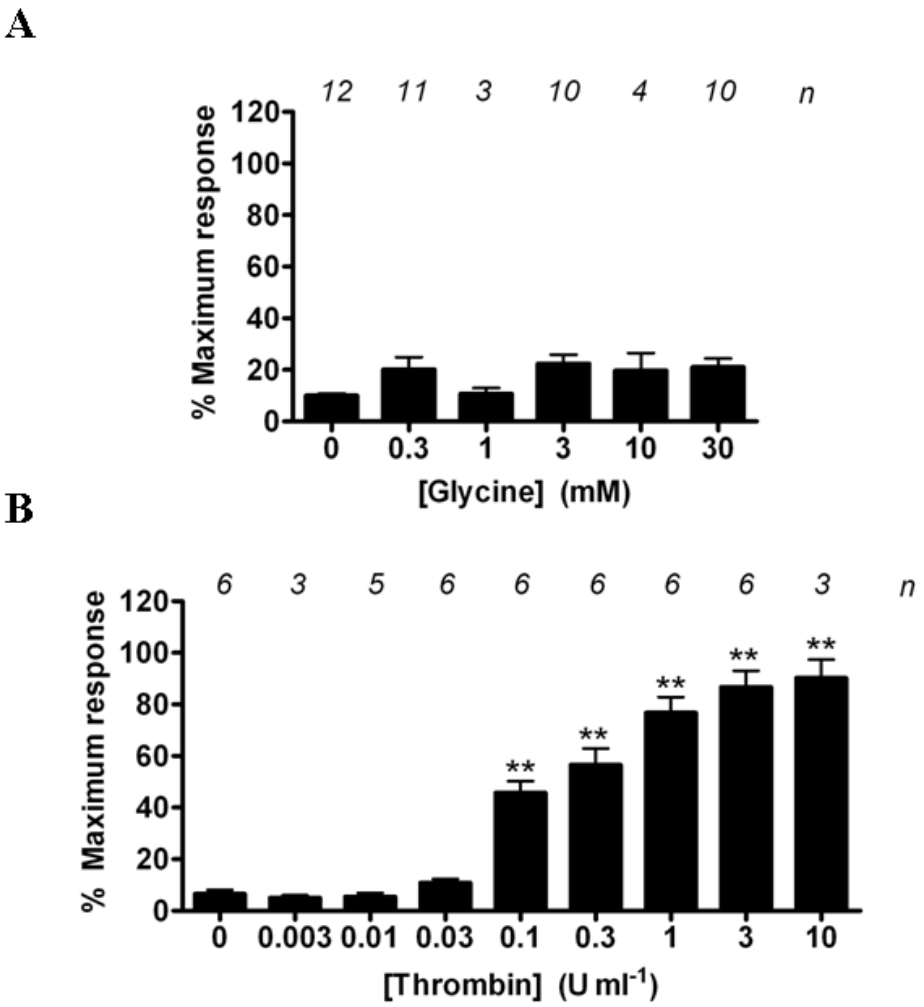

Figure 34. Comparison of the intracellular calcium responses evoked by glycine and thrombin in human platelets. A, Histogram illustrates the peak responses of glycine-evoked increases in fluo-4 fluorescence in responding human platelets in the first 2 h of the experiments (*n*= 3-12 ± S.E.M.), in comparison to those elicited by thrombin (**B**) in unpaired experiments (*n*= 3-6 ± S.E.M.). The responses to all glycine concentrations were observed to decrease over the duration of the experiment (figure 29), therefore only data obtained in the first 2 h is shown here. The thrombin responses did not vary to such an extent during the experiment and therefore all responses are shown for each concentration. While responses to thrombin increase in a dose-dependent manner, no such effect is apparent with the extracellular addition of glycine. The maximum response was determined by the addition of ionomycin (1 ug ml^{-1}) at the end of each experiment. * P< 0.05; ** P< 0.01 compared to either 0 μM glycine or 0 U ml^{-1} thrombin using a one-way ANOVA with Dunnetts post-hoc test.

Over the duration of each experiment measurements of $[Ca^{2+}]_i$ were taken between 1.5 and 5 h post isolation of the platelets. In these experiments a glycine concentration response curve was performed in triplicate, with triplicate repeats of thrombin (3 U ml^{-1}) and saline, as positive and negative controls respectively, also assessed. It was observed that responses to extracellular glycine varied between donors as illustrated in figure 32, where one demonstrates a rapid, transient increase in $[Ca^{2+}]_i$ (figure 32A), in response to glycine while in other donors glycine elicited a response comparable to that stimulated by the addition of saline (figure 32B). Therefore data was separated into that from donors who responded to the application of extracellular glycine (responders), where responses to 1 or more concentrations of glycine were observed of at least 10 % MR above that elicited by saline from the same donor, and from those who did not (non-responders) (figure 33).

It was also apparent that over the course of the experiments the responses to extracellular glycine decreased, with the greatest reduction observed after 2 h from the start of the experiments (figure 33E). The data was therefore separated into responses obtained within the first 2 h, and those obtained after 2 h (figure 33). The applications of glycine within the first 2 h were shown to increase above responses obtained for saline from 0.01 to 30 μM with the exceptions of 0.03 and 1 μM glycine in responding donors (figure 33A). The greatest increase was with 3 μM glycine which peaked at 22.42 ± 3.58 % MR (n=10) in comparison to 11.16 ± 0.93 % MR (n=12) with saline. The response elicited by saline increased over the course of the experiments to 14.22 ± 1.88 % MR (n=12) after 2 h from the start and constitutes a small sustained response (figure 32C). The peak glycine concentration drops to 0.3 μM over 2 h from the duration of the experiments (16.68 ± 5.70 % MR; n=11), with only 0.3-3 μM glycine eliciting responses above that induced by the addition of saline (figure 32C). In the non-responding donors, the increase in $[Ca^{2+}]_i$ stimulated by the addition of saline increases from 14.80 ± 2.41 to 16.64 ± 6.38 % MR (n=4) over the experiment.

In comparison it was observed that thrombin triggered a rapid, sustained response in all donors throughout the experiments (figures 33F). The peak response to thrombin was demonstrated to shift from 10 to 3 U ml^{-1} during the experiments with mean responses of 90.29 ± 7.09 and 92.21 ± 14.49 % maximum response respectively (n=3 and 6) (Appendix I). This also demonstrates that the mean peak response to thrombin at 3 U ml^{-1} is 64.32 ± 7.22 % MR larger than the mean peak response for glycine (3 μM) in responding

donors in the first 2 h of each experiment. From these data, it was determined that the glycine response is desensitised during the course of the experiments, and only data from the first 2 h of any experiment will be used for analysis. Collectively, these data demonstrate that extracellular glycine triggers a Ca^{2+} response in human platelets that desensitises over time.

The data for all donors from the first 2 h of each experiment was pooled to demonstrate the variation in responses to 3 μM glycine (figure 32I). It illustrates that $[Ca^{2+}]_i$ in platelets from 6 different donors increases upon external application with 3 μM glycine above control, with no variation from control in the remaining 4 donors. An example dose response data was obtained between different donors, illustrated in figure 32G.

4.3.2.2. D-serine responses

D-serine has a varied role as both a co-agonist for the classical NMDA NR1/ NR2 receptor and as an inhibitor in the NR1/NR3 receptor (Dingledine *et al*, 1999; Chatterton *et al*, 2002). It is therefore important to determine whether D-serine alone elicits a response from human platelets.

The addition of extracellular D-serine to fluo-4 loaded human platelets evokes a small sustained increase in fluorescence which is comparable to that elicited by the addition of saline alone (figure 35A and C, and B and D). No differences were observed over the course of the experiments in the responses to each concentration of D-serine, therefore all the data for each experiment was pooled. The largest increase above control was demonstrated to be with the extracellular application of 10 μM D-serine, with a mean increase of 3.17 ± 1.24 % MR above that induced with saline. The variation between donors is small with a range of individual responses from different donors between 6.73 and 15.27 % MR (n=5) (figure 36D). Thrombin responses were maintained between 80 and 90 % MR. From this data, it was determined that D-serine does not invoke a $[Ca^{2+}]_i$ response in platelets.

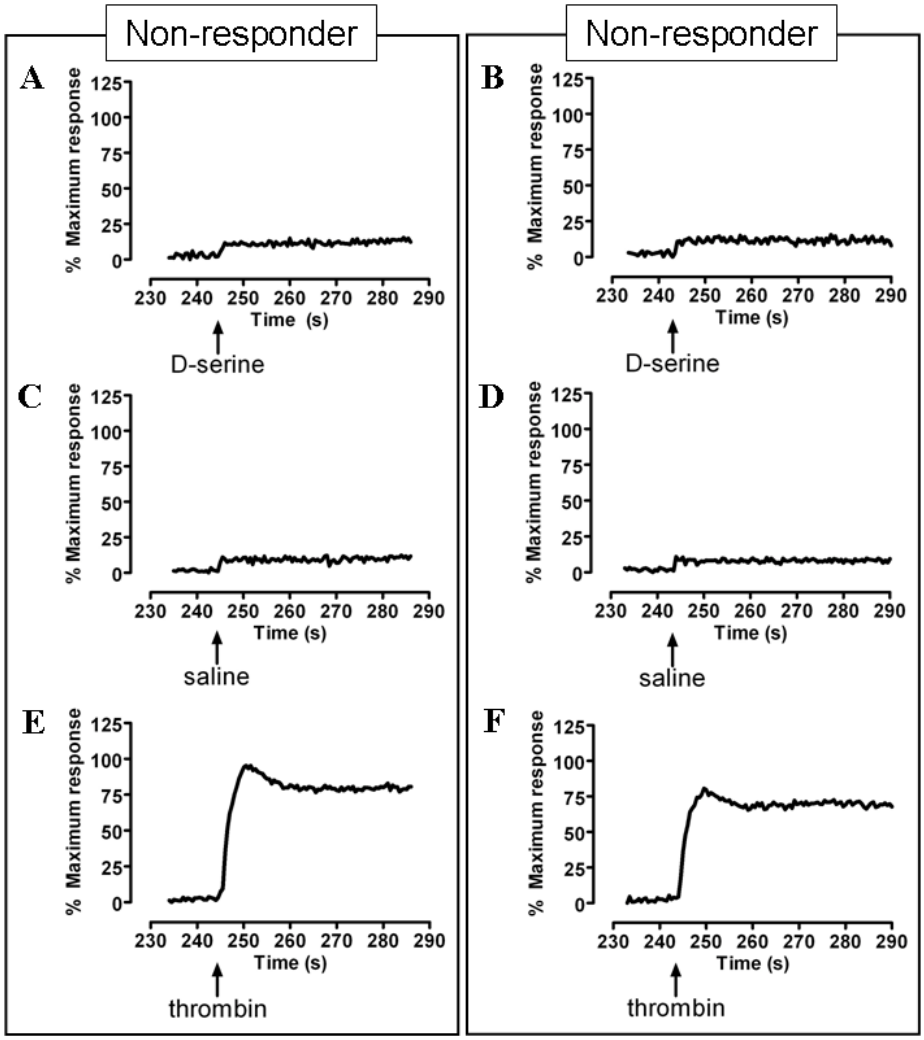

Figure 35. D-serine does not evoke an intracellular calcium response in human platelets. Representative single kinetic traces from 2 different donors illustrating variation in response to 10 μM D-serine, saline (nominally Ca^{2+}-free salt solution) and 3 U ml^{-1} thrombin. **A, B,** Representative traces demonstrating that 10 μM D-serine does not trigger an increase in fluo-4 fluorescence in human platelets. **C, D,** Control responses to the addition of saline alone (nominally Ca^{2+}-free salt solution). **E, F,** Representative traces illustrating the response to 3 U ml^{-1} thrombin (positive control) from the same donor. The addition of agonist or saline is indicated by an arrow. The % maximum response (% MR; 100 % response) is determined by the addition of 1 μg ml^{-1} ionomycin at the end of each experiment.

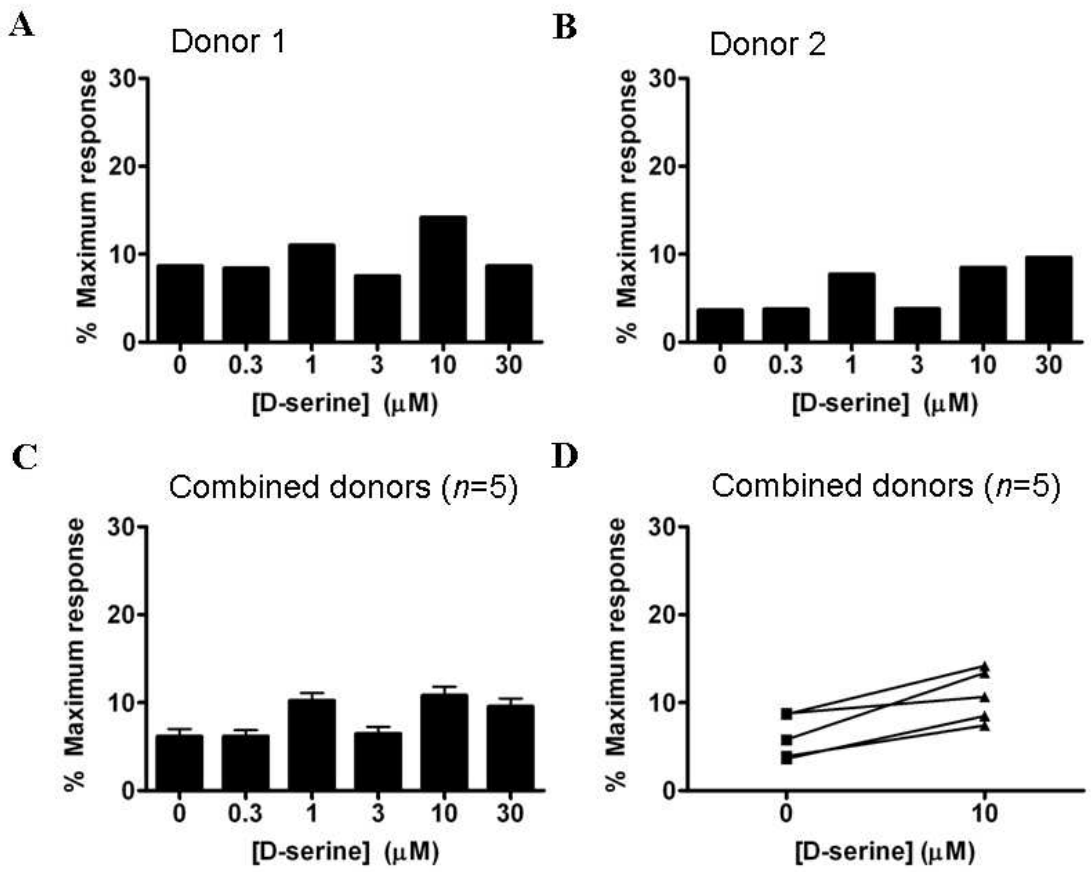

Figure 36. D-serine does not evoke an intracellular calcium response in human platelets. A, B, Each histogram represents the peak responses from a single donor where each concentration is assessed in triplicate (*n*=1). **C,** histogram illustrates the combined peak responses from 5 different donors (*n*=5 ± S.E.M). **D,** Comparing the variation in mean peak responses to 0 and 10 μM D-serine, which has the largest mean peak response, between donors (*n*= 5). Overall, D-serine does not stimulate an intracellular Ca^{2+} response in human platelets. For all concentration responses the maximum response (100 %) was obtained by the addition of 1 μg ml^{-1} ionomycin at the end of each experiment. All data was obtained within the first 2 h of each experiment.

4.3.2.3. Glycine and D-serine responses

As glycine has been shown to stimulate an increase in $[Ca^{2+}]_i$ in human platelets (section 4.3.2.1.), with D-serine alone triggering no effect (section 4.3.2.2.), the next step is to determine whether the glycine-induced responses can be inhibited by D-serine which is indicative of the NR1/ NR3 subunit combination.

The presence of D-serine induced mixed effects on the response elicited by the addition of external glycine as illustrated in figures 37A and B. These are also illustrated in figure 38D where the glycine-evoked response is either inhibited, potentiated or there is no observed effect on the response elicited with glycine alone. Example histograms are shown in figure 38A and B also demonstrating the variation between donors using only data obtained within the first 2 h of each experiment. When pooled (figure 38C), the data indicates that there is a peak in response at 3 μM glycine (24.70 ± 1.67 % MR compared to 11.06 ± 4.26 % MR with saline alone; *n*=8). This is mirrored by an increase in response with the addition of 10 μM D-serine, where the response is 22.23 ± 3.61 % MR (*n*=8) compared to that of the saline and D-serine control (11.71 ± 1.56 % MR; *n*=8). The difference between the 2 peaks is only 3.12 ± 6.03 % MR and suggests that the addition of D-serine has little effect on the glycine-induced response. However, figure 38D which compares the mean data from the 8 different donors demonstrates that there is a greater variety in response than indicated in the pooled data. It shows that in 5 out of 8 donors the application of 3 μM extracellular glycine stimulates an increase in $[Ca^{2+}]_i$, while there is no effect induced by the addition of 10 μM D-serine alone. The mixed effects of D-serine on glycine responses were shown to consist of potentiation in 3 donors, inhibition in 3 donors and no apparent effect in the remaining 2. The kinetic responses are illustrated in figure 37A and B showing that responses to extracellular glycine are rapid and transient both with and without D-serine. Together, this demonstrates that the responses induced by extracellular glycine are differentially affected by the addition of extracellular D-serine.

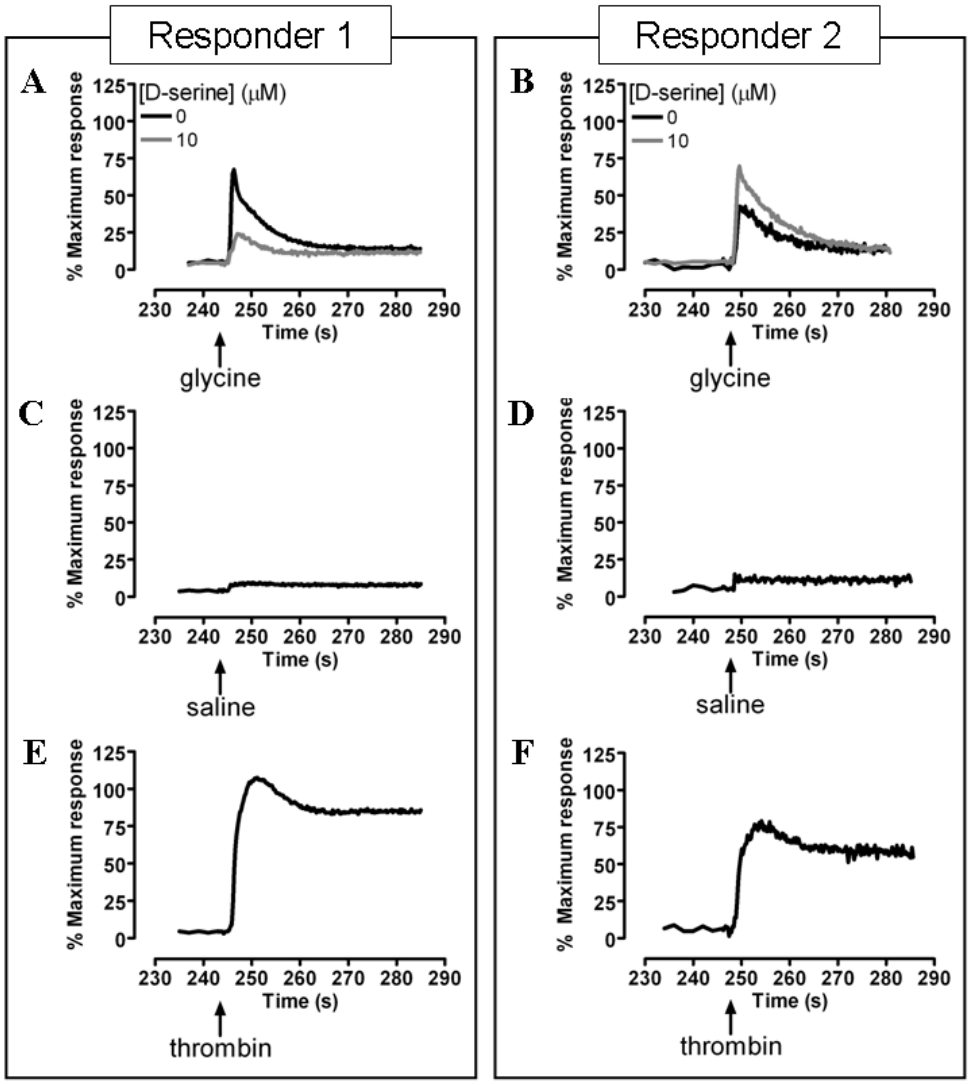

Figure 37. Glycine evokes an intracellular calcium response which is affected by the presence of D-serine in human platelets. Representative traces from 2 different donors demonstrating single kinetic responses to 3 μM glycine alone and in combination with 10 μM D-serine, saline (nominally Ca^{2+}-free salt solution) and 3 U ml^{-1} thrombin. **A, B,** Kinetic traces demonstrating that 3 μM glycine triggers an increase in fluo-4 fluorescence in human platelets which is modified by the presence of 10 μM D-serine. **C, D,** Control responses to the addition of saline (nominally Ca^{2+}-free salt solution). **E, F,** Representative traces illustrating the response to the addition of 3 U ml^{-1} thrombin (positive control) from the same donor. The addition of the agonist and saline are indicated by an arrow; the antagonist (D-serine) or saline were added at the beginning of the experiment. The % maximum response (% MR; 100 % response) is determined by the addition of 1 μg ml^{-1} ionomycin at the end of each experiment. All data was obtained within the first 2 h of each experiment.

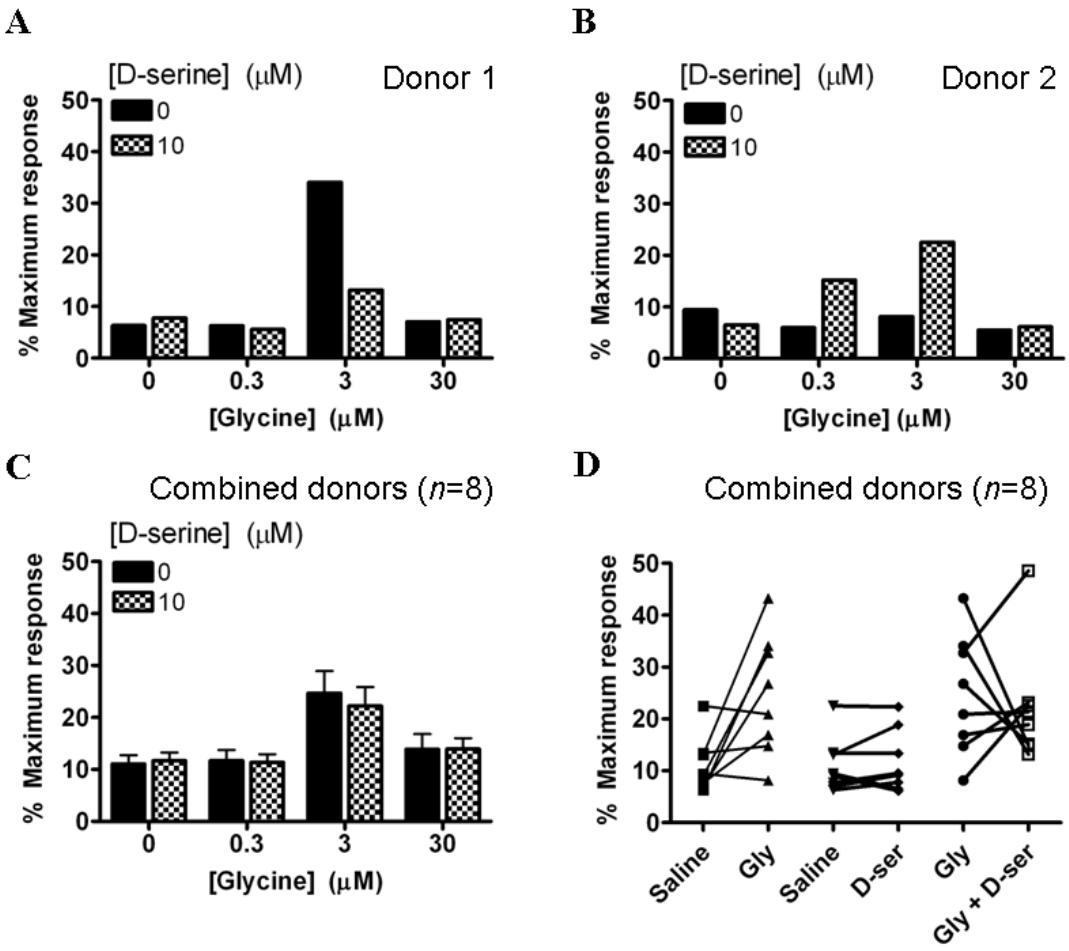

Figure 38. Glycine evokes an increase in intracellular response in human platelets which is altered by the presence of D-serine. A, B, Each histogram represents the peak responses from a single donor where all combinations of glycine and D-serine are repeated in duplicate (n= 1). **C,** Histogram illustrates the combined peak response data from 8 different donors (n=8 ± S.E.M.) **D,** The before-after plot illustrates the combined mean peak response data from 8 different donors (n=8 ± S.E.M.). This demonstrates the addition of 3 μM glycine elicits an increase in fluorescence in 5 donors with no increase in the other 3 above saline responses. The further addition of 10 μM D-serine inhibits the response in 3 donors, potentiates the responses in another 3 with no effect in the final 2 donors. D-serine alone has no effect on fluo-4 fluorescence. The maximum response (100 %) was obtained by adding ionomycin (1 μg ml^{-1}) at the end of each experiment. All data was obtained within the first 2 h of each experiment.

4.3.3. Measurement of extracellular ATP secretion from human platelets

As in Chapter 3, ATP release was investigated using the luciferase assay to determine the effects of extracellular glycine. Responses were converted to ATP concentrations using calibration curves constructed using known ATP concentrations (section 2.9). Paired saline controls were run in each experiment as negative controls to evaluate background changes in the levels of ATP detected. The addition of extracellular saline elicited a small sustained response in both responders and non-responders, 0-20 nM above baseline ATP levels in experiments to evaluate responses to glycine and D-serine comparable to that obtained in Chapter 3 (figure 23).

4.3.3.1. Glycine and thrombin responses

As in section 4.3.2.1, variation was seen in responses between donors to extracellular glycine as well as over the duration of the experiment. The data was therefore separated into that from donors who responded to at least 1 concentration of extracellular glycine, showing an increase in ATP concentration at least 40 nM above that of the saline response from the same donor, as well as by time (figures 39A and B; figure 40).

The combined data of responding donors for the first 2 h of each experiment demonstrate a bell-shaped dose response which peaks between 0.1 and 0.3 μM glycine (205.78 ± 89.93 and 126.43 ± 3.54 nM ATP released, n= 5 and 13 respectively; figure 40), where responses to glycine were shown to be rapid and sustained (figure 39A). The clear dose response effect is lost after 2h, shifting to a general trend which increases towards 1 μM glycine (228.40 ± 228.43 nM ATP, n=3), with the mean response at 0.3 μM glycine decreasing to 110.85 ± 47.72 nM ATP (n=8). The response to saline decreases from 2.44 ± 1.62 to 1.62 ± 2.61 nM ATP (n=8) over the duration of the experiment. In non-responding donors, the response to saline decreases over the experiment from -1.50 ± 1.04 nM ATP to -4.06 ± 2.73 nM ATP (n=4). The only concentration of glycine tested in donors whose platelets did not respond was 0.3 μM, which increased to 37.58 ± 28.99 nM ATP from 3.03 ± 0.75 nM ATP over the duration of the experiments. However, as the increase did not occur within the first 3 h of the tests, it does not qualify as a response. The application of extracellular thrombin (3 U ml^{-1}) elicited a rapid, transient in both responders and non-responders (figures 40C and D), which increases slightly from 7768.41 ± 1794.74 to 8708.30 ± 2883.09 nM ATP (n=6) over the duration of the experiment.

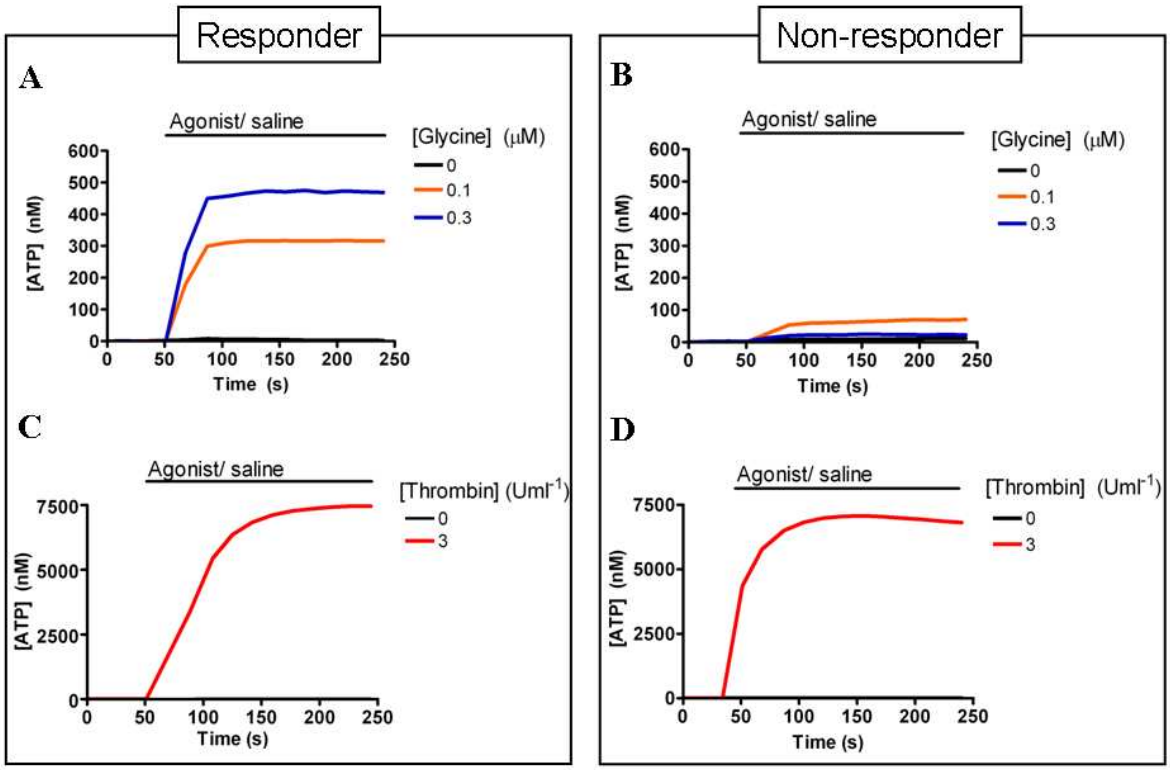
Responder
Non-responder
A
B
C
D
Agonist/ saline
[Glycine] (μM)
0
0.1
0.3
[Thrombin] (Uml-1)
3
[ATP] (nM)
Time (s)

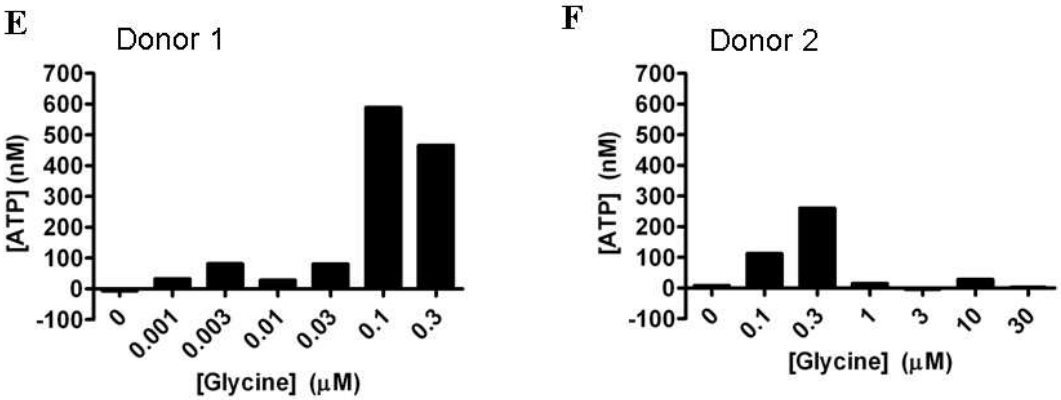
E
Donor 1
F
Donor 2
[ATP] (nM)
[Glycine] (μM)
0
0.001
0.003
0.01
0.03
0.1
0.3
1
3
10
30

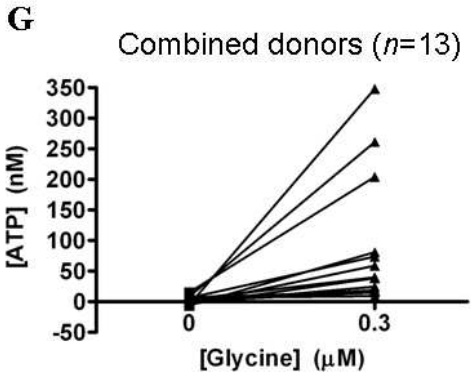
G
Combined donors (n=13)
[ATP] (nM)
[Glycine] (μM)

Figure 39. Glycine triggers ATP secretion from human platelets. A, B, Representative traces from 2 different donors illustrating single kinetic responses of ATP release elicited by the addition of 0, 0.1 and 0.3 μM glycine to human platelets. **C, D,** representative responses to the addition of 3 U ml^{-1} thrombin (positive control) for the same 2 donors. Lines indicate the duration of application of the agonist or nominally Ca^{2+}-free salt solution (saline). **E, F,** Each histogram represents the peak responses from a single donor (*n*=1). **G,** Demonstrates the variation in mean responses between responding donors to 0 and 0.3 μM glycine (*n*=8); the concentrations of glycine to which these donors responded may not include 0.3 μM. Each point represents the mean value from a single experiment for each donor, with the points joined such that the data for each donor at 0 and 0.3μM glycine is linked. All data was obtained within the first 3 h of each experiment.

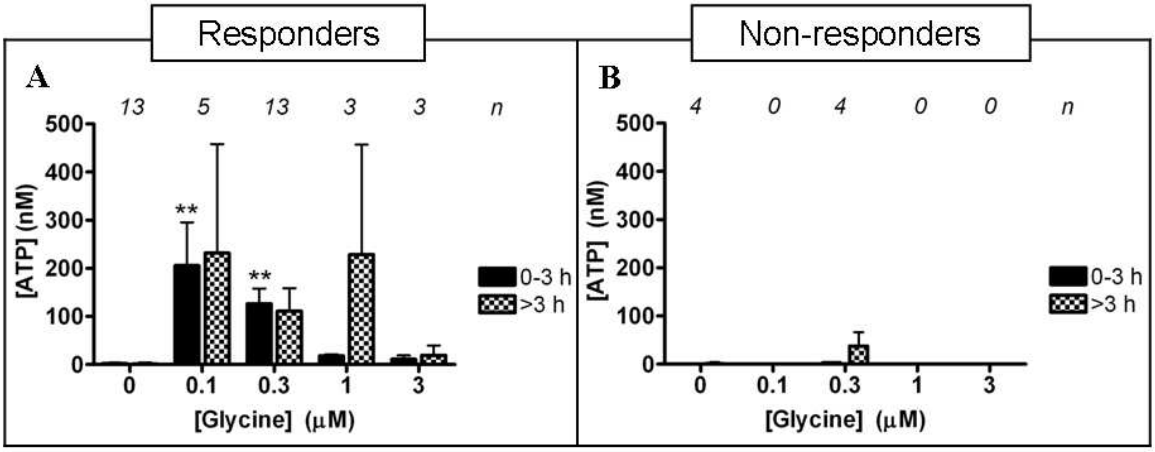

Figure 40. Glycine-evoked ATP release changes over time. A, B, The data is split into donors which responded to glycine (A) and those in which a response above control was not observed (B). Solid black bars represent responses to glycine over the first 3 h of the experiments, with responses after 3 h shown in black checked bars. They demonstrate that the ATP released on the application of extracellular glycine becomes increasingly variable more than 3 h from the start of the experiments with the responses to saline doubling after this time, from 2.78 ± 5.25 to 5.12 ± 1.74 nM ATP in responding donors, but decreasing in non-donors from 0.27 ± 0.95 to -5.52 ± 4.18 nM ATP. ATP release in the non-donors following application of extracellular glycine also decreases over the duration of the experiments (B). The numbers above the columns indicate the number of donors' data included (n=0-8). **P< 0.01 in comparison to 0 μM glycine using a one-way ANOVA with a Dunnetts post-hoc test. All data was obtained within the first 3 h of each experiment.

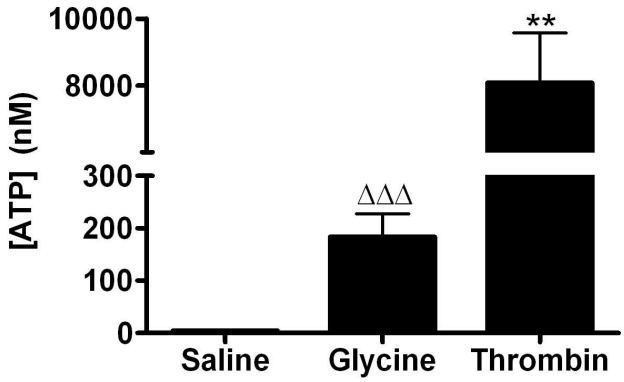

Figure 41. Comparison of peak ATP release evoked by thrombin and glycine. Histogram illustrates the peak responses for glycine (0.3 μM) and thrombin (3 U ml^{-1})- evoked ATP release in human platelets (*n*= 8 ± S.E.M. for saline (nominally Ca^{2+}-free salt solution) and glycine; *n*= 6 ± S.E.M for thrombin). This illustrates that thrombin elicits a 97.31 ± 4.44 % increase in ATP release than glycine. Data was obtained within the first 3 h of each experiment from responding donors. ** P< 0.01 compared to saline (nominally Ca^{2+}-free salt solution) using one-way ANOVA with Dunnetts post-hoc test, ΔΔΔ P< 0.001 compared to saline (nominally Ca^{2+}-free salt solution) using an unpaired, two-tailed Students *t*-test.

This again demonstrates that the ATP response to thrombin is significantly greater than the peak response to extracellular glycine, producing a difference of 7525.64 ± 1797.91 nM ATP between the peak responses (figure 41).

The pooled data for responding donors to 0.3 μM glycine in the first 2 h of each experiment illustrates the variation between responses from each donors (figure 39D). It demonstrates that out of 8 donors who respond to at least 1 concentration of glycine (from a total of 13 donors), 7 donors elicit a release of ATP from the platelets in response to the addition of 0.3 μM extracellular glycine, with 1 donor showing no apparent increase in ATP release above control at this concentration of glycine. Overall, these data demonstrate that extracellular glycine triggers ATP secretion in human platelets that varies over time and donor.

4.3.3.2. Glycine and D-serine responses

As ATP responses are elicited by the application of extracellular glycine in 13 out of 17 donors, the next stage is to determine whether the release of ATP stimulated by glycine can then be inhibited by the additional presence of 10 μM D-serine. In this study, D-serine alone has been shown to have no affect on changes in $[Ca^{2+}]_{i,}$ (figure 43), however its effects on ATP secretion must also be determined.

Extracellular D-serine (10 μM) was added to isolated human platelets and induced inhibition in 4 donors, an increase in 1 donor, and no effect above saline in the remaining 6 (figure 43D). Of the 13 donors used in these experiments, 5 demonstrated an increase in ATP release with the addition of glycine, of which 4 are inhibited by the presence of D-serine. The remaining donors showed no response to the addition of glycine, with no further effects with D-serine. This data is pooled in figure 43C, showing that overall the addition of glycine stimulates an increase in ATP concentration of 59.75 ± 21.09 nM above control. This was decreased by 34.69 ± 22.44 nM by the addition of D-serine. The kinetic responses were shown to be rapid and sustained both with and without D-serine (figures 42A and B), with variation between donors also illustrated in figures 43A and B. Overall this demonstrates that where an increase in ATP release from human platelets is obtained by the extracellular application of glycine, it can, in general, be partially inhibited by the addition of D-serine.

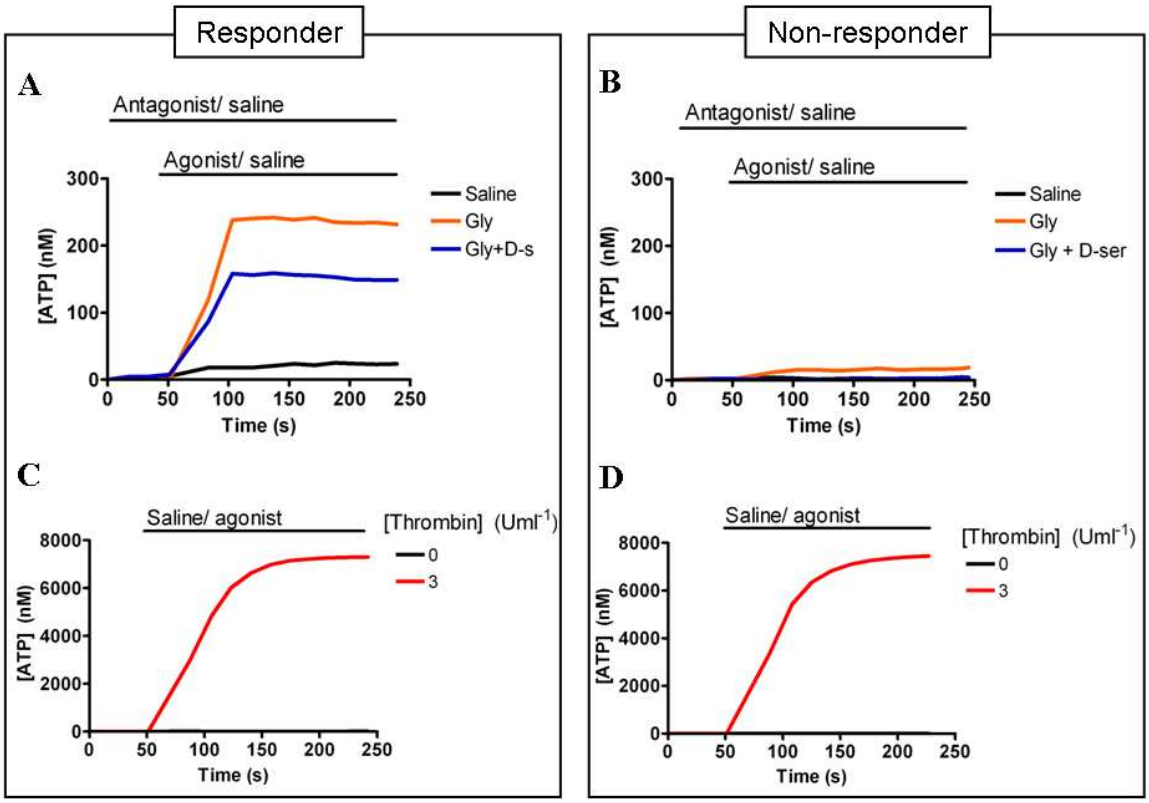

Figure 42. Glycine triggers ATP secretion from human platelets which can be inhibited by D-serine. **A, B,** Representative responses elicited by the addition of 3 μM glycine to luciferase-containing human platelet suspension in the presence and absence of 10 μM D-serine. Each trace represents single responses from 2 different donors. **C, D,** Representative responses to the addition of thrombin (3 U ml^{-1}; positive control) for the same respective donors. The lines indicate the duration of application of agonist, inhibitor and saline (nominally Ca^{2+}-free salt solution). Data was obtained within the first 3 h of each experiment.

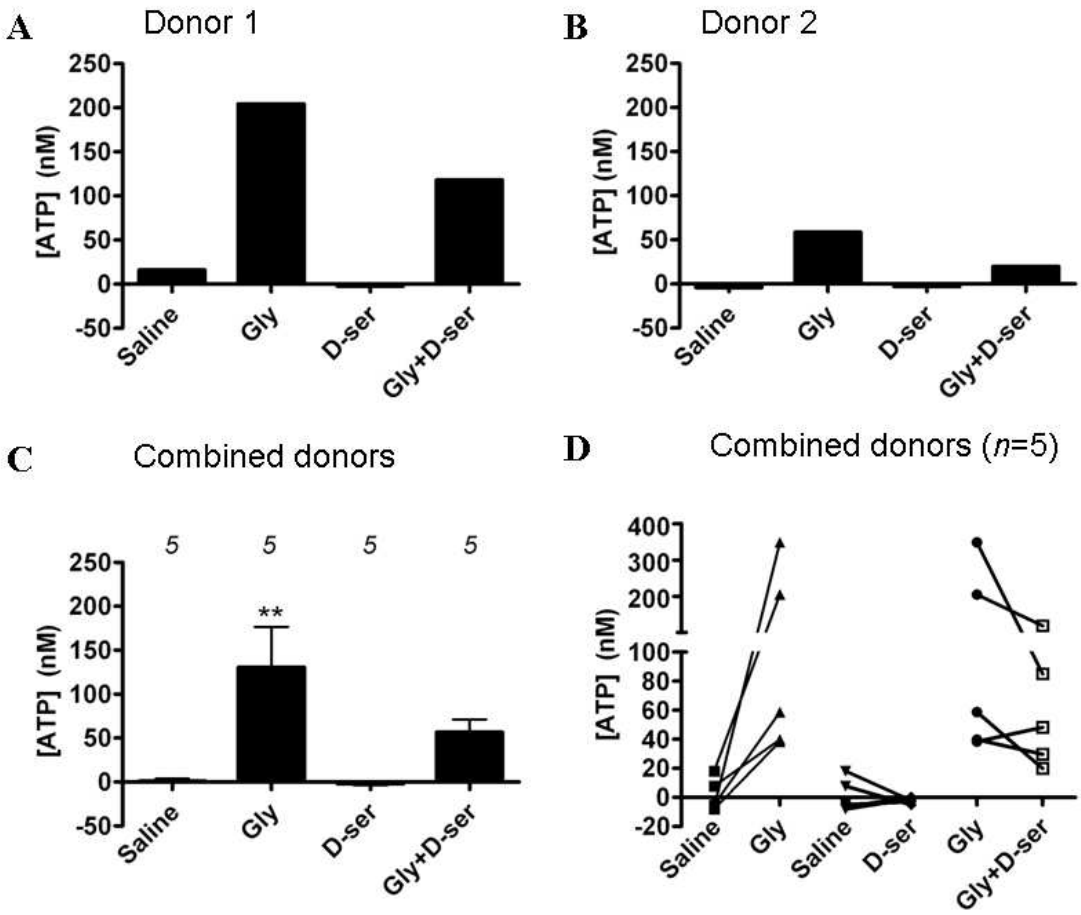

Figure 43. Glycine triggers ATP secretion from human platelets which is inhibited by D-serine. **A, B,** Each histogram exemplifies the peak responses from a single donor (*n*=1). **C,** Histogram illustrates the combined peak response data from different responding donors (*n*=5 ± S.E.M.). Saline, nominally Ca^{2+}-free salt solution; Gly, glycine; D-ser, D-serine. **D,** Plot demonstrates the combined mean peak response data from different responding donors (*n*=5). This demonstrates that 10 μM D-serine (D-ser) alone leads to a decrease in response in 2 donors with no effect in the remaining 2. The addition of 0.3 μM glycine (gly) elicits increased ATP release in 5 donors, of which responses in 4 are inhibited by the addition of D-serine. There is no effect on the remaining donor. ** P< 0.01 compared to saline (nominally Ca^{2+}-free salt solution) using one-way ANOVA with Dunnetts post-hoc test. The data was obtained within the first 3 h of each experiment.

4.4. Discussion

In this study I have demonstrated that human platelets (i) express NMDAR NR3 subunits, (ii) glycine elicits an increase in cytosolic $[Ca^{2+}]_i$ in a percentage of donors and (iii) glycine evokes ATP secretion sensitive to partial inhibition by D-serine.

4.4.1. Expression of NMDA receptor NR3 subunits

Expression of the NMDAR NR3 subunit protein was originally identified in the brain (Wong *et al*, 2002; Wee *et al*, 2008), and the mRNA has more recently been detected in the rat stomach (Wantanabe *et al*, 2008). This study has determined for the first time that the NR3 subunit protein is expressed in human platelets, which is also the first demonstration of its protein expression outside the CNS. Previous studies have shown that NR1 and NR3 subunits can form a functional receptor which requires only the binding of glycine for activation (Chatterton *et al*, 2002). As expression of the NR1 subunit protein has previously been demonstrated in human platelets (figure 13; Genever *et al*, 1999), it is possible that functional NR1/ NR3 receptors are present. To determine this, the same assays used to determine receptor function in Chapter 3 were used, Ca^{2+} influx and ATP release.

4.4.2. Glycine-evoked calcium responses

As demonstrated in the previous chapter, changes in $[Ca^{2+}]_i$ could be separated into the donors which did and those which did not respond to the application of extracellular glycine (figure 32). The timing of the recordings was also shown to have an effect on the responses obtained, with the greatest changes occurring over 2 h from the start of the experiment, which was in total 3 to 3.5 h from the whole blood being taken from the donor (figure 31). In comparison, the responses to thrombin vary only slightly over the duration of the experiment (figure 32F). The overall trend is for responses to decrease over the course of the experiments, and as with the NR1/ NR2 combination of subunit proteins, it suggests that the receptor is desensitising. The receptors have been demonstrated to rapidly resensitise upon removal of glycine, showing that this modulation is rapidly reversible (Awobuluyi *et al*, 2007). Desensitisation has been shown to be induced by the binding of glycine to the NR1 subunit through point mutagenesis and the use of a specific NR1 subunit antagonist (MDL-29951), where inhibition of the subunit increases currents induced by extracellular glycine through binding to the NR3 subunit (Awobuluyi *et al*, 2007; Madry *et al*, 2008).

As previously mentioned, the formation of Ca^{2+} micro-domains close to the intracellular face of NR1/ NR2 NMDARs has been found to play a role in desensitisation of the receptor, where increases in the level of Ca^{2+} decreases the open probability of the receptors (Rosenmund and Westbrook, 1993). NR1/ NR3 receptors are less permeable to Ca^{2+} than NR1/NR2 receptors (Chatterton *et al*, 2002), which suggests that the formation of Ca^{2+} micro-domains could be slower as the Ca^{2+} influx is reduced. Given the lack of voltage-gated Ca^{2+} channels in human platelets (Doyle and Rüegg, 1985), other receptors may also be involved, for example Na^{+} permeable channels which can induce the release of either calcium from intracellular stores or the release of ATP to trigger further influx of Ca^{2+} into the cell (figure 30).

Another factor that may contribute to receptor desensitisation is the NMDAR subunit conformation of the receptors on the platelets. This is the first demonstration of NR3 subunits in platelets and it unknown what the contribution of NR3 subunits is to the final receptor assembly. The presence of the NR3 subunit in tri-heteromeric receptors decreases the responses evoked by activating the receptor, which has the effect of reducing the influx of Ca^{2+} into the cell (Ciabarra *et al*, 1995; Sucher *et al*, 1995). It is not known comparatively, what the differences in Ca^{2+} permeability are between the different combinations of subunits (NR1/ NR2, NR1/ NR3 and NR1/ NR2/ NR3), however this could be investigated by transfecting cells without native expression of NMDAR subunit proteins with the required subunits and determine the differences. Concatemers could be used to ensure that equal amounts of DNA were inserted for each subunit required, for example NR1, NR2D and NR3A, varying the subunits included. However, as in native cells the exact combinations of subunits would not be known, but could potentially be extrapolated using a range of different combinations of subunits e.g. NR1/NR2D, NR1/NR3A, NR1/NR2D/NR3A.

4.4.3. Glycine versus thrombin-evoked calcium responses

The peak Ca^{2+} response induced by 3 μM glycine is 67.32 ± 7.22 % smaller than that elicited by 3 U ml^{-1} thrombin (figure 34). As described in Chapter 3, it is possible that the increase in $[Ca^{2+}]_i$ induced by stimulation of NR1/ NR3 receptors plays an important role in platelet activation, possibly akin to that of $P2X_1$ that induces a small Ca^{2+} influx on

activation, but which plays an important role in the initiation and continuation of thrombus formation (Hechler *et al*, 2003).

4.4.4. Receptor pharmacology: the action of D-serine

The absence of the NR2 subunit in NR1/ NR3 NMDARs means that not only is glutamate not required for receptor activation, but also that the receptor can not be inhibited by D-AP5, which competitively binds to the glutamate binding site (Costa *et al*, 2009). It has also been shown that the open channel blocker MK-801, has little or no effect on the receptor (Chatterton *et al*, 2002). Instead, D-serine which acts as a co-agonist to glutamate or NMDA in classic NMDAR conformations has been found to inhibit NR1/ NR3 glycine-induced responses in transfected oocytes (Chatterton *et al*, 2002). Prior to investigating whether D-serine has an inhibitory effect on glycine applied extracellularly to human platelets, it was important to determine whether extracellular D-serine alone could elicit increases in $[Ca^{2+}]_i$. D-serine binds to the NR1 subunit, so it is hypothetically possible that in native platelets D-serine could act as a co-agonist for glycine in NR1/ NR3 receptors, or even stimulate responses alone. Alternatively, it could repeat the results of Chatterton *et al* (2002), and inhibit the glycine-elicited responses. The NR2D subunit is also expressed in human platelets (figure 15), therefore it is possible that D-serine could stimulate a small response from NMDARs in the NR1/ NR2D subunit conformation either alone, or in combination with glutamate secreted by platelets which may have become activated by the addition of D-serine, or through the mechanical stimulation during platelet isolation. While a small response was observed upon the addition of D-serine to the platelets, it was comparable to that stimulated by the addition of saline, repeating findings published by Chatterton *et al* (2002), and demonstrating that D-serine alone does not induce an increase in $[Ca^{2+}]_i$ (figure 36).

A recent study has demonstrated that the activity of the ionotropic serotonin receptor, 5HT3 which is expressed in human platelets, is modulated by D-serine (Derkach *et al*, 1989; Shad, 2006). The presence of D-serine increases the sensitivity of the receptors to serotonin, which have been demonstrated to be permeable to a range of ions including Ca^{2+}, Na^+ and K^+ (Derkach *et al*, 1989; Yang, 1990). This suggests that activation of platelets by other agonists, for example glutamate, which trigger release of the contents of dense granules, that includes serotonin, can then trigger further stimulation of the same and nearby platelets through activation of the 5HT3 receptors, which are sensitised by the

presence of D-serine which also has a role in NMDAR activation. In the case of NR1/NR3 NMDARs, D-serine acts as an inhibitor (Chatterton *et al*, 2002), however in this study it was only demonstrated to act as a partial inhibitor. I hypothesise that D-serine inhibits NR1/NR3 NMDARs, but may also potentiate 5HT3 receptor activation through serotonin released from the dense granules. This could be further investigated using 5HT3 antagonists, for example ICS 205-930 or GR 38032F, to determine the role played by the receptor in platelet activation triggered by glycine in the presence of D-serine (Derkach *et al*, 1989) (figure 44).

The addition of D-serine to human platelets in combination with glycine had a mixed effect on $[Ca^{2+}]_i$ (figures 37A and B), either inhibiting (3 donors), potentiating (3 donors), or having no effect on the glycine-elicited response in the 2 remaining donors (figure 38D). However overall there was no net change in the mean ± S.D. % MR either with or without D-serine (figure 38C). Further study is therefore required to determine whether D-serine has a role to play in NMDAR modulation and then whether it extends to a functional role in platelet activation. D-serine is known to act as a co-agonist in classic NR1/NR2 NMDAR combinations and has more recently been determined to act as an inhibitor in the NR1/NR3 subunit conformation (Dingledine *et al*, 1999; Chatterton *et al*, 2002). NMDARs can exist as not only as heteromeric but also as triheteromeric receptors, where the presence of the NR3 subunit leads to a decrease in response to glutamate/ NMDA and glycine to that obtained with the classic NR1/NR2 combination (Ciabarra *et al*, 1995; Sucher *et al*, 1995). In this study the NR1, NR2D and NR3 subunits have been shown to be expressed in human platelets (figures 13, 15 and 31), suggesting that several different combinations of receptor subunits are present e.g. NR1/ NR2D, NR1/ NR3 (A or B), NR1/ NR3A, NR1/ NR3B and NR1/ NR2D/ NR3 (A or B). It is therefore possible that in human platelets, the NR3 subunit has a regulatory role in the level of NMDAR activation, with the simplest explanation for the differences observed with D-serine in combination with glycine being differential expression of NMDAR subunits between donors. The development of a selective NR3 antagonist will help to identify specific NR1/ NR3 responses. Currently, there are only a couple of differences between NR1/ NR3 and other glycine-activated receptors. Glycine receptors (GlyR) which permit influx of Cl^-, are widely expressed in the CNS particularly in inhibitory interneurones in the spinal cord and are reversibly inhibited by strychnine (Curtis *et al*, 1967). To date they have not been identified in platelets, and therefore further investigation is required to determine whether they are expressed, and

whether the receptors are functional. In other cell types, GlyRs have been shown to play a mixed role, with some studies demonstrating that stimulation of GlyRs leads to an increase and others showing a decrease in $[Ca^{2+}]_i$; for example in oligodendrite progenitor cells, stimulation of GlyRs lead to activation of voltage gated Ca^{2+} channel and an influx of Ca^{2+} (Belachew *et al*, 2000), and it is thought that in neutrophils stimulation of GlyRs leads to attenuation of Ca^{2+} influx (Wheeler *et al*, 2000). In comparison, NR1/ NR3 receptors induce an excitatory response and are therefore termed excitatory glycine receptors (Chatterton *et al*, 2002). They are strychnine-insensitive, enabling strychnine to be used to selectively inhibit activation of GlyRs (Chatterton *et al*, 2002). However this does not select between responses evoked by activation of NR1/ NR3 or NR1/ NR2 receptors given that glutamate may be secreted from platelet granules in response to the mechanical stimulation of agonist addition.

4.4.5. Glycine-mediated ATP release

In this study, glycine has been demonstrated to evoke the secretion of ATP from human platelets. The data from the ATP assay also illustrated a split in donors between responders and non-responders, with time also having an effect on the responses recorded (figures 39 and 40). As in Chapter 3, a 10 fold lower concentration of glycine was required to stimulate an increase above that induced by saline (0.001 μM) than in the Ca^{2+} assay (0.01 μM) (figure 23 and 40). This difference could be due to the formation of Ca^{2+} micro-domains following Ca^{2+} entry through the NR1/ NR3 receptor (figure 29), which is sufficient to stimulate the release of ATP from the dense granules at lower concentrations than required to elicit a detectable response from the fluo-4 in the Ca^{2+} assay. This could be tested by increasing the concentration of the fluo-4 used, or by reducing the concentration of the luciferase used in the ATP assay. High speed fluorescent imaging of Ca^{2+} movement could also be used. Recordings using the plate reader are limited to every 0.1 s, which means that faster bursts of Ca^{2+} (or Ca^{2+} spikes) may either not be detected or the peak of the bursts missed, whereas a high speed system is able to take up to 200-400 frames s^{-1} enabling a higher resolution and more accurate picture of the responses triggered (Sigimori *et al*, 1990).

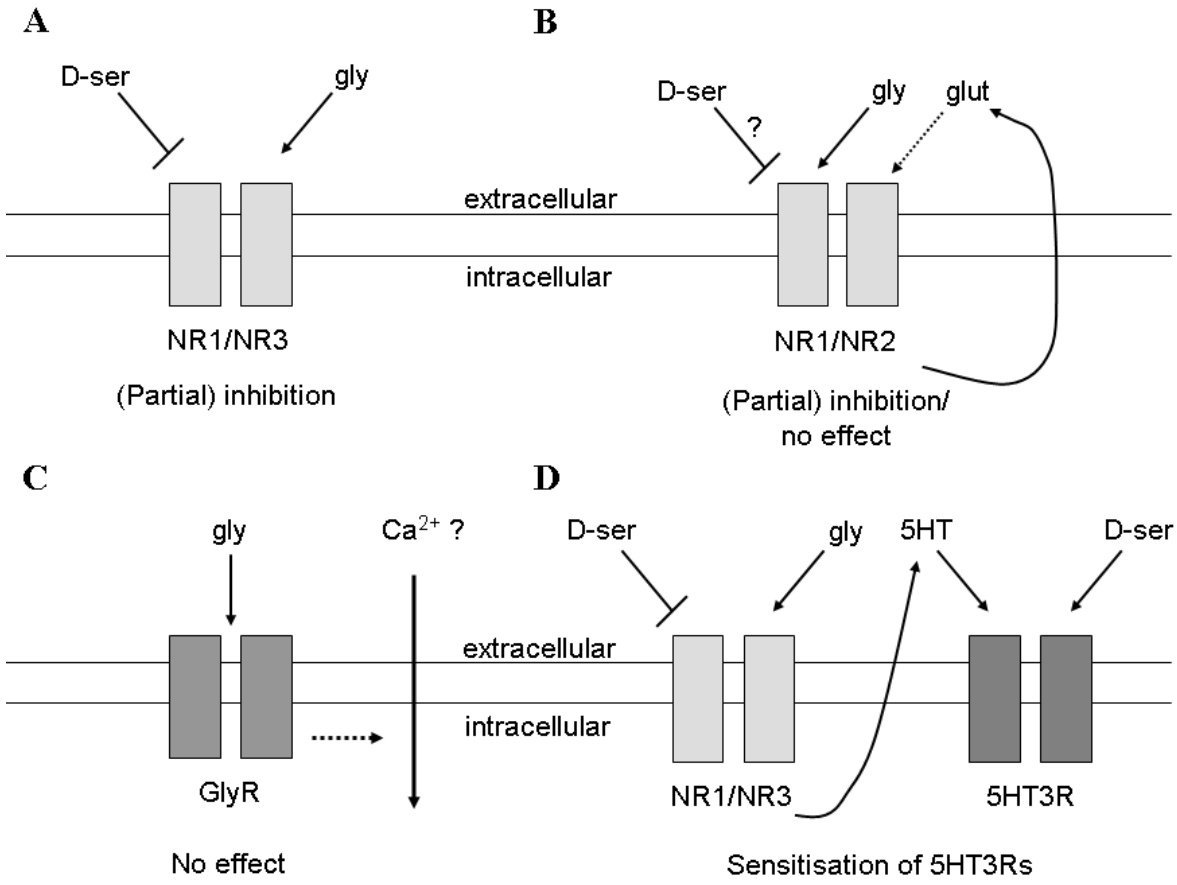

Figure 44. The potential actions of D-serine on glycine-mediated calcium influx. A, illustrates the excitatory glycine receptor, NR1/NR3, which is activated by glycine and inhibited by D-serine. In this study, 10 μM D-serine induced only a partial inhibition, however a larger concentration may induce full inhibition of Ca^{2+} influx. **B,** another variation is the effect on the classic NR1/NR2 NMDA subunit combination. Here D-serine acts as a co-agonist to glutamate or NMDA, but its role in the presence of only glycine is unknown. If the response to glycine is only partially inhibited, it is possible that the response will be sufficient to trigger glutamate release from the dense granules into the extracellular environment which could activate the NR1/NR2 receptor in a more classical manner, either by glutamate and glycine, or glutamate and D-serine. **C,** demonstrates the hypothetical role of GlyRs, which are not themselves affected by D-serine, but through their activation by glycine by can affect $[Ca^{2+}]_i$. **D,** illustrates the sensitisation effect of D-serine on 5HT3 receptors, which can be activated at lower concentrations of serotonin (5HT) in the presence of D-serine. Serotonin is released by activation of platelets and influx of Ca^{2+}, for example by stimulation of NR1/NR2 NMDARs by glutamate and glycine or D-serine. Ca^{2+} is also able to enter cells through the 5HT3 receptors.

The addition of D-serine alone to isolated human platelets induces a mixed ATP response, with no effect in 6 donors, an increased response in 1 donor, and inhibition of responses from that elicited with saline in the remaining 5 donors (figure 43). The ATP response elicited by the addition of glycine is variable between donors, and a partial inhibition is observed of the largest responses to extracellular glycine (figure 43). Overall, D-serine causes an inhibition in the responses elicited by glycine, but within the donors, those which generate the greater ATP release in responses to glycine are partially inhibited. This might suggest that (i) the expression of a second non-NMDA glycine receptor, (ii) an assembly of novel NR3 containing receptors with lower sensitivity to D-serine or an insufficient concentration of D-serine, or (iii) the concentrations published were determined using heterologous expression systems and therefore may differ in native systems.

Differences in the results obtained for the 2 different assays (changes in intracellular Ca^{2+} and ATP release) are apparent with no net change in the mean ± S.D. with the fluo-4 assay, and a noticeable, but not significant, inhibition with the addition of D-serine in ATP release (figures 38 and 43). The data is not directly comparable as different donors were used for each type of assay and the preparatory methods for the platelets were not the same. The data can therefore only be compared within each method. To obtain comparable data and to determine whether there are differences between the data obtained with the 2 methods, the platelet preparation for the ATP release assay should be changed to that used in the intracellular Ca^{2+} assay which has been published (MacKenzie *et al*, 1996) and experiments carried out in parallel for both ATP release and changes in $[Ca^{2+}]_i$.

4.4.6. Clinical relevance and overall conclusions

Until recently, glycine was thought to be implicated only in inhibitory pathways, but functional studies on the NR3 subunit discovered that when expressed in combination with the NR1 subunit protein, it elicited an excitatory response (Chatterton *et al*, 2002). Glycine has been found to be stored in human platelets, and levels have been shown to become raised during migraines (D'Andrea *et al*, 1991). Dysregulated glycine secretion could lead to stimulation of inhibitory glycine signalling pathways in the brain if signalling is raised, or could lead to stimulation of NR1/ NR3 receptors expressed on platelets. Little is known about the effects of glycine secreted from human platelets, and so further study is required.

Previous studies have been carried out on NR3 subunits which have been localised in rat brain or using cDNA isolated from rat brain and transfected in oocytes (Chatterton *et al*, 2002; Ciabarra *et al*, 1995; Sucher *et al*, 1995), but not from human cells or tissue, making this study one of the first to investigate the role of endogenous human NR1/ NR3 receptors. Therefore, all known pharmacology is derived from, and compared to, that of the rat NR3 subunit, which could potentially demonstrate variations in potency for example to glycine, with the human NR3 subunits. Knockouts have been developed of both NR3 subtypes, with the NR3A knockout showing enhanced responses to NMDA in comparison to WT littermates (Das *et al*, 1998). The number of dendritic spines was also found to increase. The mice were found to be viable and fertile with no apparent behavioural abnormalities (Das *et al*, 1998). Another study demonstrated that the NR3B knockout was also viable and fertile, with increased sociable behaviour but also exhibited increased anxiety especially in new environments (Niemann *et al*, 2007). Motor learning and co-ordination is mildly impaired in the knockout mice and activity in their home cages is also reduced (Niemann *et al*, 2007). These studies describe varied roles for each of the NR3 subunits, however further investigation is required in the animal models to more fully identify the role of the NR3 subunits in platelet activation. Further study is also required into the role of the NR3 subunit in human platelets, which would be aided by the development of a specific NR3 subunit inhibitor.

CHAPTER 5
MEGAKARYOCYTES

5.1. Summary

In this chapter, it has been demonstrated that:

- MEG-01 cells express the NMDA NR1 subunit proteins, but have not been found to express the NR2A or NR2D subunit proteins
- MEG-01 cells treated with PMA, in the presence or absence of fibrinogen, resulted in cell adhesion and an increase in cell size
- PMA-induced changes in MEG-01 morphology and cell size, in the presence or absence of fibrinogen, were not affected by NMDAR inhibitors.
- PMA-induced MEG-01 adhesion to tissue culture plastic is potentiated by NMDAR inhibitors
- Fibrinogen-dependent MEG-01 adhesion is inhibited by both NMDAR inhibitors, D-AP5 and MK-801

5.2. Introduction

In previous chapters, it has been demonstrated that human platelets express the NMDAR NR1, NR2D and NR3 subunit proteins (figures 12, 14 and 30). Evidence for the presence of functional NMDAR has also been presented, including increased ATP release with the addition of glutamate and increases in fluorescence indicative of increased intracellular Ca^{2+} on the addition of either glutamate or NMDA to fluo-4 loaded platelets (figures 23 and 26). These are indicative of the classic NMDA receptor NR1/NR2 complex. Another combination of subunits has also been determined, NR1/NR3, which is activated by glycine alone due to the lack of an NR2 subunit protein (Chatterton *et al*, 2002), and has also been demonstrated to be functional in human platelets (figures 32 and 38).

NMDAR have been primarily characterised in the brain, where they have been shown to be involved in the learning and memory pathways (Do *et al*, 2002). More recently a role has been suggested for NMDAR in MK differentiation (Genever *et al*, 1999; Hitchcock *et al*, 2003). During this process (section 1.1.3.3.), platelets are formed from the cytoplasmic contents and membrane of the parent MK, suggesting that proteins present in the parent cell are present into the daughter platelets (Italiano Jr *et al*, 2003; Patel *et al*, 2005). This study

was therefore extended to investigate the expression and functional role of NMDAR in MK differentiation using the megakaryoblastic cell line MEG-01, which was used in the initial study (Genever *et al*, 1999).

The MEG-01 cell line was established in 1985 by Ogura *et al*, using megakaryoblastic bone marrow cells isolated from the bone marrow of a male patient with Philadelphia chromosome positive chronic myelogenous leukaemia. The cells were assessed and tested for a range of markers to determine whether they are a suitable model for native megakaryocytes, which are detailed in table 39.

	Indicates...	MEG-01 cells	Native MKs
Acid phosphatase	Lysosomal enzymes	+	+
α-naphthyl acetate esterase	Non-specific monocyte and MK esterase	+	+
Periodic-Schiff reaction	Presence of carbohydrates	+	-
Naphthol AS-D choloroacetate	Granulocytes and mast cells	-	-
α-naphthyl butyrate esterase	Late stage monocytes	-	-
Leukocyte alkaline phosphatase	Late stage/ mature MKs	-	-
Myeloperoxidase	Neutrophils	-	+
Platelet peroxidise	Mature MKs to platelets	-	-
Platelet GPIIb/IIIa	Present from megakaryoblast stage to platelets	+	+
α-granules	Mature MKs	-	-
Demarcation membrane	Mature MKs	-	-

Table 39. Tests used to determine how megakaryocyte-like the MEG-01 cell line is (Pombo *et al*, 1987; Sun *et al*, 2006; Morgan and Brodsky, 1985; Okabayash *et al*, 2009; Werzel *et al*, 1967; Larson *et al*, 2006; Vainchenker *et al*, 1982).

This demonstrates that MEG-01 cells can be used as models for immature native MKs or megakaryoblasts, as they have similar properties, with the exception of the positive response to the periodic-Schiff reaction and the negative response to myleperoxidase, which is indicative of acute megakaryocytic leukaemia (Sun *et al*, 2006). NMDARs have previously been identified in MKs in 2 studies described in section 1.3.2.1.1.

5.2.1. PMA- induced differentiation

PMA has been demonstrated to stimulate MK differentiation in both cell lines and in native MKs (Genever *et al*, 1999; Nagata *et al*, 1996; Lumelsky and Schwartz, 1997). It binds to the cell membrane, through which it is able to pass partially into the cell while remaining attached to the membrane (Zhang *et al*, 1995). PMA has been shown to mimic the action of DAG in its ability to bind the members of the protein kinase C (PKC) family (Zhang *et al*, 1995).

PKC isoforms can be separated into three groups; conventional (cPKC), novel (nPKC) and atypical (aPKC). cPKC isoforms, α, βI, βII and γ, are activated by DAG, Ca^{2+} and phospholipid (PL) whereas the novel isoforms (δ, ε, η and θ) require only DAG and PL. In comparison, aPKC isoforms are insensitive to DAG and Ca^{2+} (Kikkawa *et al*, 1982; Ohno *et al*, 1988; Ono *et al*, 1989). PKC is located in the cytosol of cells, and translocates to the cell membrane where it tethers loosely in an open, inactive conformation. A pseudosubstrate is held within the substrate-binding cavity, which is released upon the enzyme tethering, exposing the C-terminus to the cytosol (Dutil and Newton, 2000). The hydrophobic region of the C-terminus is then bound by phosphoinositide-dependent kinase-1 (PDK-1) whose main substrate is Akt, but has been shown to also phosphorylate the activation loop of all PKC isoforms (figure 45) (Alessi *et* al, 1997; Gao *et al*, 2001; Dutil *et al*, 1998; Le Good *et al*, 1998; Chou *et al*, 1998). This action leads to the dissociation of PDK-1, exposing the C-terminus which enables further autophosphorylation of the turn (c, n and a isoforms) and the hydrophobic (c and n isoforms) motifs of the PKC. In combination with the re-association of the pseudosubstrate with the substrate-binding cavity, this converts the enzyme to its mature, inactive form, which dissociates from the membrane and returns to the cytosol (Newton, 2003).

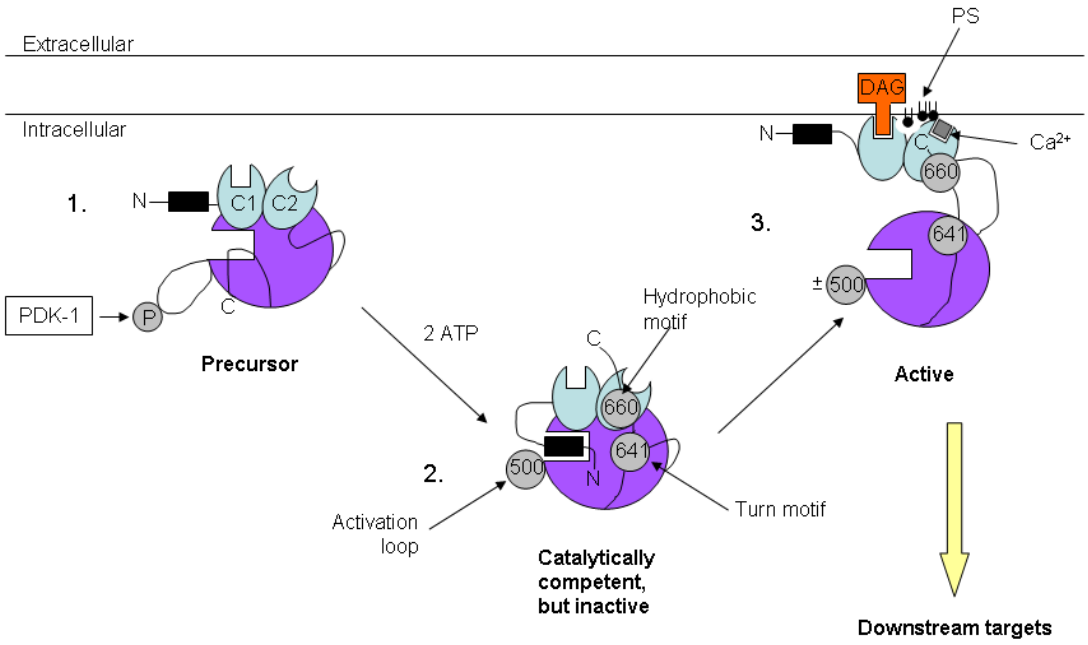

Figure 45. Schematic demonstrating the roles of the pseudosubstrate in regulation of PKC activity. C1 domain, contains the DAG (diacylglycerol) binding site; C2 domain contains the Ca^{2+} binding site (only present in conventional isoforms of PKC); PS, phosphatidylserine; PDK-1, phosphoinositide-dependent kinase-1; light grey circles indicate sites of phosphorylation, numbers indicate amino acid number phosphorylated; black rectangle, pseudosubstrate sequence; open rectangle, active site. **1**, the activation loop of PKC is exposed, enabling phosphorylation by PDK-1. **2,** this initial phosphorylation leads to autophosphorylation of the turn and hydrophobic motifs, which is halted by movement of the pseudosubstrate into the active site forming a catalytically competent, but inactive conformation, and the enzyme localises to the cytosol. **3,** Production of DAG leads to PKC translocation to the plasma membrane, where changes in conformation through binding of the C1 domain to DAG and C2 to Ca^{2+} (cPKC only) cause the release of the pseudosubstrate from the active site, activating the enzyme. Adapted from Dutil and Newton, 2000.

Under normal activation conditions, production of DAG and an increase in $[Ca^{2+}]_i$ targets the mature, inactive PKC to the membrane through binding of Ca^{2+} to the C2 region and the membrane-bound DAG to the C1 region (Nalefski and Newton, 2001). The affinity for DAG has been demonstrated to be greater in the C1 region of nPKC isoforms to aid binding to the cell membrane, as they are lacking the additional binding mediated by Ca^{2+} through the C2 region present in conventional isoforms (Giorgione *et al*, 2006). This binding leads to the release of the pseudosubstrate enabling substrate binding, phosphorylation and the induction of intracellular signalling pathways e.g. the Ras/ Raf/ MEK pathway (Griner and Kazanietz, 2007). Once activated by DAG, desensitisation is rapid, with heat-shock

protein 70 (HSP70) demonstrated to bind the dephosphorylated turn motif and stabilise the enzyme as it returns to the cytosol. The enzyme can then be rephosphorylated and recycled (Gao and Newton, 2002). When cells are stimulated with PMA, the mature, inactive PKC translocates to the membrane, binding through the C1 domain to the PMA, and triggering conformational changes which enable its activation. Binding of PKC to PMA leads to prolonged activation of the enzyme, resulting in slow dephosphorylation, down-regulation and disassociation with the membrane (Hansra *et al*, 1999).

Different PKC isoforms have been identified in platelets and MKs, the conventional α and β isoforms and the novel isoforms, δ and θ, together with the novel ε isoform in MKs and the atypical ζ isoform additionally expressed in platelets (Crosby and Poole, 2002; Grabarek *et al*, 1992; Nagata *et al*, 1996; Baldassare *et al*, 1992). The roles of activated PKC differ between MKs and platelets, from stimulating differentiation of MKs through an increase in synthesis of dense and α-granules for packaging within platelets, to an increase in expression of $\alpha_{IIb}\beta_3$, and inducing changes in cell shape (Nagata *et al*, 1996; Goto *et al*, 1992). In platelets, PKC has been demonstrated to induce expression of vWF and fibrinogen at the cell surface and stimulate thrombus formation (Konopatskaya *et al*, 2005).

From previous studies, it can be concluded that both PKC and NMDARs have a role in MK differentiation both in the MEG-01 cell line and in native MKs (Genever *et al*, 1999; Hitchcock *et al*, 2003; Nagata *et al*, 1996; Goto *et al*, 1992; Konopatskaya *et al*, 2005). These studies were extended by investigating the expression of NMDA receptor subunit proteins in MEG-01 cells differentiated with PMA.

5.2.2. Fibrinogen

Fibrinogen is a soluble glycoprotein produced by hepatocytes in the liver and in MKs, and is known to be involved in platelet adhesion and clot formation through binding to the integrin $\alpha_{IIb}\beta_3$ (Haidaris *et al*, 1989). Approximately 80000 copies of $\alpha_{IIb}\beta_3$ are present on the surface of unstimulated platelets, with additional monomers present within granules which are able to translocate to the membrane upon platelet activation (Wagner *et al*, 1996). There is also evidence that fibrinogen has a role in MK differentiation. Fibrinogen has been located in the blood sinusoids along which MKs migrate following an SDF-1 gradient as they differentiate (Wang *et al*, 1998). MKs finally adhere to fibrinogen in the sinusoids via the integrin and continue to differentiate, eventually producing proplatelets

which extend into the blood stream to release the individual platelets (Larson and Watson, 2006). The integrins have been found to be expressed only in more mature MKs, limiting fibrinogen-binding to cells which are ready to develop into proplatelets (Shiraga *et al*, 1999).

The binding of $\alpha_{IIb}\beta_3$ to fibrinogen involves 2 different signalling pathways- an inside-out and an outside-in. For the initiation of inside-out signalling, activation of the integrin is required, for example by TPO, thrombin or SDF, to stimulate binding to fibrinogen. Other signalling pathways have been found to regulate inside-out signalling such as PI3K and PKC, with their inhibitors (wortmannin and bisindolymaleimide) shown to block signalling by $\alpha_{IIb}\beta_3$, although not fibrinogen binding (Jiroušková *et al*, 2007). It has been shown that the TF, NF-E2, is required for terminal differentiation of MKs, and knockout of the p45 subunit prevents activation of NF-E2, inhibiting fibrinogen binding. The cytoplasmic tail of the β_3 integrin has been shown to interact with a number of different proteins including the cytoskeletal proteins talin, α-actinin and filamin (Calderwood *et al*, 1999; Bennett, 2005). Talin is known to also bind to actin, which has a major role in the structure of the cytoskeleton (Jiang *et al*, 2003). The second pathway, outside-in signalling, is triggered by the adhesion of MKs to fibrinogen via the $\alpha_{IIb}\beta_3$ integrin, which has been found to trigger activation of Rho GTPases including Rac and Rho. These play a role in cell spreading and cytoskeletal re-organisation, which has been observed in previous studies in MKs on culturing with fibrinogen (Shiraga *et al*, 1999). This combination of signalling pathways leads to changes in MK cell shape which characterise the later stages of differentiation.

5.3. Results

5.3.1. Detection of NMDAR subunit proteins by Western blot

The expression of NMDA NR1, NR2D and NR3 subunit proteins in human platelets has been demonstrated in Chapters 3 and 4 (figures 13, 15 and 31). The expression of these subunits together with that of the NR2A subunit was investigated in the undifferentiated megakaryoblastic cell line, MEG-01 by performing Western blots. These demonstrated that a band was detected between 100 and 150 kDa with an anti-NR1 antibody (figure 46), which corresponds to the expected molecular weight of the NR1 subunit (Moryoshi *et al*, 1991). This is in agreement with previous reports demonstrating the expression of the NR1 subunit protein in MEG-01 cells by Western blot (Genever *et al*, 1999). No bands were detected at the expected molecular weights for NR2A (figure 47) or NR2D (figure 48) in undifferentiated MEG-01 cells. From this data only the NMDA NR1 subunit protein appears to be expressed in undifferentiated MEG-01 cells.

5.3.2. Detection of NMDAR subunit mRNA by RT-PCR

Previous studies have demonstrated that mRNA for the NR1 and NR2D subunits is expressed in MEG-01 cells (Genever *et al*, 1999). This was repeated and expanded to investigate the expression of mRNA for all 7 NMDAR subunits; NR1, NR2A-D and NR3A and B. The optimal annealing temperatures for each set of primers was determined by setting up temperature gradients from 53- 63 ^{o}C on the Thermal Cycler (section 2.4.4), and using reverse transcribed human cerebellum samples (section 2.4.3). No bands were visible for the NR2D primers at either 30 or 35 cycles, not the NR3B primers at 35 cycles. From this the optimal temperatures and cycle numbers were determined (figure 49; table 40).

Table 40. Determining cycle numbers and annealing temperature for NMDAR primers

SUBUNIT	CYCLE NUMBER	ANNEALING TEMPERATURE (^{o}C)
NR1	30	59
NR2A	33	57
NR2B	33	61
NR2C	33	61
NR2D	-	-
NR3A	35	57
NR3B	-	-

PCR was therefore carried out on the remaining sets of primers using the cycle number and annealing temperatures detailed in table 40 following the programme listed in section 2.4.4 (figure 50). Reversed transcribed human cerebellum samples were also run alongside MEG-01 samples for each NMDAR subunit tested as a positive control as mRNA of all NMDAR subunits have been demonstrated in the cerebellum (Bessho *et al*, 1994; Monyer *et al*, 1994; Wong *et al*, 2002; Wee *et al*, 2008). MEG-01 and human cerebellum samples were also tested for the presence of β-actin cDNA to determine whether the loading of samples was comparable (section 2.4.4) (figure 50). This demonstrated that while all of the subunits tested were positive in the human cerebellum samples, no bands were detectable in either of the MEG-01 samples which were from 2 different passage numbers (M1- passage 10; M2- passage 12) of the same original sample (ATCC). Bands for β-actin were present for all of the samples and appeared to be equally loaded (figure 50). This demonstrates that mRNA does not appear to be expressed in MEG-01 cells at the time the samples were taken.

5.3.3. Effect of NMDAR inhibitors on cell morphology

Previous studies have reported that NMDARs play an important role in MK differentiation and have dramatic effects on cell morphology. Hitchcock *et al* (2003) demonstrated using ultrastructural analysis that during TPO-stimulated differentiation of $CD34^+$-derived MKs increased in size, induced the development of a multi-lobed nucleus, formation of α-granules and demarcation membrane together with formation of proplatelets in the absence of fibrinogen. These morphological changes could be inhibited by culturing the cells with the additional presence of MK-801. It is hypothesised that NMDARs are critical for the formation of platelets, and treatment of $CD34^+$-derived MKs with MK-801 has lead to a reduction of both the number of proplatelet forming MKs and the area of the MKs (Hitchcock *et al*, 2003). The number of MKs present at the end of the experiments is not affected by the presence of the NMDAR specific inhibitor (Hitchcock *et al*, 2003).

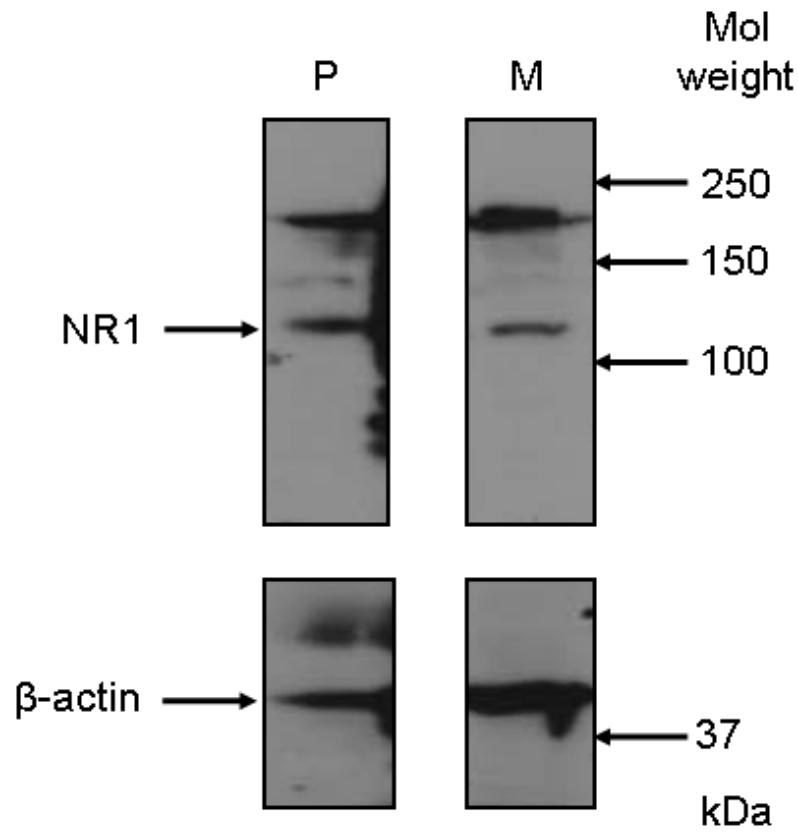

Figure 46. MEG-01 cells express NMDA receptor subunits NR1. Western blot demonstrating the expression of the NMDA NR1 subunit in undifferentiated MEG-01 human megakaryoblastic cells (M) and 1 human platelet donor (P; positive control) which were run on the same gel. The blot was split into two at approximately 70 kDa, with the top half probed for NR1 expression, and the lower half for β-actin to assess loading (expected size 42 kDa). The arrows on the right side indicate sizes predicted by protein standards (mol weight, molecular weight marker; kDa). Arrow on the left indicates the expected size of the NR1 subunit, 120 kDa. Representative blot from 12 different experiments. Approximately 15 μg protein was loaded for each sample using the Bradford assay to determine the protein concentration of each sample (section 2.4.1).

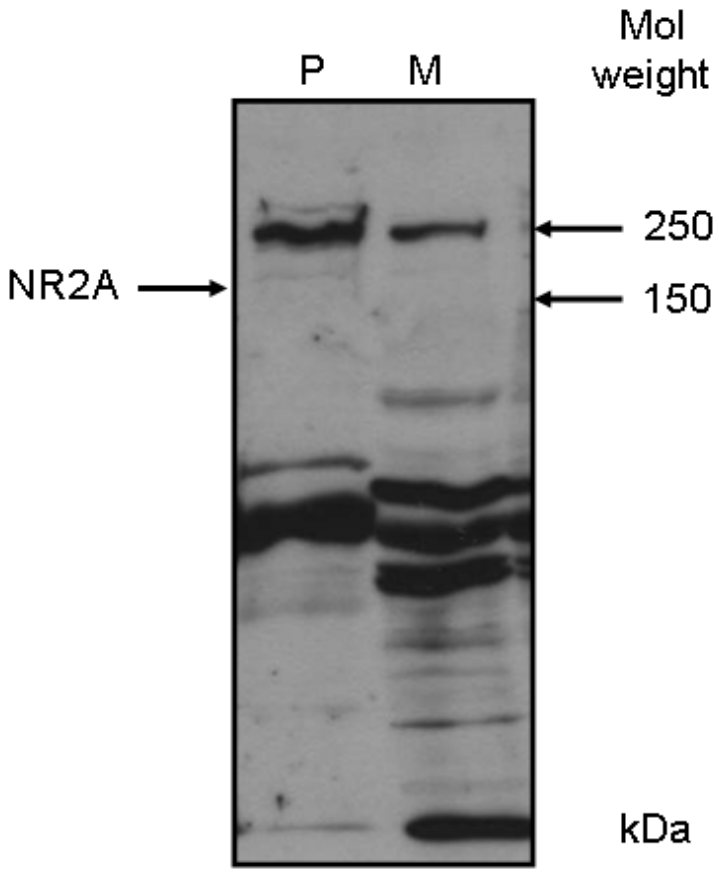

Figure 47. MEG-01 cells do not express detectable NMDA receptors subunit NR2A. Western blot demonstrating that expression of the NR2A subunit protein was not detected in undifferentiated MEG-01 human megakaryoblastic cells (M). The platelet sample (P) alongside demonstrates the apparent lack of NR2A expression in human platelets. The arrows on the right side indicate sizes predicted by the protein standards (mol weight, molecular weight marker; kDa). Arrow on the left indicates the expected size of the NR2A subunit, 180 kDa. Representative blot from 3 separate experiments. Approximately 15 μg protein was loaded for each sample using the Bradford assay to determine the protein concentration of each sample (section 2.4.1).

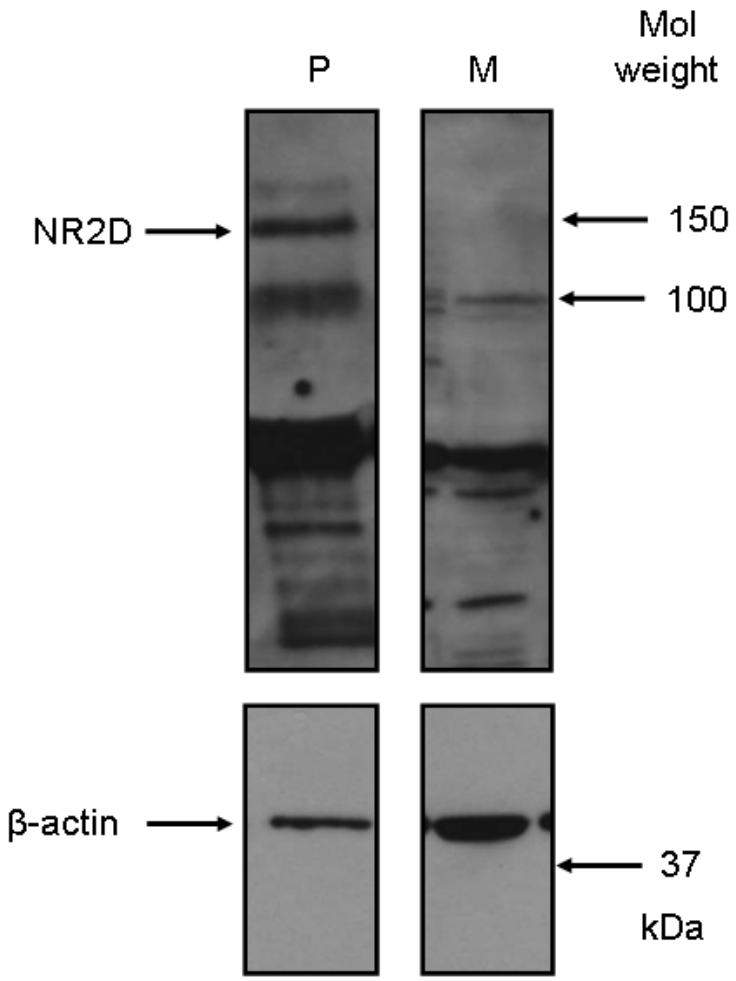

Figure 48. MEG-01 cells do not express detectable NMDA subunit NR2D. Western blot demonstrating that NR2D subunit protein expression was not detected in undifferentiated MEG-01 human megakaryoblastic cells (M). The platelet sample (P) run on the same gel demonstrates that NR2D is expressed in human platelets (positive control). The arrows on the right side indicate sizes predicted by the protein standards (mol weight, molecular weight; kDa). Arrow on the left indicates the expected size of the NR2D subunit, 150 kDa. Representative blot from 3 separate experiments. Approximately 15 μg protein was loaded for each sample using the Bradford assay to determine the protein concentration of each sample (section 2.4.1).

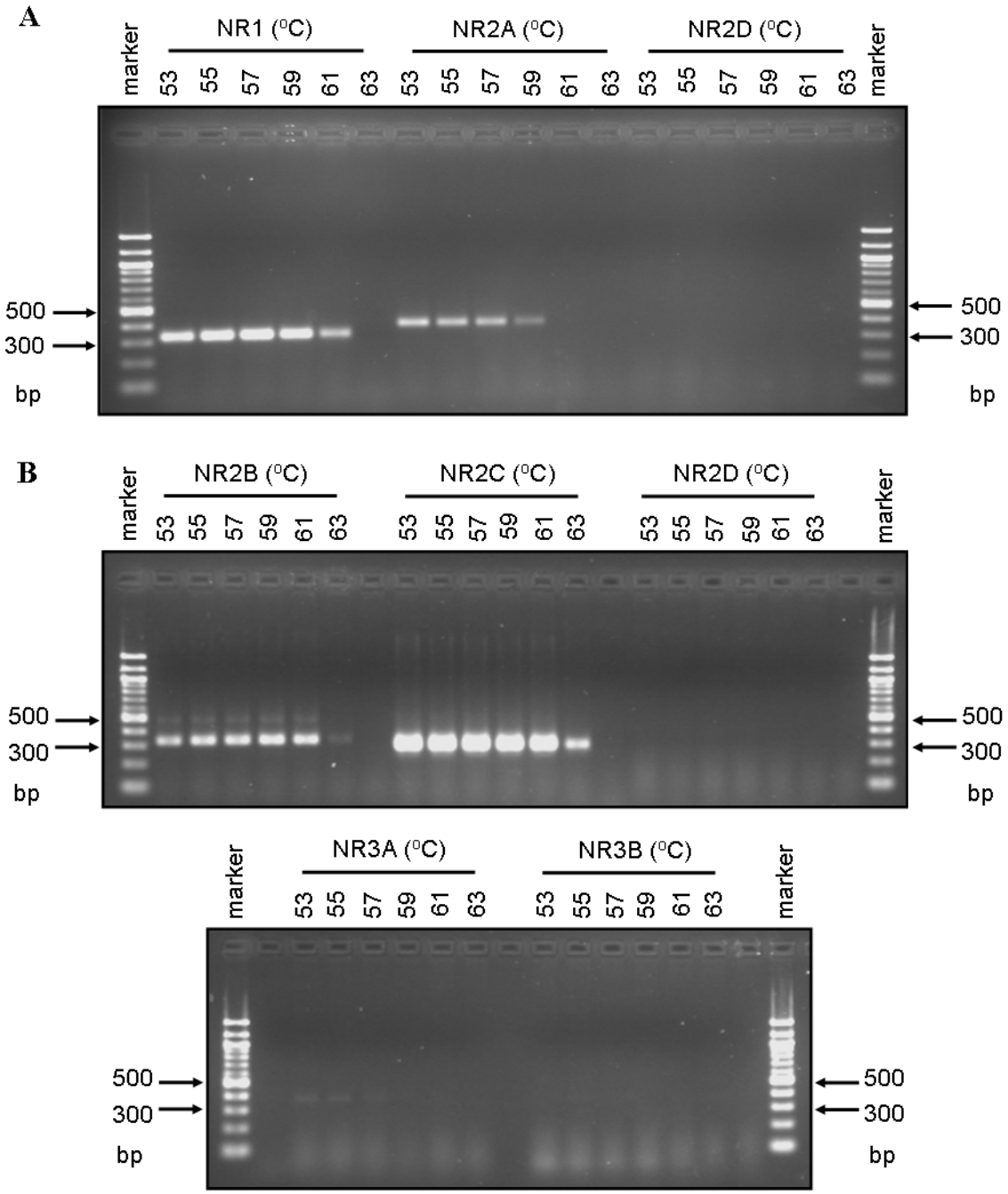

Figure 49. Temperature gradients to determine the optimal annealing temperatures for NMDAR subunit primers. A, Initially the primer sets for NR1, NR2A and NR2D were tested using 30 cycles of annealing, extension and melting. A gradient of 53- 63 °C for the annealing step were tested; temperatures are indicated above the relevant lane. Bands were visible for NR1 and NR2A but not NR2D primer sets at the expected sizes of 336, 391 and 336 bp respectively. **B,** The remaining primer sets were tested using the same gradient, using 35 cycles, the NR2D set were re-tested. Bands were visible at the expected sizes for NR2B (338 bp), NR2C (304 bp) and NR3A (352 bp), but not for NR2D (336 bp) or NR3B (385 bp). The PCR product of approximately 1 µg reverse transcribed RNA was loaded per sample.

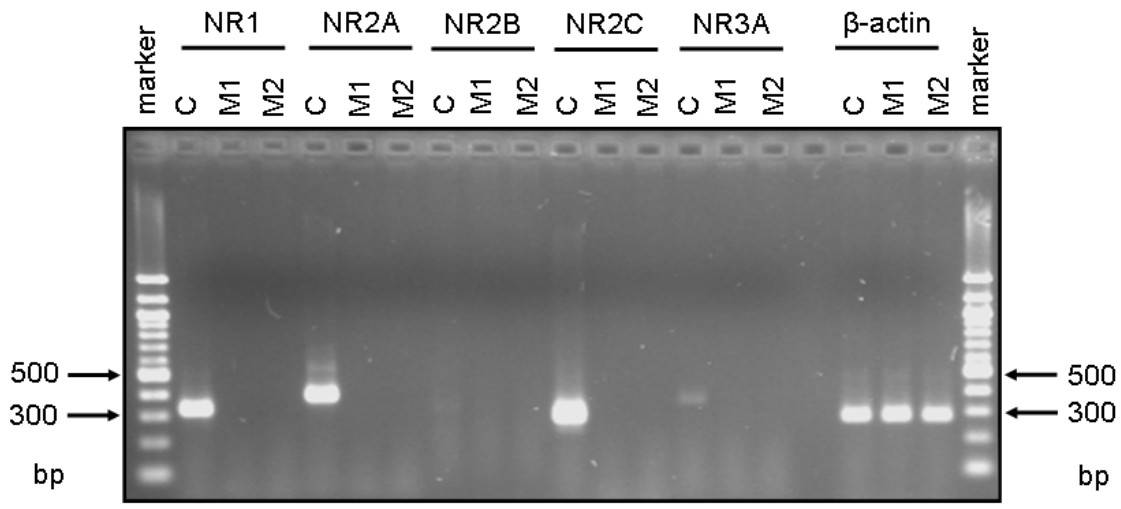

Figure 50. MEG-01 cells do not appear to express mRNA for the NMDAR subunits NR1, NR2A-C or NR3A. Two different MEG-01 samples were compared to that from human cerebellum demonstrating that the mRNA of subunits NR1, NR2A-C and NR3A are present in human cerebellum, but do not appear to be present in either MEG-1 sample at the time that the samples were taken. The samples on the right illustrate that β-actin mRNA is present in all 3 samples, and that the amount appears to be equal. The PCR product of approximately 1 μg reverse transcribed RNA was loaded per sample.

TPO has been shown to be the primary physiological regulator (Szalai *et al*, 2006) for megakaryocyte differentiation (figure 1), however PMA can also be used (Genever *et al*, 1999). PMA has previously been demonstrated to stimulate MK differentiation in both native MKs and MEG-01 cells, stimulating an increase in cell size, ploidy and adhesion, which have all been described as markers of MK differentiation (Hitchcock *et al*, 2003; Genever *et al*, 1999; Murate *et al*, 1991). PMA-mediated changes in MEG-01 cell morphology when cultured in tissue-culture treated flasks (section 2.3.2.1.) were characterised and the study extended by culturing MEG-01 cells in fibrinogen-coated dishes to compare differences. Additionally, the role of NMDAR in PMA-induced changes in cell morphology was investigated using the selective antagonists MK-801 and D-AP5.

5.3.3.1 Cell morphology in the absence of fibrinogen

Different methods were tested to differentiate MEG-01 cells using PMA in the absence of fibrinogen from 2 different published methods. The first method was described by Nagata *et al* (1996) where 1 x 10^5 cells ml^{-1} were treated with for 2 h with 10 nM PMA at 37 ^oC, washed, then resuspended at 1 x 10^5 cells ml^{-1} in fresh media and cultured for 3 d (section 2.3.2.1). The second method, described by Lacabaratz-porret *et al* (2000) used 2.4 x 10^5 cells ml^{-1} and treated MEG-01 cells for 3 d with 10 nM PMA in culture. Cultures using both methods were set up with either 10 nM PMA or 0.001 % DMSO (v/v) as a vehicle control and photographs taken after 3 d. The cells were then measured (section 2.3.2.1.1), and the results compared (figure 51). Figures 51 shows representative photographs, which demonstrate that cells treated with DMSO remain round and bright when either method 1 or method 2 was used. PMA treatment with method 1 stimulated a greater increase in size than in the DMSO match control (349.33 ± 22.75 μm^2 compared to 217.45 ± 10.57 μm^2 respectively) with some cells appearing to adhere to the bottom of the flask. The cells treated with PMA in method 2 are also larger in size than the DMSO controls, 483.82 ± 70.03 μm^2 and 163.89 ± 3.04 μm^2 respectively with the cells also becoming more irregular in shape and a larger proportion appearing to adhere to the bottom of the flask. The overall increase in cell size is greater using method 2, with an increase of 319.95 ± 70.10 μm^2 in comparison to 131.80 ± 25.06 μm^2 with method 1. Increase in cell size is one of the markers of MK differentiation and is being investigated in this study (Italiano Jr *et al*, 2003; Patel *et al*, 2005). Therefore method 2 will be used for subsequent experiments requiring PMA induced MK differentiation.

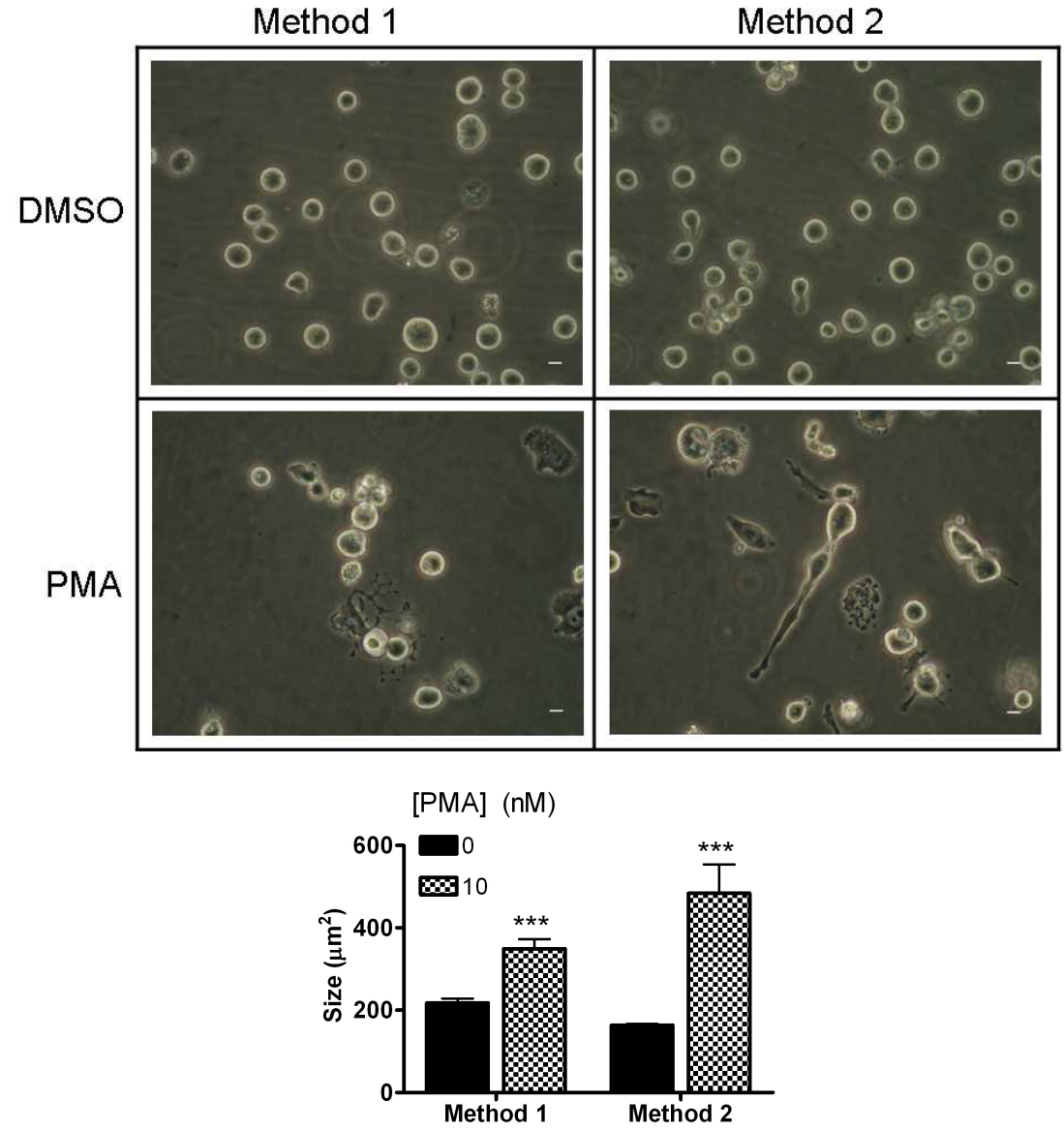

Figure 51. The size of MEG-01 cells increases with PMA-treatment. Representative pictures comparing the different treatments- method 1 where MEG-01 cells were exposed to 10 nM PMA for 2 h, washed then cultured at 1 x 10^5 cells ml^{-1} and method 2 where MEG-01 cells were chronically exposed to PMA (10 nM, 3 d) at 2.4 x 10^5 cells ml^{-1} (section 2.3.2.1). The histogram compares the differences in cell size with the 2 different methods. There is no difference between the DMSO-treated cells with either method 1 (2h exposure) or method 2 (3 d exposure), with the PMA-treated cells becoming generally larger in size than DMSO-treated cells with either method. Overall, the cells treated with PMA using method 2 are larger than those treated using method 1 (483.82 ± 70.03 μm^2 in comparison to 349.33 ± 22.75 μm^2 respectively). The data is pooled from 3 experiments (*n*=3) with 4-8 photographs taken for each treatment for each experiment, and analysed as described in section 2.3.2.1. *** P< 0.01 compared to the respective DMSO control using an unpaired, two-tailed Students *t*-test. Original magnification x 400, scale bar represents 10 μM.

5.3.3.2. Expression of NMDAR subunits in PMA-treated MEG-01 cells

MEG-01 cells were set up as described in section 2.3.2.1 (method 2) with either PMA (10 nM) or DMSO (0.001 % v/v) together with either MK-801 (100 μM) or D-AP5 (100 μM); samples were taken after 3 d in culture. The samples were prepared as described previously (lysis buffer B, section 2.4.3). Samples were run on 8 % SDS gels, transferred onto PVDF membrane (section 2.3.3-4), then probed for either the NR1, NR2A or NR2D subunit proteins (figures 52-4). Densitometry analysis was carried out on bands at the expected size for each subunit and was normalised against the intensity of bands obtained for the β-actin equal loading from the same blots (section 2.4.6). This is illustrated in figure 55. The NR1 subunit protein was shown to be expressed by both untreated and all treated MEG-01 cells, as well as in 2 different human platelet samples (figure 52). However, no overall differences were determined between the untreated or any of the differently treated MEG-01 cells. The combined analysis for donor 1 indicates that relative expression is 59.18 ± 39.61 % greater than that in untreated MEG-01 cells, with donor 2 showing a 10.98 ± 32.25 % increase in NR1 subunit protein expression above the untreated MEG-01 cells (figure 55).

In contrast, the expression of the NR2A subunit protein in MEG-01 cells is unclear. It does not appear to be expressed either by untreated MEG-01 cells or platelets (figures 14 and 47), however figure 53 demonstrates that there may be low level expression following treatment with PMA. Expression of the NR2D protein could not be detected in MEG-01 cells either with or without treatment (figure 48 and 54), however it is shown to be expressed in human platelets (figure 15 and 54) which are the terminal stage of MK differentiation. Using densitometry analysis, it was determined that the bands obtained at the expected size of 150 kDa in the platelet samples (figure 55) are 164.26 ± 25.87 % and 86.66 ± 9.75 % more intense than the matching β-actin expression for each donor respectively. Comparatively, the levels measured in the MEG-01 samples are between 5.81 ± 2.74 % and 16.56 ± 7.00 % of the matching expression levels of β-actin.

This data therefore indicates that the NR1 subunit protein is expressed by both MEG-01 cells and human platelets, with the NR2D subunit also expressed in human platelets but was not detected in MEG-01 cells. The NR2A subunit was not detected in human platelets, however its expression was potentially increased following PMA treatment for 3 d.

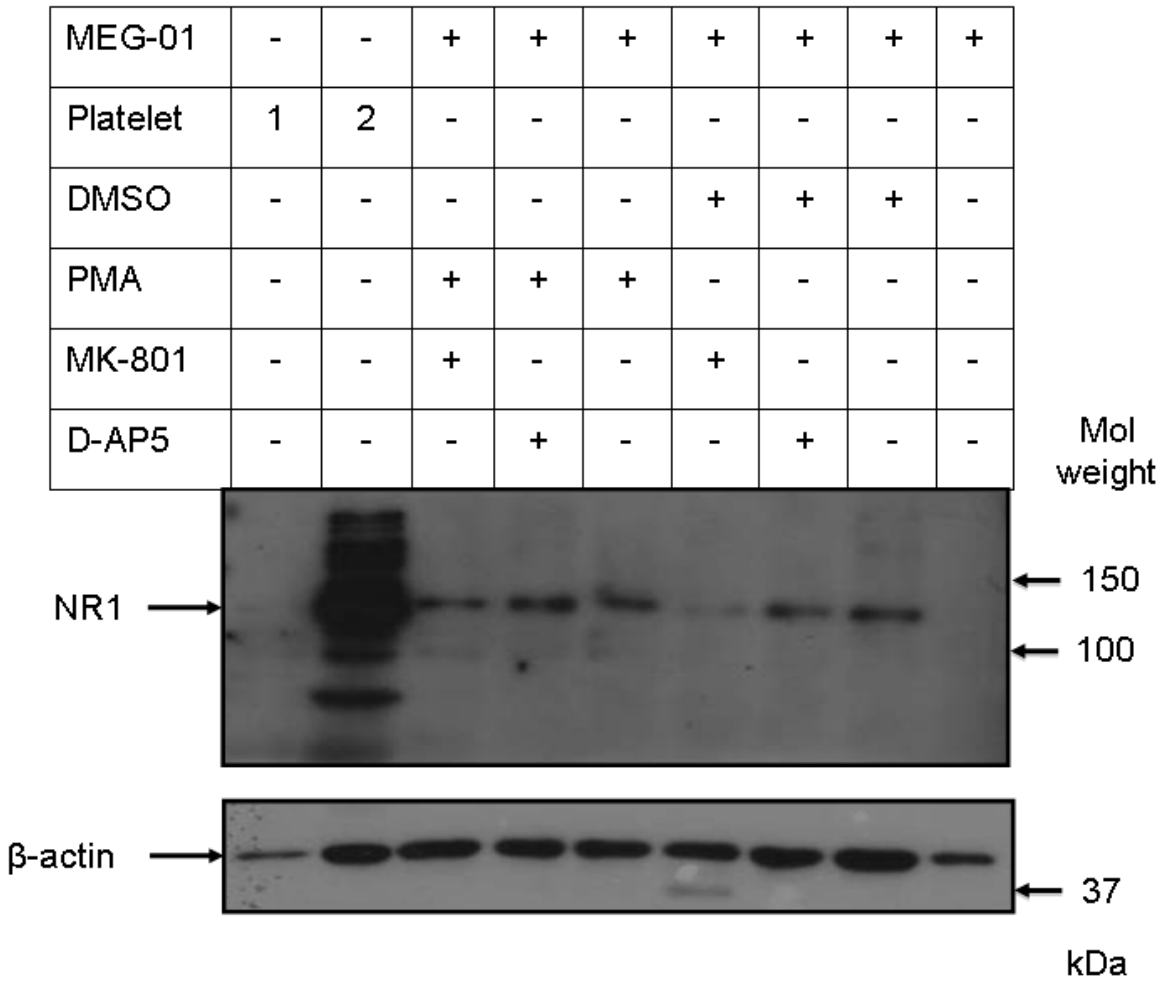

Figure 52. NMDA NR1 subunit expression in MEG-01 cells is not altered by PMA treatment or the presence of inhibitors. Western blot demonstrating the differences in expression of the NMDA NR1 subunit between undifferentiated MEG-01 cells (MEG-01), differentiated MEG-01 cells and platelets from two different donors (1 and 2) to represent terminal differentiation and as a positive control (figure 12). MEG-01 cells were treated for 3d in culture (section 2.3.2.1, method 2) with 10 nM PMA or DMSO (0.001 % v/v; vehicle control) in the presence or absence of the NMDA inhibitors MK-801 (100 μM) or D-AP5 (100 μM). The blot was split into 2 pieces at approximately 70 kDa, with the top half probed for NR1 expression, and the lower half for β-actin to compare sample loading (expected size 42 kDa). This blot is representative of 4 separate experiments, indicating that there is no discernible effect on NR1 expression through PMA treatment, with no apparent effect induced by the inhibitors. The arrows on the right indicate sizes predicated by the protein standards (mol weight, molecular weight marker; kDa). Arrow on the left indicates the expected size of the NR1 subunit, 120 kDa. Approximately 15 μg protein was loaded for each sample using the Bradford assay to determine the protein concentration of each sample (section 2.4.1).

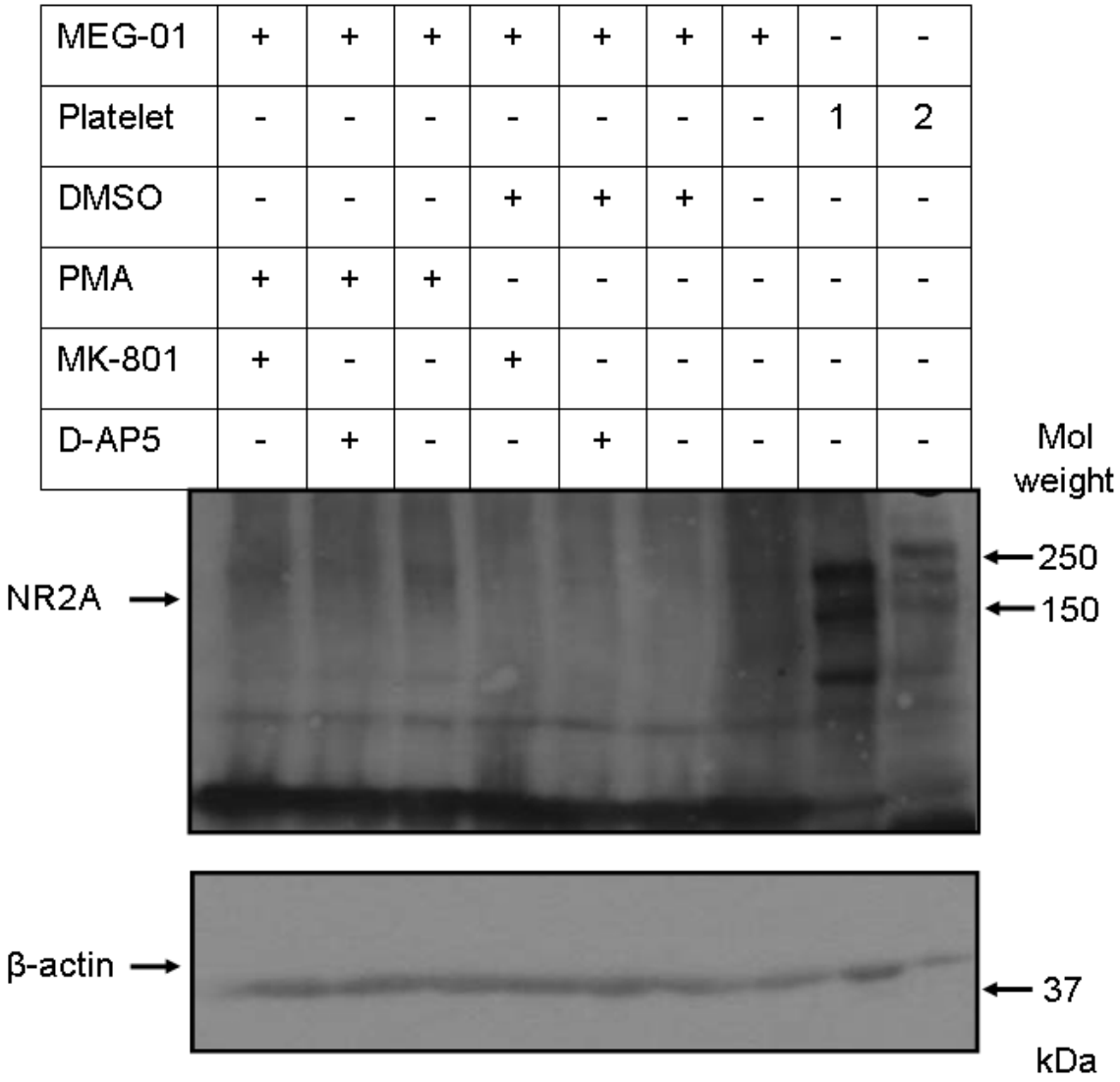

Figure 53. MEG-01 cells potentially express NMDA NR2A subunits when treated with PMA. Western blot demonstrating the differences in expression of the NMDA NR2A subunit between undifferentiated MEG-01 cells (MEG-01), differentiated MEG-01 cells and platelets from two different donors (1 and 2) to represent terminal differentiation, where NR2A is not expressed (figure 13). MEG-01 cells were treated for 3d in culture (section 2.3.2.1, method 2) with 10 nM PMA or DMSO (0.001 % v/v; vehicle control) in the presence or absence of the NMDA inhibitors MK-801 (100 μM) or D-AP5 (100 μM). The blot was stripped (section 2.4.5.) and reprobed for β-actin to compare the loading of the sample. This is illustrated in the lower blot with an expected size of 42 kDa. This blot is representative of 2 separate experiments, indicating that there is a potentially discernible effect on NR2A expression through PMA treatment. The arrows on the right indicate sizes predicted by the protein standards (mol weight, molecular weight marker; kDa). Arrow on the left indicates the expected size of the NR2A subunit, 180 kDa. Approximately 15 μg protein was loaded for each sample using the Bradford assay to determine the protein concentration of each sample (section 2.4.1).

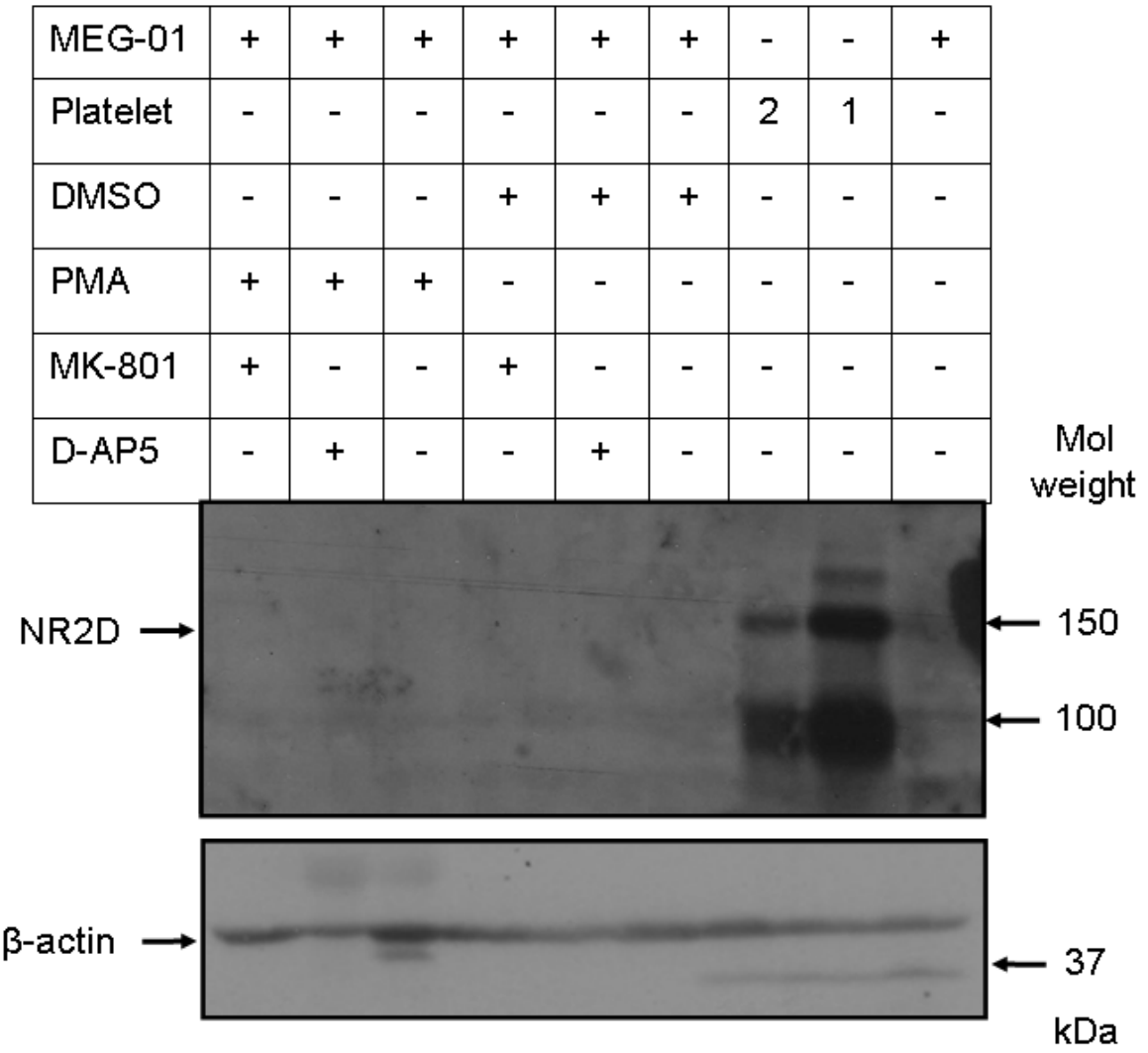

Figure 54. MEG-01 cells do not express NMDA NR2D subunits when treated with PMA. Western blot demonstrating the differences in expression of the NMDA NR2D subunit between undifferentiated MEG-01 cells (MEG-01), differentiated MEG-01 cells and platelets from two different donors (1 and 2) to represent terminal differentiation and as a positive control (figure 14). MEG-01 cells were treated for 3d in culture (section 2.3.2.1, method 2) with 10 nM PMA or DMSO (0.001 % v/v; vehicle control) in the presence or absence of the NMDA inhibitors MK-801 (100 μM) or D-AP5 (100 μM). The blot was split into 2 pieces at approximately 70 kDa, with the top half probed for NR2D expression, and the lower half for β-actin to compare sample loading (expected size 42 kDa). This blot is representative of 3 separate experiments, indicating that there is no discernible effect on NR2D expression through PMA treatment. The arrows on the right indicate sizes predicted by the protein standards (mol weight, molecular weight markers; kDa). Arrow on the left indicates the expected size of the NR2D subunit, 150 kDa. Approximately 15 μg protein was loaded for each sample using the Bradford assay to determine the protein concentration of each sample (section 2.4.1).

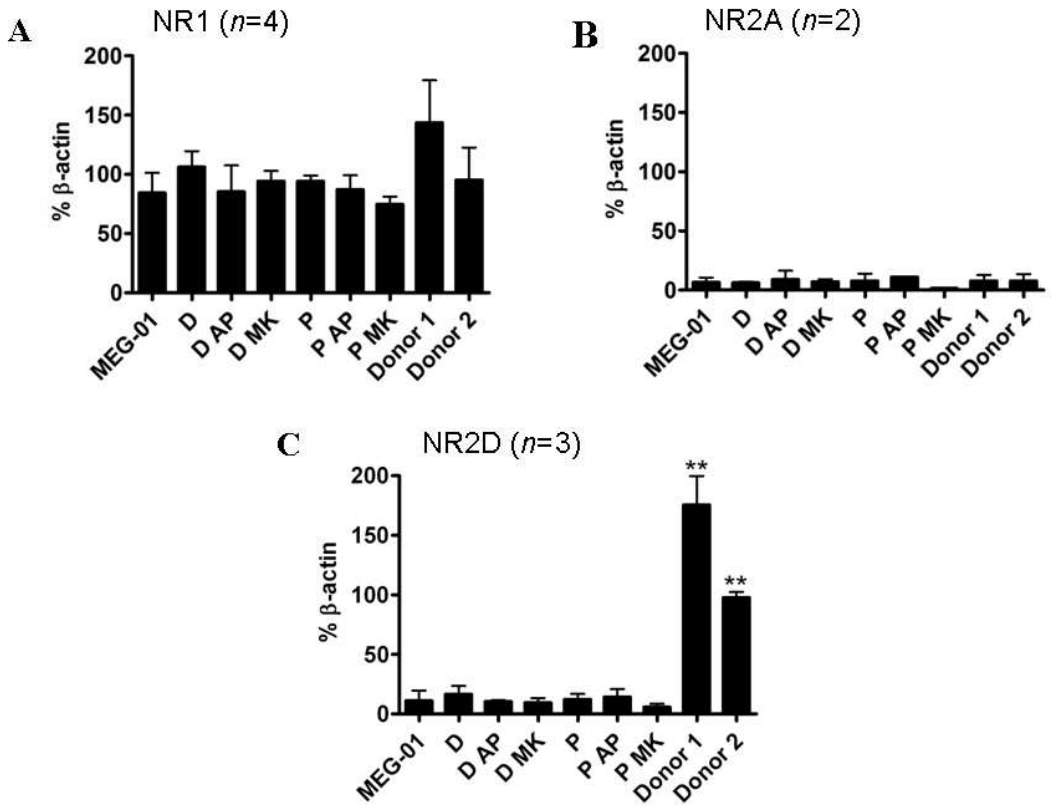

Figure 55. Differentiation of MEG-01 cells with PMA does not lead to changes in expression of NMDA receptor subunit proteins NR1, NR2A or NR2D. A, illustrates the expression of NR1 subunit proteins using densitometry (section 2.4.6.), shown as a percentage of β-actin expression (*n*=4). It demonstrates that treating MEG-01 cells with PMA for 3 d in culture has no effect on NR1 expression. The presence of either MK-801 or D-AP5 also has no effect. Samples were made from the platelets of 2 different human donors (donor 1 and donor 2), which illustrate the variation in expression between donors, and demonstrate that in these donors, NR1 expression is greater than in MEG-01 cells (143.50 ± 35.85 and 95.03 ± 27.59 % β-actin expression respectively compared to untreated MEG-01 cells (84.32 ± 16.85 % β-actin expression)). **B,** Illustrates the lack of NR2A subunit protein expression, showing no change in expression with PMA or either of the inhibitors, together a lack of expression in the 2 platelet samples as previously demonstrated (figure 13) (*n*=2). **C,** Illustrates expression of the NR2D subunit protein (*n*=3), demonstrating that there is no change in expression with PMA-treatment and no effect with either of the inhibitors. There is an increase in NR2D expression in both platelet samples of 164.26 ± 25.86 and 86.76 ± 9.75 % β-actin expression above that of untreated MEG-01 cells, again demonstrating differences in expression of NMDA receptor subunit proteins between donors. D, DMSO; P, PMA; AP, D-AP5; MK, MK-801; *n*= the number of different sets of treated MEG-01 samples and untreated human platelet samples run on Western blots and probed with each respective antibody; the same 2 platelet samples were run alongside these each time (donor 1 and 2). ** $P < 0.01$ using a one-way ANOVA with Dunnetts post-hoc test in comparison to the MEG-01 sample.

5.3.3.3. NMDAR-independent PMA-induced changes in MEG-01 morphology in the absence of fibrinogen

MEG-01 cells were cultured for 3 d using method 2 (section 2.3.2.1) with the addition of either 100 μM D-AP5 or 100 μM MK-801, both NMDAR specific antagonists. Figure 56 illustrates representative photographs taken after 3 d in culture. These show that the vehicle-treated cells (DMSO) remain round and bright even in the presence of either inhibitor, with no apparent effect on cell number. The presence of PMA leads to increases in both an increase in cell size and in the irregularity of the cells' surface membrane. Neither factor is affected by the presence of either MK-801 or D-AP5 whether with or without PMA. The histogram illustrates the pooled results from 3 separate experiments. The data demonstrates that the mean size of the cells remains at approximately 205.96 ± 5.73 μm^2 with the addition of inhibitors in untreated cells increasing to a mean size of 452.40 ± 19.14 μm^2 in the presence of PMA. The PMA-induced increase in cell size is not affected by the presence of MK-801 or D-AP5 (figure 56).

5.3.3.4. MEG-01 cell morphology in the presence of fibrinogen

Dishes were coated with 100 ng ml^{-1} fibrinogen prior to setting up cultures for differentiation (sections 2.3.5 and 2.3.2.1). MEG-01 cells were plated at a density of 1 x 10^5 cells ml^{-1} as initial experiments demonstrated that when cultured at 2.4 x 10^5 cells ml^{-1} in the presence of fibrinogen, the cells formed clumps, adhering to each other and forming a fully confluent layer making it difficult to determine the size and shape of the cells. The density of the cells was therefore decreased to 1 x 10^5 cells ml^{-1}. The cells were then treated with either 10 nM PMA or the vehicle control (0.001 % v/v DMSO) for 3 d (section 2.3.2.1). Photographs were taken after 3 d (figure 58) and the cells measured. This data was then compared to that obtained from cells cultured without fibrinogen (figure 56). Pooled data from 3 separate unpaired experiments demonstrated that culturing DMSO-treated MEG-01 cells in the presence of fibrinogen has no effect on the morphology of the cells which remain generally spherical with regular membranes (figure 58). Treating cells with 10 nM PMA in the presence of fibrinogen leads to an increase in cell size together with an increase in the irregularity of both the cell membrane and the cell shape previously observed in cells cultured without fibrinogen (figure 56). Changes in cell size are detailed in table 41 and illustrated in the histogram in figure 57. The presence of PMA significantly increases the size of the cells above that of the control cells, both in the presence and absence of fibrinogen. The addition of fibrinogen had no effect on this

pattern (figure 57), however it was determined that the size of both the control cells and those treated with PMA decreased in comparison to the non-fibrinogen treated cells.

PMA / Fibrinogen	-	+
-	205.96 ± 5.73	452.45 ± 24.66
+	170.96 ± 5.70	304.88 ± 13.00
	Cell size (μm^2)	

Table 41. Comparing the effects of PMA and fibrinogen on the size (μm^2) of MEG-01 cells in culture for 3 d.

5.3.3.5. NMDAR-independent PMA-induced changes in MEG-01 morphology in the presence of fibrinogen

MEG-01 cell cultures were set up in the presence and absence of PMA (10 nM), together with either 100 μM MK-801 or 100 μM D-AP5 as previously described (section 2.3.2.1.). Photographs were taken after 3 d (figure 57) and the cells measured (section 2.3.2.1.1.). The photographs illustrate that as previously shown without fibrinogen (figure 56), cells treated with either inhibitor in the presence of DMSO remain mainly spherical with regular membranes. The cells treated with PMA and fibrinogen, both with and without inhibitors, appear larger in size with more irregular shape and cell membranes than the DMSO controls. The data indicates both in table 42 and figure 57 that the presence of either D-AP5 or MK-801 causes the vehicle control treated cells to decrease in size from those cultured in the absence of any inhibitor. However, while there is an apparent effect on cell size when treated with both 10 nM PMA and 100 μM MK-801, the decrease is not significant given the decrease in size of the control cells with the addition of MK-801. Although PMA has been shown to increase the size of MEG-01 cells cultured in the presence of fibrinogen, the increase is smaller than in the absence of fibrinogen (figure 52). The presence of the NMDAR inhibitors D-AP5 and MK-801 therefore have effect only on the size of MEG-01 cells after 3 d in culture without PMA in the presence of fibrinogen.

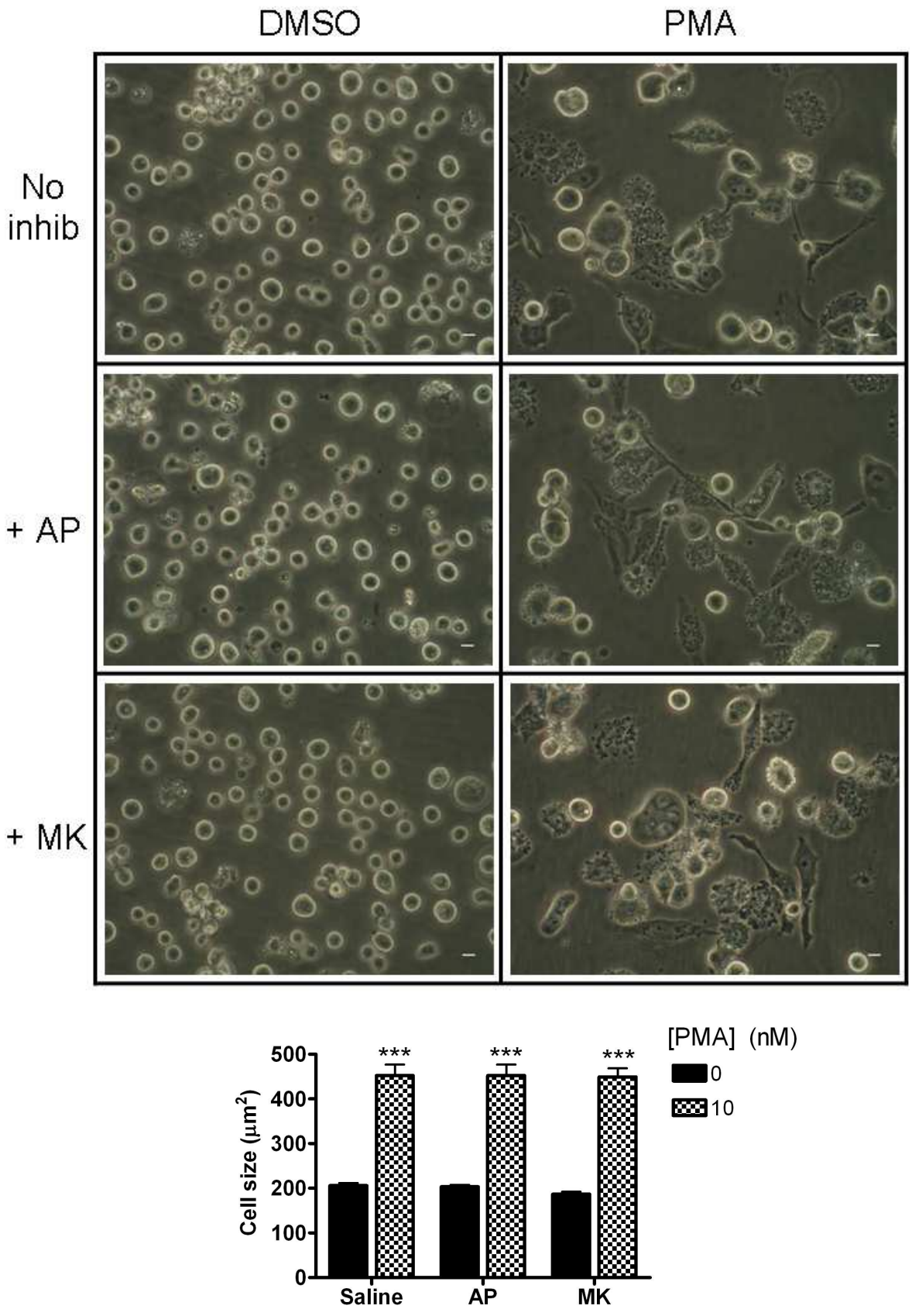
DMSO
PMA
No inhib
+ AP
+ MK
[PMA] (nM)
0
10
Cell size (μm²)
500
400
300
200
100
0
***
***
***
Saline
AP
MK

Figure 56. Inhibitors do not affect the size of MEG-01 cells when cultured in either the presence or absence of PMA and in the absence of fibrinogen. Representative pictures of MEG-01 cells cultured in the presence of either 10 nM PMA or a vehicle control (0.001 % DMSO v/v) in combination with either 100 μM D-AP5 (AP) or 100 μM MK-801 over 3 d using method 2 (section 2.3.2.1). Photographs were taken of the cells (5-8 per condition), measured and analysed as described in section 2.3.2.1. These illustrate that the presence of PMA over 3d increase the size of the cells, which become more irregular in shape and are fewer in number than those treated with DMSO. The addition of the inhibitors (inhib) does not have any further effects on the size or shape of the MEG-01 cells. The histogram illustrates pooled cell measurements from 3 separate experiments. While treatment with PMA increases the size of cells from 205.96 ± 5.73 to 452.40 ± 19.14 μm^2, the addition of inhibitors have no effect on either PMA- or DMSO-treated cells. *** $P< 0.001$ using two-way ANOVA with Bonferroni post-hoc test comparing the 2 sources of variation in the data, the use of PMA/ DMSO and the concentration of inhibitor, where PMA is shown to have an extremely significant effect, but the effect of inhibitors is not significant. In addition, *** $P< 001$ when compared to the respective 0 nM PMA (DMSO control) controls using two-tailed, unpaired Student *t*-tests. Original magnification x 400, scale bar represents 10 μM.

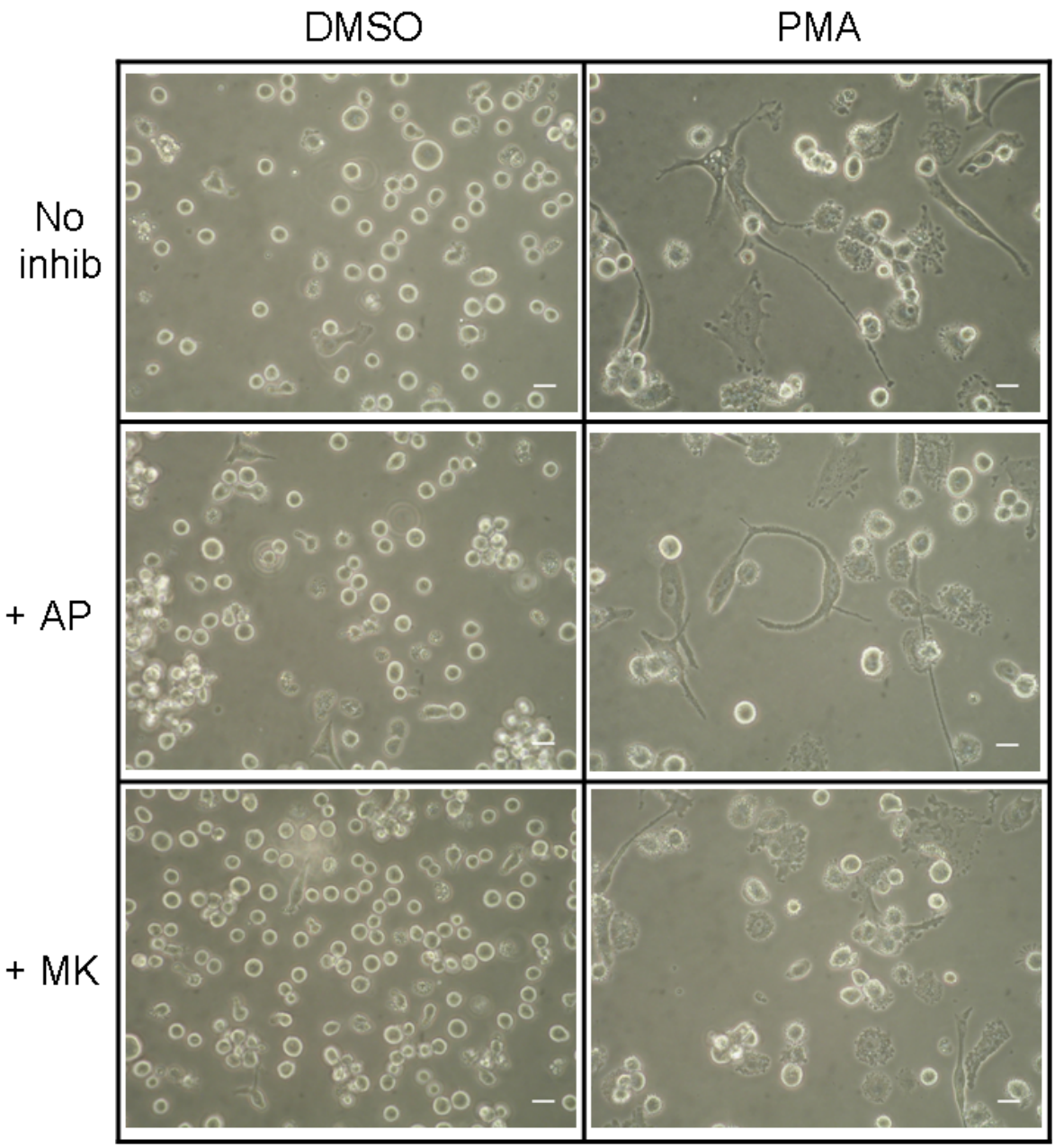
DMSO
PMA
No inhib
+ AP
+ MK

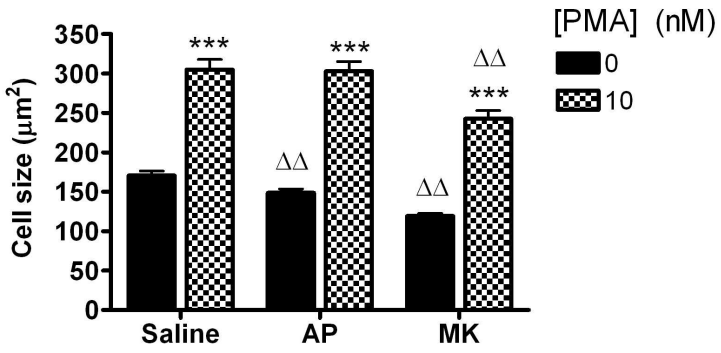
[PMA] (nM)
0
10
Cell size (μm²)
350
300
250
200
150
100
50
0
***
***
***
ΔΔ
ΔΔ
ΔΔ
Saline
AP
MK

Figure 57. Inhibitors have an effect on cell size in the presence of PMA on a fibrinogen-coated surface. MEG-01 cells were cultured in the presence of either 10 nM PMA or a vehicle control (0.001 % DMSO v/v) with either 100 μM D-AP5 or 100 μM MK-801 over 3 d (method 2, section 2.3.2.1). Photographs were then taken of the cells (5-8 per treatment combination), measured and analysed as described in section 2.3.2.1. Representative pictures of MEG-01 cells treated for 3 d with either DMSO (0.001 % v/v) or 10 nM PMA in the presence and absence of either 100 μM D-AP5 (AP) or 100 μM MK-801 (MK) on a fibrinogen-coated surface are shown above. These illustrate that the presence of PMA over 3d increase the size of the cells, which also become more irregular in shape but are fewer in number than those treated with DMSO. The addition of the inhibitors (inhib) does not appear to further affect the shape of the MEG-01 cells. The histogram illustrates pooled data from 3 separate experiments. Co-addition of NMDAR inhibitors attenuates the increase in cell size with significance achieved for MK-801 in both conditions (DMSO or PMA) and for D-AP5 in control DMSO treated MEG01 cells. *** $P< 0.001$ using a two-way ANOVA with Bonferroni post-hoc test comparing the effects of PMA and the presence of the inhibitors, showing that the addition of PMA has an extremely significant effect; also *** $P< 0.001$ using two-tailed, unpaired Student *t*-test comparing the pair of bars for each inhibitor treatment i.e. saline with 0 nM PMA (DMSO control) to saline with 10 nM PMA. ΔΔ $P< 0.01$ using a one-way ANOVA with Dunnetts post-hoc test comparing data with their respective baseline controls (either saline with 0 nM PMA (DMSO control) or saline with 10 nM PMA). Original magnification x 400, scale bar represents 10 μM.

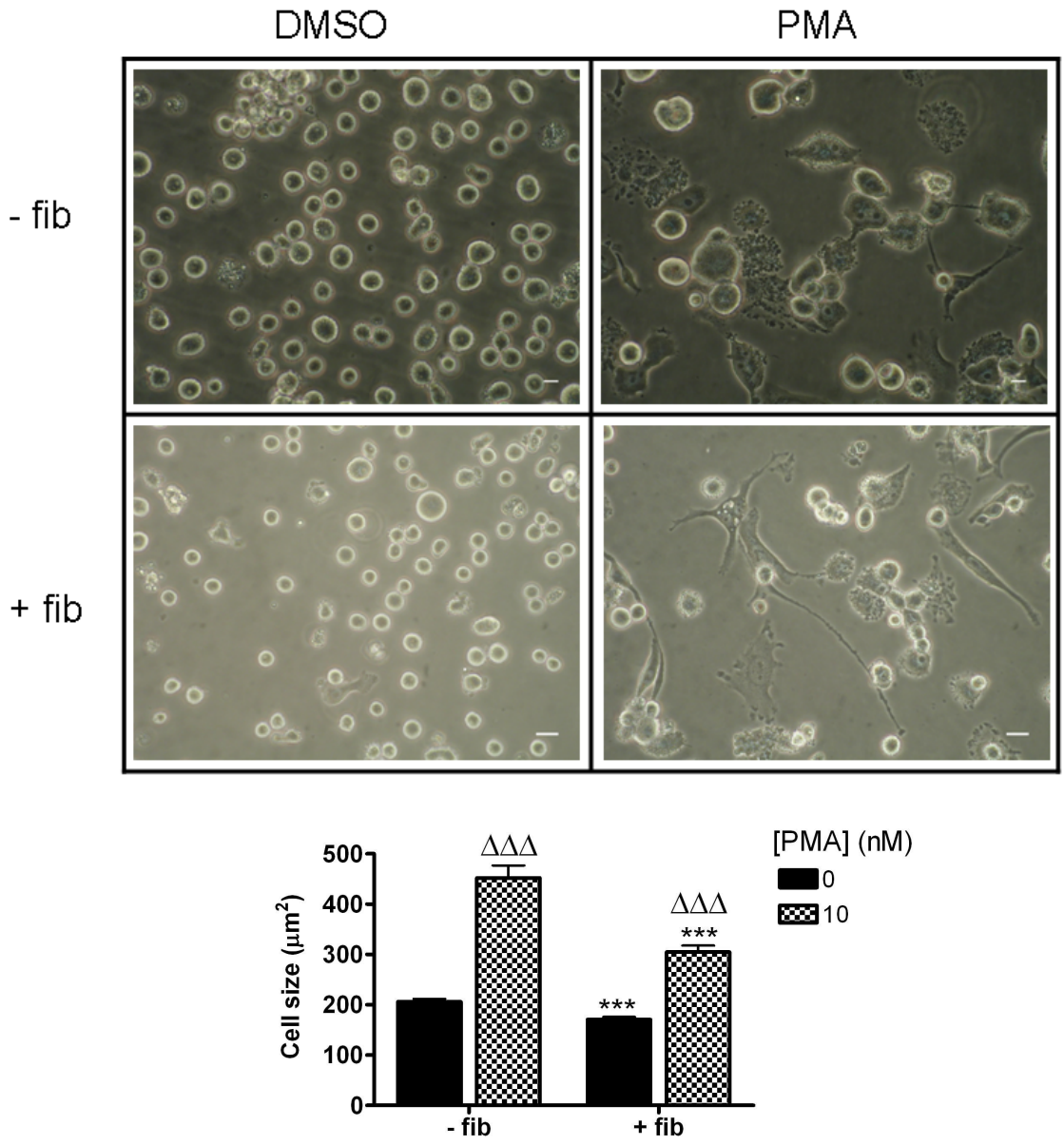

Figure 58. Culturing MEG-01 cells in the presence of fibrinogen leads to a reduction in cell size when PMA is also present. Comparing the changes in cell size and shape when MEG-01 cells are cultured in the presence and absence of 100 ng ml^{-1} fibrinogen (fib) for 3 d. The representative photographs demonstrate that in both cases, cells treated with DMSO remain spherical with regular membranes, while those treated with PMA become larger, and less regular in shape. The histogram illustrates that the increase in cell size when MEG-01 cells are cultured with PMA is maintained when fibrinogen is present (134.37 ± 14.19 μm^2). However, this increase in size is reduced when MEG-01 cells are cultured without fibrinogen (246.49 ± 25.32 μm^2). *** $P< 0.001$ compared to each - fibrinogen control, ΔΔΔ $P< 0.001$ compared to 0 nM PMA control for either with or without fibrinogen, both using unpaired, two-tailed Students *t*-tests.

PMA / Inhibitor	-	+
-	170.51 ± 5.69	304.88 ± 13.00
D-AP5	148.65 ± 4.76	302.94 ± 12.35
MK-801	119.17 ± 3.46	242.56 ± 10.43
	Cell size (μm^2)	

Table 42. Comparing the effects of the NMDAR inhibitors, MK-801 and D-AP5, on the size of MEG-01 cells (μm^2) in the presence of fibrinogen and the presence and absence of PMA for 3 d.

5.3.4. MEG-01 cell adhesion studies

Previous studies have demonstrated that NMDAR function is critical for PMA-mediated MEG-01 cell adhesion, which was repeated using the CMK cell line to ascertain that this result was not particular to the MEG-01 cell line (Genever *et al*, 1999). This earlier study use the crystal violet adhesion assay to demonstrate that adhesion of both MEG-01 and CMK cells are increased in the presence of PMA using the crystal violet adhesion assay, and that this increase can be inhibited by the addition of increasing concentrations of either MK-801 or D-AP5 (Genever *et al*, 1999). These experiments were performed using 96-well plates, which following the original study were not coated with an adhesion protein. This study has been extended to investigate the functional involvement of NMDAR in MEG-01 cell adhesion to fibrinogen-coated surfaces, which mimic conditions in the vascular sinusoids towards which MKs migrate as they differentiate in the bone marrow (Larson and Watson, 2006). Initially, the original study was repeated with MEG-01 cells, followed by an investigation into the action of NMDAR antagonists on fibrinogen-dependent cell adhesion.

5.3.4.1. NMDAR inhibition potentiates MEG-01 cell adhesion to uncoated 96-well plates

For each condition, increasing concentrations of NMDAR antagonists (MK-801 or D-AP5), were added to the MEG-01 cell culture. Adhesion was measured using a crystal violet assay which measures the absorbance of crystal violet taken up adherent MEG-01 cells which remain after non- and loosely adherent cells are washed off. The dye is then released from the cells by treatment with a citric acid solution, and the absorbance measured at 570 nm (section 2.7; Genever *et al*, 1999). The crystal violet adhesion assay was performed using 96-well plates with an initial cell density of 2.4×10^5 ml^{-1}, with either

no inhibitors or combinations of PMA, MK-801 and D-AP5. The results from 3 separate experiments were pooled and demonstrate that the presence of PMA increases adhesion where absorbance increases from 0.093 ± 0.016 to 0.22 ± 0.037 in the presence of PMA (figure 59A). The addition of D-AP5 has no effect on absorbance in the absence of PMA. However, culturing MEG-01 cells in the presence of both PMA and D-AP5 increases MEG-01 adhesion where the absorbance increases from 0.22 ± 0.037 with PMA alone to 0.39 ± 0.043 with co-addition of 10 μM D-AP5 (figure 59B).

The addition of MK-801 together with PMA also causes an increase in absorbance above that with PMA alone, but only at 100 μM MK-801 (0.21 ± 0.037 with PMA alone, increasing to 0.29 ± 0.045 with MK-801). This is mirrored in the absence of PMA, where only the addition of 100 μM MK-801 stimulates an increase above control (0.093 ± 0.12 increasing to 0.15 ± 0.024). There is no effect with other concentrations of MK-801.

To determine whether the presence of PMA or either inhibitor had an adverse effect on total cell number, matching plates were set up at the same time with the same combinations of PMA and inhibitor concentrations and the same cell density (2.5×10^4 cells $well^{-1}$). This is important to ensure that changes in cell adhesion do not reflect a change in total cell number. After 3 d, the cells were removed using 0.5 % trypsin/ EDTA and counted using a haemocytometer (section 2.3.2.1.2.). The addition of either inhibitor had a small effect on total cell number in the absence of PMA, or with MK-801 in the presence of PMA. In contrast, the inhibition stimulated by PMA was mitigated by the addition of 10 μM D-AP5 ($2.3 \times 10^4 \pm 2.8 \times 10^3$ cells $well^{-1}$ increasing to $4.8 \times 10^4 \pm 6.8 \times 10^3$ cells $well^{-1}$ respectively) (figure 59C). Overall, the presence of PMA increases adhesion while decreasing cell number, with a trend towards a decrease in cell number observed with the highest concentrations of NMDAR antagonists in the absence of PMA.

5.3.4.2. NMDAR inhibition attenuates fibrinogen-dependent MEG-01 cell adhesion

Crystal violet adhesion assays were repeated using fibrinogen-coated plates with a cell density of 1×10^4 cells ml^{-1} with the same combinations of PMA, MK-801 and D-AP5 as previously described (section 5.3.3.1). The data from 3 separate experiments was pooled and the effect of fibrinogen on adhesion compared in the presence and absence of PMA (figure 60). This demonstrates a small increase in adhesion above the baseline in the absence of PMA, where DMSO treatment without fibrinogen produced an absorbance

reading of 0.093 ± 0.012 which increased to 0.13 ± 0.0046 when the cells were cultured in the presence of fibrinogen. The presence of PMA also leads to an increase in adhesion, where absorbance increases to 0.22 ± 0.037 in the absence and 0.28 ± 0.026 in the presence of fibrinogen respectively. This indicates that the presence of fibrinogen increases MEG-01 adhesion in both the presence and absence of PMA.

The addition of the inhibitors MK-801 or D-AP5 were shown to have no effect on the adhesion of MEG-01 cells when cultured in a fibrinogen-coated 96-well plate in the absence of PMA (figures 60A and B). The increase in adhesion induced by the addition of PMA, is shown to be reduced by the presence of either inhibitor. D-AP5 induces inhibition at 1 and 10 μM concentrations, causing the absorbance measured to decrease from 0.28 ± 0.026 with PMA alone to 0.21 ± 0.014 and 0.19 ± 0.014 respectively. D-AP5 at 100 μM has no effect on absorbance in the presence of PMA. MK-801 has an overall inhibitory effect on MEG-01 cells cultured in the presence of PMA and fibrinogen. This is shown to be dose dependent (figure 61B), with the largest decrease in absorbance demonstrated with 100 μM MK-801 (PMA alone, 0.28 ± 0.026 decreasing to 0.19 ± 0.015 with 100 μM MK-801; $P< 0.01$).

As previously described in section 5.3.3.1., paired plates were set up at the same time as those for the crystal violet adhesion assay, with the same numbers of cell per well (1×10^4) and concentrations of PMA, MK-801 and D-AP5, to determine whether changes in absorbance are not a reflection of changes in cell number. As previously (figure 59), the presence of PMA when culturing MEG-01 cells prevents an increase in cell number, with cells cultured in the absence of PMA increasing from 1×10^4 cells well^{-1} when the plates were plated to $1.9 \times 10^4 \pm 2.3 \times 10^3$ cells well^{-1}, in comparison to those cultured with PMA ($0.90 \times 10^4 \pm 3.2 \times 10^3$ cells well^{-1}) (figure 61C and D). This pattern is similar to that of MEG-01 cells cultured in the presence and absence of PMA without fibrinogen, where DMSO-treated cells increase in number over 3 d in culture, with no change observed in the number of cells well^{-1} when treated with PMA (figure 59C and D.

The addition of D-AP5 to DMSO-treated control cells stimulated an increase in cell number above that of just DMSO-treated cells with the largest increase with 1μM D-AP5, from $1.9 \times 10^4 \pm 2.3 \times 10^3$ cells well^{-1} to $2.7 \times 10^4 \pm 3.7 \times 10^3$ cells well^{-1} (figure 61C). The presence of MK-801 also induced an increase in cell number above that of control cells,

with the largest increase again with 1 μM (DMSO alone, $1.9 \times 10^4 \pm 2.3 \times 10^3$ cells well^{-1}; DMSO with 1 μM MK-801, $2.7 \times 10^4 \pm 5.6 \times 10^3$ cells well^{-1}) (figure 61D). The number of cells well^{-1} then decreases with increasing concentration of both inhibitors towards that of the DMSO-only treated cells (DMSO alone, $1.9 \times 10^4 \pm 2.3 \times 10^3$ cells well^{-1}; 100 μM D-AP5, $2.5 \times 10^4 \pm 3.8 \times 10^3$ cells well^{-1}; 100 μM MK-801, $1.9 \times 10^4 \pm 3.0 \times 10^3$ cells well^{-1}). Together this indicates that both inhibitors have an inhibitory effect at specific concentrations on the adhesion of MEG-01 cells cultured in the presence of fibrinogen and the absence of PMA, with peak increases in cell number observed at 1 μM of both D-AP5 and MK-801.

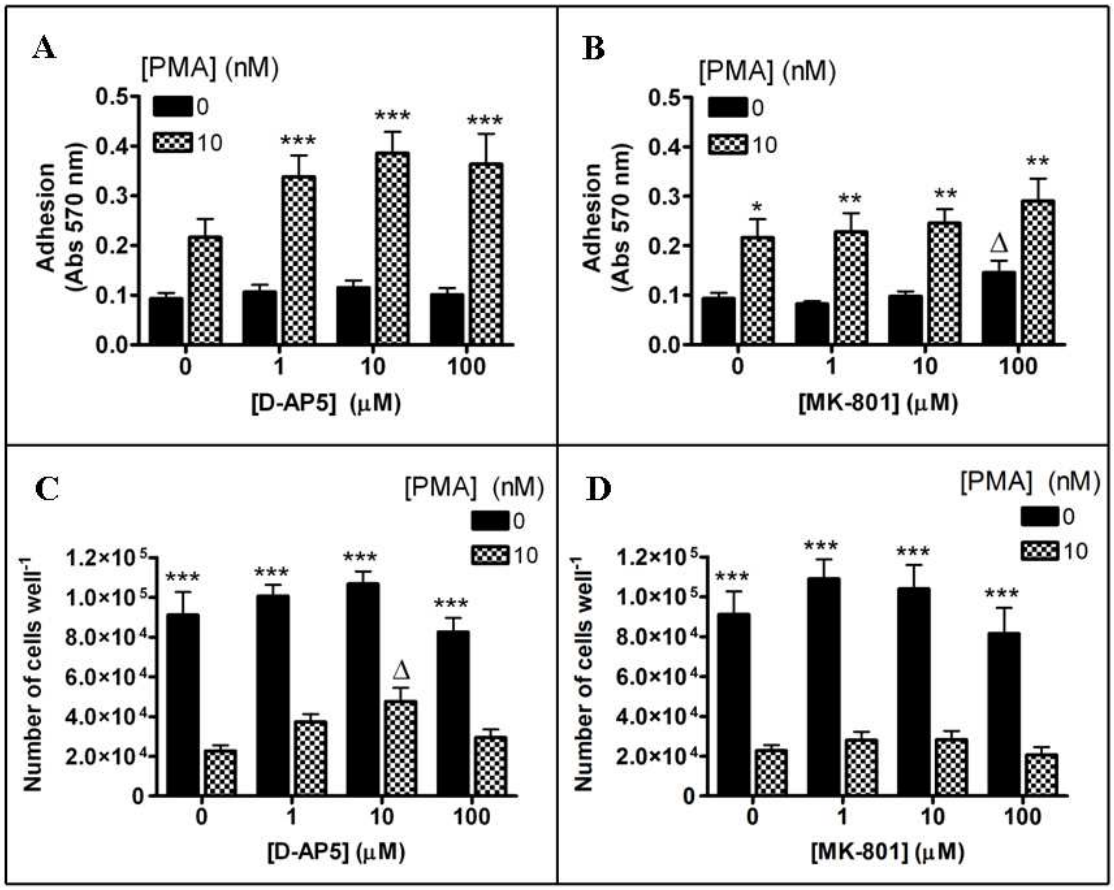

Figure 59. PMA increases adhesion of MEG-01 cells and inhibits cell proliferation, with differing actions of inhibitors in the absence of fibrinogen. MEG-01 cells were treated with either 10 nM PMA or vehicle control (0.001 % v/v DMSO) for 3d in culture at a density of 2.4 x 10^4 cells $well^{-1}$ (section 2.8) in the presence of increasing concentrations of either D-AP5 or MK-801. **A, B,** Illustrates the differences in adhesion in the presence or absence of PMA. In DMSO treated cells (control cells; solid black bars), the addition of D-AP5 has no effect on absorption, however the presence of 100 μM MK-801 leads to an increase of 0.079 ± 0.027 above the DMSO-only control. In comparison, there is a significant increase in adhesion above baseline with the addition of PMA alone and in combination with both inhibitors. The increase in absorption with D-AP5 is greatest with 10 μM D-AP5 at 0.17 ± 0.057 above the PMA control with the addition of MK-801 leading to an increase in adhesion with 100 μM MK-801 to 0.074 ± 0.059 above the PMA control. **C, D,** Parallel plates were set up at the same time as those for the crystal violet adhesion assays and cultured for 3 d with the same combinations of PMA and inhibitor concentrations. The cells were removed from the plates with 0.5 % trypsin/ EDTA and counted using a haemocytometer. These figures illustrate the total number of cells in each well after 3 d without fibrinogen. At day 0, 2.4 x 10^4 cells were plated into each well. All control cells (without PMA; solid black bars), both with and without inhibitors, increased in number over 3 d. In comparison, the number of PMA-treated cells did not increase above 2.4 x 10^4 cells $well^{-1}$ with any

combination of MK-801. The addition of PMA together with D-P5 at 1 and 10 μM concentrations leads to increases above that of PMA alone, peaking at 10 μM D-AP5 with an increase of $2.5 \times 10^4 \pm 7.4 \times 10^3$ cells well^{-1} above PMA control cells. Δ P< 0.05 compared to 0 μM inhibitor in combination with either 0 μM or 10 μM PMA using a one-way ANOVA with a Dunnetts post-hoc test. * P< 0.05, ** P < 0.01. *** P < 0.001 using a two-way ANOVA with a Bonferroni post-hoc test comparing the 2 sources of variation in the data (DMSO/ PMA and concentrations of inhibitors), where the stars refer to differences found by the post-hoc test between the DMSO and PMA mean data for each concentration of inhibitor. In all figures, the two-way ANOVA shows that the effect of PMA on the results is extremely significant, with the presence of D-AP5 having a significant effect on the results. MK-801 was shown to have no effect.

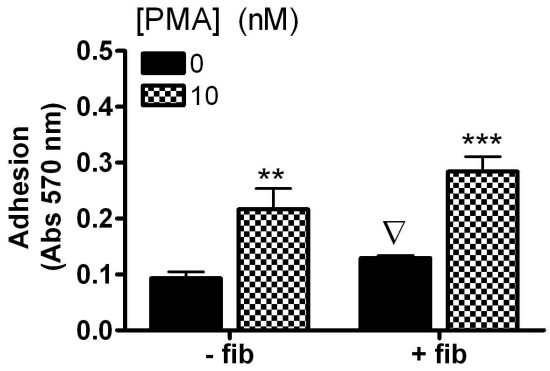

Figure 60. Fibrinogen increases adhesion of MEG-01 cells in the presence and absence of PMA. This illustrates the changes in adhesion (measured by crystal violet absorbance at 570 nm) caused by the presence of fibrinogen during culture, and represents the pooled data from unpaired separate experiments with each condition repeated in triplicate in all experiments (n=3 ± S.E.M.). It demonstrates that the presence of fibrinogen induces an increase in absorption of 0.036 ± 0.012 in the absence and an increase of 0.068 ± 0.046 in the presence of 10 nM PMA. ** P< 0.01, *** P< 0.001, compared to the respective control using an unpaired, two-tailed Students *t*-test. ∇ P< 0.05 compared to–fibrinogen with 0 nM PMA using an unpaired, two-tailed Students *t*-test.

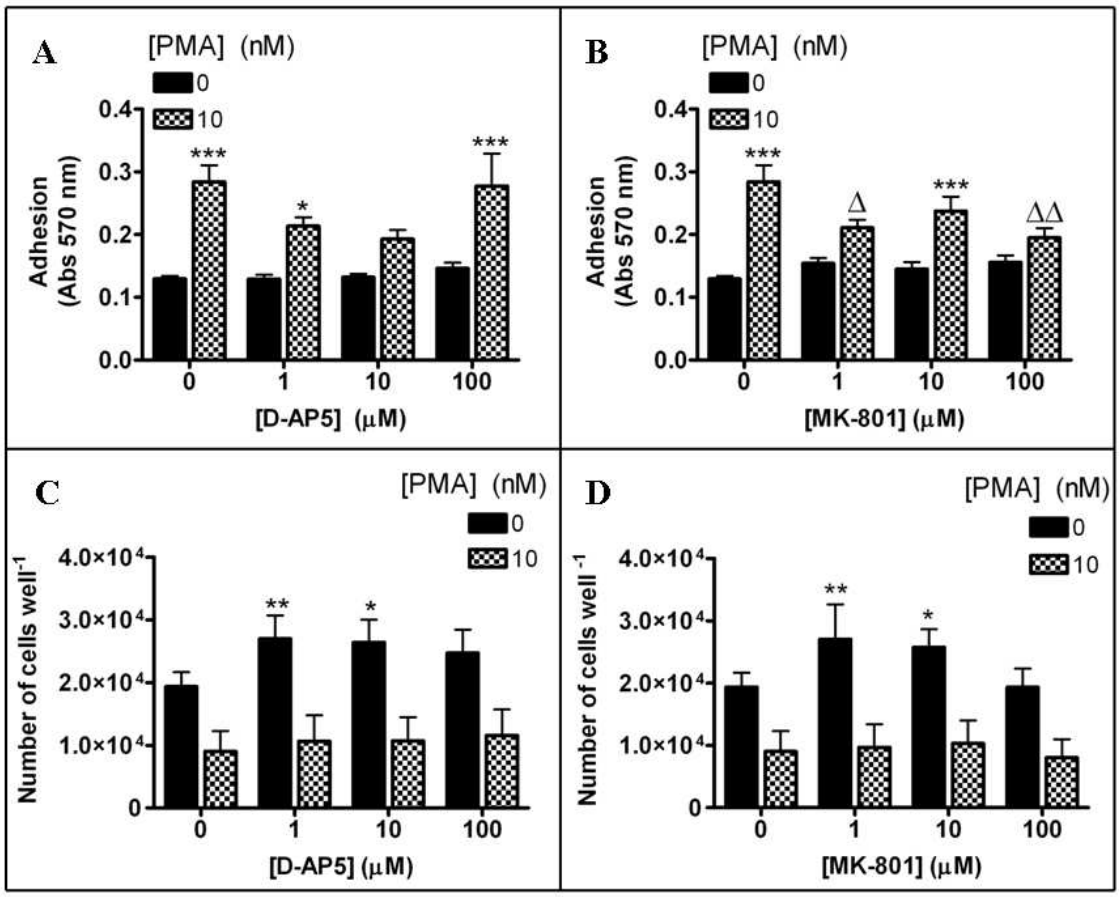

Figure 61. PMA increases adhesion of MEG-01 cells and inhibits cell proliferation, with differing actions of inhibitors in the presence of fibrinogen. MEG-01 cells were treated with either 10 nM PMA or vehicle control (0.001 % v/v DMSO) for 3d in culture (section 2.8) in the presence of increasing concentrations of either D-AP5 or MK-801 on a fibrinogen-coated surface. **A, B,** Illustrates the decrease in adhesion with increasing concentrations of either D-AP5 or MK-801 in combination with 10 nM PMA when MEG-01 cells are cultured on a fibrinogen-coated surface. The decrease in absorption from that induced with PMA alone is greatest with 10 μM D-AP5 (0.091 ± 0.030) and 100 μM MK-801 (0.089 ± 0.035). The presence of either inhibitor has no effect on cells treated with DMSO. **C, D,** Parallel plates were set up at the same times as those for the crystal violet adhesion assay at a density of 1 x 10^4 cells $well^{-1}$, and cultured for 3 d with the same combinations of PMA and increasing inhibitor concentrations. The cells were removed from the plates with 0.5 % trypsin/ EDTA and counted using a haemocytometer. These figures illustrated the total number of cells per well after 3 d in culture in the presence of fibrinogen. A lower cell density was used compared to when cells were cultured in the absence of fibrinogen, due to cells forming large clumps in the wells and becoming fully confluent within 1.5- 2 d. Therefore the starting cell density was decreased. Cells treated with PMA both with and without inhibitor remained static at approximately 1.0 x 10^4 cells $well^{-1}$. DMSO-treated cells approximately double in number, with a further increase induced by the addition of D-AP5 of around

$7.5 \times 10^3 \pm 4.0 \times 10^3$ cells well^{-1}. The addition of 1 μM MK-801 evokes a mean increase of $7.7 \times 10^3 \pm 6.0 \times 10^3$ cells well^{-1}, with increasing concentrations of MK-801 appearing to decrease the number of cells well^{-1} back to that induced with DMSO alone ($1.9 \times 10^4 \pm 2.3 \times 10^3$ cells well^{-1}).

5.4. Discussion

The aim of this chapter was to determine which NMDAR subunit proteins were expressed by the human megakaryoblastic cell line, MEG-01, and if they are, whether NMDARs play a role in MK differentiation and adhesion.

5.4.1. MEG-01 differentiation

Two published methods for MEG-01 differentiation were compared (section 2.3.2.1), of which Nagata *et al* (1996) (method 1), determined both morphological and ultrastructural changes, and Lacabaratz-porret *et al* (2000) (method 2), demonstrated increases in GPIIIa (CD61) expression upon treating the cells with PMA; these changes are all indicative of MK differentiation (Genever *et al*, 1999). In this study, changes in cell size and shape were being investigated, therefore a method was required in which observable and measureable changes in both of these characteristics could be determined. It was established that method 2, with the higher density of MEG-01 cells treated for 3 d with PMA, induced the greater change in both cell size and shape, and was therefore used for further investigation into MEG-01 cell differentiation (figure 51).

5.4.2. MEG-01 expression of NMDAR subunits

It was demonstrated that undifferentiated MEG-01 cells express the NR1 subunit protein, but do not appear to express the NR2A or NR2D subunit (figures 43-44). Both the NR1 and NR2D subunit proteins are expressed by human platelets (figures 13 and 15), the terminal stage of MK differentiation, which suggests that the NMDAR subunit protein expression alters during differentiation. NR2A subunit proteins are potentially expressed by PMA-differentiated MEG-01 cells.

The expression of NMDAR subunit mRNA has previously been investigated in undifferentiated MEG-01 cells which have been shown to express the NR1, NR2C, NR2D and NR3 subunits (Genever *et al*, 1999; Hitchcock, 2003). This has been repeated in bone-marrow derived MKs which express the NR1, NR2A and NR2D subunit mRNA (Hitchcock *et al*, 2003). In this study, the expression of mRNA for NR1, NR2A-C and NR3A was investigated and it was demonstrated that none of these subunits appear to be expressed in undifferentiated MEG-01 cells (figure 50). The contradicts the mRNA evidence in the literature and demonstrates a discrepancy with the protein expression data which illustrates that the NR1 subunit protein is expressed in undifferentiated MEG-01

cells (figure 46; Genever *et al*, 1999). One factor to take into account is that the NR1 subunit has 8 different splice variants, and whether the antibodies and primers used in both studies detect different splice variants. However, the same anti-NR1 antibody was used in both my study and that carried out by Genever (1999) and is targeted to the extracellular region between the transmembrane M3 and M4 domains, which is conserved between splice variants (Smothers and Woodward, 2009). Different primers were used in each study, and while they are targeted to different regions of the N-terminus, they are both conserved between the splice variants. Differences in the efficacy between the two different primer sets could be tested in parallel using the same undifferentiated MEG-01 sample to ascertain if the variation in results between studies is due to primer design or another factor. The presence of different NR1 splice variants in transfected HEK923 cells have been demonstrated to have varied effects on NR1/ NR3 receptors (Smothers and Woodward, 2009), and another extension of this project could be to determine which splice variants are expressed in MEG-01s and native MKs, and therefore also in platelets, and any functional differences this causes.

As such, differences in splice variant detection does not explain the apparent expression of NR1 protein together with the lack of mRNA expression in the undifferentiated MEG-01 cells. It is clear from my study that two different NMDAR antagonists (MK-801 and D-AP5) can alter MEG-01 function strongly indicating the expression of functional NMDARs. Future studies should investigate the selectivity of anti-NR1 antibodies for NR1 protein and compare binding with anti-NR1 antibodies with different epitopes on the protein. In addition, the half-life of all the NMDAR subunit mRNA (NR1, NR2A-D and NR3A and B), in MEG-01 cells should be measured and compared to that of their respective proteins.

5.4.2.1. PMA-induced MEG-01 expression of NMDAR subunits

Following PMA-treatment of MEG-01 cells in this study, the NR1 and potentially the NR2A subunit proteins were detected, suggesting increased NR2A expression during MEG-01 differentiation. RT-PCR was not carried out on differentiated MKs in this study, however Hitchcock (2003) has demonstrated that expression of the NR2A and NR2C subunit mRNA increases following PMA-treatment, while NR2D expression remains static and neither NR2B nor NR3 subunits are detected. This rise in NR2A mRNA expression illustrated by Hitchcock (2003) mirrors the possible increase in NR2A protein expression

demonstrated in this study (figure 53). An extension to this would be to determine whether these increases occur in parallel by repeating the experiment and taking paired samples for Western blot and RT-PCR. Changes in receptor functionality could be investigated by electrophysiology, and localisation of receptor subunits can be determined using immunostaining to compare differences between differentiated and undifferentiated MEG-01 cells. Obtaining new primers for the NR2D and NR3B subunit mRNAs would also assist in determining changes in expression before and after differentiation.

Differences in levels of protein expression of the NR1 subunit have been demonstrated between not only different platelet donors, but also between platelet donors and untreated MEG-01 cells (figure 52). This variation may reflect the differences in the surface area to volume ratio between platelets and MKs. Alternatively, higher expression of NR1 in platelets may indicate that NR1 expression increases during MK differentiation, however densitometry analysis demonstrated that treatment with PMA for 3 d had no effect on NR1 subunit protein expression (figure 55). This suggests that expression of the subunit protein has either peaked by the megakaryoblastic stage of differentiation, that NR1 expression increases at a later stage closer to platelet production or that expression increases within the mature platelets themselves. The higher expression in human platelet indicates that further mRNA and protein expression studies are required using primary MKs to evaluate the receptor expression profile during differentiation.

Finally, these experiments should be extended to investigate the expression of NR2 subunits in differentiated MEG-01 cells as well as primary human MKs. In Western blot studies, the expression of NR2A appears to be increased upon PMA differentiation (figure 53) and these results correlate with previous studies reporting the up regulation of NR2A mRNA expression upon PMA differentiation of (Hitchcock 2003). It is important to understand the NR2 expression profile in the differentiated MKs due to the contribution of the NR2 subunits to NMDAR pharmacology. To date, evidence suggests expression of NR2A and/or NR2D subunits from this study and previous reports in the literature. These NR2 subunits convey different properties to the assembled NMDAR. For example a stronger stimulus is required to remove the Mg^{2+} blocking the NMDAR pore if the NR2A subunit protein is present, than if the NR2D is present (Qian and Johnson, 2006; Clarke and Johnson, 2006). Additionally, affinity of MK-801 is greater for NR1/NR2A than NR1/NR2D containing receptors (Laurie and Seeburg, 1994). Electrophysiological

measurements of NMDA-gated ion channels and calcium imaging will provide further insight into the pharmacological properties of the MK NMDA receptor and may distinguish between the different NMDAR assemblies.

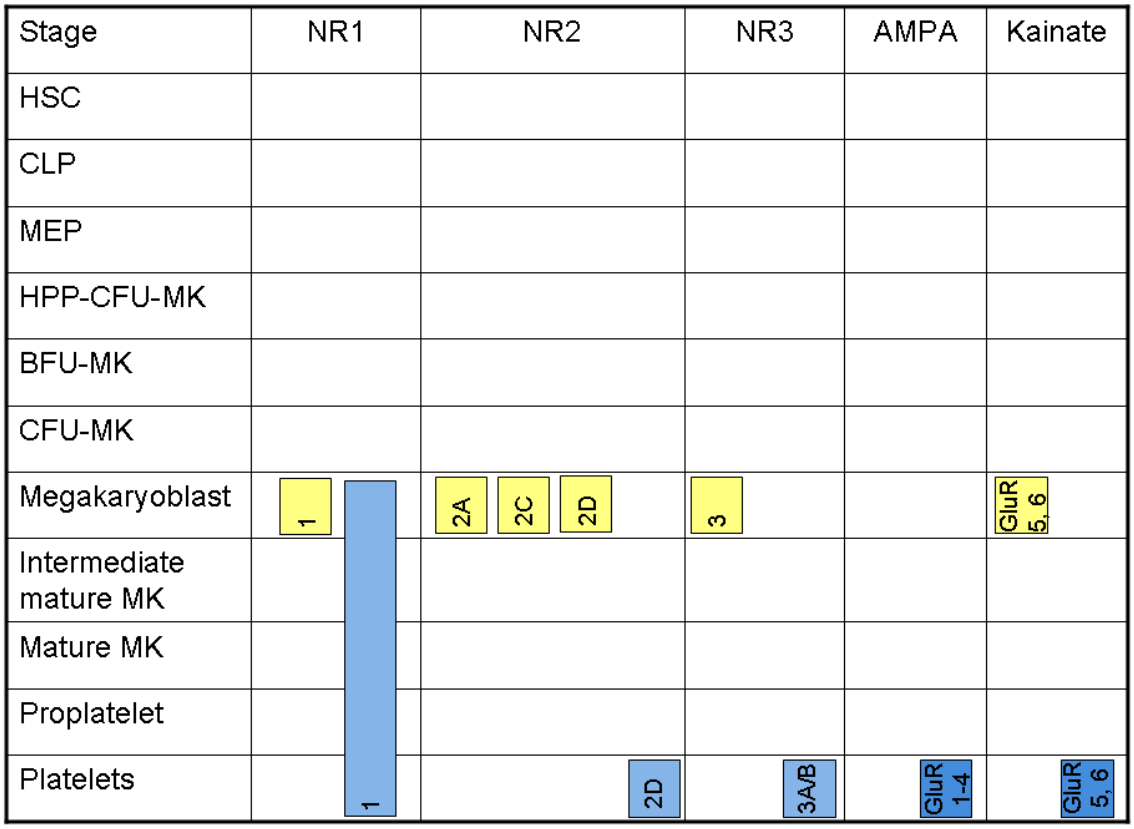

Table 43. Temporal profile of NMDAR subunit expression during haematopoiesis. Using data from this study, this figure compares the expression of the NR1, NR2 and N3 subunits. Expression of the NR2A subunit was not determined in either immature MKs (MEG-01 cells) or in platelets. Blue bars indicate protein expression as demonstrated in this study, darker blue bars indicate protein expression determined in previous studies (Morrell *et al*, 2008; Sun *et al*, 2009). Yellow bars indicate mRNA expression which was determined in other studies- NR1 in Meg-01 cells, NR2A in native human MKs, NR2C and NR2D in MEG-01 cells and native human MKs, GluR5 and 6 in MEG-01 cells (Genever *et al*, 1999; Hitchcock *et al*, 2003; Hitchcock, 2003; Sun *et al*, 2009).

5.4.2.2. MEG-01 adhesion, cell size and morphology

This study has demonstrated that NMDARs are required for fibrinogen-dependent MEG-01 adhesion. A previous study investigated whether functional NMDARs are required for the adherence of 2 different MK cell lines, MEG-01 and CMK, to tissue culture plastic (Genever *et al*, 1999). Adherence was detected using a crystal violet assay, and

shown to be inhibited by NMDAR specific inhibitors, MK-801 and D-AP5 in the presence of PMA. This work has been extended to investigate the role of NMDARs in MEG-01 cell adherence to fibrinogen as well as tissue culture plastic. It demonstrated that in contrast to the study by Genever *et al* (1999), the addition of the inhibitors potentiated adhesion to tissue culture plastic, while in the presence of fibrinogen NMDAR specific inhibitors attenuated adhesion (figures 59 and 61).

Cell number was also investigated in parallel with the crystal violet assays, which demonstrated that PMA inhibits any increase in cell density above that plated at the start of the experiment, after 3 d in culture, whether cultured on fibrinogen or tissue culture plastic (figures 59 and 61). This has previously been observed in both MEG-01 cells (Ogura *et al*, 1998; Meacci *et al*, 1996) and another megakaryoblastic cell line, HEL (Zauli *et al*, 1995). PMA has been demonstrated to differentiate both native MKs and megakaryocytic cell lines (Nagata *et al*, 1996; Goto *et al*, 1992; Genever *et al*, 1999), where one differentiation marker is that MKs cease to proliferate, instead increasing in size and moving towards platelet production (Hitchcock *et al*, 2003). This was observed in both the presence and absence of fibrinogen (figures 59 and 61), demonstrating that PMA is sufficient to stimulate differentiation alone without the additional presence of other differentiation triggering factors.

The presence of the inhibitors had mixed effects on cell number with D-AP5 (10 μM) leading to an increase in cell number in the presence of PMA but absence of fibrinogen (figure 59C). In comparison, the presence of fibrinogen and absence of PMA, 1 μM D-AP5 stimulates an increase in cell number which is then inhibited as the concentration of D-AP5 increases (figure 61C). MK-801 was found to have an inhibitory effect on MEG-01 cells cultured on fibrinogen without PMA at 100 μM, whereas lower concentrations stimulated increases in cell numbers (figure 61D). These experiments were not carried out in parallel, therefore this would need to be repeated to determine whether they are comparable, however they suggest that the presence of NMDAR specific inhibitors only have an inhibitory impact on cell density at higher concentrations (100 μM) in the presence of fibrinogen and absence of PMA. The previous literature would suggest however that their presence would inhibit the effects of the PMA, therefore halting differentiation and stimulating proliferation (Hitchcock *et al*, 2003).

Changes were also observed in the size of MEG-01 cells between those which had been cultured on fibrinogen and those on tissue culture plastic (figure 58). The cells cultured on fibrinogen were found to be smaller than those cultured on tissue culture plastic both in the presence and absence of PMA. The addition of NMDAR-specific inhibitors had no effect on cell size in either the presence or absence of fibrinogen (figures 56 and 57). The only differences in cell shape were observed between MEG-01 cells treated with PMA or the vehicle control, DMSO. DMSO-treated cells remained spherical and mostly in suspension, with PMA-treated cells becoming more irregular in shape and with a larger number appearing to adhere to the cell culture flask. Again, the addition of the inhibitors had no effect on these changes in cell morphology. These findings are in contrast to both original papers; Genever *et al* (1999) demonstrates by flow cytometry that MK-801 inhibits the increases in both cell size and CD41 expression induced by PMA, and Hitchcock *et al* (2003) that MK-801 inhibits morphological changes induced by TPO in $CD34^+$ MKs, for example increasing cell size and demarcation membrane together with formation of proplatelets and development of a multilobed nucleus. The variation between the results obtained in this study and those of the original studies require further investigation.

The crystal violet dye used in the adhesion assay binds to DNA and as the number of adherent cells increases, the amount of dye binding increases (Yang *et al*, 2001). During MK differentiation, the ploidy of the cells and therefore the amount of DNA within the cells increases, potentially leading to an increase in absorption that is not proportional to an increase in cell number. Other assays are therefore required to determine whether the effects seen are due to changes in ploidy or are in fact due to the action of the inhibitors, for example calcein-AM, a membrane permeable dye which becomes trapped in the cytoplasm of viable cells following cleavage of the AM group by non-specific esterases (Braut-Boucher *et al*, 1995). This would bypass the reliance on DNA-binding, removing the possibility of variations in ploidy affecting the results obtained.

Fibrinogen binding plays a role both in MK differentiation and in thrombus formation, with MKs binding to fibrinogen within the sinusoids such that they are able to anchor and extend proplatelets into the blood stream (Wang *et al*, 1998). The $\alpha_{IIb}\beta_3$ integrin requires activation before it is able to bind fibrinogen, and in the sinusoids this is provided by the binding of TPO or SDF (Majka *et al*, 2000). Fibrinogen also has a role in the coagulation cascade, where it is converted to fibrin by the action of FXa and FVa (figure 3) as well as in

the formation of platelet aggregates when it is released from α-granules upon platelet activation. It is possible that glutamate released by osteoclasts would be available to MKs and through binding to NMDARs, could then activate the integrin stimulating fibrinogen binding and anchoring of the MK in the sinusoids. A recent study has demonstrated that glutamate release also occurs in MKs through a SNARE (soluble NSF (N-ethylmaleimide sensitive factor))-dependent mechanism, which has been highly characterised in presynaptic neurones (Thompson *et al*, 2010). One difference between the two systems is that SNAP25 is expressed only in excitable cells, with SNAP23 present instead in non-excitable cells, and shown in the study by Thompson *et al* (2010) to be expressed in both MEG-01 cells and human MKs. Other proteins involved in vesicle-membrane fusion have also been identified in these cells including VAMP (vesicular associated membrane protein; also known as synaptobrevin) and syntaxin 4 (Thompson *et al*, 2010). These are all required to form the SNARE attachment protein receptors which are implicated in tethering of the vesicle to the cell membrane. PMA-differentiated cells were found to release higher levels of glutamate than undifferentiated MEG-01s or human MKs, and it is suggested that they release glutamate spontaneously unlike neurones which require depolarisation (Thompson *et al*, 2010).

This study could be extended by investigating the role of extracellular matrix proteins, for example collagen, and whether binding by MKs is affected by NMDAR activation or inhibition. It has previously been suggested that pre-treatment of human platelets with NMDA inhibits AA-induced Ca^{2+} influx into the cells, and potentiates the inhibition induced by the COX inhibitors ASA and indomethacin (Franconi *et al*, 1998). This could be extended by investigating whether pre-treatment with NMDA has similar effects in MKs, for example comparing the results obtained from a cell line to those using primary MKs.

Recent studies have shown that KARs and AMPARs are present on human platelets, and that activation of both receptors plays a role in platelet activation and aggregation (Morrell *et al*, 2008; Sun *et al*, 2009). Functional AMPARs have been shown to be expressed in bone marrow-isolated MKs using electrophysiology, together with functional KARs (Morrell *et al*, 2008). This suggests that these receptors may also play a role in MK differentiation, for example they may collaborate with NMDARs in the adhesion of MKs to fibrinogen, which would assist in tethering in the sinusoids, or potentially play a role in

maintaining MKs in the bone marrow. These possibilities require further investigation, but it also suggests that different iGluRs could play a combined role in MK differentiation, particularly given the differences in their ion permeability, with NMDARs permeable to both Ca^{2+} and Na^{+} whereas AMPA and KARs are permeable to Na^{+} (Dingledine *et al*, 1999).

5.4.3. Overall conclusions and clinical relevance

This study has demonstrated that the NMDAR subunit NR1 is expressed in the megakaryoblastic cell line MEG-01, and that treatment with PMA to stimulate differentiations does not appear to alter the expression of the NR1, NR2A or NR2D subunits. It has also shown that NMDARs are implicated in MEG-01 cell adhesion to fibrinogen, have a potential role in changes in cell size in the presence of fibrinogen, but not in changes to cell shape. This requires further investigation to determine whether changes in subunit expression occur during later stages of differentiation than that obtained by 3 d of PMA differentiation or whether it occurs within platelets themselves (figures 52 and 54). A previous study has also indicated that the NR2A subunit is expressed at the mRNA level in bone-marrow derived MKs, but expression has not been determined of the NR2A protein or mRNA in MEG-01 cells. Further investigations are required to determine differences between expression of the NMDA subunit proteins in the MEG-01 cell line and in native MKs as well as the presence of mRNA. Variation has been seen in subunit expression in different human donors (figures 13 and 15) indicating that studies would have to be carried out on MKs obtained from several different donors to take this variation into account.

This work could be further extended by investigating the functional expression of NMDARs in platelets from patients with disorders in platelet production, for example thrombocytopenia where the platelet count is significantly reduced (below 1×10^{8} ml^{-1}; Kaushansky *et al*, 1995) and sufferers experience spontaneous, prolonged bleeding for example, from the nose or gums (Bussel *et al*, 2009). NMDARs have been demonstrated in a previous study to play a role in MK differentiation through inhibition of proplatelet formation and increases in cell size indicative of MK differentiation in the presence of an NMDAR inhibitor, MK-801 (Hitchcock *et al*, 2003). It would therefore be interesting to determine whether the expression of NMDARs in these disorders is functionally compromised, expression reduced, or whether polymorphisms of the receptors are

expressed whose functionality is detrimentally affected. Variation in expression of the NR1 and NR2D subunit proteins was illustrated in this study (figure 13 and 15), showing that expression is not uniform between donors. Donors could also be separated into responders and non-responders, adding another facet to the variability (figures 17 and 33). Therefore a number of both patients and control donors would be required to take into account donor variation. This study could also be extended using animal models in which platelet production is compromised for example through deletions of Ets-1 or Fli-1 found in Paris-Trousseau syndrome (Raslova *et al*, 2004), to investigate changes in NMDAR expression in both the platelets and in the MKs. NMDAR expression has been demonstrated to be maintained in the absence of c-mpl expression in mice (Hitchcock *et al*, 2003), illustrating that a reduction in the ability to bind TPO, the primary regulator of MK differentiation, does not affect NR1 expression, however it was not determined whether functional receptors were formed. Therefore, NMDARs are implicated not only in the differentiation of MKs, platelet production and platelet activation, but also potentially in diseases characterised by reduced platelet numbers.

CHAPTER 6
GENERAL DISCUSSION

In this study the NR1 subunit protein has been shown to be expressed in MEG-01 cells, with human platelets found to express the NR1, NR2D and NR3 subunit proteins. There is evidence that at least 1 other NMDAR subunit protein is expressed in MEG-01 cells, as when they are cultured on fibrinogen for 3 d with MK-801, the cells are significantly smaller in size than the control cells, and the presence of MK-801 has been found to inhibit MEG-01 cells adhesion (figures 57 and 61). Functional NMDARs can not be formed solely of NR1 subunits, therefore NR2 and/ or NR3 subunits proteins must also be expressed. The observation that this effect only occurs when MEG-01 cells are cultured on fibrinogen suggests that these results are indicative of a functional role for NMDARs in the end stages of MK differentiation. Fibrinogen lines the blood sinusoids to which MKs migrate towards the latter stages of differentiation, which in this study is mimicked by the fibrinogen coating of tissue culture vessels. The inhibitory effect of MK-801 on MEG-01 cell size is suggestive that NMDARs also have a role in slightly earlier stages of MK differentiation, as MKs cease to proliferate and increase in size as a preliminary step to platelet production. This was also suggested by Hitchcock *et al* (2003) where treatment with MK-801 inhibits increases in cell size together with the formation of proplatelets, α-granules and a polyploidy nucleus.

6.1. Receptor expression

RT-PCR has demonstrated in earlier studies that undifferentiated MEG-01 cells express the NR1, NR2C and D and NR2 subunit mRNA (Genever *et al*, 1999; Hitchcock, 2003). In this investigation, primers were successfully designed for NR1 and NR2A-C subunits; a set for the NR3A subunit had previously been obtained. Two separate undifferentiated reverse transcribed MEG-01 samples were used to determine that at the time the samples were taken, the cells did not appear to express mRNA for any of the subunits tested (figure 50). Matched samples were not taken for both Western blotting and RT-PCR; implementing this would determine whether mRNA is expressed at the same time as the proteins of each subunit. This could be extended to investigate the NMDAR mRNA and proteins expressed by MEG-01 cells differentiated with PMA. There is evidence that NR2A mRNA expression increases following 3 d of PMA treatment (Hitchcock, 2003), and a possible increase in expression of the NR2A protein observed in this study (figure 53). Again,

matched samples would determine similarities and differences in timing of mRNA and protein expression. This would be assisted by the development of selective antibodies able to distinguish between the 2 NR3 subtypes, A and B, as well as obtaining another, cleaner anti-NR2A antibody and using a positive control in the Western blots, for example whole rat brain.

6.2. NMDAR localisation

The actions of NMDAR antagonists are restricted to the PMA differentiated MEG-01 cells. This maybe due to an increased expression of NR subunits, as described in the previous section, or an altered trafficking of NR subunits. NMDARs are known to be trafficked within cells, however most of the data has been obtained from work in neural cells, and would need to be repeated in MKs. NMDARs have been demonstrated to be highly mobile during in immature synapses, becoming less so once they mature (Lavezzari *et al*, 2004; Roche *et al*, 2001). Targeting of the subunits varies, with the NR2A subunit protein preferentially endocytosed via the early to the late endosomes, whereas the NR2 B subunit protein in more commonly recycled via the early endosomes back to the plasma membrane (Lavezzari *et al*, 2004). The activation of neuronal PKC has been demonstrated to induce rapid exocytosis of NMDARs to the plasma membrane (Carroll and Zukin, 2002), and the effect of PMA treatment on the localisation of NMDAR subunit proteins in MEG-01 cells could be investigated. Their movement could be tracked by labelling the different subunit proteins with antibodies labelled with different fluorescent tags and followed using live cell imaging, or alternatively following fixation at different time points after PMA treatment. Autoradiography using tritiated MK-801 could also be used which only binds to functional NMDARs, as not all clusters of NMDAR subunit proteins will form receptors (Genever *et al*, 1999).

6.3. NMDAR expression during MK differentiation

Native MKs are located in the bone marrow together with osteoblasts and osteoclasts which have been demonstrated to secrete glutamate (Morimoto *et al*, 2006; Rhangu *et al*, 2001). MKs have been found to take up glutamate via EAAT1 and store it in vesicles (Genever *et al*, 1999; Thompson *et al*, 2010), but it could also suggest that glutamate plays a role even earlier in differentiation than megakaryoblastic MEG-01 cells. It would therefore be informative to follow the expression of both the mRNA and protein for each NMDAR subunit from an earlier stage in development for example back to the progenitor cells,

HSCs, by setting up further differentiation experiments to determine when each subunit is expressed and therefore from which stage potentially functionally NMDARs could be present. This would require native MK cells or an early stage MK cell line so that changes in expression and cell morphology can be tracked through to the mature MK stage or even to platelet production. MK-801, D-AP5 and D-serine could also be used to determine the effects of NMDAR inhibition on MK differentiation. The part that NMDARs play in adhesion requires further work using a method which does not rely on a dye binding to nuclear material, for example calcein-AM, a cell permeable dye which remains within the cytoplasm making it a more accurate indicator of increases in adhesion than the dye used in this study, crystal violet, which binds to DNA. The DNA content of MKs increases during differentiation, potentially up to 128 N (Italiano *et al*, 1999), suggesting that the number of cells adhering is greater than it actually is; a cytoplasmic dye would negate this problem.

6.4. Functional expression of NMDARs in human platelets

The NMDARs expressed in human platelets have been demonstrated to be functional; activated by glutamate, glycine and NMDA; and inhibited by the receptor-specific inhibitors MK-801 and D-AP5, or the NR1/ NR3 inhibitor, D-serine. The data is not comparable between the fluo-4 and the luciferase assays, as different methods were used to isolate the platelets from the plasma for each assay. In future studies, the method used for the fluo-4 assay (section 2.7.) which has previously been published (Mackenzie *et al*, 1996) should be used for both assays. The experiments could be further improved by taking samples for Western blotting from the same platelet donation as that used for the assays so the functional results can be directly compared with the subunit proteins expressed at that time. If possible the assays should be carried out in parallel, as platelets taken from the same donor vary between each donation, which take place at least 28 d apart, and would increase the validity of the comparison. Previous studies have suggested that NMDARs play an anti-aggregatory role in human platelets (Franconi *et al*, 1996, 1998), however data obtained in this study demonstrated that the activation of NMDARs in potentially pro-aggregatory. Further study is required to investigate this, particularly experiments into the effect of treatment with NMDA prior to the addition of known pro-aggregatory agonists such as collagen and AA, which Franconi demonstrated had an inhibitory effect. Functional assays could be used alongside aggregation experiments to extend this investigation and examine more fully the role of NMDARs in platelet activation and aggregation. Glutamate release could be measured, for example using a fluorescence

detection assay (Sim *et al*, 2006) or an enzymatic probe (Morrell *et al*, 2008), and ATP release has previously been measured simultaneously with aggregation using a combined aggregometer and luminometer (Charo *et al*, 1977). *In vivo* work could investigate the effects of specific subunit knockouts or treatment of animal models with antagonists, to test the effects of NMDARs on bleeding time and thrombosis formation using induced injuries for example with ferric chloride (Morrell *et al*, 2008). A conditional knockout would be required for the NR1 subunit, as its absence during development is neonatally lethal (Li *et al*, 1994; Forrest *et al*, 1994). It would be informative to use similar conditional knockout models for the other NMDAR subunits to further determine their roles in adult systems. Treating human platelets with strychnine would determine whether inhibitory glycine receptors are also expressed and if so, whether they play a regulatory role in platelet activation. An NR2D antagonist has recently been developed, the use of which would also assist in determining the role of different subunits in platelet activation.

6.5. S-nitrosylation of NMDARs

NMDAR activity is known to be inhibited by *S*-nitrosylation through the binding of NO to specific cys residues in the extracellular regions of the NR1 and NR2A subunit proteins (Choi *et al*, 2000). Nitrosylation of the subunits has been detected in the brain using the biotin switch method (Jaffrey and Snyder, 2001). However, this is prone to producing false positives and can not be used in live cells (Jaffrey *et al*, 2001). A novel *S*-nitrosylation detection agent SNOB, has been developed at the University of Bath which can be used to detect nitrosylation of proteins in live cells and is a single step process (Appendix II). Initial optimisation was carried out using BSA which has only 1 free cys residue and demonstrated that SNOB could be used successfully at 37 ^{o}C at which only a 5 min incubation was required for binding to be detectable by Western blotting (figure 67). Human platelets were used to extend this optimisation as they are exposed to NO in the blood stream which is constitutively produced by eNOS located in the endothelium lining of the blood vessels (Dimmler *et al*, 1999), and proteins expressed on the surface of platelets are already known to be nitrosylated, for example $\alpha_{IIb}\beta_3$ (Walsh *e al*, 2007). It was therefore hypothesised that NMDARs on human platelet could be modulated by NO in the bloodstream. The data produced demonstrates that treatment with SNOB increases neutravidin-HRP binding, which can be increased further by treatment with NONOate, an NO donor, or reduced following treatment with DTT, a reducing reagent. The data obtained to date gives an overall view of nitrosylated proteins expressed on human platelets

which bind SNOB, however bands of approximately 120 kDa can be observed in figures 68 and 70, suggesting that the NR1 subunit protein may be nitrosylated by treatment with NONOate. Identification of the nitrosylated proteins required further investigation, for example using immunoprecipitation. Determination of whether the NR1, and possibly the NR2A, subunit proteins are *S*-nitrosylated will then enable functional assays to be carried out, such as the fluo-4 assay to determine the action of NO on platelet activation. Platelets could be pre-treated with NONOate or DTT before the addition of glutamate or NMDA together with glycine to determine whether the responses are altered. The addition of DTT increases the number of free thiols and mimics the reduced oxygen levels within the body (hypoxia) in comparison to that of air in the laboratory (normoxia). This should increase the sensitivity of NMDARS to NO as all 5 extracellular cys residues will be exposed as free thiols as opposed to 1 under normoxic conditions. This effect could also be achieved by carrying out the assays in a hypoxic chamber, where NONOate could be added to simulate a localised increase in NO.

6.6. Clinical relevance and overall conclusions

There are extensive clinical applications for this further understanding of platelet and MK NMDARs. Their use as neuronal models would enable testing of new agonists or antagonists to determine their effects on native human cells without having to source human brain tissue, and availability would be much higher as would the range of donors from which samples could be taken. Platelet can not be transfected, however MKs can, enabling the production of platelets containing new proteins *in vitro* that can then be analysed. The identification of the NR3 subunit protein extends the similarity of platelets to the brain, enabling further investigation into the strychnine-insensitive, excitatory glycine receptor, which demonstrates an alternative signalling role for glycine in comparison to its other, more understood roles (Curtis *et al*, 1967). Further work is required to fully understand the complete role of NMDARs in MK differentiation and platelet activation, however this study provides a good initial step.

CHAPTER 7
BIBLIOGRAPHY

Addison W. 1841. On the colourless corpuscles and on the molecules and cytoblasts in the blood. *London Med. Gaz.* NS30:144-152.

Albers GW, Clark WM, Atkinson RP, Madden K, Data JL, Whitehouse MJ. 1999. Dose escalation study of the NMDA glycine-site antagonist Licostinel in acute ischemic stroke. *Stroke* 30(3):508-13.

Alessi DR, James, SR, Downes CP, Holmes AB, Gaffney PRJ, Reese CB, Cohen P. 1997. Characterisation of a 3-phosphoinositide-dependent protein kinase which phosphorylates and activates protein kinase Bα. *Curr. Biol.* 7(4):261-69.

Alt A, Weiss B, Odgen A, Knauss J, Oler J, Ho K, Large T, Bleakman D. 2004. Pharmacological characterization of glutamatergic agonists and antagonists at recombinant human homomeric and heteromeric kainate receptors in vitro. *Neuropharmacology* 46(6):793-806.

Amisten S, Braun O, Bengtsson A, Erlinge D. 2008. Gene expression profiling for the identification of G-protein coupled receptors in human platelets. *Thrombosis Res.* 122(1):47-57.

Arundine M, Tymianski M. 2004. Molecular mechanisms of glutamate-dependent neurodegeneration in ischemia and traumatic brain injury. *Cell. Mol. Life Sci.* 61(6):657-68.

Atkinson B, Jarvis G, Watson S. 2003. Activation of GPVI by collagen is regulated by α2β1 and secondary mediators. *J. Thromb. Haemost.* 1(6):1278-87.

Atlason P, Garside M, Meddows E, Whiting P, McIlhinny R. 2007. *N*-methyl-*D*-aspartate (NMDA) receptor subunit NR1 forms the substrate for oligomeric assembly of the NMDA receptor. *J. Biol. Chem.* 282(35):25299-307.

Avecilla S, Hattori K, Heissig B, Tejada R, Liao F, Shido K, Jin D, Dias S, Zhang F, Hartman T, Hackett NR, Crystal RG, Witte L, Hicklin DJ, Bohlen P, Eaton D, Lyden D, de Sauvage F, Rafii S. 2004. Chemokine-mediated interaction of hematopoietic progenitors with the bone marrow niche is required for thrombopoiesis. *Nat. Med*. 10(1):64-71.

Awobuluyi M, Yang J, Ye Y, Chatterton J, Godzik A, Lipton S, Zhang, D. 2007. Subunit-specific roles of glycine-binding domains in activation of NR1/ NR3 *N*-methyl-*D*-aspartate receptors. *Mol. Pharmacol.* 71(1):112-22.

Bading H, Greenberg ME. 1991. Stimulation of protein tyrosine phosphorylation by NMDA receptor activation. *Science* 253(5022):912-4.

Baier P, Kocha J, Seeck-Hirschnera M, Ohlmeyera K, Wilmsa S, Aldenhoffa J, Hinze-Selch D. 2009. A flow-cytometric method to investigate glutamate-receptor-sensitivity in whole

blood platelets – Results from healthy controls and patients with schizophrenia. *J. Psychiatr. Res.* 43(6):585-91.

Baldassare J, Henderson P, Burnsell D, Loomis C, Fisher G. 1992. Translocation of protein kinase C isozymes in thrombin-stimulated human platelets. *J. Biol. Chem.* 267(22):15585-90.

Bartley T, Bogenberger J, Hunt P, Li Y, Lu H, Martin F, Chang M, Samal B, Nichol J, Swift S, Johnson MJ, Hsu R-Y, Parker VP, Suggs S, Skrine JD, Merewether LA, Clogston C, Hsu E, Hokom MM, Hornkohl A, Choi E, Pangelinan M, Sun Y, Mar V, McNinch J, Simonet L, Jacobson F, Xie C, Shutter J, Chute H, Rasu R, Selander L, Trollinger D, Sieu L, Padilla D, Trail G, Elliott G, Izumi R, Covey T, Crouse J, Garcia A, Xu W, Del Castillo J, Biron J, Cole S, Hu MC-T, Pacifici R, Ponting I, Saris C, Wen D, Yung YP, Lin H, Rosselman RA. 1994. Identification and cloning of a megakaryocyte growth and development factor that is a ligand for the cytokine receptor Mpl. *Cell* 77:1117-1124.

Battinelli E, Loscalzo J. 2000. Nitric oxide induces apoptosis in megakaryocytic cell lines. *Blood* 95(11):3451-59.

Battinelli E, Willoughby S, Foxall T, Valerie C, Loscalzo J. 2001. Induction of platelet formation from megakaryocytoid cells by nitric oxide. *Proc. Natl. Acad. Sci. U.S.A.* 98(25):14458-63.

Beelman CA, Parker R. 1995. Degradation of mRNA in eukaryotes. *Cell* 81(2):179-83.

Beeton CA, Bord S, Ireland D, Compston JE. 2006. Osteoclast formation and bone resorption are inhibited by megakaryocytes. *Bone* 39(5):985-90.

Belachew S, Malgrange B, Rigo J-M, Rogister B, Leprince P, Hans G, Nguyen L, Moonen G. 2000. Glycine triggers an intracellular calcium influx in oligodendrocyte progenitor cells which is mediated by the activation of both the ionotropic glycine receptor and Na^+-dependent transporters. *Eur. J. Neurosci.* 12(6):1924-30.

Bennett J, Weeds A. 1986. Calcium and the cytoskeleton. *Br. Med. Bull*. 42(4):385-390.

Bennett J. 2005. Structure and function of the platelet integrin αIIbβ3. *J. Clin. Invest.* 115 (12):3363-69.

Benveniste H, Drejer J, Schousboe A, Diemer N. 1984. Elevation of the extracellular concentrations of glutamate and aspartate in rat hippocampus during transient cerebral ischemia monitored by intracerebral microdialysis. *J. Neurochem.* 43(5):1369-74.

Benveniste M, Clements J, Vyklicky Jr L, Mayer M. 1990. A kinetic analysis of the modulation of *N*-methyl-D-aspartic acid receptors by glycine in mouse cultured hippocampal neurones. *J. Physiol.* 428:333-357.

Bereiter D, Bereiter DF, Hathaway CB. 1996. The NMDA receptor antagonist MK-801 reduces Fos-like immunoreactivity in central trigeminal neurons and blocks select endocrine and autonomic responses to corneal stimulate in the rat. *Pain* 64(1):179-89.

Berk M, Plein H, Belsham B. 2000. The specificity of platelet glutamate receptor supersensitivity in psychotic disorders. *J. Life. Sci* 66(25):2427-32.

Bessho Bessho, Nawa H, Nakanishi S. 1994. Selective up-regulation of an NMDA receptor subunit mRNA in cultured cerebellar granule cells by K^+-induced depolarisation and NMDA treatment. *Neuron* 12(1):87-95.

Betz U, Bloch W, van den Broek M, Yoshida K, Taga T, Kishimoto T, Addicks K, Rajewsky K, Muller W. 1998. Postnatally induced inactivation of gp130 in mice results in neurological, cardiac, hematopoietic, immunological, hepatic, and pulmonary defects. *J. Exp. Med*. 188(10):1955-65.

Bhangu P, Genever P, Spencer G, Grewal T, Skerry T. 2001. Evidence for targeted vesicular glutamate exocytosis in osteoblasts. *Bone* 29(1):16-23.

Bizzozero G. 1882. Ueber einner neuen formbestandtheil des blutes und dessen rolle bei der thrombose und der blutgerinnung. *Virchows Arch. fur Pathol. Anat. und Physiol.* 90:261-332.

Bouillet P, Metcalf D, Huang D, Tarlinton D, Kay T, Köntgen F, Adams J, Strasser A. 1999. Proapoptotic Bcl-2 relative Bim required for certain apoptotic responses, leukocyte homeostasis, and to preclude autoimmunity. *Science* 286:1735-38.

Braut-Boucher F, Pichon J, Rat P, Adolphe M, Aubery M, Font J. 1995. A non-isotopic, highly sensitive fluorimetric, cell-cell adhesion microplate assay using calcein AM-labeled lymphocytes. *J. Immunol. Methods* 178(1):41-51.

Bradford M. 1976. A rapid and sensitive method for the quantitation of microgram quantities of protein utilizing the principle of protein-dye binding. *Anal. Biochem.* 72:248-54.

Brass LF, Zhu L, Stalker TJ. 2005. Minding the gaps to promote thrombus growth and stability. *J. Clin. Invest.* 115(12):3385-92.

Briquet-Laugier V, Lavenu-Bombled C, Schmitt A, Leboeuf M, Uzan G, Dubart-Kupperschmitt A, Rosa J-P. 2004. Probing platelet factor 4 alpha granule targeting. *J. Thromb. Haemost.* 2(12):2231-40.

Broudy V, Lin N, Sabath D, Papayannopoulou T, Kaushansky K. 1997. Human platelets display high affinity receptors for thrombopoietin. *Blood* 89(6):1896-1904.

Brown CS, Dean WL. 2007. Regulation of Ca^{2+}-ATPase in human platelets by calpain. *Platelets* 18(3):207-11.

Bunting S, Widmer R, Lipari T, Rangell L, Steinmetz H, Carver-Moore K, Moore M, Keller G-A, de Sauvage F. 1997. Normal platelets and megakaryocytes are produced *in vivo* in the absence of thrombopoietin. *Blood* 90(9):3423-29.

Bussel JB, Provan D, Shamsi T, Cheng G, Psaila B, Kovaleva L, Salama A, Jenkins JM, Roychowdhury D, Mayer B, Stone N, Arning M. 2009. Effects of eltrombopag on platelet counts and bleeding during treatment of chronic idiopathic thrombocytopenic purpura: a randomised, double-blind, placebo-controlled trial. *Lancet* 373(9664):641-48.

Butt E, Immler D, Meyer H, Kotlyarov A, Laass K, Gaestel M. 2001. Heat shock protein 27 is a

substrate of cGMP-dependent protein kinase in intact human platelets: phosphorylation-induced actin polymerization caused by HSP27 mutants. *J Biol. Chem.* 276(10):7108-13.

Calderwood D, Zen R, Grant R, Rees D, Hynes R, Ginsberg M. 1999. The talin head domain binds to integrin beta subunit cytoplasmic tails and regulates integrin activation. *J. Biol. Chem.* 274(40):28071-74.

Cantor A, Katz S, Orkin S. 2002. Distinct domains of the GATA-1 cofactor FOG-1 differentailly influence erythroid versus megakaryocytic maturation. *Mol. Cell Biol*. 22(12):4268-79.

Carroll RC, Zukin RS. 2002. NMDA-receptor trafficking and targeting: implications for synaptic transmission and plasticity. *Trends. Neurosci.* 25(11):571-77.

Castillo J, Dávalos A, Noya M. 1997. Progression of ischaemic stroke and exocitotoxic amino acids. *Lancet* 349(9045):79-83.

Castillo J, Dávalos A, Naveiro J, Noya M. 1996. Neuroexcitatory amino acids and their relation to infarct size and neurological deficit in ischemic stroke. *Stroke* 27(6):1060-5.

Castro-Malaspina H, Rabellino EM, Yen A, Nachman RL, Moore MAS. 1981. Human megakaryocyte stimulation of bone marrow fibroblasts. *Blood* 57(4):781-87.

Cavallini L, Coassin M, Borean A, Alexandre A. 1996. Prostacyclin and sodium nitroprusside inhibit the activity of the platelet inositol 1, 4, 5-triphosphate receptor and promote its phosphorylation. *J Biol. Chem.* 271(10):5545-51.

Chang Y, Bluteau D, Debili N, Vainchenker W. 2007. From hematopoietic stem cell to platelets. *J. Thromb. Haemost.* 5(Suppl. 1):318-327.

Changa C-Y, Liaoa H-K, Juoc C-G, Chena S-H, Chen Y-J. 2006. Improved analysis of membrane protein by PVDF-aided, matrix-assisted laser desorption/ionization mass spectrometry. *Anal. Chim. Acta.* 556(1):237-46.

Charo IF, Feinman RD, Detwiller TC. 1977. Interrelations of platelet aggregation and secretion. *J. Clin. Invest.* 60(4):866-76.

Chatterton J, Awobuluyi M, Premkumar L, Takahashi H, Talantova M, Shin Y, Cui J, Tu S, Sevarino K, Nakanishi N et al. 2002. Excitatory glycine receptors containing the NR3 family of NMDA receptor subunits. *Nature* 415:793-98.

Chen HS, Pellegrini JW, Aggarwal SK, Lei SZ, Warach S, Jensen FE, Lipton SA. 1992. Open-channel block of N-methyl-D-aspartate (NMDA) responses by memantine: therapeutic advantage against NMDA receptor-mediated neurotoxicity. *J. Neurosci.* 12(11):4427-36.

Chen HS, Wang YF, Rayudu PV, Edgecomb P, Neill JC, Segal MM, Lipton SA, Jensen FE. 1998. Neuroprotective concentrations of the *N*-methyl-*D*-aspartate open-channel blocker memantine are effective without cytoplasmic vacuolation following post-ischemic administration and do not block maze learning or long-term potentiation. *Neuroscience* 86(4):1121-32.

Cheng L, Qasba P, Vanguri P, Thiede MA. 2000. Human mesenchymal stem cells support

megakaryocyte and pro-platelet formation from $CD34^+$ hematopoietic progenitor cells. *J. Cell. Physiol.* 184(1):58-69.

Choi Y-B, Lipton S. 2000. Redox modulation of the NMDA receptor. *Cell. Mol. Life Sci*. 57(11):1535-41.

Choi Y-B, Tenneti L, Le D, Ortiz J, Bai G, Chen H-S, Lipton S. 2000. Molecular basis of NMDA receptor-coupled ion channel modulation by *S*-nitrosylation. *Nat. Neurosci.* 3(1):15-21.

Chou MM, Hou W, Johnson J, Graham LK, Lee MH, Chen C-S, Newton AC, Schaffhausen BS, Toker A. 1998. Regulation of protein kinase C ζ by PI 3-kinase and PDK-1. *Curr. Biol.* 8(19):1069-78.

Ciabarra A, Sullivan J, Gahn L, Pecht G, Heinemann S, Sevarino K. 1995. Cloning and characterization of chi-1: a developmentally regulated member of a novel class of the ionotropic glutamate receptor family. *J. Neurosci*. 15(10):6498-508.

Clarke R, Johnson J. 2006. NMDA receptor NR2 subunit dependence of the slow component of magnesium unblock. *J. Neurosci.* 26(21):5825-5834.

Costa BM, Feng B, Tsintsadze TS, Morley RM, Irvine MW, Tsintsadze V, Lozovaya NA, Jane DE, Monaghan DT. 2009. *N*-Methyl-D-aspartate (NMDA) receptor NR2 subunit selectivity of a series of novel piperazine-2,3-dicarboxylate derivatives: preferential blockade of extrasynaptic NMDA receptors in the rat hippocampal CA3-CA1 synapse. *J. Pharmacol. Exp. Thr.* 331(2):618-26.

Coughlin S. 2000. Thrombin signalling and protease-activated receptors. *Nature* 407:258-64.

Couratier P, Lesort M, Sindou P, Esclaire F, Yardin C, Hugon J. 1996. Modifications of neuronal phosphorylated tau immunoreactivity induced by NMDA toxicity. *Mol. Chem. Neuropathol.* 27(3):259-73.

Covic L, Gresser A, Kuliopulos A. 2000. Biphasic kinetics of activation and signaling for PAR1 and PAR4 thrombin receptors in platelets. *Biochemistry* 39(18):5458-64.

Crosby D, Poole A. 2002. Interaction of Bruton's tyrosine kinase and protein kinase C in platelets. *J Biol. Chem.* 277(12):9958-65.

Cui H, Hayashi A, Sun HS, Belmares MP, Cobey C, Phan T, Schweizer J, Salter MW, Wang YT, Tasker RA, Garman D, Rabinowitz J, Lu PS, Tymianski M. 2007. PDZ protein interactions underlying NMDA receptor-mediated excitotoxicity and neuroprotection by PSD-95 inhibitors. *J. Neurosci.* 27(37):9901-15.

Curtis D, Phillis J, Watkins J. 1960. The chemical excitation of spinal neurones by certain acidic amino acids. *J. Physiol.* 150(3):656-82.

Curtis D, Phyllis J, Watkins J. 1961. Actions of amino acids on the isolated hemisected spinal cord of the toad. *Br. J. Pharmacol.* 16:262-83.

Curtis D, Hosli C, Johnston G. 1967. Inhibition of spinal neurons by glycine. *Nature* 215(1967):1502-03.

D' Andrea G, Cananzi A, Joseph R, Morra M, Zamberlan F, Ferro Milone F, Grunfeld S, Welch K. 1991. Platelet glycine, glutamate and aspartate in primary headache. *Cephalalgia* 11(4):197-200.

Das S, Sasaki Y, Rothe T, Premkumar L, Takasu M, Crandallk J, Dikkes P, Conner D, Rayudu P, Cheung W et al. 1998. Increased NMDA current and spine density in mice lacking the NMDA receptor subunit NR3A. *Nature* 393(6683): 377-81.

Davie E, Fujikawa K, Kisiel W. 1991. The coagulation cascade: initiation, maintenance and regulation. *Biochemistry* 30(43):10363-70.

de Botton S, Sabri S, Daugas E, Zermati Y, Guidotti J, Hermine O, Kroemer G, Vaichenker W, Debili N. 2002. Platelet formation is the consequence of caspase activation within megakaryocytes. *Blood* 100(4):1310-17.

de Groot R, Raaijamakers J, Lammers J-W, Koenderman L. 2000. STAT5-dependent cyclin D1 and Bcl-xL expression in Bcr-Abl-transformed cells. *Mol. Cell. Biol. Res. Commun*. 3(5):299-305.

de Sauvage F, Hass P, Spencer S, Malloy B, Gurney A, Spencer S, Carbonne W, Henzel W, Wong S, Kuang W-J et al. 1994. Stimulation of megakaryopoiesis and thrombopoiesis by the c-Mpl ligand. *Nature* 369:533-538.

Dean B, Copolov DL. 1989. Dopamine uptake by platelets is selective, temperature dependent and not influenced by the dopamine-D1 or dopamine-D2 receptor. *Life Sci.* 45(5):401-11

Debili N, Issaad C, Masse J, Guichard J, Katz A, Breton-Gorius J, Vainchenker W. 1992. Expression of CD34 and platelet glycoproteins during human megakaryocytic differentaition. *Blood* 80(12):3022-35.

Derkach V, Suprenant A, North RA. 1989. 5HT-3 receptors are membrane ion channels. *Nature* 339(6227):706-9.

Deveaux S, Filipe A, Lemarchandel V, Ghysdael J, Romeo P, Mignotte V. 1996. Analysis of the thrombopoietin receptor (MPL) promoter implicated GATA and Ets proteins in the coregulation of megakaryocyte-specific genes. *Blood* 87(11):4678-85.

Dickman KG, Youssef JG, Mathew SM, Said SI. 2004. Ionotropic glutamate receptors in lungs and airways: molecular basis for glutamate toxicity. *Am. J. Resp. Cell Mol.* 30(2):139-44.

Dimmeler S, Fleming I, Fisslthaler B, Hermann C, Busse R, Zeiher A. 1999. Activation of nitric oxide synthase in endothelial cells by Akt-dependent phosphorylation. *Nature* 399(6736):601-5.

Dingledine R, Borges K, Bowie D, Traynelfis SF. 1999. The glutamate receptor ion channels. *Pharmacol. Rev.* 51(1):7-61.

Do V, Martinez C, Jr M, JL, Derrick E. 2002. Long-term potentiation in direct perforant path projections to the hippocampal CA3 region in vivo. *J. Neurophysiol*. 87(2):669-78.

Doyle VM, Rüegg UT. 1985. Lack of evidence for voltage dependent calcium channels on

platelets. *Biochem. Biophys. Res. Comm.* 127(1):161-67.

Drachman J, Kaushansky K. 1997. Dissecting the thrombopoietin receptor: Functional elements of the Mpl cytoplasmic domain. *Proc. Natl. Acad. Sci. U.S.A.* 94(6):2350-55.

Dravid SM, Erreger K, Yuan H, Nicholson K, Le P, Lyuboslavsky P, Almonte A, Murray E, Mosley C, Barber J, French A, Balster R, Murray TF, Traynelis SF. 2007. Subunit-specific mechanisms and proton sensitivity of NMDA receptor channel block. *J. Physiol.* 251(1):107-28.

Dutil E, Newton A. 2000. Dual role of pseudosubstrate in the coordinated regulation of protein kinase C by phosphorylation and diacylglycerol. *J Biol. Chem.* 275(14):10697-701.

Dutil E, Toker A, Newton A. 1998. Regulation of conventional protein kinase C by phosphoinositide-dependent kinase-1 (PDK-1). *Curr. Biol.* 8(25):1366-75.

Elagib K, Racke F, Mogass M, Khetawat R, Delehanty L, Goldfarb A. 2003. RUNX1 and GATA-1 coexpression and cooperation in megakaryocytic differentiation. *Blood* 101(11):4333-41.

Esmon C, Owen W. 1981. Identification of an endothelial cell cofactor for thrombin-catalyzed activation of protein C. *Proc. Natl. Acad. Sci. U.S.A.* 78(4):2249-52.

Faruqi T, Weiss E, Shapiro M, Huang W, Coughlin S. 2000. Structure-function analysis of protease-activated receptor 4 tethered ligand peptides. *J Biol. Chem.* 275(26):19728-34.

Ferrarese C, Sala G, Riva R, Begni B, Zoia C, Tremolizzo L, Galimberti G, Millul A, Bastone A, Mennini T et al. 2001. Decreased platelet glutamate uptake in patients with amyotrophic lateral sclerosis. *Neurology* 56(2):270-2.

Forrest D, Yuzaki M, Soares HD, Ng L, Luk DC, Sheng M, Stewart C, Morgan JI, Connor JA, Curran T. 1994. Targeted disruption of NMDA receptor 1 gene abolishes NMDA response and results in neonatal death. *Neuron* 13(2):325-38.

Franconi F, Miceli M, Alberti L, Seghieri G, De Montis M, Tagliamonte A. 1998. Further insights into the anti-aggregating activity of NMDA in human platelets. *Br. J. Pharmacol.* 124(1):35-40.

Franconi F, Miceli M, Demonstis M, Lupis Crisafi E, Bennardini F, Tagliamonte A. 1996. NMDA receptors play an anti-aggregating role in human platelets. *Thromb. Haemost.* 76(1):84-87.

Frenette P, Johnson R, Hynes R, Wagner D. 1995. Platelets roll on stimulated endothelium *in vivo*: an interaction mediated by endothelial P-selectin. *Proc. Natl. Acad. Sci. U.S.A.* 92(16):7450-4.

Freson K, De Vos R, Wittevrongel C, Thys C, Defoor J, Vanhees L, Vermylen J, Peerlinck K, Van Geet C. 2005. The *TUBB1* Q43P functional polymorphism reduces the risk of cardiovascular disease in men by modulating platelet function and structure. *Blood* 106(7):2356-62.

Fulcher C, Gardiner J, Griffin J, Zimmerman T. 1984. Proteolytic inactivation of human factor

VIII procoagulant protein by activated human protein C and its analogy with factor V. *Blood* 63(2):486-9.

Fulton D, Gratton J, Mccabe T, Fontana J, Fujio Y, Walsh K, Franke T, Papapetropoulos A, Sessa W. 1999. Regulation of endothelium-derived nitric oxide production by the protein kinase Akt. *Nature* 399(6736):597-601.

Furie B, Furie BC. 2005. Thrombus formation in vivo. *J. Clin. Invest.* 115(12):3355-62.

Gambaryan S, Kpbsar A, Rutoyatkina N, Herterich S, Geiger J, Smolenski A, Lohmann S, Walter U. 2010. Thrombin and collagen induce a feedback inhibitory signalling pathway in platelets involving dissociation of the catalytic subunit of PKA from an NF-kB-IkB complex. *J Biol. Chem.* M109.0077602 (epub)

Gao T, Newton A. 2002. The turn motif is a phosphorylation switch that regulates the binding of Hsp70 to protein kinase. *J Biol. Chem.* 277:31585-92.

Gao T, Toker A, Newton A. 2001. The carboxyl terminus of protein kinase C provides a switch to regulate its interaction with the phsophoinositide-dependent kinase, PDK-1. *J Biol. Chem.* 276(22):19588-96.

Geddis A, Linden H, Kaushansky K. 2002. Thrombopoietin: a pan-hematopoietic cytokine. *Cytokine & Growth Factor Rev*. 13:61-73.

Gee K, Brown K, Chen W-N, Bishop-Stewart J, Gray D, Johnson I. 2000. Chemical and physiological characterization of fluo-4 Ca^{2+} -indicator dyes. *Cell Calcium* 27(2):97-106.

Genever P, Skerry TM. 2001. Regulation of spontaneous glutamate release activity in osteoblastic cells and its role in differentiation and survival: evidence for intrinsic glutamatergic signalling in bone. *FASEB J*. 15(9):1586-8.

Genever PG, Wilkinson D, Patton A, Peet N, Hong Y, Mathur A, Erusalimsky J, Skerry T. 1999. Expression of a functional N-methyl-D-aspartate-type glutamate receptor by bone marrow megakaryocytes. *Blood* 93(9):2876-83.

Genever PG, Maxfield SJ, Kennovin GD, Maltman J, Bowgen CJ, Raxworthy MJ, Skerry TM. 1999b. Evidence for a novel glutamate-mediated signalling pathway in keratinocytes. *J. Invest. Dermatol.* 112:337-42

Gielen M, Retchless BS, Mony L, Johnson JW, Paoletti. 2009. Mechanism of differential control of NMDA receptor activity by NR2 subunits. *Nature* 459:703-7.

Giorgione J, Lin J-H, McCammon J, Newton A. 2006. Increased membrane affinity of the C1 domain of protein kinase C delta compensates for the lack of involvement of its C2 domain in membrane recruitment. *J Biol. Chem.* 281(3):1660-69.

Gitlin G, Bayer EA, Wilchek M. 1987. Studies on the biotin-binding site of avidin. *Biochem. J.* 242:923-26.

Gonzalez-Cadavid NF, Ryndin I, Vernet D, Magee TR, Rajfer J. 2000. Presence of NMDA receptor subunits in the male lower urogenital tract. *J. Androl.* 21(4):566-78.

Goto S, Kobayashi M, Murate T, Hotta T, Hagiwara M, Hoshino T, Hidaka H, Saito H. 1992. Thrombin-induced shape change in megakaryoblastic leukemic cells, MEG-01, is mediated by protein kinase C. *Thromb. Res.* 68(1):87-95.

Grabarek J, Raychowdhury M, Ravid K, Kent K, Newman P, Wares J. 1992. Identification and functional characterization of protein kinase C isozymes in platelets and HEL cells. *J. Biol. Chem.* 267(14):10011-17.

Graves J, Lewis S, Kooy N. 1998. Peroxynitrite-mediated vasorelaxation: evidence against the formation of circulating S-nitrosylation. *Am. J. Physiol*. 274:H1001-H1008.

Greenamyre JT, Penney Jr JB, Yound AB, D'Amato CJ, Hicks SP, Shoulson I. 1985. Alterations in L-glutamate binding in Alzheimer's and Huntington's diseases. *Science* 227:1496-99.

Griner E, Kazanietz, MG. 2007. Protein kinase C and other diacylglyceride effectors in cancer. *Nat. Rev. Cancer.* 7:281-94.

Grynkiewicz G, Poenie M, Tsein RY. 1985. A new generation of Ca^{2+} indicators with greatly improved fluorescent properties. *J. Biol. Chem.* 260(6):3440-50.

Gu Y, Publicover S. 2000. Expression of functional metabotropic glutamate receptors in primary cultured rat osteoblasts. *J Biol. Chem.* 275(44):34252-59.

Hagen I, Bjerrum O, Solum N. 1979. Characterization of human platelet proteins solubilized with Triton X-100 and examined by crossed immunoelectrophoresis. Reference patterns of extracts from whole platelets and isolated membranes. *Eur. J. Biochem*. 99(1):9-22.

Haidaris P, Francis C, Sporn L, Arvan D, Collichio F, Marder V. 1989. Megakaryocyte and hepatocyte origins of human fibrinogen biosynthesis exhibit hepatocyte-specific expression of gamma chain-variant polypeptides. *Blood* 74(2):743-50.

Hall J, Hicks T, McLennan H, Richardson T, Wheal H. 1979. The excitation of mammalian central neurones by amino acids. *J. Physiol.* 286:29-39.

Hansra G, Garcia-Paramio P, Prevostel C, Whelan R, Bornancin F, Parker P. 1999. Multisite dephosphorylation and desensitization of conventional protein kinase C isotypes. *Biochem. J.* 342(2):337-44.

Hao G, Derakhanshan B, Shi L, Campagne F, Gross S. 2006. SNOSID, a proteomic method for identification of cysteine S-nitrosylation sites in complex protein mixtures. *Proc. Natl. Acad. Sci. U.S.A.* 103(4):1012-17.

Hardingham G, Arnold F, Bading H. 2001. A calcium microdomain near NMDA receptors: on switch for ERK-dependent synapse-to-nucleus communication. *Nat. Neurosci.* 4(6):565-66.

Hardingham GE, Fukunaga Y, Bading H. 2002. Extrasynaptic NMDARs oppose synaptic NMDARs by triggering CREB shut-off and cell death pathways. *Nature Neurosci.* 5(5):405-14.

Harker L, Marzec U, Hunt P, Kelly A, Tomer A, Cheung E, Hanson S, Stead R. 1996.

Dose-response effects of pegylated human megakaryocyte growth and development factor on platelet production and function in nonhuman primates. *Blood* 88(2):511-21.

Harper AG, Sage SO. 2007. A key role for reverse Na^{+}/Ca^{2+} exchange influenced by the actin cytoskeleton in store-operated Ca^{2+} entry in human platelets: Evidence against the *de novo* conformational coupling hypothesis. *Cell Calcium.* 42(6):606-17.

Harper AG, Brownlow SL, Sage SO. 2009. A role for TRPV1 in agonist-evoked activation of human platelets. *J. Thromb. Haemost.* 7(2):330-38.

Hechler B, Lenain N, Marchese P, Vial C, Heim V, Freund M, Cazenave J, Cattaneo M, Ruggeri Z, Evans R et al. 2003. A role of the fast ATP-gated P2X1 cation channel in thrombosis of small arteries in vivo. *J. Exp. Med.* 198(4):661-67.

Hinoi E, Fujimori S, Takarada T, Taniura H, Yoneda Y. 2002. Facilitation of glutamate release by ionotropic glutamate receptors in osteoblasts. *Biochem. Biophys. Res. Commun*. 297(3):452-58.

Hitchcock IS. 2003. Functional activity of NMDA receptors on megakaryocytes.

Hitchcock I, Skerry T, MR H, Genever P. 2003. NMDA receptor-mediated regulation of human megakaryocytopoiesis. *Blood* 102(4):1254-9.

Hoffman R, Andersen H, Walker K, Krakover J, Patel S, Stamm M, Osborn S. 1996. Peptide, disulphide, and glycosylation mapping of recombinant human thrombopoietin from Ser1 to Arg246. *Biochemistry* 35(47):14849-61.

Hollman S, Heinemann S. 1994. Cloned glutamate receptors. *Annu. Rev. Neurosci*. 17:31-108.

Hong Y, Dumenil D, van der Loo B, Goncalves F, Vainchenker W, Erusalimsky J. 1998. Protein kinase C mediates the mitogenic action of thrombopoietin in c-mpl-expressing UT-7 cells. *Blood* 91(3):813-22.

Houamed K, Kuijper J, Gilbert T, Haldman B, O'Hara P, Mulvihill E, Almers W, Hagen F. 1991. Cloning, expression, and gene structure of a G protein-coupled receptor from rat brain. *Science* 252(5010):1318-21.

Hoxie J, Ahuja M, Belmonte E, Pizarro S, Parton R, Brass L. 1993. Internalization and recycling of activate thrombin receptors. *J Biol. Chem.* 268(18):13756-63.

Ikeda K, Araki K, Inoue Y, Yagi T, Azawa S, Mishina M. 1995. Reduced spontaneous activity of mice defective in the epsilon 4 subunit of the NMDA receptor channel. *Brain. Res. Mol. Brain. Res.* 33(1):61-71.

Ikemoto A, Bole D, Ueda T. 2003. Glycolysis and glutamate accumulation into synaptic vesicles. *J. Biol. Chem.* 278(8):5929-40.

Ishii T, Moriyoshi K, Sugihara H, Sakurada K, Kadotani H, Yokoi M, Akazawa C, Shigemoto R, Mizuno N, Masu M et al. . 1993. Molecular characterisation of the family of the *N*-methyl-D-aspartate receptor subunits. *J. Biol. Chem.* 268(4): 2836-43.

Italiano Jr J, Lecine P, Shivdasani R, Hartwig J. 1999. Blood platelets are assembled principally at

the ends of proplatelet processes produced by differentiated megakaryocytes. *J. Cell. Biol*. 147(6):1299-1312.

Italiano Jr J, Shivdasani R. 2003. Megakaryocytes and beyond: the birth of platelets. *J. Thromb. Haemost.* 1:1174-82.

Jaffrey S, Erdjument H, Ferris C, Tempst P, Snyder S. 2001. Protein S-nitrosylation: a physiological signal for neuronal nitric oxide. *Nat. Cell. Biol.* 3 (2):193-97.

Jaffrey S, Snyder S. 2001. The biotin switch method for the detection of *S*-nitrosylated proteins. *Science's STKE* 86:pl1-9.

Jamieson G, Agrawal A, Greco N, Tenner TJ, Jones G, Rice K, Jacobson A, White J, Tandon N. 1992. Phencyclidine binds to blood platelets with high affinity and inhibits their activity by adrenaline. *Biochem. J*. 285(Pt1):35-9.

Jang J. 1990. Ion permeation through 5-hydroxytryptamine-gated channels in neuroblastoma N18 cells. *J. Gen. Physiol.* 96(6):1177-98.

Jenkins B, Quilici C, Roberts A, Grail D, Dunn A, Ernst. 2002. Hematopoietic abnormalities in mice deficient in gp130-mediated STAT signalling. *Ex. Hematol*. 30(11):1248-56.

Jiang G, Giannone G, Critchley DR, Fukymoto E, Sheetz, 2003. Two-piconewton slip bond between fibronectin and the cytoskeleton depends on talin. *Nature* 424(6946):334-37.

Jiroušková M, Jaiswal JK, Coller BS. 2007. Ligand density dramatically affects integrin αIIbβ3-mediated platelet signalling and spreading. *Blood* 109(2):5260-69.

Jung G, Wang J, Wlodarski P, Barylko B, Binns D, Shu H, Yin H, Albanesi J. 2008. Molecular determinants of activation and membrane targeting of phosphoinositol 4-kinase IIβ. *Biochem. J.* 409:510-9.

Junt T, Schulze H, Chen Z, Massberg S, Goerge T, Krugger A, Wagner D, Graf T, Italiano Jr J, Shivdasani R, von Andrian UH. 2007. Dynamic visualisation of thrombopoiesis within bone marrow. *Science* 317:1767-70.

Kahn M, Nakanishi M, Shapiro M, Ishihara H, Coughlin S. 1999. Protease-activated receptors 1 and 4 mediate activation of human platelets by thrombin. *J. Clin. Invest.* 103(6):879-87.

Kahn M, Zheng Y, Huang W, Bigornia V, Zeng D, Moff S, Farese Jr R, Tam C, Coughlin S. 1998. A dual thrombin receptor system for platelet activation. *Nature* 394:690-94.

Kaluzhny Y, Yu G, Sun S, Toselli P, Nieswandt B, Jackson C, Ravid K. 2002. Bcl-xL overexpression in megakaryocytes leads to impaired platelet fragmentation. *Blood* 100(5):1670-78.

Kantrowitz JT, Javitt DC. 2010. N-methyl-D-aspartate (NMDA) receptor dysfunction or dysregulation: The final common pathway on the road to schizophrenia? *Brain. Res. Bull.* doi:10.1016/j.brainresbull.2010.04.006.

Kapur S, Seeman P. 2002. NMDA receptor antagonists ketamine and PCP have direct effects on the dopamine D_2 and serotonin $5HT_2$ receptors- implications for models of schizophrenia.

Mol. Psych. 7:837-44

Káradóttir R, Cavelier P, Bergersen L, Attwell D. 2005. NMDA receptors are expressed in oligodendrocytes and activated in ischaemia. *Nature* 438(7071):1162-1166.

Kato K, Kanaji T, Russell S, Kunicki TJ, Furihata K, Kanaji S, Marchese P, Reininger A, Ruggeri ZM, Ware J. 2003. The contribution of glycoprotein VI to stable platelet adhesion and thrombus formation illustrated by targeted gene deletion. *Blood* 102(5):1701-07.

Kaushansky K. 2005. The molecular mechanisms that control thrombopoiesis. *J. Clin. Invest.* 115(12):3339-47.

Kaushansky K, Broudy V, Lin N, Jorgensen M, McCarty J, Fox N, Zucker-Franklin D, Lofton-Day C. 1995. Thrombopoietin, the Mpl ligand, is essential for full megakaryocyte development. *Proc. Natl. Acad. Sci. U.S.A.* 1992(8):3234-38.

Kaushansky K, Lok S, Holly RD, Broudy VC, Lin N, Bailey MC, Forstrom JW, Buddle MM, Oort PJ, Hagen FS, Roth GJ, Papayannopoulou T, Foster DC. 1994. Promotion of megakaryocyte progenitor expansion and differentiation by the c-Mpl ligand thrombopoietin. *Nature* 369:568-571.

Kawa K. 1990. Voltage gated potassium and calcium currents in megakaryocytes dissociated from guinea pig bone marrow. *J. Physiol.* 431:187-206.

Kawada H, Ito T, Pharr P, Spyropoulos D, Watson D, Ogawa M. 2001. Defective Megakaryopoiesis and Abnormal Erythroid Development in Fli-1 Gene–Targeted Mice. *Int. J. Hematol*. 73(4):463-8.

Kendrick SJ, Dichter MA, Wilcox KS. 1998. Characterization of desensitization in recombinant *N*-methyl-*D*-aspartate receptors: comparison with native receptors in cultured hippocampal neurons. *Mol. Brain Res.* 57(1):10-20.

Kerrigan S, Gaur M, Murphy R, Shattil S, Leavitt A. 2004. Caspase-12: a developmental link between G-protein–coupled receptors and integrin αIIbβ3 activation. *Blood* 104(5):1327-34.

Ki N, Okano Y, Nozawa Y. 1996. Protein kinase C isozymes in human megakaryoblastic leukaemia cell line, MEG-01; possible involvement of the isozymes in the differentiation process of MEG-01 cells. *Br. J. Haematol.* 93(4):762-771.

Kikkawa U, Takai Y, Minakuchi R, Inohara S, Nishizuka Y. 1982. Calcium-activated, phospholipid-dependent kinase from rat brain. *J. Biol. Chem.* 257(22):13341-48.

Kim W-K, Choi Y-B, Rayudu PV, Das P, Asaad W, Arnelle DR, Stamler JS, Lipton. 1999. Attenuation of NMDA receptor activity and neurotoxicity by nitroxyl anion, NO^-. *Neuron* 24(2):461-69.

Klages B, Brandt U, Simon MI, Schultz G, Offermanns S. 1999. Activation of G_{12}/G_{13} results in shape change and Rho/Rho-kinase-mediated myosin light chain phosphorylation in mouse platelets. *J. Cell. Biol.* 144(4):745-54.

Kokkola T, Savinainen J, Monkkonen K, Retamal M, Laitinen J. 2005. S-nitrosothiols modulate G protein-coupled receptor signalling in a reversible and highly receptor-specific manner. BMC Cell Biol. 6(1):21-37.

Konopatskaya O, Gilio K, Harper M, Zhao Y, Cosemans J, Karim Z, Whiteheart S, Molkentin J, Verkade P, Watson S et al. 1999. PKCα regulates platelet granule secretion and thrombus formation in mice. *J. Clin. Invest.* 119(2):399-407.

Krug MS, Berger SL. 1987. First-strand cDNA synthesis primed with oligo(dT). *Methods Enzymol.* 152:316-25

Krupp JJ, Vissel B, Heinemann SF, Westbrook. 1996. Calcium-dependent inactivation of recombinant *N*-methyl-*D*-aspartate receptors is NR2 subunit specific. *Mol. Pharmacol.* 50(6):1680-88.

Ku H, Yonemura Y, Kaushansky K, Ogawa M. 1996. Thrombopoietin, the ligand for the Mpl receptor, synergizes with steel factor and other early acting cytokines in supporting proliferation of primitive hematopoietic progenitors of mice. *Blood* 87(11):4544-51.

Kumari M, Ticku MK. 1998. Ethanol and regulation of the NMDA receptor subunits in fetal cortical neurons. *J. Neurochem.* 70(4):1467-76.

Kutsuwada T, Kashiwabuchi N, Mori H, Sakimura K, Kushiya E, K A, Meguro H, Masaki H, Kumanishi T, Arakawa M, Mishina M. 1992. Molecular diversity of the NMDA receptor channel. *Nature* 358(6381):36-41.

Lacabaratz-Porret C, Launay S, Corvazier E, Bredoux R, Papp B, Enouf J. 2000. Biogenesis of endoplasmic reticulum proteins involved in Ca^{2+} signalling during megakaryocytic differentiation: an in vitro study. *Biochem. J.* 350(Pt3):723-34.

Lambert M, Rauova L, Bailey M, Sola-Visner M, Kowalska M, Poncz M. 2007. Platelet factor 4 is a negative autocrine *in vivo* regulator of megakaryopoiesis: clinical and therapeutic implications. *Blood* 110(4):1153-60.

Landry P, Plante I, Ouellet D, Perron M, Rousseau G, Provost P. 2009. Existence of a microRNA pathway in anucleate platelets. *Nat. Struct. Mol. Biol*. 16(9):961-66.

Larson M, Watson S. 2008. Regulation of proplatelet formation and platelet release by integrin αIIbβ3. *Blood* 108(5):1509-14.

Laurie DJ, Seeburg PH. 1994. Ligand affinities at recombinant N-methyl-D-aspartate receptors depend on subunit composition. *Eur. J. Pharmacol.* 268(3):335-45.

Lavezzari G, McCallum J, Dewey CM, Roche KW. 2004. Subunit-specific regulation of NMDA receptor endocytosis. *J. Neuroscii.* 24(28):6383-91.

Le Good JA, Zeigler WH, Parekh DB, Alessi DR, Cohen P, Parker PJ. 1998. Protein kinase C isotypes controlled by phosphoinositide 3-kinase through the protein kinase PDK-1. *Science* 281(5385):2042-5.

Legrande P, Rosenmund C, Westbrook G. 1993. Inactivation of NMDA channels in cultured

hippocampal neurons by intracellular calcium. *J. Neurosci* 13(2):674-84.

Lehmann J, Schneider J, McPherson S, Murphy DE, Bernard P, Tsai C, Bennett OA, Pastor G, Steel DJ, Boehm C, Cheney DL, Uebman JM, Williams M, Wood PL. 1987. CPP, a selective N-methyl-D-aspartate (NMDA)-type receptor antagonist: Characterization *in vitro* and *in vivo*. *J. Pharmacol. Exp. Ther.* 420(3):737-46.

Lei S, Pan Z-H, Aggarwal S, Chen H-SV, Hartman J, Sucher N, Lipton S. 1992. Effect of nitric oxide production on the redox modulatory site of the NMDA receptor-channel complex. *Neuron* 8:1087-1099.

Léon C, Hechler B, Freund M, Eckly A, Vial C, Ohlmann P, Dierich A, LeMeur M, Cazenave J-P, Gachet C. 1999. Defective platelet aggregation and increased resistance to thrombosis in purinergic $P2Y_1$ receptor-null mice. *J. Clin. Invest.* 104(12):1731-37.

Leung JC, Travis BR, Verlander JW, Snadhu SK, Yang S-G, Zea AH, Weiner D, Silverstein DM. 2002. Expression and development regulation of the NMDA receptor subunits in the kidney and cardiovascular system. *Am. J. Physiol-Reg. I.* 283:964-71.

Li J, Xia Y, Kuter D. 1999. Interaction of thrombopoietin with the platelet c-mpl receptor in plasma: binding, internalization, stability and pharmacokinetics. *Br. J. Haematol.* 106(2):345-56.

Li L, Sengupta A, Haque N, Grundke-Iqbl I, Iqbal K. 2004. Memantine inhibits and reverses the Alzheimer type abnormal hyperphosphorylation of tau and associated neurodegeneration. *FEBS. Lett.* 566(1-3):261-69.

Li Y, Erzurumlu RS, Chen C, Jhaveri S, Tonega S. 1994. Whisker-related neuronal patterns fail to develop in the trigeminal brainstem nuclei of NMDAR1 knockout mice. *Cell* 76(3):427-37.

Linden H, Kaushansky K. 2000. The glycan domain of thrombopoietin enhances its secretion. *Biochemistry* 39(11):3044-51.

Liu C, Hermann T. 1978. Characterisation of ionomycin as a calcium ionophore. *J Biol. Chem.* 253(17):5892-94.

Lombardi G, Dianzani C, Miglio G, Canonico PL, Fantozzi R. 2001. Characterisation of ionotropic glutamate receptors in human lymphocytes. *Br. J. Pharmacol.* 133(6):936-44.

Luby ED, Choen BD, Rosenbaum G, Gorriel JS, Kelly R. 1959. Study of a new schizophrenic-like drug: Sernyl. *Arch. Neurol. Psychiat.* 81:363-69.

Lucas D, Newhouse J. 1957. The toxic effect of soodium L-glutamate on the inner layers of the retina. *AMA. Arch. Opthalmol*. 58(2):193-201.

Lumelsky N, Schwarta B. 1997. Protein kinase C in erythroid and megakaryocytic differentiation: possible role in lineage determination. *Biochim. Biophys. Acta* 1358(1):79-92.

Macaulay IC, Tijssen MR, Thijssen-Timmer DC, Gusnanto A, Steward M, Burns P, Langford CF, Ellis PD, Dudbridge F, Zwaginga J-J, Watkins NA, van der Schoot E, Ouwehand WH. 2007. Comparative gene expression profiling of in vitro differentiated megakaryocytes and

erythroblasts identifies novel activatory and inhibitory platelet membrane proteins. *Blood* 109(8):3260-69.

MacFarlane S, Seatter M, Kanke T, Hunter G, Plevin R. 2001. Protease-activated receptors. *Pharmacol. Rev*. 53(2):245-82.

MacKenzie A, Mahaut-Smith M, Sage SO. 1996. Activation of receptor-operated cation channels via P2X1 not P2T purinoceptors in human platelets. *J. Biol. Chem.* Vol. 271(6):2879-81.

MacKenzie A. 1996. Ion channels in human platelets.

Madry C, Betz H, Geiger, JRP L, B. 2008. Supralinear potentiation of NR1/ NR3A excitatory glycine receptors by Zn^{2+} and NR1 antagonist. *Proc. Natl. Acad. Sci. U.S.A.* 105(34):12563-68.

Mahaut-Smith MP, Hussain JF, Mason MJ. 1999. Depolarization-evoked Ca^{2+} release in a non-excitable cell, the rat megakaryocyte. *J. Physiol.* 515(2):385-90.

Majerus P, Smith M, Clamon G. 1969. Lipid metabolism in human platelets. I. Evidence for a complete fatty acid synthesising system. *J. Clin. Invest.* 48(1):156-64.

Majka M, Janowska A, Rataczak J, Kowalska MA, Vilaire G, Pan ZK, Honczarenko M, Marquez LA, Poncz M, Ratajczak MZ. Stromal-derived factor 1 and thrombopoietin regulate distinct aspects of human megakaryopoiesis. *Blood* 96(13):4142-51.

Mason D, Suva L, Genever P, Patton A, Steuckle S, Hillam R, Skerry T. 1997. Mechanically regulated expression of a neural glutamate transporter in bone: a role for excitatory amino acids as osteotropic agents? *Bone* 20(3):199-205.

Masu M, Tanabe Y, Tsuchida K, Shigemoto R, Nakanishi S. 1991. Sequence and expression of a metabotropic glutamate receptor. *Nature* 349:760-65.

Matsui T, Sekiguchi, M, Hashimoto A, Tomita U, Nishikawa T, Wada K. 1995. Functional comparison of D-serine and glycine in rodents: the effect of cloned NMDA receptors and the extracellular concentration. *J. Neurochem.* 65(1):454-58.

Mayer M, Vyklivky Jr L, Clements J. 1989. Regulation of NMDA receptor desensitization in mouse hippocampal neurons by glycine. *Nature* 338(6214):425-7.

McBain C, Mayer M. 1994. *N*-methyl-*D*-aspartic acid receptor structure and function. *Physiol. Rev.* 74(3):723-60.

McIlhinney R, Le Bourdellès B, Molnár E, Tricaud N, Streit P, Whiting P. 1998. Assembly, intracellular targeting and cell surface expression of the human *N*-methyl-*D*-aspartate receptor subunits NR1a and NR2A in transfected cells. *Neuropharmacology* 37(10-11):1355-67.

Meacci E, Vasta V, Farnararo M, Bruni P. 1995. Fructose 2, 6-bisphosphate metabolism during megakaryocytic differentiation of K562 and MEG-01 cells. *Mol. Cell. Biochem.* 156:125-130.

Medina I, Filippova N, Charton G, Rougeole S, Ben-Ari Y, Khrestchatisk M, Bregestovski P. 1995.

Calcium-dependent inactivation of heteromeric NMDA receptor-channels expressed in human embryonic kidney cells. *J. Physiol.* 482(3):567-73.

Meguro H, Mori H, Araki K, Kushiya E, Kutsuwada T, Yamazaki M, Kumanishi T, Arakawa M, Sakimura K, Mishina M. 1992. Functional characterization of a heteromeric NMDA receptor channel expressed from cloned cDNAs. *Nature* 357:70-74.

Melemed A, Ryder J, Vik T. 1997. Activation of the mitogen-activated protein kinase pathway is involved in and sufficient for megakaryocytic differentiation of CMK cells. *Blood* 90(9):3462-70.

Mellion B, Ignarro L, Myers C, Ohlstein E, Ballot B, Hyman A, Kadowitz P. 1983. Inhibition of human platelet aggregation by S-nitrosothiols. Heme-dependent activation of soluble guanylyl cyclase and stimulation of cyclic GMP accumulation. *Mol. Pharmacol.* 23(3):653-64.

Merezhinskaya N, Ogunwuyi S, Fishbein W. 2006. Expression of monocarboxylate transporter 4 in human platelets, leukocytes, and tissues assessed by antibodies raised against terminal versus pre-terminal peptides. *Mol. Genet. Metab*. 87(2):152-161.

Merika M, Orkin S. 1993. DNA-binding specificity of GATA family transcription factors. *Mol. Cell. Biol.* 13(7):3999-4010.

Michelson A, Benoit S, Furman M, Breckwoldt W, Rohrer M, Barnard M, Loscalzo J. 1996. Effects of nitric oxide/ endothelium-derived relaxing factor on platelet surface glycoproteins. *Am. J. Physiol.* 270(5 Pt2):H1640-48.

Micu I, Jiang Q, Coderre E, Ridsdale A, Zhang L, Woufle J, Yin X, Trapp BD, McRoy JE, Rehak R, Zamponi GW, Wang W, Stys PK. 2006. NMDA receptors mediate calcium accumulation in myelin during chemical ischaemia. *Nature* 439(7079):988-992.

Minamiguchi H, Kimura T, Urata Y, Miyazaki H, Bamba T, Abe T, Sonoda Y. 2001. Simultaneous signalling through c-mpl, c-kit and CXCR4 enhances the proliferation and differentiation of human megakaryocyte progenitors: possible roles of the PI3-K PKC and MAPK pathways. *Br. J. Haematol.* 115(1):175-85.

Minkeviciene R, Banerjee P, Tanila H. 2004. Memantine improves spatial learning in a transgenic mouse model of Alzheimer's disease. *J. Pharmacol. Exp. Ther.* 311(2):677-82.

Miura S, Li C, Cao Z, Wang H, Wardell M, Sadler J. 2000. Interaction of von Willebrand Factor domain A1 with platelet glycoprotein Ibα-(1-289). *J Biol. Chem.* 275(11):7539-46.

Mohn AR, Gainetdinov RR, Caron MG, Koller BH. 1999. Mice with reduced NMDA receptor expression display behaviours related to schizophrenia. *Cell* 98(4):427-36.

Molino M, Bainton D, Hoxie J, Coughlin S, Brass L. 1997. Thrombin receptors on human platelets. Initial localisation and subsequent redistribution during platelet activation. *J. Biol. Chem.* 272(9):6011-17.

Molńar E, Váradi A, McIlhinney J. Ashcroft SJH. 1995. Identification of functional ionotropic

glutamate receptor proteins in pancreatic β-cells and in islets of Langerhans. *FEBS Lett.* 371:253-57.

Monyer H, Burnashev N, Laurie DJ, Sakmann B, Seeburg PH. 1994. Developmental and regional expression in the rat brain and functional properties of four NMDA receptors. *Neuron* 12(3):529-40.

Monyer H, Sprengel R, Schoepfer R, Herb A, Higuchi M, Lomeli H, Burnashev N, Sakmann B, Seeburg P. 1992. Heteromeric NMDA receptors: molecular and functional distinction of subtypes. *Science* 256(5060):1217-21.

Monzoni O, Bockaert J. 1993. Nitric oxide synthase endogenously modulates NMDA receptors. *J. Neurochem.* 61(1):368-70.

Morimoto R, Uehara S, Yatsuhiro S, Juge N, Hua Z, Senoh S, Mizoguchi T, Ninomiya T, Udagawa N, Omote H, Yamamoto A, Edwards RH, Moriyama Y. 2006. Secretion of L-glutamate from osteoclasts through transcytosis. *EMBO J.* 25(18):4175-86.

Morrell C, Sun H, Ikeda M, Beique J, Swaim A, Mason E, Martin T, Thrompson L, Gozen O, Ampagoomain D, Sprengel R, Rothstein J, Faraday N, Huganir R, Lowenstein CJ. 2008. Glutamate mediates platelet activation through the AMPA receptor. *J. Exp. Med.* 205(3):575-84.

Morris GF, Bullock R, Marshall SB, Marmarou A, Maas A, Marchall LF. 1999. Failure of the competitive *N*-methyl-*D*-aspartate antagonist Selfotel (CGS 19755) in the treatment of severe head injury: results of two phase III clinical trials. *J. Neurosurg.* 91(5):737-43.

Murate T, Hotta T, Tsushita K, Suzuki M, Yoshida T, Saga S, Saito H, Yoshida S. 1991. Aphidicolin, an inhibitor of DNA replication, blocks the TPA-induced differentiation of a human megakaryoblastic cell line, MEG-01. *Blood* 78(12):3168-77.

Muto T, Feese M, Shimada Y, Kudou Y, Okamoto T, Ozawa T, Tahara T, Ohashi H, Ogami K, Kato T, Miyazaki H, Kuroki R. 2000. Functional analysis of the C-terminal region of recombinant human thrombopoietin. C-terminal region of thrombopoietin is a 'shuttle' peptide to help secretion. *J Biol. Chem.* 275(16):12090-4.

Nagata KI, Okano Y, Nozawa Y. 1996. Protein kinase C isozymes in human megakaryoblastic leukaemia cell line, MEG-01; possible involvement of the isozymes in the differentiation process of MEG-01 cells. *Br. J. Haematol.* 93(4):762-71

Nagata Y, Nagahisa H, Aida Y, Okutomi K, Nagasawa T, Todokoro K. 1995. Thrombopoietin induced megakaryocyte differentiation in hematopoietic progenitor FDC-P2 cells. *J. Biol. Chem.* 270(34):19673-75.

Neben TY, Loebelenz J, Hayes L, McCarthy K, Stoudemire J, Schaub R, Goldman SJ. 1993. Recombinant human interleukin-11 stimulates megakaryocytopoiesis and increases peripheral platelets in normal and spleenectomized mice. *Blood* 81(4):901-08.

Newton A. 2003. Regulation of the ABC kinases by phosphorylation: protein kinase C as a

paradigm. *Biochem. J*. 370:361-71.

Newton A, Nalefski E. 2001. Membrane binding kinetics of protein kinase C βII mediated by the C2 domain. *Biochemistry* 40:13216-29.

Ni H, Denis C, Subbarao S, Degen J, Sato T, Hynes R, Wagner D. 2000. Persistence of platelet thrombus formation in arterioles of mice lacking both von Willebrand factor and fibrinogen. *J. Clin. Invest.* 106(3):385-92.

Nicoll D, Longoni S, Philipson. 1990. Molecular cloning and functional expression of the cardiac sarcolemmal Na(+)-Ca^{2+} exchanger. *Science* 250(4980):562-565.

Niemann S, Kanki H, Fukui Y, Takao K, Fukaya M, Hynynen N, Churchill MJ, Shefner JM, Bronson RT, Brown Jr Watanabe M, Miyakawa T, Itohara S, Hayashi Y. 2007. Genetic ablation of NMDA receptor subunit NR3B in mouse reveals motoneuronal and nonmotoneuronal phenotypes. *Eur. J. Neurosci.* 26(6):1407-20.

Niiya K, Hodson E, Bader R, Byers-Ward V, Koziol J, Plow E, Ruggeri Z. 1987. Increased surface expression of the membrane glycoprotein IIb/IIIa complex induced by platelet activation. Relationship to the binding of fibrinogen and platelet aggregation. *Blood* 70(2):475-83.

Nishi M, Hinds H, Lu H-P, Kawata M, Hayashi Y. 2001. Motoneuron-specific expression of NR3B, a novel NMDA-type glutamate receptor subunit that works in a dominant-negative manner. *J. Neurosci* 21(RC185):1-6.

Oberpreiler N, Roberts W, Riba R, Graham A, Homer-Vanniansinkam S, Naseem K. 2007. Cyclic GMP-independent inhibition of integrin αIIb βIIIa-mediated platelet adhesion and outside-in signalling by nitric oxide. *FEBS. Lett.* 581(7):1529-34.

Oblak M, Prezelj A, Pecar S, Solmajer T. 2004. Thiol-reactive clenbuterol analogues conjugated to bovine serum albumin. *J. Biosci.* 59(11-12):880-86.

Ogilvy S, Metcalf D, Print C, Bath M, Harris A, Adams J. 1999. Constitutive bcl-2 expression throughout the haematopoietic compartment affects multiple lineages and enhances progenitor cell survival. *Proc. Natl. Acad. Sci. U.S.A.* 96(26):14943-48.

Ogura M, Morishima Y, Ohno R, Kato Y, Hirabayashi N, Nagura H, Saito H. 1985. Establishment of a novel human megakaryoblastic leukemia cell line, MEG-01, with positive Philadelphia chromosome. *Blood* 66(6):1384-92.

Ogura M, Morishima Y, Okamura M, Hotta T, Takamoto S, Ohna, R, Hiabayashi N, Nagura H, Saito H. 1988. Functional and morphological differentiation induction of a human megakaryoblastic leukaemia cell line (MEG-01s) by phorbol diesters. *Blood* 72(1):49-60.

Ohno S, Akita Y, Konno Y, Imajoh S, Suzuki K. 1988. A novel phorbol ester receptor/ kinase, nPKC, distantly related to the protein kinase C family. *Cell* 53(5):731-41.

Olney J, Ho O, Rhee V. 1971. Cytotoxic effects of acidic and sulfur containing amino acids on the infant mouse central nervous system. *Exp. Brain. Res*. 14(1):61-70.

Olney J, Sharpe L. 1969. Brain lesions in an infant rhesus monkey treated with monosodium

glutamate. *Science* 166(903):386-8.

Ono Y, Fujii T, Ogita K, Kikkawa U, Igarashi K, Nishizuka Y. 1989. Protein kinase C ζ subspecies from rat brain: Its structure, expression and properties. *Proc. Natl. Acad. Sci. U.S.A.* 86(9):3099-103

Orcutt S, Krishnaswamy S. 2004. Binding of substrate in two conformations to human prothrombinase drives consecutive cleavage at two sites in prothrombin. *J. Biol. Chem.* 279(52):54927–36.

Ouwehand WH. 2007. Platelet genomics and the risk of atherothrombosis. *J. Thromb. Haemost.* 5(Suppl.1):188-95.

Pang L, Weiss M, Poncz M. 2005. Megakaryocyte biology and related disorders. *J. Clin. Invest.* 115(12):3332-38.

Pasquet J-M, Gross B, Gratacap M-P, Quek L, Pasquet S, Payrastre B, van W, G, Mountford J, Watson S. 2000. Thrombopoietin potentiates collagen receptor signalling in platelets through a phosphatidylinositol 3-kinase-dependent pathway. *Blood* 95(11):3429-34.

Patel S, Hartwig J, Italiano Jr J. 2005a. The biogenesis of platelets from megakaryocyte proplatelets. *J. Clin. Invest.* 115(12):3348-54.

Patel S, Richardson J, Schultze H, Kahle E, Galjart N, Drabek K, Shivdasani R, Hartwig J, Italiano Jr J. 2005b. Differential roles of microtubule assembly and sliding in proplatelet formation by megakaryocytes. *Blood* 106(13):4076-85.

Patton AJ, Genever PG, Birch MA, Suva LJ, Skerry TM. 1998. Expression of an *N*-methyl-*D*-aspartate-type receptor by human and rat osteoblasts and osteoclasts suggest a novel glutamate signalling pathway in bone. *Bone* 22(6):645-49.

Peeters M, Gunthorpe MJ, Strijbos PJLM, Goldsmith P, Upton N, James MF. 2007. Effects of pan- and subtype-selective *N*-methyl-*D*-aspartate receptor antagonists on cortical spreading depression in the rat: therapeutic potential for migraine. *J. Pharmacol. Exp. Ther.* 321(2):564-72.

Peng M, Li H, Wu L, Zheng Q, Chen Y, G W. 2005. Porous poly(vinylidene fluoride) membrane with highly hydrophobic surface. *J. App. Polym. Sci.* 98(3):1358-63.

Perez-Otano I, Schulteis C, Contractor A, Lipton S, Trimmer J, Sucher N, Heinemann S. 2001. Assembly with the NR1 subunit is required for surface expression of NR3A-containing NMDA receptors. *J. Neurosci.* 21(4):1228-37.

Porter RHP, Greene JG, Higgins Jr DS, Greenamyre JT. 1994. Polysynaptic regulation of glutamate receptors and mitochondrial enzyme activities in the basal ganglia of rats with unilateral dopamine depletion. *J. Neurosci.* 14(11):7192-99.

Qian A, Johnson J. 2006. Permeant ion effects on external Mg^{2+} block of NR1/2D NMDA receptors. *J. Neurosci.* 26(42):10899-910.

Quesenberry PJ, Ihle JN, McGrath E. 1985. The effect of interleukin 3 and GM-CSA-2 on

megakaryocyte and myeloid clonal colony formation. *Blood* 65(1):214-17.

Radley J, Haller J. 1983. Fate of senescent megakaryocytes in the bone marrow. *Br. J. Haematol.* 53(1):277-87.

Rameau GA, Chiu L-Y, Ziff EB. 2003. NMDA receptor regulation of nNOS phosphorylation and induction of neuron death. *Neurobiol. Aging* 24(8):1123-33.

Raslova H, Komura E, Le Couédic JP, Larbret F, Debili N, Feunteun J, Danos O, Albagli O, Vainchenker W, Favier R. 2004. *FLI1* monoallelic expression combined with its hemizygous loss underlies Paris-Trousseau/ Jacobson thrombopenia. *J. Clin. Invest.* 114(1):77-87.

Raslova H, Baccini V, Loussaief L, Comba B, Larghero J, Debili V, W. 2006. Mammalian target of rapamycin (mTOR) regulates both proliferation of megakaryocyte progenitors and late stages of megakaryocyte differentiation. *Blood* 107(6):2303-10.

Ricci A, Bronzetti E, Mannino F, Mignini F, Morosetti C, Tayebati SK, Amenta F. 2001. Dopamine receptors in human platelets. *Arch. Pharmacol.* 363:376-82.

Richardson J, Shivdasani R, Boers C, Hartwig J, Italiano Jr J. 2005. Mechanisms of organelle transport and capture along proplatelets during platelet production. *Blood* 106(13):4066-75.

Richardson P, Kaushansky K. 2001. Actin reorganisation and proplatelet formation in murine megakaryocyte: the role of protein kinase C. *Blood* 97(1):154-61.

Robinson BE, McGrath HE, Quesenberry PJ. 1987. Recombinant murine granulocyte macrophage colony-stimulating factor has megakaryocyte colony-stimulating activity and augments megakaryocyte colony stimulation by interleukin 3. *J. Clin. Invest.* 79(6):1648-52.

Roche KW, Standley S, MacCallum J, Dune LC, Ehlers MD, Wenthold RJ. 2001. Molecular determinants of NMDA receptor internalization. *Nat. Neurosci.* 4(8):794-802.

Romijn R, Bouma B, Wuyster W, Gros P, Kroon J, Sixma J, Huizinga E. 2001. Identification of the collagen-binding site of the von Willebrand Factor A3-domain. *J. Biol. Chem.* 276(13):9985-91.

Rosenmund C, Westbrook G. 1993. Rundown of N-methyl-D-aspartate channels during whole-cell recording in rat hippocampal neurons: role of Ca^{2+} and ATP. *J. Physiol.* 470(1):705-29.

Rosenmund C, Westbrook G. 1993b. Calcium-induced actin depolymerization reduces NMDA channel activity. *Neuron* 10(5):805-14.

Ruggeri Z. 2007. The role of von Willebrand factor in thrombus formation. *Thromb. Res.* 120:55-59.

Saito M, Takada K, Yamada T, Fujimoto J. 1996. Overexpression of granulocyte colony-stimulation factor in vivo decreases the level of polyploidization of mouse bone marrow megakaryocytes. *Stem Cells* 14(1):124-31.

Sase K, Michel T. 1995. Expression of constitutive endothelial nitric oxide synthase in human

blood platelets. *Life Sci*. 57(22):2049-55.

Sato T, Fuse A, Eguchi M, Hayashi Y, Ryo R, Adachi M, Kishimoto Y, Teramura M, Mizoguchi H, Shima Y, Komori I. Sunami S; Okomoto Y, Nakajima. 1989. Establishment of a human leukaemic cell line (CMK) with megakaryocytic characteristics from a Down's syndrome patient with acute megakaryoblastic leukaemia. *Br. J. Haematol.* 72(2):184-190.

Schatzmann H. 1966. ATP-dependent Ca^{2+} extrusion from human red cells. *Experimentia Basel* 22(6):364-65.

Scheid M, Schubert K, Duronio V. 1999. Regulation of bad phosphorylation and association with Bl-x(L) by the MAP/Erk kinase. *J Biol. Chem.* 274(43):31108-13.

Schipke CG, Ohlemeyer C, Matyash M, Nolte C, Kettenmann H, Kirchhoff F. 2001. Astrocytes of the mouse neocortex express functional *N*-methyl-*D*-aspartate receptors. *FASEB J.* 16(2):1270-72.

Schliwa M, Nakamura T, Porter K, Euteneuer U. 1984. A tumor promoter induces rapid and coordinate reorganiszation of actin and vinculin in cultured cells. *J. Cell. Biol*. 99(3):1045-59.

Schmitz J, Weissenbach M, Haan S, Heinrich P, Schaper F. 2000. SOCS3 exerts its inhibitory function on interleukin-6 signal transduction through the SHP2 recruitment site of gp130. *J Biol. Chem.* 275(17):12848-56.

Schorge S, Colquhoun D. 2003. Studies of NMDA receptor function and stoichiometry with truncated and tandem subunits. *J. Neurosci.* 23(4):1151-58.

Schuler T, Mesic I, Madry C, Bartholomaus I, Laube B. 2008. Formation of NR1/NR2 and NR1/NR3 hetero-dimers constitutes the initial step in *N*-methyl-*D*-aspartate receptor assembly. *J. Biol. Chem.* 283(1):37-46.

Shad KF. 2006. Effect of D-serine on the serotonin receptors of human platelets. *Exp. Brain. Res.* 173(2):353-56.

Shapiro M, Weiss E, Faruqi T, Coughlin S. 2000. Protease-activated receptors 1 and 4 are shut off with distinct kinetics after activation by thrombin. *J Biol. Chem.* 275(33):25216-21.

Sheu J, Fong T, Liu, CM, Shen M, Chen T, Chang Y, Lu M, Hsiao G. 2004. Expression of matrix metalloproteinase-9 in human platelets: regulation of platelet activation in in vitro and in vivo studies. *Br. J. Pharmacol*. 143(1):193-201.

Shidasani R, Fujiwara Y, McDevitt M, Orkin S. 1997. A lineage-selective knockout establishes the critical role of transcription factor GATA-1 in megakaryocyte growth and platelet development. *EMBO J*. 16(13):3965-73.

Sim ATR, Herd L, Proctor DT, Baldwin ML, Meunier FA, Rostas JAP. 2006. High throughput analysis of endogenous glutamate release using a fluorescence plate reader. *J. Neurosci. Methods* 153(1):43-47.

Simon RP, Swan JH, Griggiths T, Meldrum BS. 1984. Blockade of N-methyl-D-aspartate

receptors may protect against ischemic damage in the brain. *Science* 226(4647):850-52.

Simpson A. 2005. Calcium signalling protocols, Chapter 1 Fluorescent measurement of $[Ca2+]_i$: Basic practical considerations.

Sitnicka E, Lin N, Priestley G, Fox N, Broudy V, Wolf N, Kaushansky K. 1996. The effect of thrombopoietin on the proliferation and differentiation of murine hemopoietic stem cells. *Blood* 87(12):4998-5005.

Skaer R, Emmines J, Skaer H. 1979. The fine ultrastructure of cell contacts in platelet aggregation. *J. Ultrastruct. Res*. 69(1):28-42.

Skerry TM, Genever PG. 2001. Glutamate signalling in non-neuronal tissues. *Trends Pharmacol. Sci.* 22(4):174-81.

Skoda R, Seldin D, Chiang M, Peichel C, Vogt T, Leder. 1993. Murine c-mpl: a member of the hematopoietic growth factor receptor superfamily that transduces a proliferative signal. *EMBO J.* 12(7):2645-53.

Smothers CT, Woodward JJ. 2009. Expression of glycine-activated diheteromeric NR1/NR3 receptors in human embryonic kidney 293 cells is NR1 splice variant-dependent. *J. Pharmacol. Exp. Therapeut.* 331(3):975-84.

Stahl N, Boulton T, Farruggella T, Ip N, Davie S, Witthuhn B, Quelle F, Silvennoninen O, Barieri G, Pellegrini S. 1994. Association and activation of Jak-Tyk kinases by CNTF-LIF-OSM-IL-6 beta receptor components. *Science* 263:89-92.

Sucher N, Akbarian S, Chi C, Leclerc C, Awobuluyi M, Deitcher D, Wu M, Yuan J, Jones E, Lipton. 1995. Developmental and regional expression pattern of a novel NMDA receptor-like subunit (NMDAR-L) in the rodent brain. *J. Neurosci.* 15(10):6509-20.

Sun H, Swaim A, Herrera J, Becker D, Becker L, Srivastava K, Thrompson L, Shero M, Perez-Tamayo A, Sukitipat B, Mathias R, Contractor A, Faraday N, Morrell CN. 2009. Platelet kainate receptor signalling promotes thrombosis by stimulating cyclooxygenase activation. *Circ. Res*. 105(6):595-603.

Szalai G, LaRue A, Watson D. 2006. Molecular mechanisms of megakaryopoiesis. *Cell. Mol. Life Sci.* 63(21):2460-76.

Tanabe Y, Masu M, Ishii T, Shigemoto R, Nakanishi S. 1992. A family of metabotropic glutamate receptors. *Neuron* 8(1):169-79.

Thompson CJ, Schilling T, Howard MR, Genever PG. 2010. SNARE-dependent glutamate release in megakaryocytes. *Exp. Haematol.* DOI:10.1016/j.exphem.2010.03.11.

Thon JN, Devine DV. 2007. Translation of glycoprotein IIIa in stored blood platelets. *Transfusion* 47(12):2269-70.

Toth-Zsamboki E, Oury C, Cornelissen H, Vos D, Vermylem J, Hoylaerts M. 2003. P2X1-mediated ERK2 activation amplifies the collagen-induced platelet secretion by enhancing myosin light chain kinase activation. *J. Biol. Chem.* 278(47):46661-67.

Towbin H, Staehelint T, Gordon J. 1979. Electrophoretic transfer of proteins from polyacrylamide gels to nitrocellulose sheets: Procedure and some applications. *Proc. Natl. Acad. Sci. U.S.A* 76(9):4350-54.

Tracey P, Mann K. 1983. Prothombinase complex assembled on the platelet surface is mediated through the 74, 000-dalton component of factor Va. *Proc. Natl. Acad. Sci. U.S.A* 80(8):2380-84.

Trejo J, Hammes S, Coughlin S. 1998. Termination of signaling by protease-activated receptor-1 is linked to lysosomal sorting. *Proc. Natl. Acad. Sci. U.S.A*. 95(23):13698-702.

Tremolizzo L, DiFrancesco JC, Rodriguez-Menendez V, Sirtori E, Longoni M, Cassetti A, Bossi M, El Mestikawy S, Cavaletti G, Ferrarese C. 2006. Human platelets express the synaptic markers VGLUT1 and 2 and release glutamate following aggregation. *Neurosci. Letts.* 404:626-5.

Tsai F-Y, G K, Kuo F, Weiss M, Chen J, Rosenblatt M, Alt F, Orkin S. 1994. An early heamatopoietic defect in mice lacking the transcription factor GATA-2. *Nature* 371(6494)221-26.

Tsang A, Fujiwara Y, Hom D, Orkin S. 1998. Failure of megakaryopoiesis and arrested erythropoiesis in mice lacking the GATA-1 transcriptional cofactor FOG. *Genes. Dev*. 12:1176-88.

Tsikas D, Ikic M, Tewes K, Kaida M, Frolich J. 1999. Inhibition of platelet aggregation by S-nitroso-cysteine via cyclic GMP-independent mechanisms: evidence of inhibition of thromboxane A2 synthesis in human blood platelets. *FEBS Lett*. 442(2-3):162-66.

Tymvios C, Moore C, Jones S, Solomon A, Sanz-Rosa D, Emerson M. 2009. Platelet aggregation responses are critically regulated *in vivo* by endogenous nitric oxide but not by endothelial nitric oxide synthase. *Br. J. Pharmacol.* 158(7):1735-42.

Vainchenker V, Deschamps J, Bastin J, Guichard J, Titeux M, Breton-Gorius J, McMicheal A. 1982. Two monoclonal antiplatelet antibodies as markers of human normal and leukemic patients peroxidase detection in megakaryocyte colonies and in in vivo cells from megakaryocyte maturation: immunofluorescent staining and platelet. *Blood* 59(3):514-21.

van Os E, Wu Y-P, Pouwels J, Ijsseldijk M, Sixma J. 2003. Thrombopoietin increases platelet adhesion under flow. *Br. J. Haematol.* 121(3):482-90.

Verkhratsky A, Kirchhoff F. 2007. NMDA receptors in glia. *Neuroscientist* 13(1):28-37.

Vermes I, Haanen C, Steffens-Nakken H, Reutellingsperger C. 1995. A novel assay for apoptosis. Flow cytometric detection of phosphatidylserine expression on early apoptotic cells using fluorescein labelled Annexin V. *J. Immuno. Methods*. 184(1):39-51.

Vigon I, Florindo C, Fichelson S, Guenet J, Mattei M, Souyri M, Cosman D, Gisselbrecht S. 1993. Characterization of the murine Mpl proto-oncogene, a member of the hematopoietic cytokine receptor family: molecular cloning, chromocomal location and evidence for a

function in cell growth. *Oncogene* 8(10):2607-15.

Vigon I, Mornon J-P, Cocault L, Mitjavila T, Tambourin P, Gosselbrecht S, Souyri M. 1992. Molecular cloning and characterization of *MPL,* the human homolog of the v-*mpl* oncogene: identification of a member of the haematopoietic growth factor receptor superfamily. *Proc. Natl. Acad. Sci. U.S.A.* 89(12):5640-44.

Vu T-K, Hung D, Wheaton V, Coughlin S. 1991. Molecular cloning of a functional thrombin receptor reveals a novel proteolytic mechanism of receptor activation. *Cell* 64(6):1057-68.

Vyas P, Ault K, Jackson C, Orkin S, Shivdasani R. 1999. Consequences of GATA-1 deficiency in megakaryocytes and platelets. *Blood* 93(9):2876-75.

Wagner CL, Mascelli MA, Neblock DS, Weisman HF, Coller BS, Jordan RE. 1996. Analysis of GPIIb/IIIa receptor number by quantification of 7E3 binding to human platelets. *Blood* 88(3): 907-14.

Wakikawa T, Shioi A, Hino M, Inaba M, Nishizawa Y, Tatsumi N, Morii H, Otani S. 1997. Thrombopoietin inhibits *in vitro* osteoclastogenesis from murine bone marrow cells. *Endocrinology* 138(10):4160-66.

Walsh GM, Leane D, Moran N, Keves TE, Forster RJ, Kenny D, O'Neill S. 2007. *S*-nitrosylation of αIIbβ3 as revealed by Raman spectroscopy. *Biochemistry* 46(21):6429-36.

Wang J, Liu Z-L, Jerome E. Groopman J. 1998. The alpha-chemokine receptor CXCR4 is expressed on the megakaryocytic lineage from progenitor to platelets and modulates migration and adhesion. *Blood* 92(3):756-64.

Watkins J, Evans R. 1981. Excitatory amino acid transmitters. *Ann. Rev. Pharmacol. Toxicol.* 21:165-204.

Watkins J, Jane D. 2006. The glutamate story. *Br. J. Pharmacol.* 147:S100-8.

Watts AG, Hobbs, CM, Gibson J, Glover C, Katenar T, Resende, R, MacKenzie AB. 2010. S-NO binding (SNOB) reagents for the direct visualization and characterisation of protein *S*-nitrosylation. *In submission.*

Wee K-L, Zhang Y, Khanna SL, C-M. 2008. Immunolocalisation of NMDA receptor subunit NR3B in selected structures in the rat forebrain, cerebellum and lumbar spinal cord. *J. Comp. Neurol*. 509(1):118-35.

Wheeler M, Stachlewitz RF, Yamashina S, Ikejima K, Morrow AL, Thurman RG. 2000. Glycine-gated chloride channels in neutrophils attenuate calcium influx and superoxide production. *FASEB J.* 14(3):476-484.

Wong H-K, Liu X-B, Matos, MF, Chan S, Perez-Otano I, Boysen M, Cui J, Nakanishi N, Trimmer J, Jones E, Lipton S, Sucher NJ. 2002. Temporal and regional expression of NMDA receptor subunit NR3A in the mammalian brain. *J. Comp. Neurol* 450(4):303-17.

Wood M, Vandongen H, Vandogen A. 1995. Structural conservation of ion conduction pathways in K channels and glutamate receptors. *Proc. Natl. Acad. Sci. USA.* 92(11):4882-6.

Wright J. 1906. The origin and nature of the blood plates. *Boston Med. Surg. J.* 23:643-45.

Xu W, H A, Whitmore T, Presnell S, Yee D, Ching A, Gilbert T, Davie E, Foster D. 1998. Cloning and characterization of human protease-activated receptor 4. *Proc. Natl. Acad. Sci. U.S.A.* 95(12):6642-46.

Yang Y-I. Jung D-W, Bai D-G, Yoo G-S, Choi J-K. 2001. Counterion-dye staining method for DNA in agarose gels using crystal violet and methyl orange. *Electorphoresis* 22(5):855-59.

Yoshida K, Taga T, Saito M, Suematsu S, Kumanogoh A, Tanaka T, Fujiwara H, Hirata M, Yamagami T, Nakahata T, Hirabayashi T, Yoneda Y, Tanaka K, Wang WZ, Mori C, Shiota K, Yoshida N, Kishimoto T. 1996. Targeted disruption of gp130, a common signal transducer for the interleukin 6 family of cytokines, leads to hyocardial and hematological disorders. *Proc. Natl. Acad. Sci. U.S.A.* 93(1):407-11.

Young M, Pelegrin P, Surprenant A. 2007. Amino acid residues in the P2X7 receptor that mediate differential sensitivity to ATP and BzATP. *Mol. Pharmacol*. 71(1):92-100.

Zauli G, Bassini A, Catani L, Gibellini D, Celechini C, Borgatti P, Carmelli E, Guidotti L, Capitani S. 1995. PMA-induced megakaryocyte differentiation of HEL cells is accompanied by striking modifications of protein kinase C catalytic activity and isoform composition at the nuclear level. *Br. J. Haematol.* 92:530-36.

Zhang G, Kazanietz M, Blumberg P, Hurley J. 1995. Crystal structure of the cys2 activator-binding domain of protein kinase C delta in complex with phorbol ester. *Cell* 81(6):917-24.

Zhang H, Nimmer P, Tahir S, Chen J, Fryer R, Hahn K, Iciek L, Morgan S, Nasarre M, Nelson R, Preusser LC, Reinhart GA, Smith ML, Rosenberg SH, Elmore SW, Tse C. 2007. Bcl-2 family proteins are essential for platelet survival. *Cell Death Differ.* 14(5):943-51.

Zimmet J, Ravid K. 2000. Polyploidy: Occurrence in nature, mechanisms, and significance for the megakaryocyte-platelet system. *Exp. Hematol*. 28(1):3-16.

Zoia C, Cogliati T, Taglibue E, Cavaletti G, Sala G, Galimberti G, Rivolta I, Rossi V, Frattola L, Ferrarese C. 2004. Glutamate transporters in platelets: EAAT1 decrease in aging and in Alzheimers disease. *Neurobiol. Aging.* 25(2):149-57.

APPENDIX I
THROMBIN DOSE RESPONSE

Thrombin responses were detected in all donors, both those which responded to the agonist tested and those which did not. It was observed that responses to all of the agonists used in the fluo-4 assay desensitised over the duration of the experiments, therefore thrombin dose response data was also separated by time to determine whether this effect also occurred.

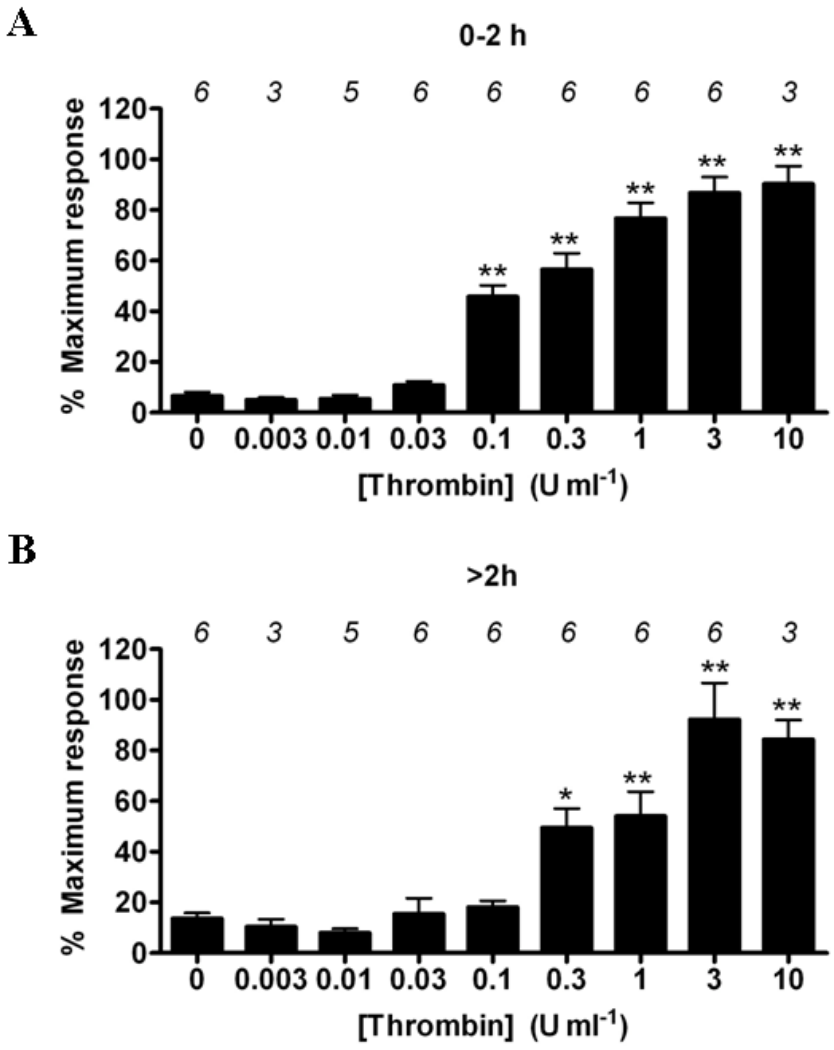

Figure 62. Thrombin evokes an intracellular calcium response in human platelet which decreases over the duration of each experiment. *P< 0.05; **P< 001 in comparison to 0 μM thrombin using a one-way ANOVA with a Dunnetts post-hoc test.

The data is split into that obtained within the first 2 h of each experiment (A) and that obtained over 2 h from the start of the experiments (B). The figure demonstrated that responses to thrombin decrease for 0.3, 1 and 10 U ml^{-1} over the course of each experiment, with a small increase in that elicited with 3 U ml^{-1} (86.74 ± 6.27 rising to 92.21 ± 14.49 % MR). It was decided that thrombin would be used as a positive control at 3 Uml^{-1} for the rest of the study.

APPENDIX II
NITROSYLATION

AII.1. Summary

In this appendix, it has been demonstrated that *S*-nitrosylation binding (SNOB) reagents bind to platelet proteins where:

- SNOB reactivity is time and temperature dependent
- SNOB binding is increased by incubation of platelets with NO donors
- SNOB binding is decreased by incubation of platelets with DTT, which is predicted to reduce S-nitrosylation.

AII.2. Introduction

AII.2.1. NMDAR S-nitrosylation

NMDAR subunits NR1 and NR2A contain cysteine (cys) residues within their extracellular regions- cys744 and 798 in the M3-M4 extracellular loop of NR1 and cys78, 320 and 399 in the N-terminus of NR2A (Choi *et al*, 2000). All 5 sites can be modulated by *S*-nitrosylation, with NR2A cys399 identified as the primary modulation site and located in the linker region between the ligand binding and the regulatory domains of the N-terminus (Choi *et al*, 2000). NO binds to free thiol groups (-SH) forming an *S*-nitrosothiol group (-SNO) (equation 1).

$$\text{R-SH} + \text{NO} \longleftrightarrow \text{R-SNO} + \text{H}$$

Equation 1. R= any amino acid

The other extracellular cysteine residues have been shown to form disulphide bonds (-S-S-), cys744 and cys798 (NR1) and cys78 and 320 (NR2A), and therefore can not bind NO. However under low oxygen, or hypoxic, conditions, for example in the brain, these have been demonstrated to preferentially exist as separate free thiols (Takahashi *et al*, 2007). It has been suggested that the free NR1 cysteine residues form a 'molecular oxygen sensor' which enhances the extent of down-regulation of NMDAR activity by *S*-nitrosylation, under hypoxic conditions (Takahashi *et al*, 2007). It is then hypothesised that the *S*-nitrosylation of these residues exerts an allosteric influence on the *S*-nitrosylation of other thiols in the receptor for example cys399 of the NR2A subunit.

It has been shown that NMDARs can be modulated by both endogenous and exogenous NO (Choi *et al,* 2000; Monzoni and Bockaert, 1993). Exogenous NO is provided by NO donors such as SNOC or NONOate, with endogenous NO produced by NO synthase (NOS), for example neuronal NOS (nNOS) in the brain (Choi *et al*, 2000). NMDAR NR1 subunits have been found to be coupled to nNOS via postsynaptic density 95 (PSD95) in some neurones, and it has been shown that activation of NMDAR leads in turn to the production of NO (Choi *et al*, 2000). This inhibits further activation of NMDARs, and desensitises already activated receptors, preventing overstimulation which can occur for example during an ischemic event. Localised levels of glutamate increase rapidly, stimulating large increases in Ca^{2+} influx into the cells triggering not only NO production but also mitochondrial dysfunction and activation of caspases-3 and -9, which can trigger apoptosis (Rameau *et al*, 2003; Hardingham *et al*, 2002; Arundine and Tymianski, 2004). Reducing their activation can halt the damage which is done to not only the immediate area of the insult, but also the surrounding area, limiting the damage caused (Choi *et al*, 2000).

Reducing agents such as DTT, which reduce –SNO groups and disulphide bonds to free thiols (-SH) mimic the effects of hypoxia, and leads to the removal of the *S*-nitrosylation induced inhibition of NMDARs (Kim *et al,* 1999; Takahashi *et al*, 2007).

$$2R\text{-}SNO + DTT\ (2H) \longleftrightarrow 2R\text{-}SH + 2NO + oxDTT$$

$$R\text{-}SS\text{-}R + DTT\ (2H) \longleftrightarrow 2R\text{-}SH + oxDTT$$

Equation 2. R= any amino acid

AII.2.2. Detection of S-nitrosylation

Previously, the biotin switch method (Jaffrey and Snyder, 2001) has been used to detect nitrosylation of proteins, however a new single step process has been developed using an *S*-nitrosylation binding protein (SNOB) (Watts *et al*, in submission). SNOB is a long chain molecule with a formula of $C_{25}H_{43}N_5O_4S$ and molecular weight of 509.71 g mol^{-1} (figure 63), that contains a terminal alkene group which can react with the unique –SNO bond and directly functionalise the group with biotin. It binds to *S*-nitrosylated cysteine residues within proteins through the mechanism detailed in figure 59 catalysed by light or

heat. The biotin switch is an indirect approach to detect *S*-nitrosylation, where thiols are blocked by methyl methanethiosulfonate (MMTS) and the protein denatured by SDS, excess MMTS is then removed, after which nitrosothiols are reduced to thiols by acetone before the addition of biotin-(*N*-[6-(biotinamido)hexyl]-3'-(2'-pyridyldithio)propionamide (biotin-HPDP) which labels the exposed thiols with biotin (figure 64) (Jaffrey *et al*, 2001). In contrast, SNOB binds directly to *S*-nitrosylated cysteines without the need for protein denaturation, which suggests that SNOB could be used to detect *S*-nitrosylation of surface proteins expressed in live cells. The biotin switch is prone to false positive results as it works on the premise that MMTS blocks all exposed thiol groups and that acetone only reduces the *S*-nitrosylated cysteine residues. It is however feasible for exposed disulphide bonds to also be reduced by the acetone, increasing the number of free thiols together with those not blocked by MMTS, which can then be bound by the biotin-HPDP molecule (Jaffrey *et al* 2001). It is also possible that if the protein is not sufficiently reduced, thiols may not be blocked by MMTS, but still be accessible to biotin-HPDP, again increasing the amount of biotin binding and suggesting a greater level of *S*-nitrosylation than is actually present. The single step SNOB method does not use reducing agents, and is therefore free from this potential problem. The mechanism by which SNOB functions is described in figure 65 with the final step occurring under acidic aqueous conditions such as those used for the preparation of samples for mass spectroscopy analysis. The presence of the bound biotin either through biotin switch or SNOB methods can be detected by different methods for example running samples on SDS PAGE and detecting changes in protein biotinylation using Neutravidin-HRP which utilises the strong avidin-biotin bond (Giltin *et al*, 1987). Alternatively, samples can be digested, for example with trypsin, so that the fragments can be analysed by mass spectrometry to identify where the SNOB is bound to the protein (figure 64). SNOB reagent binding to S-nitrosylated cysteines has been characterised using recombinant bovine serum albumin (BSA) and human platelet membrane proteins.

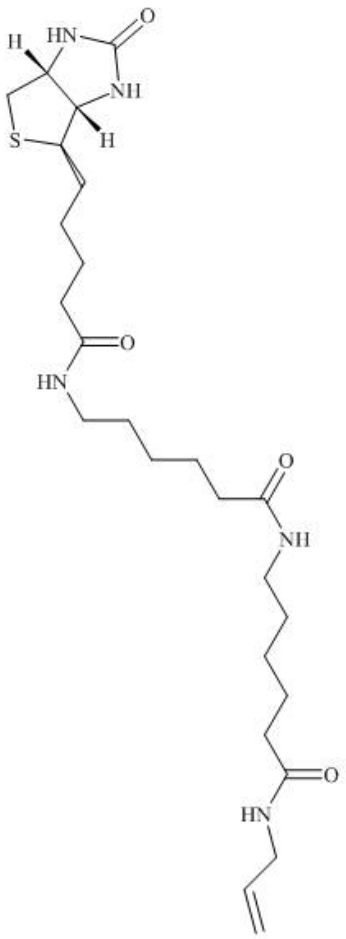

Figure 63. Structure of SNOB. *S*-nitrosylation binding protein 6 (SNOB6) has a chemical formula of $C_{25}H_{43}N_5O_4S$ and a molecular weight of 509.71 g mol^{-1}. A biotin group is located at the N-terminus which can be detected through SNOB binding (Watts *et al*, in submission).

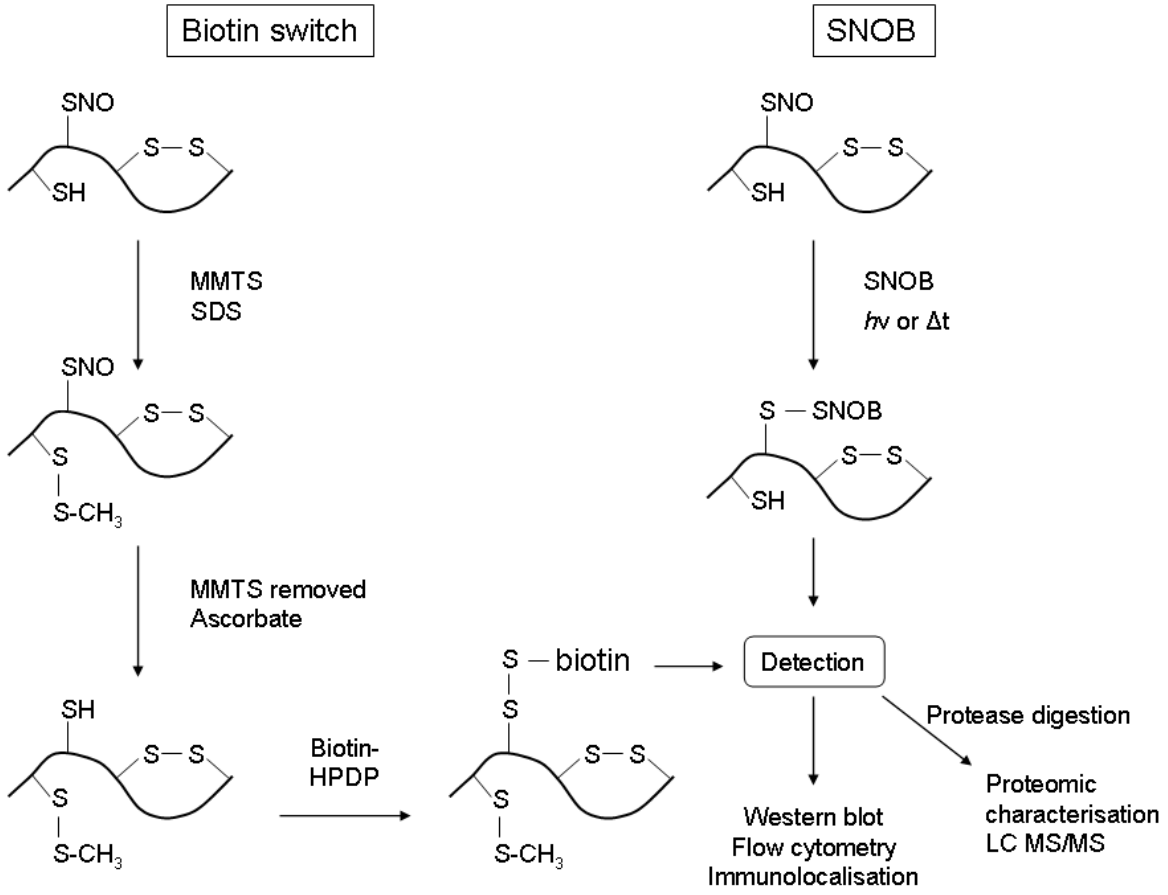

Figure 64. Comparison of the biotin switch and SNOB methods of detecting *S*-nitrosylated proteins. The biotin switch method is an indirect assay which can not be used on live cells, whereas the SNOB method is a single step process which does not require denaturation of the protein being labelled, and can therefore be used on live cells. In the biotin switch assay, proteins are denatured with sodium dodecyl sulphate (SDS) and the free thiols (-SH) methylthiolated with methyl methanethiosulfonate (MMTS) to render them unreactive. The excess MMTS is then removed and the proteins treated with acetone to denitrosylate the –SNO groups to free thiols. Finally the protein is reacted with a thiol-modifying reagent biotin-HPDP (*N*-[6-(biotinamido)hexyl]-3'-(2'-pyridyldithio)propionamide) which labels the thiols with biotin. In comparison, the SNOB reagent requires only an increase in temperature (Δt) or the presence of light (*hv*) to react making it a single step process; detailed mechanism shown in figure 60. With both methods, once the proteins have been labelled, the biotin can be detected through a range of methods, including Western blot using avidin-containing reagents e.g. Neutravidin-HRP, flow cytometry or immunolocalisation with fluorescently tagged avidin. The proteins can also be digested with enzymatically, for example with trypsin and the fragments found which are labelled and the sites of *S*-nitrosylation identified through LC MS/MS.

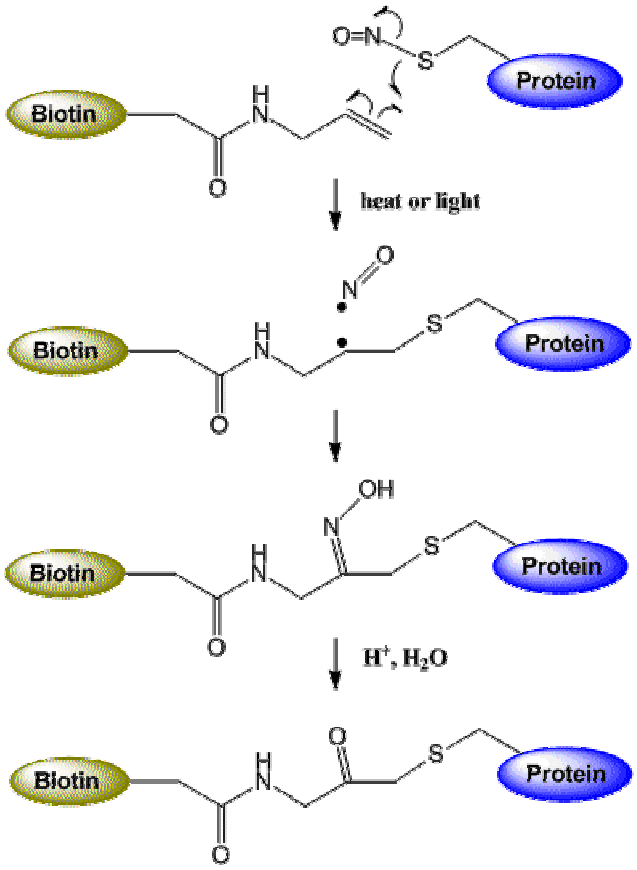

Figure 65. Proposed mechanism for the reaction of SNOB reagents with *S*-nitrosylated cysteines. This illustrates the proposed mechanism of activity for SNOB reagents. The SNOB reagent is shown as the left-hand molecule with the green biotin tag, with the protein of interest shown on the right in blue. The movement of electrons in the -SNO group cause denitrosylation, which leads to binding of the SNOB reagent to the exposed cysteine residue of the protein. Unpaired electrons in the NO group and at the link between the protein and SNOB form a double bond, adding an –N-OH group to the complex. This is then converted to a ketone by the loss of the –OH group under aqueous acidic conditions (Watts *et al*, in submission).

AII.3. Methods

*AII3.1. Reagent –*S*-nitrosocysteine (SNOC)*

Table 44. SNOC

REAGENT	CONCENTRATION (M)
L-cysteine	0.2
Sodium nitrite	0.2
HCl	10

Equal volumes of 200 mM L-cysteine and 200 mM sodium nitrite, both made in nominally Ca^{2+}-free salt solution (saline), were combined to produce 100 mM SNOC, a clear colourless solution. The addition of 10 M HCl to a final concentration of 0.5 M activates SNOC, which becomes clear red in colour. Once activated, SNOC must be kept on wet ice and used within 2 h (Graves *et al*, 1998; Lei *et al*, 1992).

AII.3.2. Detection of S-nitrosylation

PRP was separated into the number of 2 ml aliquots required and centrifuged at 350 x*g* for 20 min. Each platelet pellet was washed and resuspended in 500 µl nominally Ca^{2+}-free salt solution warmed to 37 ^{o}C. From this point the platelets were kept at 37 ^{o}C in the dark as both DEA NONOate (NONOate) and SNOB are light-sensitive. NONOate (5 mM) or SNOC (100 µM; section 2.1.1) were added to platelet suspensions as required and incubated for 20 min. These are both exogenous sources of NO, which generate and release NO into solution (Jaffrey *et al*, 2001; Lei *et al*, 1992). The cells were centrifuged (20 min, 350 *x*g) and resuspended in warmed nominally Ca^{2+}-free salt solution. DTT (20 mM) was also added for 20 min either to previously untreated platelets or following NONOate incubation. DTT is a reducing agent, which can maintain thiol (-SH) groups and reduce disulphide bridges; it was used to determine whether baseline or induced nitrosylation of platelet membrane proteins by NONOate or SNOC can be reduced (Choi and Lipton, 2000). Finally the SNOB (450 µM) was added for 5 min, after which the platelet suspension was centrifuged for 20 min at 350 x*g*, washed and the pellet resuspended in 50 µl lysis buffer B. The resuspended platelets were then rocked gently for 1 h at 4 ^{o}C and centrifuged at 19000 x*g* for 10 min at 4 ^{o}C.

The supernatant was then removed and either run immediately on a Western blot (section 2.4.3) or stored at -80 ^{o}C. Coomassie gels were run alongside the gels for immunoblotting to ensure that the samples were equally loaded. Once the protein was transferred, the membrane was blocked overnight in 5 % BSA-TTBS at 4 ^{o}C on a rocker (5-10 rpm). The membrane was then washed briefly in TTBS and incubated in 0.5 μg ml^{-1} neutravidin-HRP in BSA-TTBS for 30 min at RT, rocking gently. Following this the membrane was washed six times for 5 min in TTBS. Biotinylated proteins and markers were visualised using the ECL chemiluminescent detection agent.

AII.4. Results

AII.4.1. SNOB and BSA

BSA was chosen as a model protein as it is known to contain 35 cysteine residues of which 24 form 12 disulphide bridges with 1 free surface cysteine residue, cys58 (Oblak *et al*, 2004). Mass spectrometry data has demonstrated that SNOB binds to the QQCP sequence in BSA which includes the exposed cys58 residue corresponding to the peak at 998.29 amu (figure 66).

BSA (1 mg ml^{-1}) was nitrosylated with 1 mM NONOate in light limited conditions at pH 7, with a control sample that was not NONOate treated. Samples were treated with 450 μM SNOB for 0, 5, 10, 15, 30 and 60 min at 4, 10 or 37 ^{o}C and run on Western blots. Biotin was detected by probing with Neutravidin-HRP (figure 67). At 4 ^{o}C, binding of SNOB was detected after 30 min of SNOB treatment. This was decreased to 15 min treatment at 10 ^{o}C, and reduced further to 5 min at 37 ^{o}C. Further investigations used 5 min treatment with 450 μM SNOB at 37 ^{o}C.

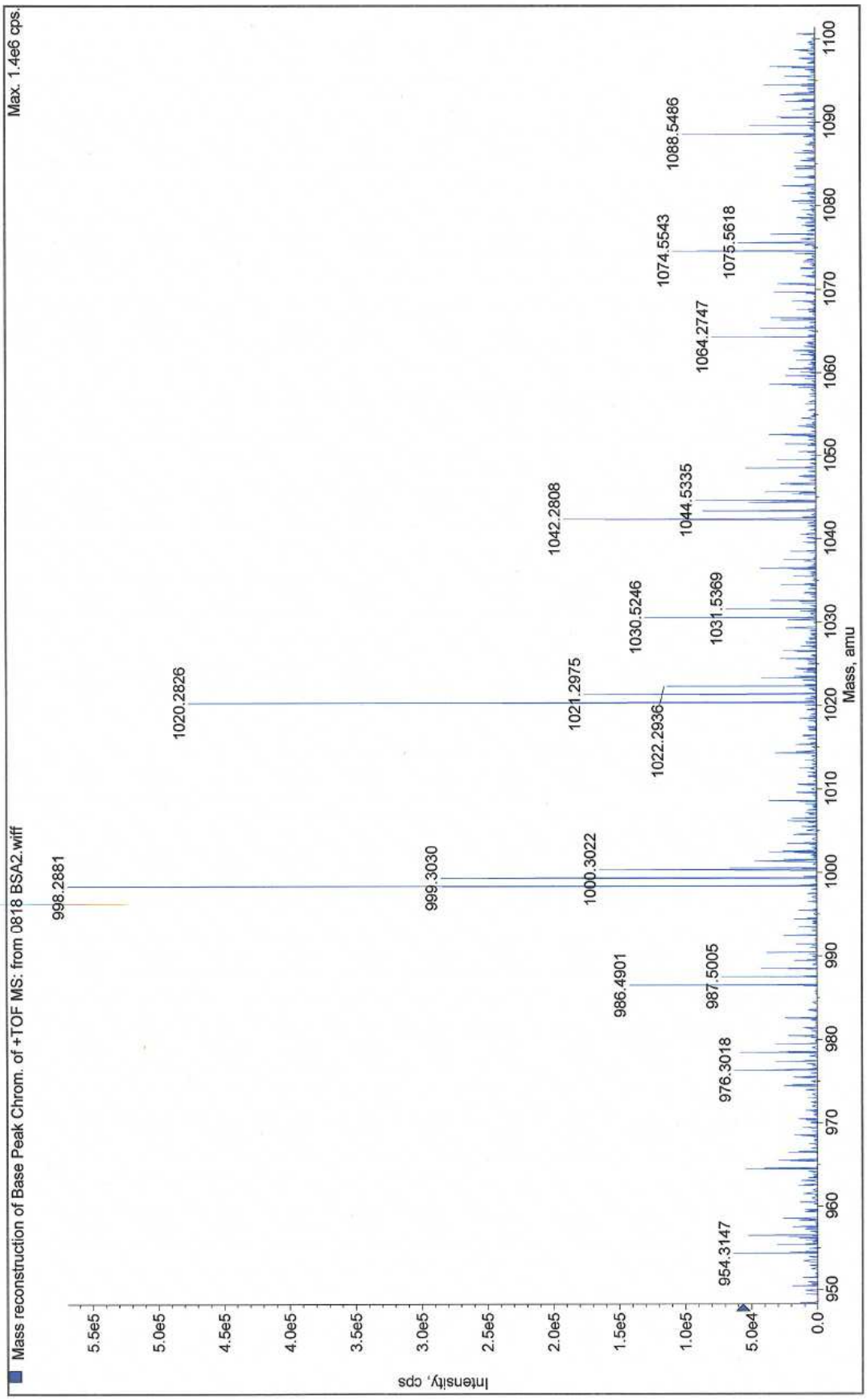
Mass reconstruction of Base Peak Chrom. of +TOF MS: from 0818 BSA2.wiff
Max. 1.4e6 cps.
Intensity, cps
Mass, amu
998.2881
999.3030
1000.3022
1020.2826
1021.2975
1022.2936
1030.5246
1031.5369
1042.2808
1044.5335
1064.2747
1074.5543
1075.5618
1088.5486
986.4901
987.5005
976.3018
954.3147

Figure 66. Mass spectrometry data for BSA bound SNOB. Liquid chromatography mass spectrometry (LC MS/MS) spectrum of SNOB bound to BSA. The BSA is subjected to peptic digestion (pH 3, 4 hours) prior to running on the mass spectrometer, separating the BSA into small fragments. This spectrum illustrates the binding of the SNOB to the peptide fragment QQCP (998.29 amu peak) which contains the exposed cysteine residue (Cys^{58}) (Watts *et al*, in submission).

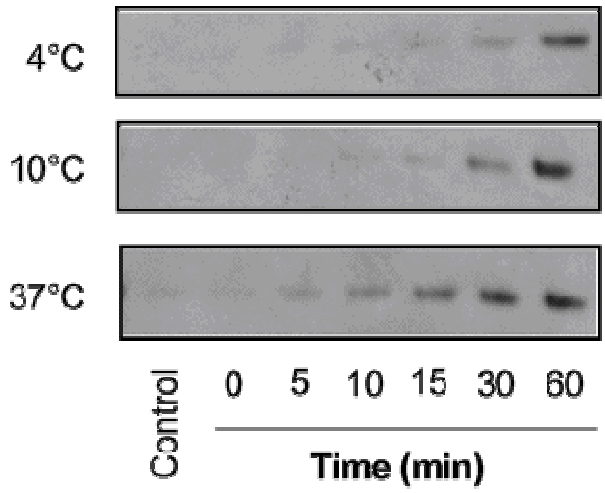

Figure 67. Effects of time and temperature on SNOB binding to BSA. Nitrosylated BSA (1 mg ml^{-1}) was treated with 450 μM SNOB at 4, 10 and 37 ^{o}C with samples treated for 0, 5, 10, 15, 30 and 60 min. Samples were run on SDS PAGE and developed on Western blot using Neutravidin-HRP which binds the biotin present in the SNOB reagent. This demonstrates that the level of SNOB binding to the BSA is distinguishable above baseline from 30 min at 4 ^{o}C, 15 min at 10 ^{o}C and from 5 min at 37 ^{o}C. The control lane demonstrates the baseline biotin levels in the absence of both DEA NONOate and SNOB (Data from Jodie Gibson, 2008).

AII.4.2. Treating live cells with SNOB

Other methods of detecting *S*-nitrosylation such as biotin switch or SNOSID (SNO-site identification) (Jaffrey and Snyder, 2001; Hao *et al*, 2006) are not suitable for use on live cells, and it was hypothesised from the data obtained with BSA that as the SNOB reagent can be used under physiological conditions (pH 7, 37 ^{o}C), it could be used to detect *S*-nitrosylation of proteins on the surface of living cells. To investigate this, freshly isolated human platelets were used as they express proteins on their surface for example NMDARs which are known to be modulated by *S*-nitrosylation (Jaffrey and Snyder, 2001).

AII.4.2.1. Temperature

Figure 63 compares the binding of SNOB at either room temperature (RT; 20-22 ^{o}C) or at 37 ^{o}C under different conditions. The background controls indicate that there are no observable differences in the level of biotin detected in live platelets when treated at either temperature. The addition of 450 μM SNOB increases the level of protein-bound biotin at RT, which is enhanced further following incubation at 37 ^{o}C, indicating a greater increase in *S*-nitrosylation. DTT is a reducing agent, which has been shown to reverse *S*-nitrosylation (Kim *et al*, 1999). It was added to live platelets prior to SNOB treatment to determine whether any changes were observed in biotin binding, which is indicative of changes in *S*-nitrosylation. This was shown to occur at both temperatures, with the levels of biotinylation decreasing to nearly that of the control samples. Overall this indicates that levels of biotinylation are higher at 37 ^{o}C than at RT, therefore all further experiments were carried out at 37 ^{o}C.

AII.4.2.2. SNOB concentration

Different concentrations of SNOB were tested to determine which to use for further experiments (figure 69). These were assessed in combination with DTT as previously described (section 6.3.3.1), together with the addition of DEA NONOate (NONOate), an NO donor. NONOate was added to determine whether the levels of biotinylation linked to changes in nitrosylation, could be raised by the presence of increased NO. DTT was added to determine whether both the baseline levels and levels of biotinylation enhanced by previous NONOate treatment, could be decreased.

The presence of 300 μM SNOB elicited a small increase in biotinylation above the no SNOB control, which was increased further by the addition of NONOate prior to SNOB

treatment. Treating platelets with DTT following incubation with NONOate reduced the level of biotinylation, but not to the same level as the no treatment control. Increasing the concentration of SNOB to 450 μM, increased the levels of biotinylation above that with 300 μM SNOB. As with 300 μM SNOB, the addition of DTT before SNOB treatment (450 μM) reduced the levels of biotinylation. The addition of NONOate increased biotinylation above that detected by SNOB alone, particularly in bands at approximately 90 kDa. Detection of background biotinylation is decreased by treatment with DTT suggestive of decreases in *S*-nitrosylation, however levels do not return to those of the SNOB only control. From this, 450 μM SNOB will be used for further experiments.

AII.4.2.3. SNOC

S-nitrosocysteine (SNOC) (table 44) is another NO donor, which was tested to determine whether it could raise levels of biotinylation linked to increased nitrosylation comparatively to NONOate. SNOC is shown to increase the levels of biotinylation above that detected with SNOB alone, with a larger increase induced by a 10 min SNOC incubation (figure 70). These increases can then be reduced by the addition with DTT to similar levels to the baseline in the absence of SNOB. However this demonstrates that the increase in nitrosylation-linked biotinylation with SNOC is not as great as that in the presence of NONOate.

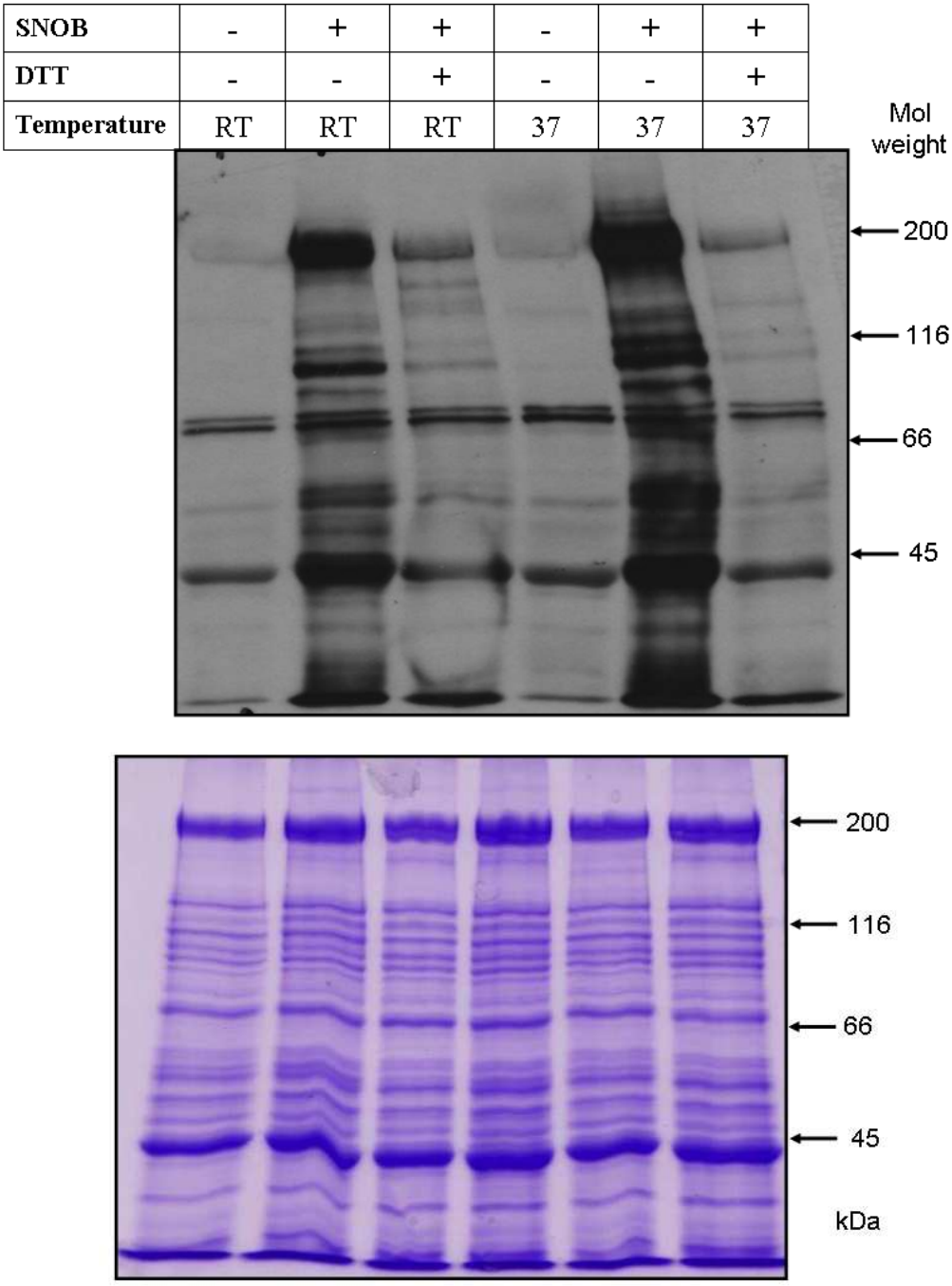

Figure 68. Nitrosylation of human platelet membrane proteins is increased with temperature. Western blot demonstrating SNOB binding to membrane proteins of human platelets at room temperature (RT; 20-22 ^{o}C) and at 37 ^{o}C. The table indicates the application of 450 µM SNOB and 20 mM DTT. At both temperatures the signal increases in strength with the addition of 450 µM SNOB, which is reduced to almost baseline amounts with the addition of DTT, a reducing agent. The increase in signal with SNOB alone above baseline is higher at 37 ^{o}C than RT indicating a greater level of binding. The gel below was run alongside the upper gel using the same samples to demonstrate equal loading and stained with coomassie blue dye (n=1). Approximately 15 µg of protein was loaded per sample.

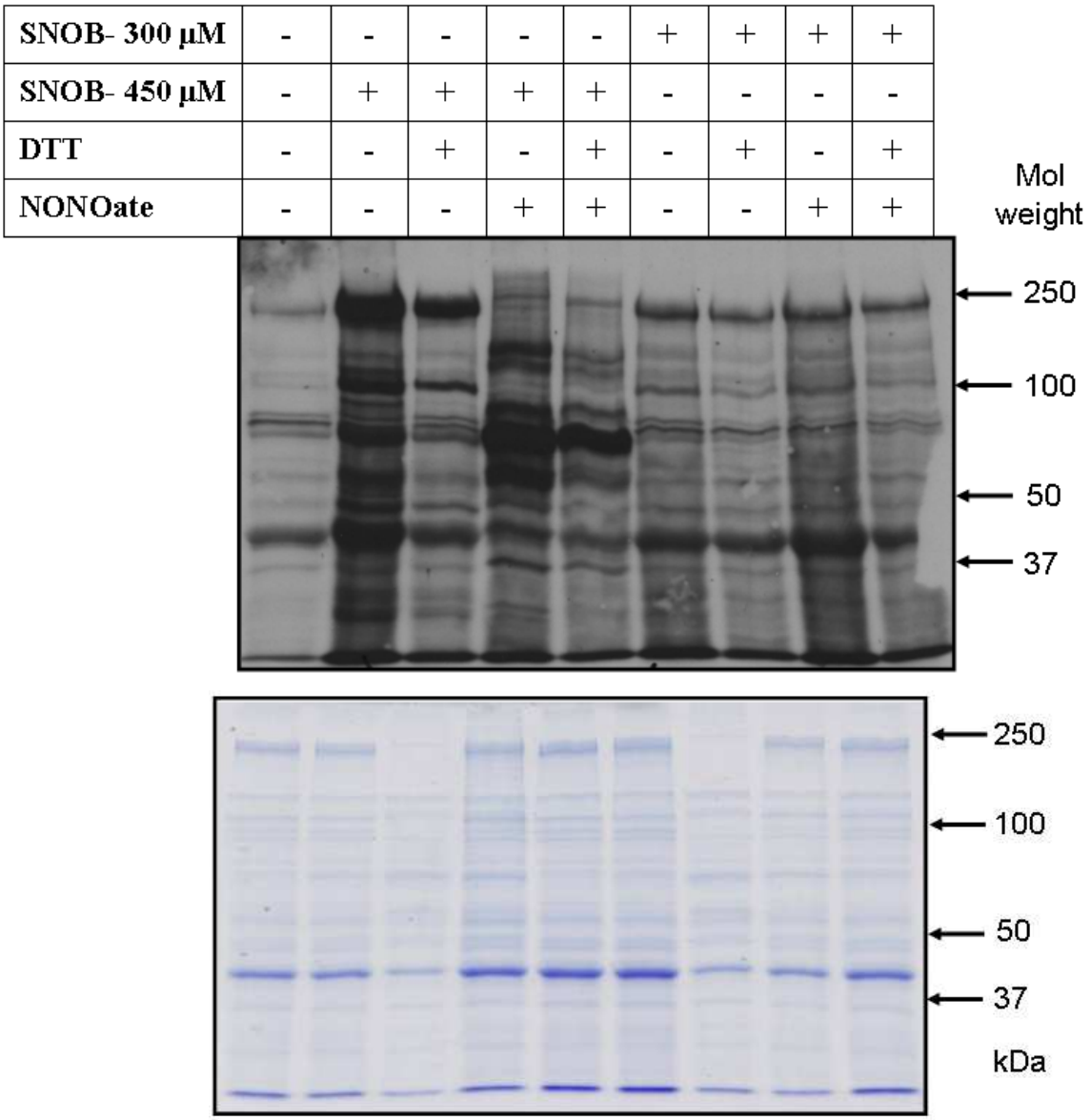

Figure 69. Increasing SNOB concentration leads to greater detection of nitrosylated human platelet membrane proteins. Western blot demonstrates the effect of increasing the concentration of SNOB used to detect nitrosylated proteins on human platelet membrane surface. With both concentrations of SNOB, the level of nitrosylation detected decreases when platelets are incubated with 20 mM DTT and increases above baseline with the addition of 5 mM NONOate (NO donor) to the platelet suspension. Treatment of platelets with NONOate, then DTT and finally SNOB reduced the level of protein biotinylation compared to platelets treated with the NO donor. In all cases 450 µM SNOB gives a greater signal than the corresponding sample with 300 µM. The table indicates the application of SNOB, DTT and NONOate. This is a representative blot from 3 repeats from 3 different human donors. The gel below was run alongside the upper gel using the same samples to demonstrate equal loading and stained with coomassie blue dye (n=3). Approximately 15 µg protein was loaded per sample.

SNOB	-	+	+	+	+	+	+	+	+
DTT	-	-	-	+	+	-	+	-	+
NONO	-	-	+	-	+	-	-	-	-
SNOC- 5'	-	-	-	-	-	+	+	-	-
SNOC- 10'	-	-	-	-	-	-	-	+	+

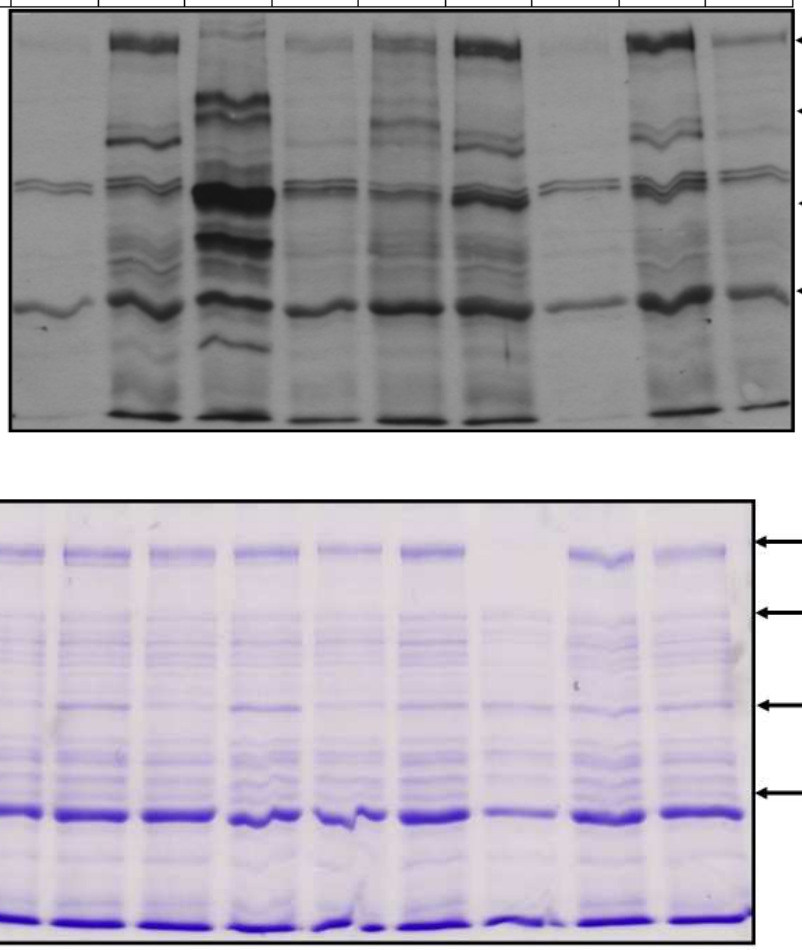

Figure 70. *S*-nitrosocysteine increases nitrosylation of human platelet membrane proteins. This illustrates that another NO donor, *S*-nitrosocysteine, (SNOC; 100 μM) can increase nitrosylation of human platelet membrane proteins above the baseline that can be detected using SNOB reagents. The SNOC-mediated *S*-nitrosylation detected by SNOB reagents can be reduced in turn by the addition of DTT to the platelet suspension. This increase can be reduced in turn by the addition of DTT. However the increases with SNOC are not as great as that achieved with the addition of NONOate. The table indicates the application of 450 μM SNOB, 20 mM DTT, 5 mM NONOate and 100 μM SNOC. Representative blot from 3 separate experiments using platelets from 3 different donors. The gel below was run alongside the upper gel using the same samples to demonstrate equal loading and stained with coomassie blue dye (n=3). Approximately 15 μg protein was loaded per sample.

AII.5. Discussion

AII.5.1. NMDAR S-nitrosylation in the CNS

NMDARs have been highly characterised in the CNS, where they are activated by extracellular glutamate and glycine (Matsui *et al*, 1995). Glutamate levels are tightly controlled within the CNS, increasing briefly when glutamate is released in a controlled manner from a presynaptic terminal to stimulate post-synaptic receptors. Sustained exposure of neuronal cells to high levels of glutamate has been shown to cause cell death (Lucas and Newhouse, 1957), in a process named excitotoxicity found to be a common action of high concentrations of excitatory amino acids in the CNS (Olney and Sharpe, 1969; Olney *et al*, 1971). Regulation of receptors is therefore important, and one mechanism by which this occurs is *S*-nitrosylation of extracellular cysteine residues. NMDARs have 5 extracellular cysteine residues, of which 4 (2 in the NR1 subunit protein and 2 in the NR2A subunit) form disulphide bonds, while the final residue, cys399 on NR2A subunit, is the primary regulator of *S*-nitrosylation (Choi *et al*, 2000). Under reducing or hypoxic conditions, the disulphide bonds of the other cysteine residues are reduced, increasing the number of free thiol groups for *S*-nitrosylation. Previous studies have shown that *S*-nitrosylation of NMDARs inhibits NMDA-evoked currents, and that generation of endogenous NO also stimulates this effect (Choi *et al*, 2000). NMDAR NR1 subunits are located in close proximity to nNOS via the scaffolding protein PSD95, and activation of NMDARs has been shown to activate nNOS through increasing $[Ca^{2+}]_i$. This leads to further production of NO which acts as a regulatory feedback mechanism to minimise further NMDAR activation (Cui *et al*, 2007).

AII.5.2. Role of S-nitrosylation in platelet activation

S-nitrosylation also plays an inhibitory role in platelet activation and aggregation. NO is produced in the endothelium by constitutive eNOS, and production is stimulated by fluid shear stress generated by the flow of blood over the endothelial cell surface (Dimmeler *et al*, 1999). This leads to activation of PI3K and Akt which phosphorylates eNOS stimulating production of NO which can then diffuse into the blood stream, inhibiting platelet aggregation (Dimmeler *et al*, 1999; Fulton *et al*, 1999). There is also evidence that NO is produced in platelets following the identification of eNOS expression, however this remains a contentious issue (Sase and Michel, 1995; Tymvios *et al*, 2009). Endogenous NO plays an inhibitory role in platelet aggregation through a combination of cyclic guanosine monophosphate (cGMP)-dependent and –independent pathways. The binding of

NO to soluble guanylyl cyclase (sGC) leads to an increase in cGMP (Mellion *et al*, 1983), activating protein kinase G (PKG) or cGMP-dependent protein kinase, which has been found to inhibit a range of functions within platelets including release of Ca^{2+} from intracellular stores (Cavellini *et al*, 1996), granule secretion (Michelson *et al*, 1996), and cytoskeleton re-organisation (Butt *et al*, 2001), as well as $\alpha_{IIb}\beta_3$ and P-selectin expression on the surface of cells (Michelson *et al*, 1996). The cGMP-independent pathways include the inhibition of $\alpha_{IIb}\beta_3$ phosphorylation (Oberprieler *et al*, 2007), $P2Y_{12}$ activation (Kokkola *et al*, 2005) and thromboxane A2 synthesis (Tsikas *et al*, 1999). Together, these pathways lead to a reduction in the initiation and continuation of aggregate formation which leads to increased bleeding times (Michelson *et al*, 1996).

AII.5.2.1. NMDARs and human platelets

The NMDAR subunit proteins, NR1 and NR2A have been shown in this study to be expressed in human platelets, and there is evidence of nitrosylation of both the receptor and other platelet surface proteins in the literature (Jaffrey and Snyder, 2001; Walsh *et al*, 2007; Mellion *et al*, 1983). It was therefore hypothesised that nitrosylation of NMDARs could act as a regulatory step in platelet activation. This would help to limit activation during an ischemic event where localised concentrations of both glutamate and NO increase, with the activation of NMDARs inducing further NO production (Choi *et al*, 2000). Nitrosylation of other platelet proteins would also prevent the cell from aggregating within the site of injury, decreasing the potential for further injury. *S*-nitrosylation of proteins has previously been detected using the biotin switch method, for example NR1 and NR2A in the brain (Jaffrey and Snyder, 2001; Jaffrey *et al*, 2001). This method is however susceptible to false positives, and can not be used on live cells. A novel compound, SNOB, has been developed in collaboration with Dr Andrew Watts (University of Bath, UK) to detect cell surface *S*-nitrosylation in live cells, and specifically in human platelets. The eventual aim was to evaluate the *S*-nitrosylation of NMDARs expressed on human platelets and their potential regulation by NO. This appendix presents the data evaluating the compound using recombinant proteins, which has been extended to investigate the *S*-nitrosylation of membrane proteins in live platelets.

Initial work demonstrated that *S*-nitrosylated cysteines could be detected in BSA following a 5 min incubation with SNOB at 37 ^{o}C, pH 7, which was repeated with live human platelets, demonstrating that SNOB reacted under physiological conditions (figures 66 and

68). Low levels of biotin binding were detected in the absence of SNOB in human platelets, suggesting that they contain endogenously biotinylated proteins, although further investigation is required to identify these.

Initial studies investigated variations in biotinylation indicative of changes in SNOB binding, demonstrating that increases in exogenous NO using an NO donor enhances biotinylation, indicative of augmented *S*-nitrosylation of platelet proteins. Treatment of human platelets with a reducing agent demonstrated that SNOB binding can be reduced, however the intensity of some bands, for example at approximately 40 and 70 kDa, remain unaltered (figure 68). This suggests that these bands contain endogenously biotinylated proteins which are present within the platelets, and are inaccessible to the action of the reducing agent, but are exposed upon lysis of the platelets in preparation of gel electrophoresis. The action of reducing agents mimics the effects of hypoxia, the oxygen conditions under which platelets circulate within the body (Takahashi *et al*, 2007). Using a combined approach, the reduction of platelet membrane proteins followed by the addition of exogenous NO, produces a physiological insight into the reactions of platelet membrane proteins within the body, with increased SNOB binding above that observed with no SNOB treatment and a variation in expression to that with SNOB treatment (figures 69 and 70).

AII.5.3. Overall conclusions and further studies

Previous evidence demonstrates that *S*-nitrosylation of NR1 and NR2A subunit proteins within the brain can be detected by biotin switch (Jaffrey *et al*, 2001), therefore it follows that they could be detected using the SNOB reagent. This study has however demonstrated that the NR1 and not the NR2A subunit proteins are detectable in human platelets (figures 12 and 13), and it is therefore possible that while the NR2A subunit protein is expressed in human platelets, it is to a lesser extent than the NR1 subunit protein; greater study is required to investigate this further. A previous study has shown that *S*-nitrosylation of just the NR1 N-terminal cysteine residues under hypoxic conditions has a only small inhibitory effect on NMDA-evoked currents (Choi *et al*, 2000); under normoxic conditions these form a disulphide bond and are therefore not accessible for *S*-nitrosylation. While this effect is small, it is possible that it is sufficient to mediate a partial inhibitory response in NMDAR activation and requires additional study. The Western blots in theis study identified several bands of different sizeds, one of which at approximately 120 kDa could potentially contain the biotinylated NR1 subunit protein (figures 68 and 70). Further work is needed to verify

the nitrosylation of NMDAR subunit proteins for example immunoprecipitation (IP) experiments and MS. This could be extended further using SNOB to identify the *S*-nitrosylated cys residues in NMDAR subunit proteins, detecting the biotinylation using LC-MS/MS with IPs to investigate regulation of *S*-nitrosylation under different conditions. Once this has been determined, the effect of *S*-nitrosylation and denitrosylation on NMDAR function can be measured using electrophysiology and calcium imaging for example.

The SNOB reagent can be used to determine which other proteins expressed by platelets are regulated by *S*-nitrosylation and their role in platelet activation and thrombus formation. Other platelet proteins are known to be *S*-nitrosylated for example $\alpha_{IIb}\beta_{3,}$ which could be inhibited by generation of NO by eNOS into the bloodstream (Dimmler *et al*, 1999). Given the differences in oxygen concentration between normoxia and hypoxia, and the potential disparities in effects on protein activation through exposure of different numbers of free thiols, additional study is required under hypoxic conditions to determine more accurately roles of proteins such as NMDARs, under physiological conditions.